# Nonaqueous Liquid Electrolytes for Lithium-Based Rechargeable Batteries

Kang Xu

*Electrochemistry Branch, Sensor and Electron Devices Directorate, U.S. Army Research Laboratory, Adelphi, Maryland 20783-1197*

## Contents

## 1. Introduction and Scope

### 1.1. Fundamentals of Battery Electrolytes

Electrolytes are ubiquitous and indispensable in all electrochemical devices, and their basic function is independent of the much diversified chemistries and applications of these devices. In this sense, the role of electrolytes in electrolytic cells, capacitors, fuel cells, or batteries would remain the same: to serve as the medium for the transfer of charges, which are in the form of ions, between a pair of electrodes. The vast majority of the electrolytes are electrolytic solution-types that consist of salts (also called "electrolyte solutes") dissolved in solvents, either water (aqueous) or organic molecules (nonaqueous), and are in a liquid state in the service-temperature range. [Although "nonaqueous" has been used overwhelmingly in the literature, "aprotic" would be a more precise term. Either anhydrous ammonia or ethanol qualifies as a "nonaqueous solvent" but is unstable with lithium because of the active protons. Nevertheless, this review will conform to the convention and use "nonaqueous" in place of "aprotic".]

Because of its physical location in the electrochemical devices, that is, being sandwiched between positive and negative electrodes, the electrolyte is in close interaction with both electrodes; therefore, when new electrode materials come into use, the need for

Kang Xu was born in Chengdu, China, and received his B.S. degree in Chemistry from Southwest Normal University in Chongqing, China, in 1985 and M.S. in Polymer Chemistry from Lanzhou Institute of Chemical Physics, Academy of Sciences, in 1988. After working on polymer electrolyte materials from 1988 to 1992 at Chengdu Institute of Organic Chemistry, Academy of Sciences, he went to Arizona State University and received a Ph.D. degree in Chemistry in 1996 under the tutelage of C. Austen Angell. From 1997 to 2002, he was awarded the National Research Council Research Associate Fellowship and the American Society for Engineer Education Postdoctoral Fellowship, respectively, and he served during the tenures as a guest researcher at U.S. Army Research Laboratory with T. Richard Jow as academic advisor. He was employed by the U.S. Army Research Laboratory in 2002. His research interests concern materials development for electrochemical energy storage applications, which include lithium or lithium ion batteries and electrochemical capacitors. He won R&D Achievement Awards from the Department of the Army in 1999, 2001, and 2002 for his work on electrolyte materials. He authored over 60 research publications and 11 patents and is a member of the Electrochemical Society.

compatible electrolytes usually arises. The interfaces between the electrolyte and the two electrodes often dictate the performance of the devices. In fact, these electrified interfaces have been the focus of interest since the dawn of modern electrochemistry[1] and remain so in the contemporary lithium-based rechargeable battery technologies.

In a battery,[2] the chemical nature of positive and negative electrodes (also called cathode and anode, respectively, although by a more strict definition, this convention is only correct during discharge) decides the energy output, while the electrolyte, in most situations, defines how fast the energy could be released by controlling the rate of mass flow within the battery. Conceptually, the electrolyte should undergo no net chemical changes during the operation of the battery, and all Faradaic processes are expected to occur within the electrodes. Therefore, in an oversimplified expression, an electrolyte could be viewed as the inert component in the battery, and it must demonstrate stability against both cathode and anode surfaces. This electrochemical stability of the electrolyte, which in actual devices is usually realized in a kinetic (passivation) rather than thermodynamic manner, is of especial importance to rechargeable battery systems, but it is often challenged by the strong oxidizing and reducing nature of the cathode and the anode, respectively. The severity of this challenge is ever increasing with the pursuit of new battery systems with higher energy densities, which drives the exploration of a more oxidizing cathode and a more reducing anode as

candidate electrode materials, and thus constantly requests improvements in electrolyte stability. Ad hoc surface chemistry is often necessary for the kinetic stability of these new electrolyte/electrode interfaces. While the potencies of electrode materials are usually quantified by the redox potential in volts against some certain reference potential,[3] the stability of an electrolyte can also be quantified by the range in volts between its oxidative and reductive decomposition limits, which is known as the "electrochemical window". Obviously, the redox potential of both electrode materials must fall within this electrochemical window to enable a rechargeable battery operation.

Certainly, electrochemical stability is only one of the requirements that an electrolyte should meet. A generalized list of these minimal requirements should include the following: (1) It should be a good ionic conductor and electronic insulator, so that ion transport can be facile and self-discharge can be kept to a minimum. (2) It should have a wide electrochemical window, so that electrolyte degradation would not occur within the range of the working potentials of both the cathode and the anode. (3) It should also be inert to other cell components such as cell separators, electrode substrates, and cell packaging materials. (4) It should be robust against various abuses, such as electrical, mechanical, or thermal ones. (5) Its components should be environmentally friendly.

## 1.2. The Attraction of "Lithium" and Its Challenge

Lithium has long received much attention as a promising anode material. The interest in this alkali metal has arisen from the combination of its two unique properties: (1) it is the most electronegative metal ($\sim -3.0$ V vs SHE), and (2) it is the lightest metal (0.534 g cm$^{-3}$).[3] The former confers upon it a negative potential that translates into high cell voltage when matched with certain cathodes, and the latter makes it an anode of high specific capacity (3.86 A h g$^{-1}$). In the 1950s lithium metal was found to be stable in a number of nonaqueous solvents despite its reactivity,[4] and this stabilization was attributed to the formation of a passivation film on the lithium surface, which prevents it from having a sustained reaction with electrolytes. Intensified research activities resulted in the commercialization of a series of lithium-based primary cells in the 1960s and 1970s, and the electrolyte solvents ranged from organic (propylene carbonate) to inorganic (thionyl chloride and sulfur dioxide).[5-8]

The continued efforts to expand lithium chemistry into rechargeable technology, however, encountered severe difficulties in terms of the cycle life and safety.[9,10] Soon it was realized that the source of the problems was the morphology of the lithium crystals newly deposited from the electrolytes upon recharge.[11,12] Needlelike lithium crystals (called "dendrite") grow on the anode upon charge and, during the subsequent discharge, become electrically isolated from the substrate due to nonuniform dissolution rates at different sites of the dendrite. The direct victim of such lithium loss is energy density, because excessive lithium has to be used in the cell to make up for the loss.[13] But more seriously, a hazard could

be caused by such "dead lithium" crystals, which are electrochemically inactive but chemically hyper-reactive due to their high surface area. When dendrite growth pierces the separator and results in an internal short, thermal runaway and explosion ensue.

The work on rechargeable lithium batteries from the 1970s to 1980s overwhelmingly concentrated on the electrolyte formulation, in the hope that proper choices of electrolyte solvents or salts would suppress or even eliminate the dendritic deposition of lithium. Among the numerous electrolyte systems investigated, an ether-based solution developed by an Israeli company seems to have achieved the apex for lithium metal-based rechargeable batteries.[14] A lithium electrode is highly stable in this solution up to 120 °C because of excellent surface passivation,[15] and over 300 depth discharge cycles have been reported.[16] A novel redox mechanism between the salt, $LiAsF_6$, and solvent, 1,3-dioxolane, shuts down the cell chemistry at temperatures higher than 125 °C, thus preventing thermal runaway.[16,17] However, dendrite formation, especially at high charge rates, still results in capacity fade.[18] In 1989 incidents of fire due to lithium rechargeable batteries in the electronic devices, followed by the manufacturer recalls, highlighted the end of general enthusiasm in lithium metal as an anode.[19]

## 1.3. From "Lithium" to "Lithium Ion"

The failure of lithium as an anode due to dendrite formation prompted the search for a way to circumvent the drastic morphological change of the anode during cell cycling. As a result, "host−guest" chemistry was considered. Also known as "intercalation"- or "insertion"-type electrodes, this concept of reversible chemistry had been applied earlier to cathode materials for lithium batteries, as represented by the trail-blazing work of Whittingham[20,21] and the significant improvements by Goodenough et al. and others.[22,23] Most of the host materials are transition metal oxides or chalcogenides with stable crystal lattices, and their layer or tunnel structures provide the pathways for guest ions such as the lithium ion to diffuse. By injecting or extracting electrons, the redox reactions occur on the host lattice while mobile guest ions intercalate into or deintercalate from the host matrix to compensate for regional electroneutrality. During the whole intercalation/deintercalation cycle, there are no Faradaic changes in the "guest ion". If a similar intercalation host could be found and used as an anode material, then a battery employing such intercalation cathodes and anodes would only require the lithium ion to shuttle back and forth between the electrodes without the presence of lithium metal. The nickname "rocking-chair battery" was given to such a device that uses dual intercalation electrodes,[24] the working principle of which is schematically depicted in Figure 1, using the example of the state-of-the-art lithium ion chemistry.

The concept of rocking-chair lithium batteries was confirmed experimentally by using lithiated oxides ($Li_6Fe_2O_3$, $LiWO_2$) as interaction anodes and other oxides ($WO_3$, $TiS_2$, $V_2O_5$) as cathodes in nonaqueous
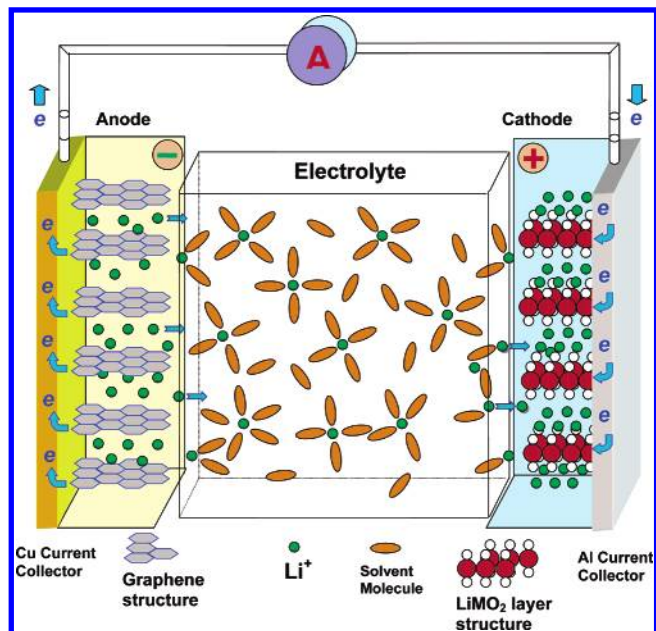


**Figure 1.** Schematic description of a "(lithium ion) rocking-chair" cell that employs graphitic carbon as anode and transition metal oxide as cathode. The undergoing electrochemical process is lithium ion deintercalation from the graphene structure of the anode and simultaneous intercalation into the layered structure of the metal oxide cathode. For the cell, this process is discharge, since the reaction is spontaneous.

electrolytes.[25,26] However, the enhanced safety and extended cycle life were not sufficient to offset the penalty in energy density caused by the replacement of lithium metal; hence, these systems were never commercialized.[27,28]

A breakthrough was made when Japanese researchers exploited an old concept of using carbonaceous materials as anode intercalation host.[29−31] The term "lithium ion battery" that was introduced by those researchers eventually prevailed and replaced the other aliases such as "rocking-chair",[24] "shuttlecock",[32] or "swing" batteries.[33] In the charged state of these carbonaceous anodes, lithium exists in its ionic rather than metallic state, thus eliminating any possibility of dendrite lithium. The advantage of this new host is highlighted by the low cost of carbon and the high lithium ion activity in the intercalation compound; the latter renders an anode potential close to that of lithium metal and minimizes the energetic penalty. In 1990 both Sony[34] and Moli[35] announced the commercialization of cells based on petroleum coke and $LiCoO_2$, though Sony was generally credited for making this technology a commercial reality. In the same year Dahn and co-workers published their seminal report on the principle of lithium intercalation chemistry with graphitic anodes and the effect of electrolyte solvent in the process.[36] In fact, the conclusions drawn therein constitute the foundation for the current lithium ion battery industry:

(1) Electrolyte solvents decompose reductively on the carbonaceous anode, and the decomposition product forms a protective film. When the surface of the anode is covered, the film prevents further decomposition of the electrolyte components. This film is an ionic conductor but an electronic insulator.

(2) This reductive decomposition process occurs only during the first charge and is absent in the following cycles so that the carbonaceous anode can be cycled many times in the electrolyte, yielding stable capacity.

(3) The chemical structure of the electrolyte solvents critically influences the nature of the protective film, and ethylene carbonate was found to be an essential component of the solvents that protects the highly crystalline structure of graphite.

Obviously, the film formed on a carbonaceous anode plays a critical role in enabling a lithium ion device to work reversibly. Presuming that the surface nature of the carbonaceous anode at low potentials is similar to that of lithium metal in nonaqueous electrolytes, Dahn and co-workers adopted a model developed earlier by Peled to describe the passivation on lithium metal[37] and named this surface film on carbonaceous anodes a "solid electrolyte interface" (SEI). This term soon became the most frequently used key word in publications concerning lithium ion technology in the following decade. Although it will turn out later that the exact mechanism involved in the formation is far more complicated and remains a controversial topic even today, it has been generally agreed that the electrolyte reduction products are the main components of an SEI and dictate the chemical as well as thermal properties of the electrode.

The decade following Dahn's publication witnessed an explosive growth in lithium ion technology research, and essentially all aspects of lithium ion technology were explored with state-of-the-art techniques, while the main excitement revolved around developing new materials such as carbonaceous anode and metal oxide cathode materials and the electrolyte solvents and salts compatible with them. The result of those intensified efforts was the successful commercialization and the rapid thriving of this youngest battery chemistry. By 2000, the quantity of lithium ion cells manufactured reached ~620 million units with a market value of ~1 billion dollars,[38] accounting for more than a 90% share of the rechargeable battery market[39] or 63% of total sales in portable batteries. The employment of new materials and novel engineering designs has pushed the cycle life, energy, and power density of this technology to more than 2000 cycles, 160 W h kg$^{-1}$, and 5000 W kg$^{-1}$, respectively.[40] The major driving force of this market remains the so-called "small formula batteries" with capacities smaller than 1 A h; however, industry-size lithium ion cells are increasingly being used in space, military, and other special applications, especially as traction power sources for electric or hybrid electric vehicle (EV/HEV) applications.[40]

## 1.4. Scope of This Review

Since the inception of lithium ion technology, there have been several reviews summarizing the knowledge accumulated about this new technology from various perspectives, with the latest being in 2003.[41−48] Because electrolytes interact closely with both cathode and anode materials during the operation, their effect on cell performance has been discussed in almost every one of these reviews. On the other hand, attention has always been focused on electrode materials, especially the anodes, and electrolytes as an important component of the cell have not been comprehensively treated in any dedicated reviews.

This review intends to fill this deficit by summarizing the progress made during the last 10 years in the research and development of electrolytes for lithium-based batteries. Since lithium ion chemistry is by far the only successfully commercialized rechargeable lithium-based technology, emphasis will be placed on the electrolytes developed for this system. Liquid electrolytes will take the central stage, and the scope of the review will include their ionics, phase diagrams, interfaces with cathode and anode materials, long-term chemical stability in the device, thermal properties and performance at extreme temperatures, and safety characterizations. Whenever an interdisciplinary topic involving both electrolyte and other cell components is encountered (i.e., electrolyte/electrode interface and passivation of electrodes), emphasis will be placed on the role and effect of electrolyte components.

For the convenience of this discussion, a somewhat arbitrary demarcation was drawn between "state-of-the-art" (SOA) and "novel" electrolyte systems, with the former referring to the ones currently used in commercialized lithium ion cells and the latter to the ones improved over the SOA systems but still under development. It should be pointed out that the exact electrolyte compositions in commercialized devices are usually proprietary knowledge, but publications from the affiliated researchers normally disclose sufficient information to reveal the skeletal electrolyte components employed. The distinction made in this review concerning the previously mentioned demarcation is based on such open literature.

This review will focus on the literature published from 1990 to the middle of 2003. Meanwhile, a certain amount of attention will also be allocated to the electrolytes for lithium batteries to avoid omitting the important progress made in these closely related fields. When selecting references, efforts were made to ensure academic quality as well as ready public accessibility. For this reason, patents, various technical reports, and conference/workshop presentations/abstracts were avoided to the extent possible. There were exceptions, though, when there was no alternative reference source. Finally, although comprehensive coverage was attempted, it is essentially impossible to cover every aspect in an exhaustive manner. The choice of the references and the organization of the content reflect the personal view of the author only.

## 2. Electrolyte Components: History and State of the Art

Most compositions of lithium electrolytes are based on solutions of one or more lithium salts in mixtures of two or more solvents, and single-solvent formulations are very rare, if there are any. The rationale behind this mixed solvent formulation is that the diverse and often contradicting requirements of bat-

**Table 1. Organic Carbonates and Esters as Electrolyte Solvents**

| Solvent | Structure | M. Wt | $T_m$/ °C | $T_b$/ °C | $\eta$/cP 25 °C | $\epsilon$ 25 °C | Dipole Moment/debye | $T_f$/ °C | d/gcm⁻³, 25 °C |
|---------|-----------|-------|-----------|-----------|-----------------|------------------|---------------------|-----------|----------------|
| EC | | 88 | 36.4 | 248 | 1.90, (40 °C) | 89.78 | 4.61 | 160 | 1.321 |
| PC | | 102 | -48.8 | 242 | 2.53 | 64.92 | 4.81 | 132 | 1.200 |
| BC | | 116 | -53 | 240 | 3.2 | 53 | | | |
| γBL | | 86 | -43.5 | 204 | 1.73 | 39 | 4.23 | 97 | 1.199 |
| γVL | | 100 | -31 | 208 | 2.0 | 34 | 4.29 | 81 | 1.057 |
| NMO | | 101 | 15 | 270 | 2.5 | 78 | 4.52 | 110 | 1.17 |
| DMC | | 90 | 4.6 | 91 | 0.59 (20 °C) | 3.107 | 0.76 | 18 | 1.063 |
| DEC | | 118 | -74.3 [a] | 126 | 0.75 | 2.805 | 0.96 | 31 | 0.969 |
| EMC | | 104 | -53 | 110 | 0.65 | 2.958 | 0.89 | | 1.006 |
| EA | | 88 | -84 | 77 | 0.45 | 6.02 | | -3 | 0.902 |
| MB | | 102 | -84 | 102 | 0.6 | | | 11 | 0.898 |
| EB | | 116 | -93 | 120 | 0.71 | | | 19 | 0.878 |

[a] The mp of DEC recorded in various literature sources (books, papers, commercial catalogs) has been −43 °C, which was corrected by a very recent measurement (ref 50e). This widespread error of 30° seems to stem from a single source in 1921, which was then registered by *Beilstein Handbuch* and escaped detection for approximately eight decades.

tery applications can hardly be met by any individual compound, for example, high fluidity versus high dielectric constant; therefore, solvents of very different physical and chemical natures are often used together to perform various functions simultaneously. A mixture of salts, on the other hand, is usually not used, because anion choice is usually limited, and performance advantages or improvements are not readily demonstrated.

Solid polymer and gel polymer electrolytes could be viewed as the special variation of the solution-type electrolyte. In the former, the solvents are polar macromolecules that dissolve salts, while, in the latter, only a small portion of high polymer is employed as the mechanical matrix, which is either soaked with or swollen by essentially the same liquid electrolytes. One exception exists: molten salt (ionic liquid) electrolytes where no solvent is present and the dissociation of opposite ions is solely achieved by the thermal disintegration of the salt lattice (melting). Polymer electrolyte will be reviewed in section 8 ("Novel Electrolyte Systems"), although lithium ion technology based on gel polymer electrolytes has in fact entered the market and accounted for 4% of lithium ion cells manufactured in 2000.[38] On the other hand, ionic liquid electrolytes will be omitted, due to both the limited literature concerning this topic and the fact that the application of ionic liquid electrolytes in lithium ion devices remains dubious. Since most of the ionic liquid systems are still in a supercooled state at ambient temperature, it is unlikely that the metastable liquid state could be maintained in an actual electrochemical device, wherein electrode materials would serve as effective nucleation sites for crystallization.

## 2.1. Solvents

In accordance with the basic requirements for electrolytes, an ideal electrolyte solvent should meet the following minimal criteria: (1) It should be able to dissolve salts to sufficient concentration. In other words, it should have a high dielectric constant ($\epsilon$). (2) It should be fluid (low viscosity $\eta$), so that facile ion transport can occur. (3) It should remain inert to all cell components, especially the charged surfaces of the cathode and the anode, during cell operation. (4) It should remain liquid in a wide temperature range. In other words, its melting point ($T_m$) should be low and its boiling point ($T_b$) high. (5) It should also be safe (high flash point $T_f$), nontoxic, and economical.

For lithium-based batteries, the active nature of the strongly reducing anodes (lithium metal or the highly lithiated carbon) and the strongly oxidizing cathodes (transition metal based oxides) rules out the use of any solvents that have active protons despite their excellent power in solvating salts, because the reduction of such protons and/or the oxidation of the corresponding anions generally occurs within 2.0–4.0 V versus Li,[49] while the charged potentials of the anode and the cathode in the current rechargeable lithium devices average 0.0–0.2 V and 3.0–4.5 V, respectively. On the other hand, the nonaqueous compounds that qualify as electrolyte solvents must be able to dissolve sufficient amounts of lithium salt; therefore, only those with polar groups such as carbonyl (C=O), nitrile (C≡N), sulfonyl (S=O), and ether-linkage (−O−) merit consideration.

Since the inception of nonaqueous electrolytes, a wide spectrum of polar solvents has been investigated, and the majority of them fall into either one of the following families: organic esters and ethers. The most commonly used solvents from these families, along with their physical properties, are listed in Tables 1 and 2, respectively,[50] where the melting temperature of diethyl carbonate (DEC) deserves special attention because a significant correction has been made recently.[50e]

**Table 2. Organic Ethers as Electrolyte Solvents**

| Solvent | Structure | M. Wt | $T_m$/ °C | $T_b$/ °C | $\eta$/cP 25 °C | $\epsilon$ 25 °C | Dipole Moment/debye | $T_f$/ °C | d/gcm$^{-3}$, 25 °C |
|---|---|---|---|---|---|---|---|---|---|
| DMM | | 76 | -105 | 41 | 0.33 | 2.7 | 2.41 | −17 | 0.86 |
| DME | | 90 | -58 | 84 | 0.46 | 7.2 | 1.15 | 0 | 0.86 |
| DEE | | 118 | -74 | 121 | | | | 20 | 0.84 |
| THF | | 72 | -109 | 66 | 0.46 | 7.4 | 1.7 | -17 | 0.88 |
| 2-Me-THF | | 86 | -137 | 80 | 0.47 | 6.2 | 1.6 | -11 | 0.85 |
| 1,3-DL | | 74 | -95 | 78 | 0.59 | 7.1 | 1.25 | 1 | 1.06 |
| 4-Me-1,3-DL | | 88 | -125 | 85 | 0.60 | 6.8 | 1.43 | -2 | 0.983 |
| 2-Me-1,3-DL | | 88 | | | 0.54 | 4.39 | | | |

An interesting observation should be made concerning the dependence of the physical properties on molecular cyclicity, since it will have a significant effect on the formulation of electrolytes for lithium ion cells. While all of the ethers, cyclic or acyclic, demonstrate similar moderate dielectric constants (2−7) and low viscosities (0.3−0.6 cP), cyclic and acyclic esters behave like two entirely different kinds of compounds in terms of dielectric constant and viscosity; that is, all cyclic esters are uniformly polar ($\epsilon = 40-90$) and rather viscous ($\eta = 1.7-2.0$ cP), and all acyclic esters are weakly polar ($\epsilon = 3-6$) and fluid ($\eta = 0.4-0.7$ cP). The origin for the effect of molecular cyclicity on the dielectric constant has been attributed to the intramolecular strain of the cyclic structures that favors the conformation of better alignment of molecular dipoles, while the more flexible and open structure of linear carbonates results in the mutual cancellation of these dipoles.

### 2.1.1. Propylene Carbonate (PC)

Among these solvents, cyclic diesters of carbonic acid have undoubtedly attracted the main research attention throughout the entire history of lithium batteries, especially in the past decade, when their role in forming an SEI on carbonaceous anodes became recognized. However, the early interest in these compounds arose solely from their high dielectric constant and, hence, their ability to dissolve a wide variety of lithium salts. In 1958, it was observed that lithium could be electrodeposited from a solution of LiClO$_4$ in PC,[51] and PC became the immediate focus of investigation.[4,9,10] Its wide liquid range (defined by the difference between $T_m$ and $T_b$, Table 1), high dielectric constant, and static stability with lithium made it a preferred solvent, and considerable efforts were made to purify it[52] when a less-than-ideal stripping/plating efficiency ($\leq$ 85%) for lithium was observed during cycling. The capacity of lithium cells with PC electrolytes also fades accordingly.[4,9,10,54] However, it was soon realized that this poor cycling efficiency was more intrinsic to the electrolyte solvent than contaminant-originated, and the reaction between the PC and the newly deposited lithium particles was thought to be the cause.[9] More recent studies employing spectroscopic means have confirmed the PC reduction on a newly formed lithium

**Scheme 1. Reduction of PC on a Lithium Surface: One-Electron Process**
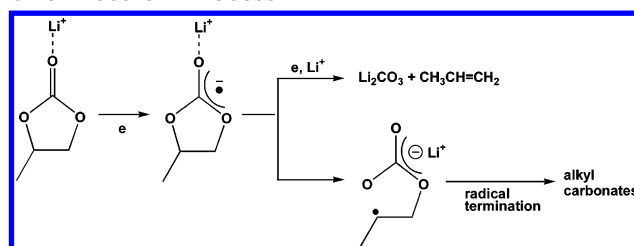


surface, and a one-electron reduction process has been proposed (see Scheme 1).[55]

The overall capacity fading of lithium cells using PC-based electrolytes, however, is a more complicated mechanism, although Scheme 1 plays a part in it. The static stability of PC against a lithium surface had been attributed earlier to the existence of a protective layer,[37,56] which consists of the decomposition products shown in Scheme 1, and prevents the sustained reaction of PC with lithium.[55] On the other hand, it was the dynamic reactivity that results in the lithium loss during cycling,[9] for which the main cause is related to the nonuniform morphological change of the lithium surface rather than chemical corrosion. Figure 2 schematically shows this nonuniformity of the lithium surface during the cycling process, where uneven growth of the electrodeposited lithium crystals results in dendrites that in subsequent discharge processes (lithium dissolution) produce lithium particles that are electrically isolated from the lithium anode. Microscopic studies have confirmed the existence of dendrites (Figure 3) and have attributed their formation to the presence of a passivation film.[37,57] Serious safety hazards are often caused by the generation of both dendrites and isolated lithium crystals.[58,59] The former creates internal shorts, and the latter is chemically active with the electrolyte solvents due to their huge surface areas.

### 2.1.2. Ethers

In view of the poor cycling efficiency and the potential hazards associated with PC, people turned to ethers for improved lithium morphology. In the 1980s, ethers were widely preferred by researchers as an alternative candidate, because of their low
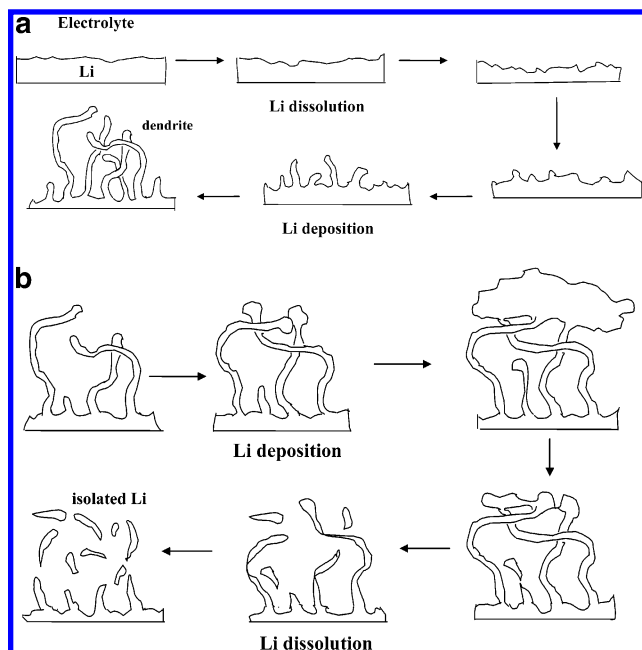
**Figure 2.** (a) Schematic description for the growth of dendrite crystals on a Li surface. The film consisting of decomposition products as shown in Scheme 1 prevents the growth of large granular crystals but rather promotes the formation of treelike dendrites. (b) Schematic description for the formation of isolated lithium particles from Li dendrites. The uneven dissolution of the dendrites leaves lithium crystals detached from the lithium substrate. The isolated lithium crystals become electrochemically "dead" but chemically reactive due to their high surface area.
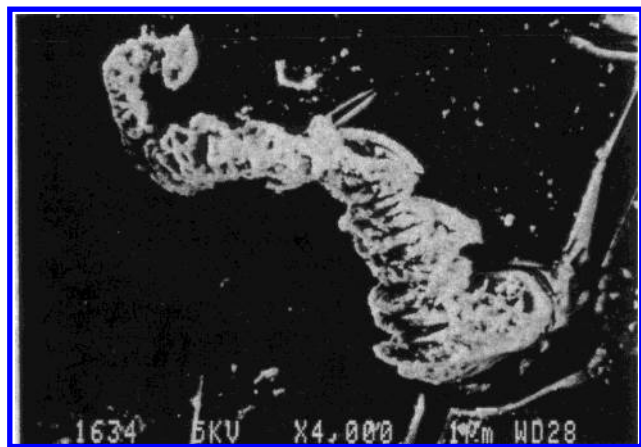


**Figure 3.** Micrograph of a single dendrite lithium grown in PC. (Reproduced with permission from ref 57 (Figure 6a). Copyright 1989 The Electrochemical Society.)

viscosity and resultant high ionic conductivity, but, most of all, the better lithium morphology during cycling.[60] The cycling efficiency of lithium was reported to be 88% in tetrahydrofuran (THF),[60-62] an average of 96% in 2-methyltetrahydrofuran (2-Me-THF),[62-65] 97% in polymethoxy ethers[66] and dimethoxy propane,[67] and 98% in diethyl ether,[62,68] although the safety concern over the high vapor pressure of diethyl ether renders it an impractical candidate. The formation of dendritic lithium seemed to be sufficiently suppressed in these solvents even at high charge rates.[62] However, efforts to incorporate ether-based electrolytes in lithium cells were still troubled by the poor capacity retention,[68-70] and prolonged cycling

(>100 cycles) of the cells still produced dendrite deposition,[71] which terminated the cells by creating shorts,[72] despite the improved lithium morphology observed in the short term.

In addition to the problem with the lithium anode, a new factor contributing to the capacity fade surfaced as the oxidative decomposition of ether-based compounds on the cathode surface.[61,67,73] Electrochemical studies on these ether-based electrolytes placed the potential for the oxidative breakdown of the ether functionality at relatively low potentials. On a platinum surface, for example, THF was found to be oxidized at 4.0 V vs Li, while PC remained stable up to 5.0 V.[74] In an actual cell, ethers are more readily decomposed at even lower potentials, because of the highly catalytic surface of cathode materials.[76] With the application of more potent 4.0 V cathode materials ($Li_xMO_2$, M = Mn, Ni, or Co) in lithium or lithium ion cells, the possibility of using ether compounds as solvents or cosolvents diminished.[75,77] During the 1990s, various ethers were gradually phased out in most of the electrolyte systems under investigation. The failure of ether-based electrolytes served as a perfect example to illustrate that, in a battery, the electrolyte (solvents and salts) must cope with challenges from both the anode and the cathode. On the other hand, the advantage of organic esters, especially cyclic alkyl carbonates, was rediscovered because of their excellent stability against oxidation on cathode surfaces.[74,78,79]

### 2.1.3. Ethylene Carbonate (EC)

The interest in alkyl carbonates was renewed with the emergence of the lithium ion "shuttle" concept.[24-31] Gone with the lithium anode is the difficult issue of lithium morphology; subsequently, the higher anodic stability of PC made it once again a promising candidate. In the first generation of the commercial lithium ion cells, a PC-based electrolyte was used by Sony along with $Li_xCoO_2$ as the cathode and petroleum coke as the anode.[31] However, the real renaissance for using alkyl carbonates as lithium electrolyte solvents was not brought about by PC but, quite unexpectedly, by its high melting cousin EC.

Compared with PC, EC has comparable viscosity and slightly higher dielectric constant, which are favorable merits for a solvent candidate (Table 1). In fact, its dielectric constant is even higher than that of the the most common electrolyte solvent on the earth: water ($\epsilon \sim 79$).[3] However, because of its high melting point ($\sim 36$ °C), it was never favored as an ambient-temperature electrolyte solvent in the early days of lithium battery research: the liquid range of the electrolytes based on it would be too restricted. Its higher melting point than those of other members of the carbonate family (Table 1) is believed to arise from its high molecular symmetry, which renders it a better stabilized crystalline lattice.[80, 81]

EC was considered as an electrolyte cosolvent for the first time by Elliot in 1964, who noted that, due to the high dielectric constant and low viscosity of EC, the addition of it to electrolyte solutions would favor ion conductivity.[82] The findings did not attract particular attention from the battery community

until the early 1970s, when Scrosati and Pistoia exploited it to advantages for lithium battery electrolytes. They reported that, owing to the suppression of the melting point by the presence of the solute, a room-temperature melt would form, and extra suppression could be obtained when a small percentage (9%) of PC was added.[83] Further investigation found that electrolytes based on EC as compared with PC demonstrated improvements, not only in bulk ion conductivity but also in interfacial properties such as lower polarization on various cathode surfaces.[84] Following these reports, EC began to appear as an electrolyte cosolvent in a number of new electrolyte systems under investigation, many of which still contained ethers.[72,73,85−88] However, the first commercialized rechargeable lithium battery used an ether-free composition, an EC/PC mixture, as the electrolyte solvent.[89,90] Despite the melting-point suppression by the solute and other cosolvents, the higher liquidus temperatures of the electrolyte due to EC remained a factor limiting the low-temperature applications of the lithium cell.

The unique position of EC as a lithium battery electrolyte was established in 1990 when Dahn and co-workers reported the fundamental difference between EC and PC in their effects on the reversibility of lithium ion intercalation/deintercalation with graphitic anodes.[36] Despite the seemingly minute difference in molecular structure between the two, EC was found to form an effective protective film (SEI) on a graphitic anode that prevented any sustained electrolyte decomposition on the anode, while this protection could not be realized with PC and the graphene structure eventually disintegrated in a process termed "exfoliation" because of PC cointercalation. The reason for the effectiveness of the SEI has incited a lot of research interest in the past decade but remains an unsolved mystery, although it is generally believed that EC undergoes a reduction process on the carbonaceous anode via a similar path to that shown in Scheme 1. Because of the important role this SEI plays in lithium ion chemistry, the research efforts on this topic will be reviewed in a dedicated section (section 6).

### 2.1.4. Linear Carbonates

After Sony successfully marketed the first generation lithium ion cells, numerous competitors emerged and a pursuit for higher energy density started. With the energetic advantage of highly crystalline carbon (graphitic) over disordered carbon being recognized, EC became the core and indispensable component of the electrolyte formulation.

During the early 1990s, efforts were made to expand the limited liquid range of EC-based electrolytes by using different cosolvents, including PC,[91,92] THF and 2-Me-THF,[73,85−88] diethoxyethane (DEE),[93,94] and dimethoxyethane (DME).[45,95−97] None of these cosolvents performed satisfactorily though, because the presence of PC usually caused a large irreversible capacity in the initial cycle of the lithium ion cell,[36,91,92] while the ethers were found to be unstable against the oxidation catalyzed by the surface of the charged cathode.[93,94] Thus, it was generally realized that, for

a lithium ion cell that employs graphite as an anode and 4.0 V metal oxide (LiMO₂, M = Co, Ni) as a cathode, the electrolyte must have oxidative stability up to ~5 V vs Li.[95−97]
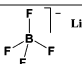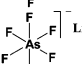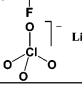
In 1994 a formulation that successfully met such a standard was first described in open literature by Tarascon and Guyomard, who used a linear carbonate, dimethyl carbonate (DMC), as a cosolvent with EC.[98,99] As it has been pointed out, linear carbonates differ from their cyclic cousins by their low boiling points, low viscosity, and low dielectric constant. They can form homogeneous mixtures with EC at any ratio, and the resultant mixed electrolytes benefit not only from the melting-temperature suppression of EC but also from the low viscosity (higher ion conductivity) of DMC. But what surprises researchers is the wide electrochemical stability window of this mixture electrolyte: it remains stable on a spinel cathode surface up to 5.0 V. Considering that these linear carbonates, in the absence of EC, are readily liable to oxidation on cathode surfaces at ~4.0 V vs Li,[76] the origin for the above improvement in the electrochemical window remains unclear, because the anodic stabilities of the ether-based electrolytes were hardly raised by their mixing with EC[93,94] or PC.[95,96] It seems that a synergistic effect is achieved when EC and DMC (or other linear carbonates) are mixed because the merits of each individual solvent are imparted on to the resultant mixture: high anodic stability of EC on cathode surfaces, high solvation power of EC toward lithium salts, and low viscosity of DMC to promote ion transport.

This new formulation of electrolytes based on a mixture of EC with a linear carbonate set the main theme for the state-of-the-art lithium ion electrolytes and was quickly adopted by the researchers and manufacturers.[97,100−103] Other linear carbonates were also explored, including DEC,[104−106] ethylmethyl carbonate (EMC),[107] and propylmethyl carbonate (PMC),[108,109] and no significant differences were found between them and DMC in terms of electrochemical characteristics. The direct impact of this electrolyte innovation is that the first generation carbonaceous anode petroleum coke was soon replaced by graphitic anode materials in essentially all of the lithium ion cells manufactured after 1993. At present, the electrolyte solvents used in the over one billion lithium ion cells manufactured each year are almost exclusively based on the mixture of EC with one or more of these linear carbonates, although each individual manufacture may have its own proprietary electrolyte formulation.

## 2.2. Lithium Salts

An ideal electrolyte solute for ambient rechargeable lithium batteries should meet the following minimal requirements: (1) It should be able to completely dissolve and dissociate in the nonaqueous media, and the solvated ions (especially lithium cation) should be able to move in the media with high mobility. (2) The anion should be stable against oxidative decomposition at the cathode. (3) The anion should be inert to electrolyte solvents. (4) Both the anion and the cation should remain inert toward the other cell components such as separator, electrode substrate,

**Table 3. Lithium Salts as Electrolyte Solutes**

| Salt | Structure | M. Wt | $T_m/$ °C | $T_{decomp.,}/$ °C in solution | Al-corrosion | $\sigma$ /mScm$^{-1}$ (1.0 M, 25 °C) in PC | in EC/DMC |
|------|-----------|-------|-----------|-------------------------------|--------------|-----------|-----------|
| LiBF$_4$ | (structure) | 93.9 | 293 (d) | > 100 | N | 3.4 [a] | 4.9 [c] |
| LiPF$_6$ | (structure) | 151.9 | 200 (d) | ~ 80 (EC/DMC) | N | 5.8 [a] | 10.7 [d] |
| LiAsF$_6$ | (structure) | 195.9 | 340 | > 100 | N | 5.7 [a] | 11.1 [e] |
| LiClO$_4$ | (structure) | 106.4 | 236 | >100 | N | 5.6 [a] | 8.4 [d] |
| Li Triflate | Li$^+$ CF$_3$SO$_3^-$ | 155.9 | >300 | >100 | Y | 1.7 [a] | |
| Li Imide | Li$^+$ [N(SO$_2$CF$_3$)$_2$]$^-$ | 286.9 | 234 [b] | >100 | Y | 5.1 [a] | 9.0 [e] |
| Li Beti | Li$^+$ [N(SO$_2$CF$_2$CF$_3$)$_2$]$^-$ | | | | N | | |

[a] Reference 111. [b] Reference 146. [c] Reference 114. [d] Reference 115. [e] Reference 116.

and cell packaging materials. (5) The anion should be nontoxic and remain stable against thermally induced reactions with electrolyte solvents and other cell components.

The available choice of lithium salts for electrolyte application is rather limited when compared to the wide spectrum of aprotic organic compounds that could make possible electrolyte solvents. This difference could be more clearly reflected in a comprehensive report summarizing nonaqueous electrolytes developed for rechargeable lithium cells, in which Dahn and co-workers described over 150 electrolyte solvent compositions that were formulated based on 27 basic solvents but only 5 lithium salts.[50b]

Because of the small ionic radius of lithium ion, most simple salts of lithium fail to meet the minimum solubility requirement in low dielectric media. Examples are halides, LiX (where X = Cl and F), or the oxides Li$_2$O. Although solubility in nonaqueous solvents would increase if the anion is replaced by a so-called "soft Lewis base" such as Br$^-$, I$^-$, S$^{2-}$, or carboxylates (R$-$CO$_2^-$), the improvement is usually realized at the expense of the anodic stability of the salt because these anions are readily oxidized on the charged surfaces of cathode materials at <4.0 V vs Li.

Most of the lithium salts that are qualified for the minimal solubility standard are based on complex anions that are composed of a simple anion core stabilized by a Lewis acid agent. For example, the anion of lithium hexafluorophosphate (LiPF$_6$) could be viewed as F$^-$ complexed by the Lewis acid PF$_5$. Such anions, also known as anions of superacids, have a structure in which the formal negative charge is well distributed by the strongly electron-withdrawing Lewis acid ligands, and the corresponding complex salts are usually lower melting and better soluble in low dielectric media than their parent salts.

The requirement for chemical inertness further excluded a family of lithium salts that have been widely used in primary lithium batteries: LiAlX$_4$ (X = halides).[110] Since the Lewis acidities of the AlX$_3$ are so strong, their complexation with the moderate bases such as Cl$^-$ does not fully neutralize their activity, and as a result, they would attack most of the nonaqueous solvents, especially ethers. The AlX$_4^-$ anions also cause severe corrosion to other cell components such as the separators, usually made of polypropylene, and the insulating sealant, as well as the metallic packaging materials. On the other hand, anions based on milder Lewis acids can remain stable with organic solvents under normal conditions (e.g., ambient temperature) and have been preferentially investigated by researchers. These salts include lithium perchlorate (LiClO$_4$) and various lithium borates, arsenates, phosphates, and antimonates, LiMX$_n$ (where M = B or As, P, and Sb and $n$ = 4 or 6, respectively). Table 3 lists some examples of these salts along with some basic physical properties,[50c] including ion conductivity data at room temperature in PC or EC/DMC (1:1), respectively.[50d,111−116] A brief summary of a few selected lithium salts of significance during the development of lithium cell electrolytes is given below.

### 2.2.1. Lithium Perchlorate (LiClO$_4$)

LiClO$_4$ has been a popular electrolyte solute owing to its satisfactory solubility and high conductivity (~9.0 mS cm$^{-1}$ in EC/DMC at 20 °C) as well as its high anodic stability (up to 5.1 V on a spinel cathode surface in EC/DMC).[99] Recent studies found that SEI films formed in LiClO$_4$ electrolytes, on both lithium and carbonaceous anode surfaces, are of lower impedance than those formed in LiPF$_6$ or lithium tetrafluoroborate (LiBF$_4$) electrolytes, because the HF is absent in the former.[104,117] It is believed that HF, generated as the hydrolysis product of LiPF$_6$ and LiBF$_4$ by trace moisture in the electrolyte solvents, reacts with either alkyl carbonate or Li$_2$CO$_3$ and forms the highly resistive LiF.[117,118] Compared with other lithium salts, LiClO$_4$ also has the merits of being relatively less hygroscopic and is stable to ambient moisture.

However, the high oxidation state of chlorine (VII) in perchlorate makes it a strong oxidant, which readily reacts with most organic species in violent ways under certain conditions such as high temper-

**Scheme 2. Reaction between LiAsF$_6$ and Ether Solvents**
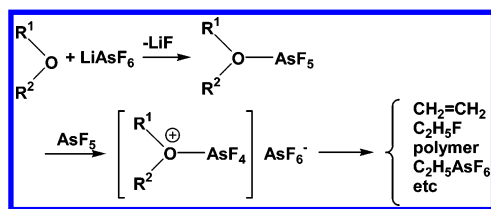


ature and high current charge.[58,119] Actually, back in the 1970s it had already been realized that LiClO$_4$ was impractical as an electrolyte solute for industry purposes;[119] nevertheless, it is still frequently used as a salt of convenience in various laboratory tests because it is easy to handle and economical.[43,79,91,94]

### 2.2.2. Lithium Hexafluoroarsenate (LiAsF$_6$)

While researchers focused on the morphology of lithium cycling in nonaqueous electrolytes during the late 1970s, it was found that the salt plays an important role beside the solvents, and in general, LiAsF$_6$ was a superior salt to LiClO$_4$ as an electrolyte solute for lithium batteries.[54] For a long period, the combination of LiAsF$_6$ with various ethers became the most popular system under investigation.[60,62,68,69,78] On average, lithium cycling efficiencies could reach >95% in these systems,[54,62,66] although long-term cycling in these electrolytes still promoted the growth of lithium dendrites.[71] Chemical deterioration was also detected, as indicated by the discoloration of the LiAsF$_6$/2-Me-THF solution with time, and a reaction between LiAsF$_6$ and the solvent was suspected.[65,68] A mechanism was proposed based on the Lewis acidity of As(V), which cleaves the ether linkage and produces a series of gaseous and polymeric products (see Scheme 2).[68]

The cathodic stability of the AsF$_6^-$ anion was studied on a glassy carbon surface, and a reduction process was found at ~1.15 V vs Li:[120]

$$AsF_6^- + 2e \rightleftharpoons AsF_3 + 3F^-$$
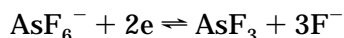
The above process was observed only in the initial cycles. Nevertheless, any electrochemical reduction of As(V) would raise concern about the safety of using LiAsF$_6$ in a commercial battery, because, while arsenate in its high oxidation state (V) is not particularly toxic, As(III) and As(0) species are.[68,120−122] From the electrochemical point of view, however, the above reduction could be a benefit, especially for lithium ion cells, since an SEI formed on an anode at >1.0 V vs lithium would be very stable during the operation of a lithium ion cell according to a semi-empirical rule,[106] which will be discussed in more detail in section 6.

Very similar to the case of LiClO$_4$, an SEI formed from LiAsF$_6$-based electrolytes, either on a lithium or carbonaceous anode, mainly consists of alkyl carbonates or Li$_2$CO$_3$ rather than LiF, as one would expect from the behavior of its close structural brothers LiPF$_6$ or LiBF$_4$.[104,117,118] This can be attributed to the much less labile As−F bond that is resistive to hydrolysis.[120]

The anodic stability of the AsF$_6^-$ anion proved to be high. In proper solvents, such as esters rather than ethers, the electrolyte based on this salt can remain stable up to 4.5 V on various cathode surfaces.[78,99] The combination of cathodic and anodic stability would have made LiAsF$_6$ a very promising candidate salt for both lithium and lithium ion batteries had the toxicity not been a source of concern. Instead, it was never used in any commercialized cells but is still frequently used in laboratory tests even today.[14−18,123−125]

### 2.2.3. Lithium Tetrafluoroborate (LiBF$_4$)

Like LiAsF$_6$, LiBF$_4$ is a salt based on an inorganic superacid anion and has moderate ion conductivity in nonaqueous solvents (Table 3). It was out of favor in the early days of lithium battery research because the ether-based electrolytes containing it were found to result in poor lithium cycling efficiencies, which decayed rapidly with cycle number.[60,126−128] The reactivity of LiBF$_4$ with lithium was suspected as discoloration occurred with time or heating.[128]

The researchers who initiated the study on LiBF$_4$ mentioned the multiple advantages of LiBF$_4$ as compared with other salts (e.g., less toxicity than LiAsF$_6$ and higher safety than LiClO$_4$),[128] but its moderate ion conductivity has been a major obstacle to its application. More recent studies on its ionics and limiting properties in various nonaqueous systems established that, among the most common anions encountered, BF$_4^-$ has the highest mobility, but its dissociation constant is significantly smaller than those of LiAsF$_6$ and LiPF$_6$.[111,129] The unfavorable balance of these two properties results in the moderate ion conductivity.

Electrochemically, the BF$_4^-$ anion was found to be stable against oxidation on a glassy carbon (GC) surface up to 3.6 V vs a standard calomel electrode (SCE), which translates into ~5.0 V vs lithium.[130,131] When a distinction is made, this stability limit is somehow lower than those of AsF$_6^-$ and PF$_6^-$ anions; however, caution must be exercised here, as these data were measured on GC with quaternary ammonium as supporting electrolyte, instead of on a surface of cathode materials. This could result in substantial difference.[76]

The use of LiBF$_4$ in lithium-based cells has been rare because of its inferior ion conductivity until recently, when the thermal instability of LiPF$_6$ and the moisture sensitivity became recognized. Attempts to replace LiPF$_6$ in lithium ion cells have been made, and the cells based on LiBF$_4$ electrolytes showed improved performance, not only at elevated temperatures up to 50 °C[132] but, surprisingly, also at low temperatures as well.[132−135] These observations could bring this salt back to research favor.

### 2.2.4. Lithium Trifluoromethanesulfonate (LiTf)

Another family of lithium salts is based on the conjugate bases of the organic superacids, where acid strength is increased because of the stabilization of anions by the strongly electron-withdrawing groups, usually perfluorinated alkyls. In these anions, the

delocalization of the formal negative charge is practically realized by a combination of the inductive effect of the electron-withdrawing groups and the conjugated structures:
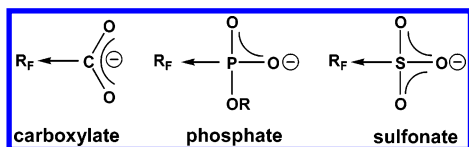


The attempt to use these salts originated from the hope that their dissociation constants would be high even in low dielectric media, and the organic nature of perfluorinated alkyls would always assist the solubility of the salts in nonaqueous solvents. Because of the requirement for electrochemical stability, lithium carboxylates ($R_F$–$CO_2Li$, where $R_F^-$ = perfluorinated alkyls) are excluded from consideration, because their oxidation still occurs at ~3.5 V vs lithium, which is similar to the cases of their nonfluorinated counterparts.[22] Obviously, the electron-withdrawing groups do not stabilize the carboxylate anions sufficiently to alter their oxidative stability.

On the other hand, sulfonate ($-SO_3Li$) became the anion of choice because it is highly resistant to oxidation, thermally stable, nontoxic, and insensitive to ambient moisture as compared with $LiPF_6$ or $LiBF_4$.[122] As the simplest member of this category ($R_F = CF_3$), lithium triflate (LiTf) received extensive research as a candidate for lithium/lithium ion cells. Other similar salts studied include perfluoroethyl sulfonate ($R_F = C_2F_5$), perfluorobutylsulfonate ($R_F = C_4F_9$),[129–131] and the oligomeric versions that are based on polyether linkages.[136,137]

One major drawback of these sulfonate salts is their poor ion conductivity in nonaqueous solvents as compared with other salts. In fact, among all the salts listed in Table 3, LiTf affords the lowest conducting solution. This is believed to be caused by the combination of its low dissociation constant in low dielectric media[122,138] and its moderate ion mobility[129] as compared with those of other salts. Serious ion pairing in LiTf-based electrolytes is expected, especially when solvents of low dielectric constant such as ethers are used.[111,122]

The stability of the Tf⁻ anion toward lithium has been studied by both electrochemical and spectroscopic means.[139] While the surface analysis using X-ray photoelectron spectra (XPS) found only a trace of LiF, in addition to $Li_2CO_3$, present on the lithium surface, indicating that this anion was not reactive with lithium, a poor lithium morphology was identified in LiTf-based electrolytes. Electrochemical quartz crystal microbalance (EQCM) detected a very rough surface of the cycled lithium, most likely related to the formation of dendritic lithium. A simultaneous impedance measurement confirmed the poor morphology with ever-increasing interfacial impedance due to the incessant reactions between the rough lithium surface and the electrolyte. This sustained reaction resulted in a thick and resistive SEI film that was not favorable to battery operation. However, in at least one case, LiTf was found to outperform the state-of-the-art solute $LiPF_6$, where an atypical

**Scheme 3. Resonance States of the Imide (Im) Anion**
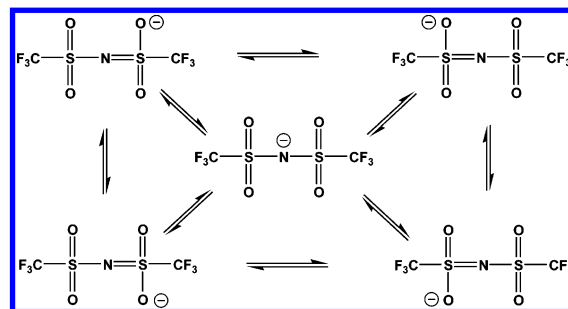


anode (carbon fiber) was used, and LiTf-based electrolytes in various solvent mixtures (EC/DMC, PC/DMC, or EC/DME) showed better Coulombic efficiency (~98%) and discharge capacity.[140]

The anodic stability of the Tf⁻ anion, as measured on a GC surface, was not found to be particularly high:[130] inferior to $BF_4^-$ and $PF_6^-$ but better than $ClO_4^-$. Ab initio calculations yielded similar conclusions,[131] and results measured on porous carbon electrodes were consistent with those measured on GC.[81]

The real obstacle that eventually eliminated LiTf as a candidate for lithium ion battery application is the serious aluminum corrosion that occurred in LiTf-based electrolytes. Used as the substrate material to carry cathode active material in the cell, Al is constantly subject to high potentials during cell operation and, thus, must maintain inertness against anodic dissolution. However, because of a special interaction between the Tf⁻ anion and Al, the latter dissolves anodically at ~2.7 V and starts to pit at ~3.0 V.[141] At 4.0 V vs lithium, the normal working potential of a charged cell, the anodic dissolution current is ~20 mA/cm² in PC. This high corrosion rate leaves LiTf virtually little possibility of being used as an electrolyte solute for any high voltage cells, either lithium or lithium ion.

### 2.2.5. Lithium Bis(trifluoromethanesulfonyl)imide (LiIm) and Its Derivatives

In 1984, Foropoulos and DesMarteau reported a new acid based on an imide anion stabilized by two trifluoromethanesulfonyl (triflic) groups.[142] Because of the strong electron-withdrawing nature of the triflic groups and the conjugation between them and the lone electron pair on the nitrogen, the formal negative charge in the anion is well delocalized, as shown by the resonance structures in Scheme 3.

As a result, the acid strength of the proton is approximately equivalent to that of sulfuric acid in nonaqueous media.[142] In view of the excellent miscibility of this anion with organic nonpolar materials, Armand et al. proposed using its lithium salt (later nicknamed "lithium imide", or LiIm) in solid polymer electrolytes, based mainly on oligomeric or macromolecular ethers.[143] In no time, researchers adopted its use in liquid electrolytes as well, and initial results with the carbonaceous anode materials seemed promising.[95] The commercialization of this new salt by 3M Corporation in the early 1990s sparked considerable hope that it might replace the poorly

conducting LiTf, the hazardous $LiClO_4$, the thermally unstable $LiBF_4$ and $LiPF_6$, and the toxic $LiAsF_6$ in lithium battery applications.[122] Extensive studies of this salt were carried out to determine its ionics in nonaqueous solutions[111,116,129,130,131,139] and its applications in lithium or lithium ion cells.[45,96,144,145]

LiIm proved to be safe, thermally stable, and highly conducting: it melts at 236 °C without decomposition (a rarity among lithium salts) and does not decompose until 360 °C.[146] Its ion conductivity in THF is an order of magnitude higher than that of LiTf, although lower than those of $LiAsF_6$ and $LiPF_6$,[111,116,122] and when no Al is used, a lithium ion cell based on a $LiNiO_2$ cathode and a petroleum coke anode can yield up to 1000 deep discharge cycles with LiIm in an EC/DMC solution.[45]

Ionics studies by Webber and Ue revealed that this salt dissociates very well even in low dielectric solvents, although its large anion size usually results in a higher solution viscosity than those of other salts in a given solvent system. Thus, its good ion conductivity should be the result of a compromise between a high degree of dissociation and low mobility.[122,129] In this sense, LiIm favors solvents with a low dielectric constant. Electrochemical stability tests were carried out on a GC electrode, and $Im^-$ was found to be stable against oxidation in EC/DMC up to 2.5 V vs a $Ag^+/Ag$ reference, which translates to ∼5.0 V vs Li, an oxidation limit lower than those for $LiBF_4$ and $LiPF_6$,[130,131] but still high enough to be practical. The morphology of cycling lithium in LiIm-based electrolytes is apparently superior to that in other salt-based electrolytes.[139]
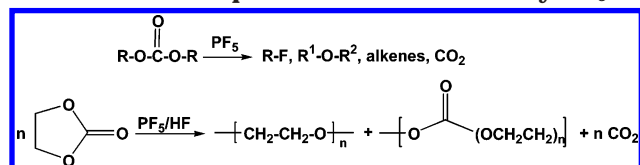
Despite all of these merits, the application of LiIm in lithium ion cells never materialized because it caused severe Al corrosion in electrolytes based on it.[141] In situ surface studies using EQCM established a reaction between the $Im^-$ anion and the Al substrate in which $Al(Im)_3$ is produced and adsorbed on the Al surface.[147] Undoubtedly, this corrosion of a key component of the cell by $Im^-$ greatly restricts the possible application of LiIm, because the role of Al as a cathode substrate in the lithium-based battery industry is hard to replace, due to its light weight, resistance to oxidation at high potential, excellent processability, and low cost.

Efforts were made to reduce the reactivity of $Im^-$ toward Al. Other salts that could passivate Al were used as additives with LiIm, and the results were encouraging.[147] Also, structural modification of the imide anion was made by extending the perfluorinated alkyl chain and was found to be effective, although at the price of lower ion conductivity.[141,148] Although LiIm has never been used in any commercial lithium ion devices, it remains an interesting salt to be investigated, especially for the polymer-based electrolytes.[47]
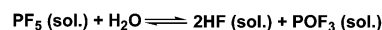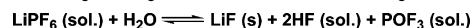
### 2.2.6. Lithium Hexafluorophosphate (LiPF₆)

Among the numerous salts vying for lithium/ lithium ion batteries, $LiPF_6$ was the obvious winner and was eventually commercialized. The success of $LiPF_6$ was not achieved by any single outstanding property but, rather, by the combination of a series

**Scheme 4. Decomposition of Carbonates by PF₅**



**Scheme 5. Hydrolysis of LiPF₆ Salts by Moisture**

$$LiPF_6 \text{ (sol.)} + H_2O \rightleftharpoons LiF \text{ (s)} + 2HF \text{ (sol.)} + POF_3 \text{ (sol.)}$$

$$PF_5 \text{ (sol.)} + H_2O \rightleftharpoons 2HF \text{ (sol.)} + POF_3 \text{ (sol.)}$$

of well-balanced properties with concomitant compromises and restrictions. For example, in the commonly used carbonate solvent mixtures it has a lower conductivity than $LiAsF_6$ (Table 3),[99,111,116] a lower dissociation constant than LiIm,[129] a lower ionic mobility than $LiBF_4$,[129] a lower thermal stability than most of the other salts,[149] a lower anodic stability than $LiAsF_6$ and $LiSbF_6$,[130,131] and a lower chemical stability toward ambient moisture than $LiClO_4$, LiIm, and LiTf. However, none of these other salts could meet all these multifaceted requirements simultaneously as well as $LiPF_6$ does.

$LiPF_6$ was proposed as an electrolyte solute for lithium-based batteries in the late 1960s,[149] and soon its chemical and thermal instabilities were known.[150] Even at room temperature, an equilibrium exists:

$$LiPF_6(s) \rightleftharpoons LiF(s) + PF_5(g)$$

The generation of the gaseous product, $PF_5$, drives the equilibrium to the right, and this process is favored by elevated temperatures. In the presence of nonaqueous solvents, the strong Lewis acid $PF_5$ tends to initiate a series of reactions, such as ring-opening polymerization or cleavage of ether linkages (Schemes 2 and 4).[68,151,152]

On the other hand, the P−F bond is rather labile toward hydrolysis by even trace amounts of moisture in nonaqueous solvents, producing a series of corrosive products (Scheme 5). Thermal gravimetric analysis (TGA) reveals that, in a dry state, $LiPF_6$ loses 50% of its weight at >200 °C[141] but that, in nonaqueous solutions, the deterioration occurs at substantially lower temperatures, for example, as low as 70 °C.

The sensitivity of $LiPF_6$ toward ambient moisture, solvents, and high temperature not only restricts its range of applications, especially in nonaqueous batteries, but also causes tremendous difficulty in its preparation and purification.[150] Before the 1990s, most of the commercially available $LiPF_6$ had high amounts of LiF and HF, and the purity issue became part of the reason the potential of $LiPF_6$ was not fully realized until recently. The manufacture of high-purity $LiPF_6$ (HF < 10 ppm) in industrial scale was achieved by Japanese companies in the late 1980s, finally leading to the commercialization of lithium ion technology and the ensuing extensive research.[86,120,122]

In nonaqueous solvents based on mixed alkyl carbonates, $LiPF_6$ remains one of the most conducting salts. For example, in EC/DMC (1:1) the conductivity is 10.7 mS cm$^{-1}$, only fractionally lower than that of

LiAsF$_6$. According to the ionics studies on the limiting properties in various solvents, this excellent conductivity results from the combination of its ionic mobility and dissociation constant, although in neither category does LiPF$_6$ stand at the most outstanding position:[111,129]

Average ion mobility: $\mathrm{LiBF_4 > LiClO_4 > }$
$$\mathbf{LiPF_6} > \mathrm{LiAsF_6 > LiTf > LiIm}$$

Dissociation constant: $\mathrm{LiTf < LiBF_4 < LiClO_4 < }$
$$\mathbf{LiPF_6} < \mathrm{LiAsF_6 < LiIm}$$

The reversed order in the above two properties clearly demonstrates the conflicting nature of the requirements and the advantage of the well-balanced properties of LiPF$_6$.

Electrochemical studies on a GC electrode and various metal oxide-based cathode surfaces confirm that the solution of LiPF$_6$ in mixed carbonates can effectively resist oxidation up to 5.1 V,[99,130] thus making it one of the few salts that can actually support the operation of 4.0 V cathode materials. LiPF$_6$ also effectively passivates an Al substrate at high potentials.[141,153,154] It is generally accepted that the anion participated in forming a protective film on Al, although there is no concensus as yet concerning the mechanism of the process.[141,153−156]

The above merits made LiPF$_6$ the salt of choice when lithium ion technology leaped from concept into product. In 1990, it was used by Sony in the first generation lithium ion cell,[157] and since then, its position in the lithium ion industry has remained unchallenged. Like EC as an indispensable solvent component, LiPF$_6$ has become the indispensable electrolyte solute for almost all lithium ion devices manufactured in the past decade.

## 2.3. Brief Summary

After more than a decade of exploration, the skeletal components of the electrolyte for the commercialized lithium ion devices have been identified. Within the various brands of lithium ion cells, the exact electrolyte composition differs from manufacturer to manufacturer, and the formulas remain proprietary information; however, the overwhelming majority of these are apparently based on two indispensable components: EC as the solvent and LiPF$_6$ as the solute. In most cases, one or more linear carbonates, selected from DMC, DEC, or EMC, are also used as cosolvents to increase the fluidity and reduce the melting point of the electrolyte, thus forming the popular composition consisting of LiPF$_6$/EC/linear carbonate(s).

However, certain restrictions on battery performance arise from these state-of-the-art electrolytes, for which these two indispensable components are mainly responsible: (1) a low-temperature limit (−20 °C) set by EC due to the high melting point and the high liquidus temperature it confers upon the solvent mixture, and (2) a high-temperature limit (50 °C) set by LiPF$_6$ due to its reactivity with solvents. As a result, the commercialized lithium ion batteries can only deliver their rated capacity and power in the temperature range −20 to 50 °C. Below temperatures from −20 to −30 °C, both the capacity utilized and the rate at which it is delivered (power) are decimated. This reduction in performance at low temperatures is usually temporary, and rated capacity can be recovered once the battery is brought back to >20 °C. However, at temperatures higher than 60 °C, the performance deterioration is permanent, because the reactions between the electrolyte solute and solvents are irreversible. Furthermore, the decomposition products of these irreversible processes, which are often gaseous, can lead to hazardous pressure build-up within the batteries.

## 3. Liquid Range of Electrolyte Solutions

The liquid range of a nonaqueous electrolyte system is defined at the upper limit by the temperature at which one of its components begins to vaporize (also called the bubble temperature, $\theta_b$) and at the lower limit by the temperature at which one of its components begins to crystallize (liquidus temperature, $\theta_l$).[158] Apparently, along with restrictions imposed by other factors, this range could serve as the main basis for estimating the operating limits of lithium-based devices that employ such an electrolyte system. Surprisingly, despite the significance of this issue to practical applications, there have been rather few studies dedicated to the thermophysical properties of the electrolytes, especially considering the large amount of effort spent on studying ion conduction and electrochemical properties.

Tarascon and Guyomard were perhaps the first researchers to try to delineate a temperature range for lithium ion electrolytes.[99] Following their seminal formulation of new electrolytes based on cyclic and linear carbonates, they measured boiling (bp) and melting points (mp) for LiPF$_6$/EC/DMC solutions as the function of EC/DMC compositions. They found that the bp of the electrolytes as a function of composition exhibits a monotonic decrease from that of EC (248 °C) to that of DMC (91 °C) with such a severe curvature that, for most of the compositions, it is dominated by the lower boiling component. The same trend was observed in a similar system (PC/DEC) by Ding recently,[158] who made the observation that enhancing the bp for a mixed solvent system by adding a higher boiling component would have little effect because of the previously mentioned dependence. In other words, the upper limit of the liquid range for a binary system is mainly determined by the bp of the lower boiling component. There is sufficient reason to believe that this rule would hold true for ternary or higher order systems.

It must be pointed out that, in the state-of-the-art electrolytes, the actual high-temperature limits for application in cells are usually not set by the upper boundary of the liquid range because other factors might push the limits far lower. For example, the upper boundary of the liquid range is ∼90 °C for DMC-, 110 °C for EMC-, and 120 °C for DEC-based electrolytes, all of which are far above the high-temperature limit set by the salt LiPF$_6$ (70 °C).[152]

Even if LiPF$_6$ is replaced by more thermally stable salts, the thermal stability of passivation films on both the anode and the cathode would still keep the high-temperature limits lower than 90 °C, as do the thermal stability of the separator (<90 °C for polypropylene), the chemical stability of the insulating coatings/sealants used in the cell packaging, and the polymeric binder agents used in both cathode and anode composites.

The lower boundary of the liquid range, on the other hand, does usually serve as the low-temperature limit for the electrolytes. The mp of LiPF$_6$/EC/DMC was determined as a function of solvent composition by Tarascon and Guyomard, who concluded that LiPF$_6$/EC/DMC could be used in the solvent compositions between 3:7 and 8:2 at temperatures down to −25 °C.[99] The mp-dependence on solvent composition that was reported in the work, however, does not seem to be rational, since it shows a long plateau at ∼ −10 °C in 30−90% DMC after an initial drop from 20 °C at 20% DMC,[99] whereas a typical simple eutectic feature would be expected instead. When a closer comparison is made between the results by Tarascon and Guyomard and the more recent studies by Ding et al.,[50e,159,160] it becomes obvious that in the former work no distinction was made between the liquidus and solidus temperatures; that is, the mp's at 20% and 90% DMC are liquidus temperatures, while the rest (the plateau section) seem to be solidus temperatures as measured by Ding et al. This confusion could have arisen from the fact that, for the intermediate compositions between 30% and 80% DMC, the liquidus transition usually appears as a broad peak of relatively negligible thermal effect that could evade notice, while the solidus transition usually appears as a sharp and conspicuous peak.

Systematic construction of carbonate mixture phase diagrams was performed by Ding et al.[50e,159,160] for a series of binary carbonate solvent systems that are frequently used as lithium ion electrolyte solvents. It was found that all of the binary combinations between EC, PC, DMC, EMC, and DEC yield the same basic feature of simple eutectic-type phase diagrams, characterized by the V-shaped liquidus lines intersecting at the eutectic composition with a horizontal solidus line, although the details of each individual diagram vary greatly depending on their mp and cyclicity. Figure 4 shows a collection of such phase diagrams mapped for some EC-based binary solvent systems.

In these phase diagrams, the liquidus line represents the temperature at which one of the components crystallizes, while, below the solidus line, the whole system solidifies. Between the solidus and liquidus lines are the regions where solid and liquid coexist. Since there is no solid phase above the liquidus lines and the liquid is thermodynamically stable, Ding et al. suggested that the liquidus temperatures should be adopted as the lower boundary of the liquid phase, instead of the solidus temperatures.[159,160] The patterns of these phase diagrams are typical of binary systems in which the two components are mutually soluble in their liquid states but
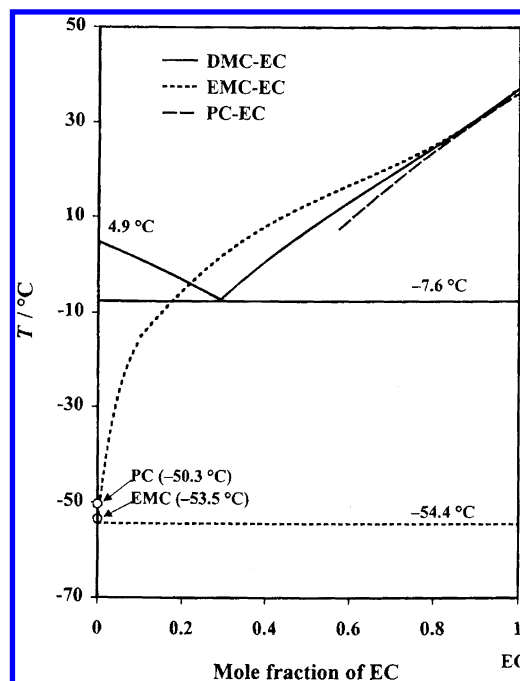


**Figure 4.** Liquid−solid phase diagrams of EC/DMC, EC/EMC, and PC/EC. (Reproduced with permission from ref 159 (Figure 9). Copyright 2000 The Electrochemical Society.)

insoluble in their solid states; therefore, solid solutions do not form below solidus temperatures, and the binary system exists in the form of a heterogeneous mixture of both solids.

Typically, the liquidus lines of a binary system curve down and intersect with the solidus line at the eutectic point, where a liquid coexists with the solid phases of both components. In this sense, the mixture of two solvents should have an expanded liquid range with a lower melting temperature than that of either solvent individually. As Figure 4 shows, the most popular solvent combination used for lithium ion technology, LiPF$_6$/EC/DMC, has liquidus lines below the mp of either EC or DMC, and the eutectic point lies at −7.6 °C with molar fractions of ∼0.30 EC and ∼0.70 DMC. This composition corresponds to volume fractions of 0.24 EC and 0.76 DMC or weight fractions of 0.28 EC and 0.71 DMC. Due to the high mp of both EC (36 °C) and DMC (4.6 °C), this low-temperature limit is rather high and needs improvement if applications in cold environments are to be considered.

A rather counterintuitive conclusion that can be extracted from these phase diagrams, however, is that simply introducing a low-melting component does not necessarily extend the liquid range, as evidenced by the replacement of DMC by the lower melting EMC (−53 °C) in an EC-based binary solvent system (Figure 4). The mismatch between the EC and EMC mp's creates a liquidus line that approaches the mp of EC for most of the compositions; therefore, the liquid range toward the low-temperature end actually shrinks as compared with that of the EC/DMC binary system. The replacement of DMC by another low-melting linear carbonate, DEC (−74 °C), produces a similar effect.[23d] It was proposed later that this poor compatibility between EC and linear carbonates

originates from the intrinsic differences found at the molecular level, that is, in the number of structural conformations that was allowed for by their freely rotatable single bonds.[158]

The comparison between the phase diagrams has led to the conclusion that the compatibility between different solvents is determined by two factors: (1) molecular structure similarity and (2) melting point proximity.[50e,158−160] Thus, from the viewpoint of phase diagram study alone, the effort to advance the liquid range toward lower temperature would be far more effective if cyclic−cyclic or linear−linear binary systems were formulated rather than the cyclic−linear combination that is currently used as the state-of-the-art lithium ion electrolytes. Unfortunately, most of the possible formulations under these categories would be vetoed by other considerations such as ion conductivity, electrochemical stability, and SEI formation on electrodes, and the cyclic−linear combination remains the formulation of choice. Viewed from another angle, the low-temperature limit on the device will remain a challenge as long as the high-melting EC remains an indispensable solvent component for the lithium ion electrolytes, because it will dominate the lower boundary of the liquid range no matter what linear cosolvents were used.

The phase diagrams shown in Figure 4 only describe the thermal properties of the binary *solvents*, while in practical applications the *salt solutions* of these solvent mixtures would be of greater interest. Ding et al. studied the effect of salt on the liquidus and solidus line locations at various concentrations up to 1.0 M and concluded that both lines would be depressed on temperature axes by a limited number of degrees.[159] At the salt concentrations investigated, it seems that the basic shape of the phase diagram remains unchanged, while the liquidus and solidus lines parallel those of the corresponding solvents. Thus, one can reliably estimate the phase transition temperatures of an electrolyte to be formed from a solvent with a known phase diagram.

In the actual application of the electrolytes at low temperatures, another thermal property that is closely related to the phase diagram and should not be ignored is the so-called "supercooling" behavior,[161−163] which occurs when the liquid circumvents crystallization at its mp or liquidus/solidus temperature, usually because the high viscosity of the solvent system at this temperature prevents the timely reorganization of molecules to ordered conformations. As a result, the solvent remains fluid at the temperatures below their thermodynamic freezing point, and this metastable liquid is called a "supercooled liquid". The supercooled state ends when the glass transition occurs at some lower temperature and turns the system into a disordered (noncrystalline) solid phase. Since supercooling actually delays or even eliminates crystallization of solvent components, the liquid range of the solvent system could be substantially extended from the liquidus down to the glass transition temperature ($T_g$). This extended range could potentially benefit the operation of the electrolyte at low temperatures, and there are numerous examples in which electrolytes were tested at temperatures far

below their liquidus temperatures without pronounced deterioration.[164,165]

However, an electrolyte is only kinetically stable below its liquidus line, and the presence of any nucleating agent could trigger the formation of a solid phase. In an electrochemical device, the rough surface of the electrode composite, the fibers of the separator, or the edges of current collectors and tabs can all act as such a nucleating agent; therefore, the extended liquid range of electrolytes by supercooling seems rather unreliable. Ding et al. studied the supercooling behavior of the EC/EMC system and the effect of various carbon particles on its diminution.[166] They found that, in this particular carbonate mixture, only the liquidus temperature could be successfully bypassed at a given cooling rate (10 °C/min), while, at the solidus temperature, binary crystallization occurs with negligible supercooling. Carbon particles effectively diminish the supercooling by providing nucleation seeds and effectively promoting the primary crystallization of EC at or near its liquidus temperature. The effectiveness of these carbon particles lies in the order

$$MCMB > activated\ carbon > carbon\ black$$

where MCMB stands for mesocarbon microbeads, a popular carbonaceous anode material used in the lithium ion batteries.

On the other hand, the presence of the salt, $LiPF_6$, assists the occurrence of supercooling by increasing the solution viscosity and by depressing the liquidus temperature. At practical concentrations of $LiPF_6$ (∼1.0 M), even the solidus temperature can be circumvented, since there is no crystallization process observed for $LiPF_6$/EC/EMC solution down to −120 °C, while the glass transition occurs at −103 °C. In such concentrated solutions, even the presence of MCMB cannot initiate crystallization, and the supercooling is completely suppressed at the cooling rate of 10 °C/min.

Thus, in actual applications, supercooling might well exist when electrolytes are used at low temperatures and result in an extended liquid range. However, it should be emphasized that such an extended range remains fragile, since the supercooling as a kinetically stable behavior is highly conditional and unpredictable during the operation of the device. The diminution or even elimination of supercooling is entirely possible if a slower cooling rate is employed or long-term storage at low temperature is exercised, but almost certainly, any prolonged operation of an electrolyte below the liquidus line would eventually encounter precipitation of solvent components and result in performance deterioration. Therefore, the reliable low-temperature limit should still be set by the liquidus lines as depicted in the phase diagram.

Following the seminal formulation of electrolytes based on carbonates by Tarascon and Guyomard,[98,99] a lot of effort had been made to modify those binary lithium ion electrolytes. Often, ternary, quaternary, and even higher order solvent systems were proposed, and the difficulty in constructing the phase diagrams for these systems increased dramatically
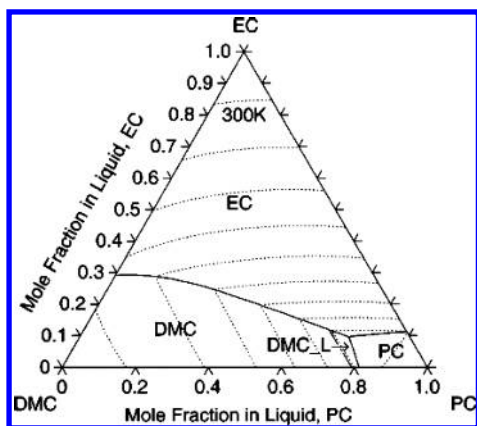
**Figure 5.** Calculated ternary phase diagram for EC/PC/DMC as expressed in the form of a composition triangle plane. The dotted lines represent the isotherms with 10 K intervals with 300 K marked. (Reproduced with permission from ref 167 (Figure 12). Copyright 2003 The Electrochemical Society.)

due to the amount of experimental work required. Consequently, the possibility of using computer modeling to circumvent the laborious experimental mapping was considered.[167] Because a phase diagram is merely a graphic representation of thermodynamics through minimizations in the free energy of the system under certain constraints, free-energy modeling of individual phases in a multicomponent system should represent the phase boundary through phase equilibrium calculations. Since the electrolyte systems are usually used at constant pressure conditions, the Gibbs free energy is the quantity minimized in calculating phase equilibria, and the computational approach commonly known as the CALPHAD method was used by Liu. The initial attempt seemed to be successful because phase diagrams of unary systems for neat DMC, EC, and PC, and of binary systems of EC/DMC, PC/DMC, and EC/PC were reproduced with satisfactory accuracy when compared with the work of Ding et al. Furthermore, by combining the three binary systems, a ternary phase diagram for EC/PC/DMC was predicted as shown in Figure 5. As one would expect, the eutectic composition was heavily PC-rich because PC was the lowest melting of the three components. Although the eutectic composition as predicted in the ternary phase diagram (0.10 EC/0.15 DMC/0.75 PC) was impractical for cell applications because of PC's destructive effect on most carbonaceous anodes, the effectiveness of PC, when used in smaller amounts (<30%), in improving low-temperature performance had been confirmed.[168] Undoubtedly, continued efforts to predict the thermal properties of ternary or higher order systems should be encouraged for prospective electrolytes, as they would provide useful knowledge for estimating their operating temperature range.

## 4. Ion Transport Properties

The ability to conduct ions is the basic function of electrolytes, which would determine how fast the energy stored in electrodes can be delivered. In liquid electrolytes, the transport of ions is realized via a two-step process: (1) the solvation and dissociation

of ionic compounds (usually crystalline salts) by polar solvent molecules and (2) the migration of these solvated ions through the solvent media.

During the solvation, the stability of the salt crystal lattice is energetically compensated by the coordination of solvent dipoles with the naked ions (especially cations); therefore, these ions should always migrate with a "solvation sheath" around them, which consists of a certain number of oriented solvent molecules. According to the results obtained from various modeling approaches including ab initio quantum mechanics, the small ionic radius of lithium usually allows no more than four solvent molecules in its solvation sheath.[129,169−171] Using a new mass spectrum (MS) technique, a more recent determination of the coordination number (CN) for lithium ions seems to support these computational results: among the various solvated lithium ion species, the peaks corresponding to $Li(solv)_{2\sim3}^+$ are the most abundant no matter whether the solvent is EC, PC, or $\gamma$-butyrolactone ($\gamma$BL).[172,173] This latter experimental observation also revealed the stability of the solvation sheath, which obviously remains intact even during the electrospraying under vacuum and the subsequent ionization process. Therefore, there should be sufficient confidence in the general belief that the composition of solvated lithium ion remains unchanged during its migration in an electrolyte solution.[1] Considering that both cation and anion could be coordinated by solvents, ion conduction actually consists of the oriented movement of ion/solvent complexes of both charges.

Ionic conductivity $\sigma$, which quantifies the ion conduction ability, reflects the influence of these two aspects, that is, solvation/dissociation and the subsequent migration, in terms of the free ion number $n_i$ and the ionic mobility $\mu_i$:

$$\sigma = \sum_i n_i \mu_i Z_i e \qquad (1)$$

where $Z_i$ is the valence order of ionic species $i$, and $e$ is the unit charge of electrons. For a single salt solution, the cations and anions are the only two charged species present.[174]

Ion conductivity has essentially become the quantity used as the field-trial standard for any prospective electrolytes, because it can be easily measured with simple instrumentation, and the results are highly accurate and reproducible. The methodology and the fundamental principles involved with the measurement have been summarized in a detailed review.[175] On the other hand, no reliable method has been available so far for the exact determination of ion mobility (or a related property, diffusivity $D_i$) and ionization degree, especially in electrolyte solutions in the concentration ranges of practical interest.[1]

The lack of ionic mobility data causes a serious inconvenience when the ion conduction ability of an electrolyte is evaluated, because the measured conductivity is the result of the overall migration of both anions and cations, while for lithium batteries only the portion of the current that was carried by the lithium cation matters. This portion of the current from lithium ion movement, which determines the

rate at which the battery operates, is quantified by the lithium ion transference number ($t_{Li}$):

$$t_{Li} = \frac{\mu_{Li}}{\sum_i \mu_i} \qquad (2)$$

There have been numerous efforts aimed at estimating the lithium ion transference numbers in nonaqueous solutions, and the data obtained via different approaches vary appreciably. Nevertheless, it is generally accepted that, in much diluted nonaqueous solutions, lithium ion transference numbers range from 0.20 to 0.40, depending on the properties of salts and solvents.[1,111,129,138,176−178] In other words, the anions are much more mobile than the lithium ions in nonaqueous electrolytes. The small cation current portion in nonaqueous electrolytes is believed to be caused by the high surface charge density on the cations (especially lithium ion) due to their small ionic radii, so they are much more favorably solvated and must move at slower speed with the solvation sheath, while high populations of anions could remain relatively "naked". Solvation enthalpy calculations for cations and anions support this argument:[169,176,178] in typical carbonate solvents, the former range between 20 and 50 kcal mol$^{-1}$ while the latter are below 10 kcal mol$^{-1}$.

A lithium ion transference number significantly less than 1 is certainly an undesired property, because the resultant overwhelming anion movement and enrichment near electrode surfaces would cause concentration polarization during battery operation, especially when the local viscosity is high (such as in polymer electrolytes), and extra impedance to the ion transport would occur as a consequence at the interfaces. Fortunately, in liquid electrolytes, this polarization factor is not seriously pronounced.

The unavailability of data on dissociation degree and mobility has thus made ion conductivity an alternative metric that has been universally adopted by the battery research and development community to evaluate the transport ability of electrolytes. However, it should always be remembered that such a metric of convenience is based on an unstated assumption; that is, the increase in the overall conductivity should originate, at least partially, from the improvement in the cation conductivity. Qualitatively, this assumption holds true, since a correlation does usually exist between ion conductivity and power performance in batteries, although quantitatively the distribution of this increase between anions and cations is unknown.

The efforts to improve ion conductivity have revolved around eq 1, that is, aiming at increasing either the salt dissociation degree ($n_i$) or the ionic mobility ($\mu_i$). Since these two factors are decided simultaneously by the physicochemical natures of the salt and solvents, different approaches involving either of these electrolyte components have been adopted.

For lithium electrolytes, the only variable in salt structure is the anion. In a given nonaqueous solvent system, the dissociation of a lithium salt would be facilitated if the anion is well stabilized by electron-withdrawing functionalities. Successful examples of such anions include $PF_6^-$ or $Im^-$, whose lithium salts dissociate readily as compared to those based on the parental anions (LiF and lithium alkylamide, respectively).

On the other hand, the mobility of an ion is known to vary inversely with its solvation radius $r_i$ according to the Stokes−Einstein relation:[1]

$$\mu_i = \frac{1}{6\pi\eta r_i} \qquad (3)$$

where $\eta$ is the viscosity of the media. With the cation species fixed, this approach seems to be of little use to increase cation mobility. However, a larger anion with lower anion mobility shows the application of this approach in another way, which results in a higher cation transference number, although the overall conductivity could decrease because of the reduction in the anion contribution. This effect was observed in imide and its derivatives.[138] The extremity of this approach was represented by the salts with oligomeric or polymeric anions, where $t_+$ approaches 1.0 but the overall ion conductivities suffer drastically.[136,137,179−182] Hence, the approach of using large anions to enhance $t_{Li}$ is not widely pursued in liquid electrolytes.

So far, very few attempts at improving ion conductivity have been realized via the salt approach, because the choice of anions suitable for lithium electrolyte solute is limited. Instead, solvent composition tailoring has been the main tool for manipulating electrolyte ion conductivity due to the availability of a vast number of candidate solvents. Considerable knowledge has been accumulated on the correlation between solvent properties and ion conductivity,[1] and the most important are the two bulk properties of the solvents, dielectric constant $\epsilon$ and viscosity $\eta$, which determine the charge carrier number ($n_i$) and ion mobility ($\mu_i$), respectively.

In order for a solvated ion to migrate under an electric field, it must be prevented from forming close ion pairs with its counterions by the solvating solvent. The effectiveness of the solvent molecule in shielding the interionic Coulombic attraction is closely related with its dielectric constant. The critical distance for the ion pair formation $q$ is given by eq 4 according to Bjerrum's treatment, with the hypothesis that ion-pair formation occurs if the interionic distance is smaller than $q$:[1,183]

$$q = \frac{|z_i z_j| e^2}{8\pi\epsilon_0\epsilon kT} \qquad (4)$$

where $z$, $\epsilon_0$, $k$, and $T$ are the valence orders of ions, the dielectric constant of vacuum, Boltzmann's constant, and temperature, respectively. Apparently, in a solvent with a higher dielectric constant, ions would have a higher probability of staying free at a given salt concentration and ion association would be less likely to occur. Most of these solvents are of high boiling temperature and high viscosity (Table 1).
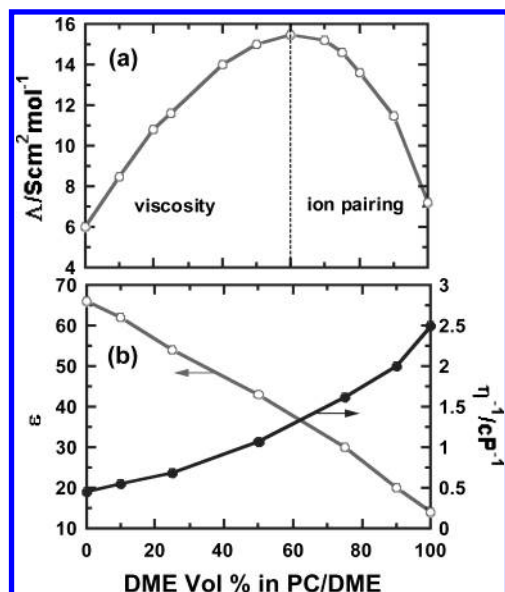
**Figure 6.** (a) Optimization of ion conductivity in mixed solvents: 1.0 M LiClO$_4$ in PC/DME. (b) Dependence of dielectric constant ($\epsilon$) and fluidity ($\eta^{-1}$) on solvent composition. These plots are reconstructed based on the data reported in refs 187 and 194, respectively.

When solvated ions migrate within the electrolyte, the drag force applied by the surrounding solvent molecules is measured by solvent viscosity $\eta$. Thus, in a solvent of lower viscosity, the solvated ions would move more easily in response to an applied electric field, as expressed by the Einstein–Stokes relation (eq 3). Solvents of low viscosity have always been considered the ideal candidates for electrolyte application; however, their actual use was restricted because most of these solvents have low dielectric constants (Tables 1 and 2) and cannot dissociate ions effectively enough to prevent ion pairing.

Since a high dielectric constant and low viscosity usually cannot be integrated into a single solvent,[184] a solvent mixture, usually binary with one of the components selected for $\epsilon$ and the other for $\eta$, was used to formulate electrolytes for lithium batteries with the hope that a balance between these two properties could be arrived at via such mixing.[185–187] The concept was rapidly accepted by researchers of the 1980s, usually using cyclic carbonates for their high $\epsilon$ and linear or cyclic ethers for their low $\eta$.[72,73,78,87,89,127,188–191] In almost all the cases, ion conductivity in mixed solvents is superior to that in single solvents, as Figure 6a shows for LiClO$_4$ in PC/DME, and a maximum in conductivity is usually realized in medium compositions.

A series of works by Matsuda et al. composed perhaps the first systematic study to explore the physical foundation for such a mixing effect.[127,187,193,194] Using PC/DME as a model system, they investigated the dependence of vapor pressure, dielectric constant, and viscosity on solvent composition, and they correlated these variations with ion conductions. It was found that the dielectric constant varied with solvent composition by following an almost linear relation, with slight positive deviations, while viscosity always showed a pronounced negative deviation from what a linear relation would predict (Figure 6b). For such binary solvent systems, approximate quantifications

of the solvent mixing effect on these two properties were given:[195,196]

$$\epsilon_s = (1 - x_2)\epsilon_1 + x_2\epsilon_2 \qquad (5)$$

$$\eta_s = \eta_1^{(1-x_2)}\eta_2^{x_2} \qquad (6)$$

where $\epsilon_s$, $\eta_s$, $\epsilon_i$, $\eta_i$, and $x_i$ are the dielectric constant and viscosity of the mixture or the pure solvent components and the volume fraction of the individual solvent component, respectively.

Either $\epsilon_s$ or $\eta_s$ varies with solvent composition in a monotonic way, and the additive effect of each term seems to be able to account for the manner in which ion conductivity varies with solvent composition. At low DME concentration in the PC/DME system, the mixture has a high dielectric constant, so that the salt dissociates more completely. However, in this region, the high viscosity, which impedes ionic movement, dominates the ion conduction (Figure 6a). With increasing DME content, the dielectric constant remains relatively high, but the system viscosity falls drastically and the solvated ions migrate with higher mobility. As a result, a net increase in ion conductivity is achieved. Further increases in DME content (or low PC content) result in a very low dielectric medium where the effect of ion pair formation outweighs that of low viscosity; thus, ion conductivity drops with the increase in DME content. Therefore, the maximum in ion conductivity versus solvent composition as shown in Figure 6a is actually the result of the compromise between the effects of the dielectric constant and viscosity. Such a compromise illustrates the superiority of mixed solvent versus single solvent electrolytes.

A simple mathematical treatment based on this model successfully reproduced the variation in ion conductivity with solvent composition as observed in experiments on numerous different systems. It also proposed that, in an ideal situation where no ion pair formation is present, the change in ion conductivity should follow a linear relation as predicted by the semiempirical Walden's law:[194]

$$\Lambda\eta_s = \text{constant} \qquad (7)$$

where $\Lambda$ is the ion conductivity as normalized against salt concentration (molar conductivity). The Walden product ($\Lambda\eta_s$) can be viewed as an ion conduction metric that is normalized against both the solvent viscosity and the salt concentration (i.e., the free ion number if no ion pairing occurs); therefore, its value serves to the first approximation as a quantification of ion dissociation degree in electrolytes with either a given solvent or a given salt.[111,122]

Although the above findings came from studies on mixtures of the cyclic carbonate PC with ethers, they remain qualitatively true for mixtures of cyclic and linear carbonates, that is, compositions of the state-of-the-art lithium electrolytes. Most likely, it was the work by Matsuda et al. that delineated the basic guidelines for electrolyte formulation, which eventually led to the formulations by Tarascon and Guyomard using cyclic (high $\epsilon$) and linear (low $\eta$) carbonate mixtures.[93,98,99]

Further analysis of related studies seems to argue that the success of the high-$\epsilon$/low-$\eta$ combination might not be due to the simple additive effect of these two properties but, rather, a synergistic action of these two variables through a mechanism that involves the solvent's preference for cations in its solvation sheath. During the dissolution process of a certain salt lattice in mixed solvents, the solvation of the ions by a solvent molecule of a higher dielectric constant would be energetically favored over that by a molecule of a lower dielectric constant. Consequently, it would be reasonable to expect that, after equilibrium is established in the solution, the ions would have solvation sheaths that are mainly composed of the high-$\epsilon$ solvents. Modeling results using molecular quantum mechanics support this hypothesis by showing that the less favored solvent molecules (low $\epsilon$) actually could be readily replaced by the favored ones.[197] Thus, in the EC/EMC system, the solvation shell should be predominantly composed of EC.[171] The most forceful evidence of this comes from the experimental observation, where a new MS technique employing low-energy ionization was applied to electrolytes based on a series of binary compositions, including EC/DEC, EC/DMC, PC/DEC, PC/DMC, $\gamma$BL/DEC, and $\gamma$BL/DMC. In each of these systems, the overwhelmingly abundant species detected were the solvation complexes of lithium with the cyclic solvents (EC, PC, or $\gamma$BL), with coordination numbers between 2 and 3.[173]

This selective solvation of lithium ions by high-$\epsilon$ solvent molecules would exclude the solvents of low-$\eta$ from the solvation sheath and leave the latter as free, noncoordinating solvent molecules. As a result, the media in which the solvated ions migrate are mainly composed of these free solvent molecules, which impart their low-$\eta$ to benefit the movement of the solvated ions. In this way, a synergistic participation from both high-$\epsilon$ and low-$\eta$ solvents contributes to the optimization of ion conduction.

The implication of such a picture of the solution structure on the microscopic level not only concerns ion transport but also further relates to the electrochemical stability of the electrolytes in lithium ion cells, because these solvent molecules in the solvation sheath, such as EC or PC, migrate with the ions to electrode surfaces and are probably more involved in the oxidative or reductive processes than the noncoordinating, low-$\eta$ solvent molecules, such as the linear carbonates. This could have a profound impact on the chemical nature of the electrolyte/electrode interfaces (section 6).

Knowing how ion conduction is determined by the interplay between the dielectric constant and viscosity, the dependence of ion conductivity on different variables that are of practical interest can be explained consistently. Extensive studies have been carried out on the effects of salt concentration, solvent composition, and temperature on ion conductivity in different electrolyte systems,[113,195,196,198,199] among which the most representative is the meticulous work by Ding et al. on a series of binary systems pertinent to the state-of-the-art lithium ion cells.[195,196] Figure 7 shows the LiPF$_6$/EC/DMC system as an example

of surface plots based on the close fit of experimental data to a fourth degree trivariant polynomial function:

$$\sigma = f(m, x, T) \qquad (8)$$

where $\sigma$, $m$, $x$, and $T$ are ion conductivity in mS cm$^{-1}$, salt concentration in mol kg$^{-1}$, the mole fraction of EC, and temperature in °C, respectively. Figure 7 summarizes the changes in ion conductivity with these variables and exhibits a general trend which has been observed repeatedly for various electrolyte systems. This trend allows the tailoring of salt concentration and solvent composition to maximize ion conductivity at a given temperature for practical interests:

**(1) Salt Concentration ($m$).** At low salt concentrations ($<1.0$ m), the number of free ions increases with salt concentration; consequently, ion conductivity also increases until it peaks at a higher concentration. After this conductivity maximum, any increase in salt concentration results in higher ion aggregation and higher viscosity of the solution, which reduces both the free-ion number and the ionic mobility simultaneously. The location of this maximum conductivity on the salt concentration axes ($m_{max}$) is decided by the dielectric constant of the solvents as well as temperature. Generally speaking, a higher dielectric constant would shift the occurrence of ion pairing to higher salt concentrations, while a higher temperature reduces the solution viscosity. The common result of both scenarios is the shift of $m_{max}$ to higher salt concentrations.

**(2) Solvent Composition ($x_{EC}$).** At a given temperature, the solvent composition determines the outcome of the interplay between dielectric constant and viscosity; hence, a similar relation between $\sigma$ and $x_{EC}$ as shown for the PC/DME system in Figure 6a should be expected, as is indeed the case. However, temperature and salt concentration have such a pronounced effect on this dependence of conductivity on solvent composition that sometimes this relation will appear as monotonic in the given range of solvent compositions.

For example, at a given salt concentration of 1.6 m, solvents with a higher $x_{EC}$ are favored at high temperatures ($>50$ °C) because the influence of viscosity is less pronounced and $\sigma$ increases monotonically with $x_{EC}$. At low temperatures ($<10$ °C), this relation is reversed because of the predominate role of viscosity. At intermediate temperatures between 20 and 40 °C, $\sigma$ peaks versus $x_{EC}$, indicating that at neither high nor low $x_{EC}$ is the compromise between $\epsilon$ and $\eta$ able to optimize ion conduction. Similarly, salt concentration also affects the dependence of conductivity on solvent composition and produces the various shapes in $\sigma - x_{EC}$ relations shown in Figure 7, including single maximum curves and monotonic increases or decreases at different salt concentrations and temperatures.

**(3) Temperature ($T$).** With other variables being the same, ion conductivity increases with temperature monotonically until at very high temperatures the dielectric constant outweighs the viscosity in affecting ion conduction. Such high temperatures,
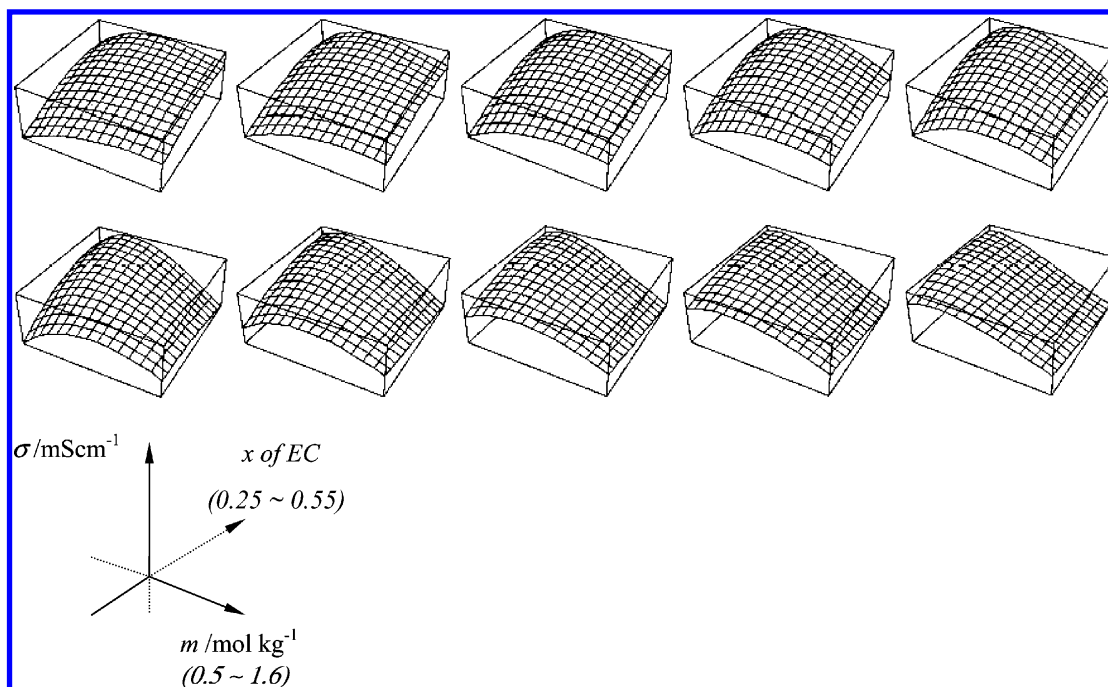
**Figure 7.** Detailed mapping of the dependence of ion conductivity on salt concentration ($m$), solvent composition ($x$), and temperature ($T$) in a commonly used binary solvent system EC/DMC by surface plots. The orientations, titles, and units of the axes used in the plots are shown in the bottom portion of the figure, and the temperatures for these plots are, in order of their appearance, from 60 to −30 °C in 10 °C increments. The $\sigma$ ranges for the surface plots are, in order of their appearance, (8.49, 16.7), (7.78, 14.6), (7.03, 12.6), (6.23, 10.6), (5.44, 8.7), (4.63, 7.00), (3.14, 5.47), (1.93, 4.14), (1.04, 3.00), and (0.46, 2.06) mS cm$^{-1}$. (Reproduced with permission from ref 195 (Figure 4). Copyright 2001 The Electrochemical Society.)

however, are usually beyond the range of practical interest.[195,200] Conversely, ion conductivity at sub-ambient temperatures is predominately determined by the increase in solution viscosity, although the dielectric constant becomes higher simultaneously.

A higher salt concentration accelerates the drop of ion conductivity with decreasing temperature, because it contributes to a higher viscosity. The combined effect of higher viscosity and low temperature is shown by the steeper $\sigma$−$T$ curves of higher $m$. Solvent composition, on the other hand, also has a definite though mild influence on the temperature-dependence of ion conductivity. The surface plots in Figure 7 reveal that the change of conductivity with temperature speeds up as the solvent becomes EC-richer,[195] though different mechanisms involving either predominant $\epsilon$ or $\eta$ at low or high salt concentrations, respectively, are believed to be at work.

To see more clearly the temperature effect on ion conduction, the logarithmic molal conductivity was plotted against the inverse of temperature, and the resultant plots showed apparent non-Arrhenius behavior, which can be nicely fitted to the Vogel−Tamman−Fulcher (VTF) equation:

$$\sigma = AT^{-1/2}e^{-B/R(T-T_0)} \tag{9}$$

where $A$ and $B$ are constants characteristic of the conduction process and $T_0$ is the vanishing conductivity temperature, which can be determined through fitting. The $T_0$ values obtained were found to be closely related to the glass transition temperatures of the solution systems, which agreed with the

general knowledge that ion transport in liquids or any noncrystalline polymer media is coupled with solvent media.[162,163,200]

In summary, these trends in the change of conductivity with $m$, $x_{EC}$, and $T$ can be consistently interpreted in terms of the change of $\epsilon$ and $\eta$ with these same variables. Since these factors and their effect on ion conductivity are not unique to the system illustrated, LiPF$_6$/EC/DMC, these trends should provide general guidance as to how ion conductivities of other electrolyte systems with similar compositions would change with these same variables, and they should constitute a useful database for the understanding of more complex systems, such as ternary or quaternary mixtures.

## 5. Electrochemical Stability: on Inert Electrodes

The cycle life of a rechargeable battery depends on the long-term reversibility of cell chemistries, and the electrochemical stability of the electrolyte plays a crucial role in maintaining this reversibility. In electrochemistry, there have been numerous techniques developed to measure and quantify the electrochemical stability of electrolyte components, and the most frequently used technique is cyclic voltammetry (CV) in its many variations.[201,202]

In voltammetric experiments, the oxidative or reductive decompositions of the investigated electrolyte components (solvents or salts) are made to occur on an electrode whose potential is controlled, and the corresponding decomposition current recorded as the function of the potential is used as the criterion for

the stability limits. However, in contrast to the simpler task of measuring ion conduction or determining phase boundaries, the electrochemical decomposition is often a very complicated process, determined not only by thermodynamic factors but, more importantly, also by kinetic factors such as the electrode surface, scan rate, and concentration of the species under study. Therefore, electrochemical stability data for a given substance depend heavily on the conditions under which they are measured and defined, and the electrochemical stability limits as reported in the literature are not always consistent with each other. Depending on the concentration of the target component in the solution under study and the working electrode used, the voltammetry techniques favored by the researchers of the battery community fall into three major categories.

The first approach is the standard voltammetry technique used in conventional analytical electrochemistry.[202] Normally the target components are dissolved at much diluted concentrations in a supporting electrolyte, and the electrodes used are made of inert materials such as glassy carbon (GC), nickel (Ni), and noble metals such as gold (Au), silver (Ag), and platinum (Pt). The advantages of this approach include the following: (1) the diffusion pattern of the investigated species is well-defined in the diluted solution so that the redox properties thus determined can be more reliably linked to the thermodynamic properties;[201] (2) it is possible to study the decomposition behavior of solvents and salts separately so that their contributions to the overall stability of the electrolyte can be distinguished. However, the wide application of this approach is restricted by the availability of supporting electrolytes, which are supposed to be stable in the potential ranges where the target components decompose. In the case of lithium-based electrolytes, the wide electrochemical stability window of the electrolyte solvents and salts makes it hardly possible to find a supporting medium that is more resistant against decomposition. An additional disadvantage of this approach also includes the fact that the surface of the inert electrode, usually nonporous, is very different in catalytic activity from the porous surfaces of the composite electrode materials used in real electrochemical devices. As a consequence, this approach could overestimate the electrochemical stability of the components.[76]

The second approach is an adaptation of the voltammetry technique to the working environment of electrolytes in an operational electrochemical device. Therefore, neat electrolyte solutions are used and the working electrodes are made of active electrode materials that would be used in an actual electrochemical device. The stability limits thus determined should more reliably describe the actual electrochemical behavior of the investigated electrolytes in real life operations, because the possible extension or contraction of the stability window, due to either various passivation processes of the electrode surface by electrolyte components or electrochemical decomposition of these components catalyzed by the electrode surfaces, would have been reflected.[75,76,93,94,98,99] However, since neat electrolyte solutions are used as both the targets of study and the supporting electrolyte, the observed stability is the result of the possible contributions from all components, and it is often difficult to distinguish whether the stability limits are set by the solvent or the salt decompositions, especially in the case of anodic (oxidation) limits. Because of the high concentration of electrolytes used, it is also difficult to apply a thermodynamic interpretation to the stability data obtained in this way. Furthermore, the coexistence of the reversible redox processes that may occur simultaneously on these active electrode materials can make the determination of electrochemical stability limits difficult, and frequently even the definition of electrochemical stability becomes ambiguous because of the passivation on active electrodes. The stability data for various lithium ion cell electrolytes determined in this way are therefore still scarce despite their importance.

As a compromise between the above two approaches, the third approach adopts nonactive (inert) materials as working electrodes with neat electrolyte solutions and is the most widely used voltammetry technique for the characterization of electrolytes for batteries, capacitors, and fuel cells. Its advantage is the absence of the reversible redox processes and passivations that occur with active electrode materials, and therefore, a well-defined onset or threshold current can usually be determined. However, there is still a certain arbitrariness involved in this approach in the definition of onset of decomposition, and disparities often occur for a given electrolyte system when reported by different authors[50d,75,76,130,131,203] Therefore, caution should be taken when electrochemical stability data from different sources are compared.

This section will discuss the electrochemical stabilities of different solvents and salts used in state-of-the-art electrolytes that were determined with nonactive electrodes (i.e., in the first and the third approaches). When active rather than inert electrodes are used as working surfaces, many complicated processes, including the reversible electrochemical redox chemistries as well as surface passivation, occur simultaneously. These related materials will be dealt with in a dedicated section (section 6).

## 5.1. Anion of Lithium Salts

Table 4 lists selected electrochemical stability data for various lithium salt anions that are commonly used in lithium-based electrolytes, with the measurement approaches indicated. Although it has been known that the reduction of anions does occur, sometimes at high potentials, the corresponding processes are usually sluggish and a definite potential for such reductions is often hard to determine. The reduction of solvents, occurring simultaneously with that of anions on the electrode, further complicates the interpretation efforts. For this reason, only the anodic stability of salt anions is of interest, while the cathodic limit of the salt in most cases is set by the reduction of its cation (i.e., lithium deposition potential).

**Table 4. Anodic Stability of Electrolyte Solutes:  Nonactive Electrodes**

| salt | solvent | conc/M | working electrode | $E_a{}^a$ ($i$/(mA cm$^{-2}$)) | approach | ref |
|------|---------|--------|-------------------|--------------------------------|----------|-----|
| $ClO_4^-$ | PC | 0.65 | GC | 6.1 (1.0) | 3 | 130, 131[b] |
| | PC | | Pt | 4.6 | 3 | 204 |
| $BF_4^-$ | PC | 0.65 | GC | 6.6 (1.0) | 3 | 130, 131, 81[c] |
| | EC/DMC | 1.0 | AC | 4.78 | 2 | |
| $PF_6^-$ | THF | 0.001 | GC | 4.4 (0.1) | 1 | 120[d] |
| | SL | 0.001 | GC | 4.8 (0.1) | 1 | 120 |
| | PC | 0.65 | GC | 6.8 (1.0) | 3 | 130, 131 |
| | none[e] | none | GC | 4.94 (1.0) | 3 | 206 |
| | none | none | Pt | 5.00 (1.0) | 3 | 206 |
| | EC/DMC | 1.0 | AC | 4.55 | 2 | 81 |
| $AsF_6^-$ | PC | 0.65 | GC | 6.8 (1.0) | 3 | 130, 131 |
| | none | none | GC | 5.05 (1.0) | 3 | 206 |
| | none | none | Pt | 5.10 (1.0) | 2 | 206 |
| | EC/DMC | 1.0 | AC | 4.96 | 3 | 81 |
| | THF | 1.0 | GC | 4.25 (0.1) | 1 | 120 |
| | THF | 0.009 | GC | | 1 | 120 |
| | SL | 0.8 | GC | 4.69 (0.1) | 1 | 120 |
| $SbF_6^-$ | THF | 1.0 | GC | 4.10 (0.1) | 1 | 120 |
| | PC | 0.65 | GC | 7.1 (1.0) | 3 | 130, 131 |
| $Tf^-$ | PC | 0.65 | GC | 6.0 (1.0) | 3 | 130, 131 |
| | PC | 0.10 | Pt | 5.0 (0.5) | 3 | 207 |
| | EC/DMC | 1.0 | AC | 4.29 | 2 | 81 |
| $Beti^-$ | PC | 0.65 | GC | 6.3 (1.0) | 3 | 130, 131 |
| | PC | 0.1 | GC | 6.2 (0.5) | 3 | 207 |
| $Im^-$ | PC | 0.65 | GC | 6.3 (1.0) | 3 | 130, 131 |
| | PC | 0.1 | Pt | 5.3 (0.5) | 3 | 130, 131 |
| | none | none | GC | 5.06 (1.0) | 3 | 206 |
| | none | none | Pt | 5.13 (1.0) | 3 | 206 |
| | EC/DMC | 1.0 | AC | 4.33 | 2 | 81 |

[a] Anodic limit, potential referred to Li$^+$/Li, cutoff current density in parentheses. [b] Scan rate:  5 mV s$^{-1}$. [c] Activated carbon as working surface. Scan rate:  10 mV s$^{-1}$. [d] Supporting electrolyte 0.1 M Bu$_4$NBF$_4$. Scan rate:  100 mV s$^{-1}$. [e] The solvent-free condition was realized by using an ionic liquid based on imidazolium cation, at 80 °C. Scan rate:  20 mV s$^{-1}$.

The most noteworthy observation among the entries of Table 4 is that these anodic stability data are widely diversified depending on the conditions under which they were obtained. For example, the anodic stability limits of $PF_6^-$, $AsF_6^-$, and $SbF_6^-$ determined in THF solutions are obviously lower than those determined in carbonate solutions, and a possible explanation lies in the fact that THF itself is not an oxidation-resistant solvent; therefore, its own decomposition is most likely responsible for these limits.[120]

The rather systematic work was performed by Ue et al., who used tetraalkylammonium salts as supporting electrolytes and measured the oxidation potential of a number of anions, most of which were considered promising candidates for lithium-based batteries.[50d,130,131] Figure 8 shows the linear sweep voltammograms obtained from these solutions with a GC electrode.[50d] The reduction limits seem to be caused by the decomposition of the ammonium cations, as evidenced by the similar cathodic current response for all of these solutions in Figure 8 and further confirmed by the analysis conducted on the decomposition products.[204] On the other hand, the oxidation limits were determined simultaneously by both salt and solvent. For example, the anodic limits were set by the unstable anions (Tf$^-$ and $ClO_4^-$), whereas solvent PC would be oxidized first if stable anions such as $BF_4^-$ and $PF_6^-$ are present. By using a more oxidation-resistant solvent, glutaronitrile

(GLN), the stability order of these anionic species was determined as[130]

$$SbF_6^- > AsF_6^- \geq PF_6^- > BF_4^- > Im^- > Tf > ClO_4^-$$
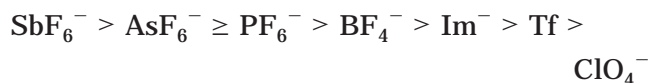
It should be pointed out that the above anodic stability order is highly conditional, since the order had been determined by approach 2 above, where the stability limits are defined as the potential at which the decomposition current density reaches an arbitrary value (1.0 mA cm$^{-2}$ in this case). Any change in this criterion could result in a reversal of the order.

The coupling effects of solvent/salt on electrolyte stability can also be observed when mixture solvents are used, and the stability of the electrolyte can be much improved when a stable solvent/salt is selected. For example, the room-temperature breakdown voltage of electrolytes LiX/EC/DEE lies in the order[205]

$$ClO_4^- > Im^- > Tf^- > AsF_6^- > PF_6^- > BF_4^-$$
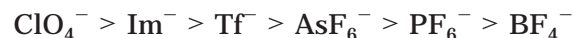
However, when a linear carbonate replaces the unstable ether DEE, the order changes into

$$ClO_4^- \sim PF_6^- \sim BF_4^- > AsF_6^- > Im^- > Tf^-$$
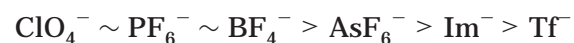
It is believed that the reactivity of DEE toward Lewis acids, $PF_6^-$ and $BF_4^-$, contributes to the early decomposition of the electrolytes.

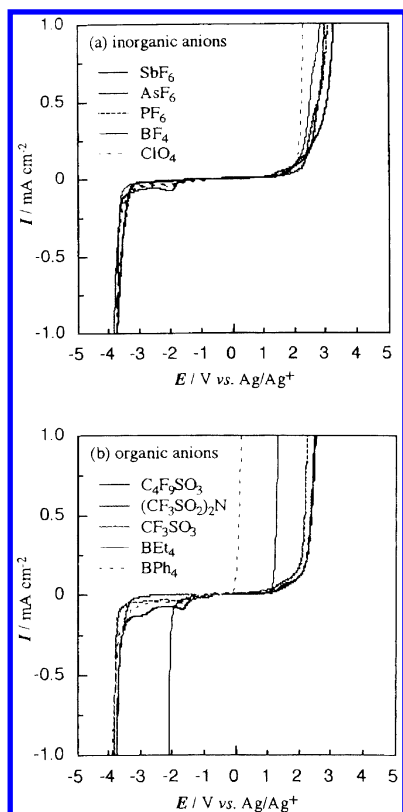To exclude the solvent's effect on the anodic stability of salt anions, Koch et al. made a series of salts

**Figure 8.** Determination of anodic stability for various anions in PC solution on GC. (Reproduced with permission from ref 130 (Figure 1a and b). Copyright 1997 The Electrochemical Society.)

**Scheme 6. Electrochemical Oxidation of the $PF_6^-$ Anion: the Solvents or the Trace Moisture in the Electrolyte Serves as the Proton Source of H-Abstraction**

$$PF_6^- \xrightarrow{-e} PF_6^\bullet \longrightarrow PF_5 + F^\bullet \xrightarrow{\text{H-abst.}} HF$$

based on a low-melting organic cation and measured the oxidation limits of these solvent-free molten salts on the surfaces of GC, tungsten, and Pt, respectively.[206] The "intrinsic anodic stability" measured by them follows an order completely different from the one determined in solvents:

$$Im^- \sim AsF_6^- > PF_6^-$$

A mechanism was also proposed for the instability of the $PF_6^-$ anion (see Scheme 6).

The above stability order is supported by the results of ab initio calculations, where a correlation has been established between the oxidation limits of these anions and the energy level of their highest occupied molecular orbital (HOMO). However, the gapping discrepancies that exist between "intrinsic" and solution stability limits remain to be explained.

## 5.2. Solvents

A solvent with an ideal electrochemical stability for a high-energy-density battery purpose should possess high oxidation and low reduction potentials at the same time. Table 5 lists selected electrochemical

**Scheme 7. Proposed Single-Electron Mechanism for the Reduction of EC and DEC**
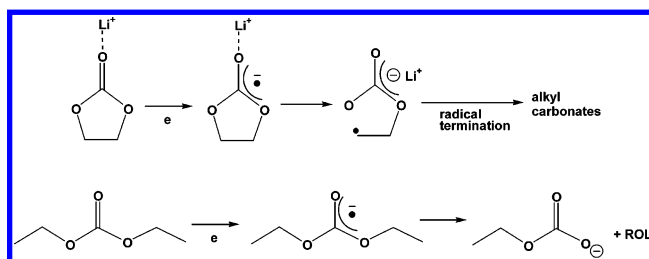


stability limits for some nonaqueous solvents commonly used in lithium-based battery research. Despite the inconsistency created by the varying measurement conditions, these data express a general trend that we have discussed in section 2; that is, carbonates and esters are more anodically stable, while ethers are more resistant to cathodic decompositions.

Among cyclic carbonates and esters, EC seems to be more liable toward reduction on nonactive electrodes,[210–214] which agrees with molecular orbital ab initio calculations of the corresponding radical anions. The difference between EC and PC in reductive reactivity is attributed to the steric effect introduced by the methyl on PC rather than the electronic effect, as supported by the molecular orbital ab initio calculations for the corresponding radical anions.[212] On the other hand, the reduction of PC seems to be a rather sluggish process, as evidenced by the high background current level distributed in a broad potential range during voltammetric scans. The slow kinetics of PC toward cathodic reduction is correlated with its readiness to cointercalate into a graphene structure of carbonaceous anodes and then decompose, causing exfoliation of the latter.[214]

Aurbach and co-workers performed a series of ex situ as well as in situ spectroscopic analyses on the surface of the working electrode upon which the cyclic voltammetry of electrolytes was carried out.[210–213] On the basis of the functionalities detected in FT-IR, X-ray microanalysis, and nuclear magnetic resonance (NMR) studies, they were able to investigate the mechanisms involved in the reduction process of carbonate solvents and proposed that, upon reduction, these solvents mainly form lithium alkyl carbonates ($RCO_3Li$), which are sensitive to various contaminants in the electrolyte system. For example, the presence of $CO_2$ or trace moisture would cause the formation of $Li_2CO_3$. This peculiar reduction product has been observed on all occasions when cyclic carbonates are present, and it seems to be independent of the nature of the working electrodes. A single electron mechanism has been shown for PC reduction in Scheme 1, while those of EC and linear carbonates are shown in Scheme 7.[214]

The radical anion is considered to be the common intermediate formed for these carbonate molecules, and its existence in the electrochemical reductions has been confirmed experimentally.[178] As will be revealed later, this mechanism seems to be universal for carbonates, whether on inert or active electrodes, and alkyl carbonates have been widely believed to be a key component in forming a protective interface

**Table 5. Electrochemical Stability of Electrolyte Solvents:  Nonactive Electrodes**

| solvent | salt/conc (M) | working electrode | $E_a{}^a$ | $E_c{}^b$ | ref |
|---------|---------------|-------------------|-----------|-----------|-----|
| PC | Et$_4$NBF$_4$/0.65 | GC | 6.6 | | 130, 131 |
| | none$^c$ | Pt | 5.0 | ~1.0 | 74 |
| | Bu$_4$NPF$_6$ | Ni | | 0.5 | 212 |
| | LiClO$_4$/0.1 | Au, Pt | | 1.0−1.2 | 214 |
| | LiClO$_4$/0.5 | porous Pt | 4.0 | | 305 |
| | LiClO$_4$ | Pt | 4.7 | | 177 |
| | LiClO$_4$ | Au | 5.5 | | 306 |
| | LiAsF$_6$ | Pt | 4.8 | | 177 |
| EC | Et$_4$NBF$_4$/0.65 | GC | 6.2 | | 130, 131 |
| | Bu$_4$NPF$_6$ | Ni | | 0.9 | 212 |
| | LiClO$_4$/0.1 | Au, Pt | | 1.36 | 214 |
| DMC | Et$_4$NBF$_4$/0.65 | GC | 6.7 | | 130, 131 |
| | LiClO$_4$/0.1 | Au, Pt | | 1.32 | 214 |
| | LiPF$_6$/1.0 | GC | 6.3 | | 76 |
| | LiF | GC | 5.0 | | 312 |
| DEC | Et$_4$NBF$_4$/0.65 | GC | 6.7 | | 130, 131 |
| | LiClO$_4$/0.1 | Au, Pt | | 1.32 | 214 |
| EMC | Et$_4$NBF$_4$/0.65 | GC | 6.7 | | 130, 131 |
| | LiPF$_6$/1.0 | GC | 6.7 | | 76 |
| $\gamma$BL | LiAsF$_6$/0.5 | Au, Ag | | 1.25 | 208 |
| THF | Et$_4$NBF$_4$/0.65 | GC | 5.2 | | 130, 131 |
| | LiClO$_4$ | Pt | 4.2 | | 177 |
| | LiAsF$_6$/1.0 | GC | 4.25 (0.1) | | 214 |
| | none$^c$ | Pt | 4.0 | < −2.0 | 74 |
| | LiAsF$_6$/1.0 | GC | 4.2 | | 64 |
| | LiAsF$_6$ | Pt | 4.2 | | 177 |
| 2-Me-THF | LiClO$_4$ | Pt | 4.1 | | 177 |
| | LiAsF$_6$/1.0 | GC | 4.15 (0.1) | | 214 |
| | LiAsF$_6$/1.0 | GC | 4.2 | | 64 |
| | LiAsF$_6$ | Pt | 4.1 | | 177 |
| DME | Et$_4$NBF$_4$/0.65 | GC | 5.1 | | 130, 131 |
| | LiClO$_4$ | Pt | 4.5 | | 177 |
| | LiAsF$_6$ | Pt | 4.5 | | 177 |

$^{a,b}$ Anodic and cathodic limits, potential referred to Li$^+$/Li. $^c$ The salt-free condition was realized via an ultramicroelectrode technique.

between active electrodes and electrolytes. In a more general context, since the surface chemistries on both inert and active electrodes have been found to be very similar in most of the nonaqueous electrolytes when these electrodes are polarized to low potentials, the early analytical work, mainly performed by Aurbach and co-workers, should be recognized as the foundation for the later understandings of the SEI on carbonaceous anodes.

## 6. Electrochemical Stability: on Active Electrodes

The requirement that electrolytes be inert toward both anode and cathode materials is usually realized by the kinetic rather than thermodynamic stability of the former against reductions and oxidations. Given the strong reducing and oxidizing potency of the electrode materials employed in the high-energy-density battery chemistries, the possibility of a thermodynamically stable electrolyte is usually non-existent, and it is the chemical passivation of these reducing or oxidizing surfaces that ensures the inertness of the bulk electrolytes during cell chemistry.

Passivation is a process where the products from the initial decomposition of electrolyte form a dense, protective film that covers up the pristine surface of the electrode and prevents any sustained decomposition. The electrolyte components that are sacrificed to form such a protective film would have a deter-

mining influence on the physicochemical nature of the new electrode surface, such as thermal and chemical stability, as well as its impedance to ionic conduction. The occurrence of passivation constitutes the foundation upon which many high-energy-density battery chemistries are built, including lithium-based chemistry. For this reason, the electrolyte/electrode interface has been the focus of research interest for both lithium and lithium ion chemistries.

On the other hand, it should be pointed out that, in addition to the protective effect of passivation, the passivated interface also acts as a barrier to the facile ion transport that occurs between the electrode and electrolyte. More often than not, the bottleneck for the overall battery chemistry is constituted by passivation. Excessive passivation is especially undesired because it reduces the power performance of the cell. For lithium ion cells, this power reduction usually happens on the cathode surface.

### 6.1. Passivation on Lithium Anode

Almost immediately after lithium metal was found to be stable in nonaqueous electrolytes, researchers suggested that the passivation of the lithium surface by electrolytes is the origin of this unexpected stability, because the reduction potentials of these organic solvents are far above that of lithium.[4,215−217] Peled was the first author to formally introduce the concept of a protective interface between lithium and elec-

**Scheme 8. Proposed Two-Electron Mechanism for the Reduction of PC**
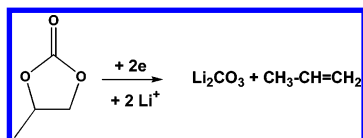


trolytes and describe the fundamental physicochemical properties of such an interface.[37] He argued that, because of the high electronegativity of lithium, the free contact between it and the electrolyte components never actually exists; instead, the reaction between the lithium electrode and electrolyte components occurs instantaneously, and the solid products from this reaction compose a thin film that grows on the lithium with the reaction. The decomposition could only stop when this film, which is nonconductive to electrons but conductive to ions, covers the whole surface of the lithium and attains a certain thickness. Once formed, the film stays on the lithium surface at all times, and it cannot be completely removed even by the stripping/deposition of lithium. Since this film acts like an electrolyte in its conductive preference, Peled named it the "solid electrolyte interface (or interphase)" (SEI). Considering the low ionic conductivity of solid-state electrolytes, he also proposed that the rate determining step for a redox process on such surfaces would be the diffusion of lithium ions through the SEI,[218] instead of the electron charge-transfer between electrode and solution species, as was believed before.

Using a parallel capacitor model, Peled and Straze calculated the apparent thickness of the SEI for a series of active metal electrodes, including lithium, calcium, and magnesium, with the equation[219]

$$L = \frac{\epsilon A}{C\pi(3.6 \times 10^{12})} \quad (10)$$

where $A$, $L$, $C$, and $\epsilon$ are the electrode area, the thickness, the capacitance, and the dielectric constant of SEI, respectively. They estimated that the average SEI thickness of lithium in nonaqueous electrolytes is 25–100 Å.[218,219] Electrons tunneling through the film of this thickness are believed to be minimal.

The chemical composition of the SEI is believed to be closely related to the electrolyte composition. For example, in thionyl chloride-based electrolytes, the SEI is proposed to be mainly composed of LiCl,[218] while it becomes $Li_2S_2O_4$ in sulfur dioxide-based electrolytes[218] or $Li_2O$ in ether-based electrolytes.[56] After performing microscopic observations of lithium surfaces treated with PC-based electrolytes, Dey believed the main component of this interface to be $Li_2CO_3$, which is the decomposition product of PC through a two-electron mechanism (see Scheme 8).[56] This conclusion seems to be supported by results from Auger electron spectroscopy (AES) and X-ray photoelectron spectroscopy (XPS).[220,221] However, more recent studies suggest that the above process might be oversimplified, and the actual process involves a complex competition between a number of reductive reactions of different components.

With surface-sensitive spectroscopic means, Aurbach et al. argued that the main component in the

SEI on lithium is not $Li_2CO_3$ but the lithium salt of alkyl carbonate, and it was most probably formed via a one-electron mechanism followed by radical termination paths as shown in Scheme 1.[55] This compound has an FT-IR signature at ~1650 cm$^{-1}$ for the carbonyl stretching, which was confirmed by the characterization of a synthesized authentic sample of a lithium alkyl carbonate, $CH_3CH_2CH_2CO_3Li$.[55] Since XPS also detected the decomposition products from lithium salts, which are in the form of simple halides, alkoxides, or oxides, a competition between solvents and salts obviously exists. However, the formation of alkyl carbonate seems to be dominant when EC is present because of the more reactive nature of EC toward cathodic reductions.[117,209] The formation of lithium alkyl carbonate was also confirmed in an independent diagnosis work, where the reduction products of EC in a supporting electrolyte were hydrolyzed by $D_2O$ and then subject to NMR analysis, which identified ethylene glycol as the main species formed, as indicated by the singlet at $\delta = 3.7$ ppm vs TMS.[208,212] Thus, Aurbach and co-workers concluded that PC and EC were reduced to the following lithium alkyl dicarbonates, respectively:
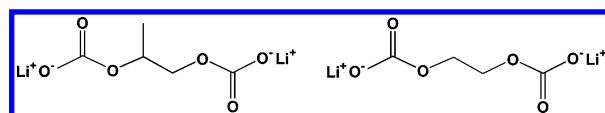


Further studies demonstrated that alkyl carbonate is very sensitive to the common contaminants in electrolytes, which is probably the reason that early work identified $Li_2CO_3$ as the main component in the SEI.[118] For example, trace moisture produces $Li_2CO_3$ when the salt anion is stable (such as $ClO_4^-$ or $AsF_6^-$):[249]
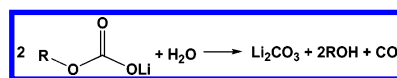


However, when the salt anion is susceptible to hydrolysis by trace moisture (such as $BF_4^-$ or $PF_6^-$), the generated HF eliminates alkyl carbonate as a surface species and only LiF can be observed as the overwhelming species in the SEI:[117]
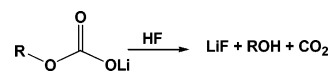


Alkyl carbonate is also unstable upon storage on the lithium electrode, probably because of its continuous electrochemical reduction.[118] Thus, Aurbach et al. further proposed that the SEI might have a multilayer structure within which the simple inorganic species such as $Li_2CO_3$ and $Li_2O$ are more stable and closer to lithium, while alkyl carbonate is more likely to be distributed in the outer layers.[117,118]

Kanamura et al. carried out detailed XPS studies on lithium electrodes that were either statically treated with or cycled in $LiBF_4$-based electrolytes.[222,223] By sputtering the surface of the lithium electrode, they were able to record the depth profile of the related chemical species. Their conclusions are in good agreement with the hypothesis by Aurbach et al.;[117,118] that is, while alkyl carbonate can be detected
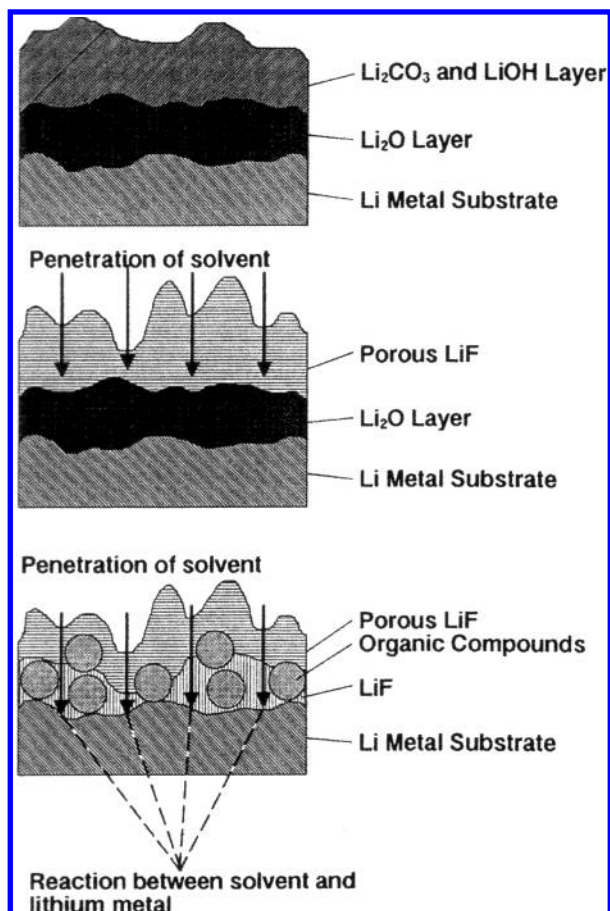
**Figure 9.** Schematic illustrations of the surface film formed on lithium in nonaqueous electrolytes based on LiBF$_4$ solutions and the subsequent reactions. (Reproduced with permission from ref 222 (Figure 12). Copyright 1995 The Electrochemical Society.)
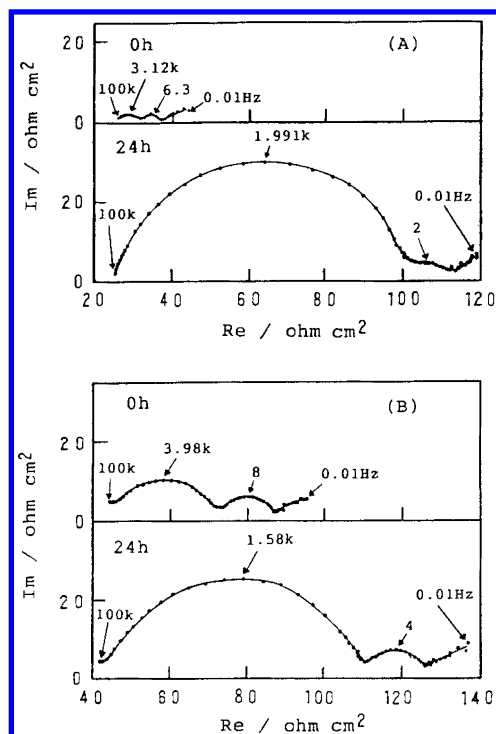


**Figure 10.** Impedance complex plane (Nyquist plots) of lithium electrode in (A) 1.0 M LiPF$_6$/EC/PC and (B) 1.0 M LiClO$_4$/EC/PC at initial time (0.0 h) and after 24 h. Re and Im stand for the real and imaginary parts of the impedance measured, respectively. Frequency was indicated in the figure for selected data points. Note that the first semicircle corresponds to SEI impedance. (Reproduced with permission from ref 86 (Figure 2). Copyright 1992 The Electrochemical Society.)

in the outlaying layer of the SEI, as indicated by its signature binding energy of 289.0 eV at the C 1s region, its abundance rapidly decreases with sputtering time. On the other hand, O 1s spectra clearly reveal the increasing abundance of Li$_2$O species. LiF exists throughout the SEI and is relatively independent of sputtering, a result of the sensitivity of BF$_4^-$ anion toward trace moisture in electrolytes. Kanamura et al. proposed two possible paths for the formation of LiF: (1) simple acid−base reaction between HF and alkyl carbonate or Li$_2$CO$_3$, or (2) direct reduction of BF$_4^-$ anion by lithium.[222,223] Additional reactions between the solvents and the lithium electrode also seem possible after the initial formation of the SEI, since the abundance of organic species increases in the inner layer with storage time increases, according to C 1s spectra. These organic species might be some polymeric products that resulted from PC or other carbonates instead of alkyl carbonates alone, as evidenced by the C 1s signal around 286 eV and by an earlier XPS work.[224] This latter process is attributed to the permeation of solvent through the SEI and its subsequent reaction with lithium. The resulting polymeric films, most likely polyether moieties, are embedded with LiF crystals. Figure 9 schematically shows the lithium surface structure and these subsequent reactions of the SEI.[222]

Aside from voltammetric techniques, ac impedance is also a powerful tool widely used to study the interfacial properties of lithium in nonaqueous electrolytes. It is one of the few in situ techniques and therefore is often used in combination with voltammetry, known as electrochemical impedance spectroscopy (EIS). As an example, Figure 10 shows the impedance response of a symmetrical cell, lithium|1.0 M LiX in PC/EC|lithium, drawn in the Nyquist plot, where LiX is LiPF$_6$ or LiClO$_4$. Typically, two semicircles would be observed for such cells at high and medium frequencies, if the time constants for each component are sufficiently separated, along with a spike at the low-frequency end.[175] It is generally accepted that the semicircle at medium frequency corresponds to the ionic migration process in the SEI and the one at lower frequency to the charge-transfer process on lithium, whereas the intercept at the high frequency end with the real axis represents bulk electrolyte resistance. Examination of the interfacial resistance in various electrolyte solutions reveals that the SEI on lithium grows with time of exposure to electrolytes, and the chemical nature of both solvent and salt anion seems to relate closely to the semicircle for the interfacial film.[86,225−227] For example, the resistance of the SEI that formed in the LiPF$_6$-based electrolyte is smaller than the one formed in the LiClO$_4$-based electrolyte, and the presence of EC also renders a more conductive SEI on lithium.[86,225−227] An empirical rule (with frequent exceptions though) might be stated here concerning the resistance of the

SEI: an electrolyte with higher bulk ion conductivity usually results in an SEI of lower impedance, either on a lithium or carbonaceous electrode, as will be discuss in later sections.

As a mass sensor with nanogram sensitivity, a quartz crystal microbalance (QCM) was used in combination with voltammetry by Naoi et al. to monitor the change occurring on the lithium surface during SEI formation.[228] Like EIS, it is one of the few analytical tools that can reveal in situ information on the interfacial process, which includes the change in mass as well as the surface morphology of the lithium electrode. It was found that, during the cycling process, the already-formed SEI was repeatedly destroyed and rebuilt, as indicated by the consistent mass increase with cycle numbers. Among the various combinations of salts and solvents tested, the $LiPF_6$-based electrolyte seems to have the most rapid reaction kinetics with lithium, since the lithium electrode in it was observed to gain net mass even during the stripping step, suggesting that the reaction kinetics between the fresh lithium surface and the electrolyte is fast enough to compensate for the mass loss caused by the lithium dissolution. On the other hand, the net mass accumulated on lithium is much higher in $LiClO_4$- and LiTf-based electrolytes than in the $LiPF_6$-based electrolyte. The conclusion from the above two observations seems to point to a more efficient and protective SEI formed by the $LiPF_6$-based electrolyte. The author ascribed this result to the trace amount of LiF in the SEI, which is absent in $LiClO_4$- and LiTf-based electrolytes.[118] The measurement of lithium surface roughness also reveals $LiPF_6$ as the favored salt in electrolytes because it forms a smoother and more uniform SEI, thus minimizing the probability of dendrite growth on a relative scale as compared with the cases of the other salts studied.

The significance of an SEI on lithium stability should be evaluated from two different angles: one is the static stability that relates to standing storage, and the other is the dynamic stability that relates to reversibility. It is the SEI formation on the lithium surface that leaves lithium statically stable in a nonaqueous electrolyte; conversely, the SEI also renders a nonuniform surface morphology for deposited lithium, so that the current density across the surface is unevenly distributed during the lithium stripping/deposition, with the direct consequence being dendrite growth.

The roughness of the SEI depends heavily on the chemical nature of the electrolyte. For example, it was argued that an SEI consisting of $LiF/Li_2O$ would provide a much more uniform current distribution,[223] while in numerous earlier works it was also observed that trace moisture has a positive effect on the lithium cycling efficiency in nonaqueous electrolytes by assisting in forming a compact and uniform SEI.[57,229] Nevertheless, the dendrite issue is a major challenge to lithium metal-based chemistry that still remains unresolved. The prospects for this battery technology, still attractive because of its high energy density as compared with the state-of-the-art lithium ion technology, rely on the discovery of a new electrolyte system that can suppress or even eliminate lithium dendrite formation.

## 6.2. Electrolyte/Carbonaceous Anode Interface: SEI

### 6.2.1. Exfoliation and Irreversible Capacities on a Carbonaceous Anode

It has been known since the mid 1950s that graphite can form intercalation compounds with lithium ions, which are accommodated in the interstitial region between the planar graphene sheets.[230–232,233] The most lithium-enriched intercalation compound of this family has a stoichiometry of $LiC_6$, and its chemical reactivity is very similar to that of lithium metal. There have been a number of different chemical approaches to the preparation of these compounds, for example, by direct reactions of graphite with molten lithium at 350 °C,[232] with lithium vapor at >400 °C,[234] or with lithium powder under high pressure,[235,236] and so forth.

On the other hand, the electrochemical synthesis of these lithium graphite intercalation compounds (Li-GIC) has been proven difficult. In earlier work, it had been found that the most commonly used electrolyte solvent, PC, decomposed reductively on the graphite electrode at a potential of ~0.80 V, and the irreversible process led to the physical disintegration of graphite.[237] The occurrence of this irreversible reduction apparently prohibits any possibility of the lithium ion intercalating into graphite, which should happen at a much lower (and therefore more reductive) potential. The destruction of graphite by PC was repeatedly observed in different electrolytes based on PC, and this disintegrating process of the graphite structure was named "exfoliation".[238–243] Besenhard et al. proposed that the exfoliation was caused by the cointercalation of PC molecules with lithium ions into the interplanar structure of the graphite and the subsequent decomposition therein.[239–242] As a result, the multilayer structure of graphite, which is only held together by weak van de Waals forces, falls apart because of the strain introduced by the gaseous products, believed to be mostly propylene.[234–237,243]

Realizing that the solvent must be the key to the exfoliation, later researchers explored different polar organic molecules such as dimethyl sulfoxide (DMSO) and DME as candidates to replace PC, in the hope that they would not cointercalate or decompose; but most of these efforts failed to endorse the usefulness of Li-GIC as a negative electrode to replace lithium.[239–241] In the 1980s, the only successful example of electrochemical intercalation of lithium into graphite was reported by Yazami and Touzain in 1983 with a polymer electrolyte based on poly(ethylene oxide) (PEO).[244] As it is essentially impossible for the macromolecular solvent PEO to cointercalate, this electrolyte supported the reversible lithium ion intercalation into and deintercalation from natural graphite. Using electrochemical titration techniques, the potential of the stage I and II Li-GIC was determined to be between 0.50 and 0.20 V vs Li, thus confirming the conceptual feasibility that Li-GIC

could be used as a negative electrode to replace lithium with minimal energetic penalty. Thus, a negative electrode based on the stage I Li-GIC would have the following reversible chemistry:

$$\text{Li}_x\text{C}_6 \xrightleftharpoons[\text{charge}]{\text{discharge}} x\text{Li}^+ + 6\text{C} + x\text{e}$$
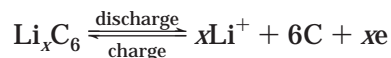
In the ideal situation of 100% utilization ($x = 1.0$), the capacity corresponding to the above anode half reaction is 372 mA h g$^{-1}$. However, due to the low ion conductivity of the polymer electrolyte and the high interfacial impedance between it and the graphite electrode, this elegant example of electrochemical preparation of lithiated graphite is of limited practical significance.

Considering the vulnerability of the highly crystalline structure of graphite, some researchers in the late 1980s focused their attention on carbon structure instead of electrolyte formulation. Successes were seen with various amorphous carbon electrodes, including carbon fiber,[245] pyrolytic carbons,[246] and petroleum coke.[247] The insensitivity of these carbonaceous materials to solvent cointercalation seems to be related to their amorphous portion, which has stacking defects that coexist with the tiny crystalline sectors and serve to pin the graphene layers together to suppress the lattice expansion that occurs during the solvent cointercalation. Thus, the indefinite "exfoliation plateau" at 0.80 V is completely absent from these amorphous carbon anodes in PC-based electrolytes,[36] and reversible lithium ion intercalation is realized up to >10$^3$ cycles in various nonaqueous electrolytes, although the initial cycles are always accompanied by a portion of irreversible capacity that depends on the nature of the carbon and the composition of the electrolytes.[36,157] These efforts eventually led to the commercialization of the first generation lithium ion cells.[29−31,34−35]

However, two penalties, both associated with energy density, arise from the disordered anode structure: (1) a smaller Coulombic capacity than the theoretical value for LiC$_6$ and (2) a sloping potential profile during both charging and discharging.[43,157] The former is caused by the small crystallinity of these amorphous carbons, because it is in the highly ordered graphene sheets where lithium ion could be accommodated, while the latter is caused by a broad distribution of adsorption site energies in the disordered carbons, which leads to a broad potential range within which lithium intercalation occurs.[125] Figure 11 compares the cycling behavior of an amorphous carbon anode with that of graphite in a half anode cell[248] and clearly demonstrates the above two penalties.[36] While the latter is certainly disadvantageous because of the unstable cell voltage, the combination of these two results in a much lower energy density that Li-GIC can offer theoretically.

Hence, a dilemma was encountered between energy density and stability for these various forms of carbonaceous materials; that is, as the carbonaceous anode is more graphitic in structure, the degree of lithium ion intercalation may be closer to the ideal ($x = 1.0$), and its potential profile may be closer to that of Li$^+$/Li and remain relatively flat (therefore
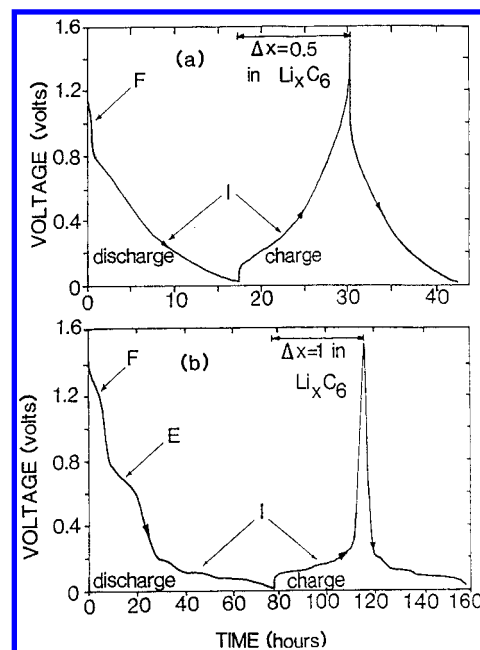


**Figure 11.** (a) Initial 1$^1$/$_2$ cycles of a Li/petroleum coke cell. The cell was cycled at a rate of 12.5 h for $\Delta x = 0.5$ in Li$_x$C$_6$. (b) Initial 1$^1$/$_2$ cycles of a Li/graphite cell. The cell was cycled at a rate of 40 h for $\Delta x = 0.5$ in Li$_x$C$_6$. F denotes the irreversible capacity associated with SEI formation, E the irreversible capacity due to exfoliation, and I the reversible capacity due to lithium intercalation into carbon. 1.0 M LiAsF$_6$ in EC/PC was used as electrolyte. (Reproduced with permission from ref 36 (Figure 2). Copyright 1990 The Electrochemical Society.)

attractive as an anode candidate), it also becomes more liable to solvent co-intercalation.[43,96,249,250] It was only after Dahn and co-workers revealed the role of the SEI on the reversibility of carbonaceous electrodes and the effect of EC therein that the energetic advantage of highly graphitic carbonaceous materials regained practical significance for the lithium ion industry.[36] As a direct consequence of improvements in electrolyte formulations aided by the knowledge gained in SEI chemistry, amorphous carbonaceous anode materials were gradually phased out from commercial lithium ion technology, starting in the 1990s.[38]

In retrospect, the significance of Dahn's seminal work lies in two aspects: (1) the fundamental understanding of how carbonaceous materials operate in nonaqueous electrolytes and (2) the more practical side of how the above dilemma concerning energy density and reversibility can be overcome. This knowledge dictates the development of electrolytes for state-of-the-art lithium ion chemistry.

On the fundamental front, Dahn et al. successfully accounted for the irreversible capacity that accompanies all carbonaceous anodes in the first cycling. They observed that the irreversible capacity around 1.2 V follows an almost linear relation with the surface area of the carbonaceous anodes and that this irreversible process is essentially absent in the following cycles.[36] Therefore, they speculated that a passivation film that resembles the one formed on lithium electrode in nonaqueous electrolyte[37,218,219] must also be formed on a carbonaceous electrode via similar electrolyte decompositions, and only because

of the more porous surface of the latter would the capacity associated with the reduction process become noticeable. Once formed, the physicochemical property of this film should be similar to the solid electrolyte model that Peled had proposed for the lithium surface; that is, it is an ionic conductor and an electronic insulator,[37] and therefore, the sustained reductive decomposition could be prevented. Hence, the term SEI that Peled had invented for the passivation of lithium electrode was transplanted on the carbonaceous anode materials.

On the practical side, Dahn's work demonstrated that, by altering the electrolyte composition, the exfoliation of graphitic materials could be eliminated, since the chemical nature of the SEI is dictated by electrolyte composition, especially by the solvents. The "magic ingredient" identified in this case is EC, whose structural difference with PC is merely a methyl substituent. As Figure 11 shows, the presence of EC not only prevents the physical disintegration of graphite that occurs at 0.8 V but also supports the reversible intercalation (during the discharge of the half-cell) and deintercalation (during the corresponding charge) of lithium ions at a very low potential, <0.20 V, with Coulombic capacity approximately approaching the theoretical value of $LiC_6$. Because PC is present in the electrolyte, a certain degree of graphite exfoliation can still be observed, but obviously EC plays an effective role in suppressing the destruction of the graphite structure. The latter development in electrolyte formulation made by Tarascon and Guyomard effectively suppressed this side reaction to a negligible level,[44,98,99] although a certain irreversible capacity was always present, accounting for the material supply required by the SEI formation. The irreversible capacity, or the ratio of this capacity to the total reversible capacity (called Coulombic inefficiency), has become one of the parameters for measuring the performance of a certain electrolyte on carbonaceous anodes.

The commercial lithium ion cells on the consumer market nowadays have already undergone a so-called "forming process" at the manufacture sites, during which a stable SEI was formed to ensure that no more irreversible process was left. The Coulombic efficiency of these cells ought to be 100% under the conditions specified for their application. On the other hand, any accidental misuse such as overcharge, high temperature exposure, and mechanic impact might damage the already formed SEI, resulting in more irreversible reactions during charging and consequently a loss from the rated capacity.

### 6.2.2. Mechanism of SEI Formation

According to Peled's model, the existence of an SEI constitutes the foundation on which lithium ion chemistry could operate reversibly. Therefore, an ideal SEI should meet the following requirements: (1) electron transference number $t_e = 0$ (otherwise, electron tunneling would occur and enable continuous electrolyte decomposition), (2) high ion conductivity so that lithium ions can readily migrate to intercalate into or deintercalate from graphene layers, (3) uniform morphology and chemical composition for ho-

mogeneous current distribution, (4) good adhesion to the carbonaceous anode surface, (5) good mechanical strength and flexibility so that it allows the expansion and contraction of the graphene lattice during the reversible intercalation/deintercalation process, and (6) low solubility in electrolytes so that continuous dissolution of SEI would not occur, resulting in persistent decomposition of electrolyte and consummation of the limited source of lithium from the cathode.

There has been considerable controversy concerning the mechanism of SEI formation on a carbonaceous anode, but it is generally agreed that the initial electrolyte decomposition is responsible and that a competition among a variety of reactions involving the solvent as well as the salt components is also present.

*6.2.2.1. Peled's Model: Anode/Electrolyte Interface Film.* In their proposal of SEI formation on a carbonaceous electrode in nonaqueous electrolytes, Dahn actually adopted Peled's model for lithium's surface and extended it to carbonaceous electrodes. By this model, a two-dimensional passivation film is established via a surface reaction.

Because of the similar potentials between fully lithiated graphite and lithium metal, it has been suggested that the chemical nature of the SEIs in both cases should be similar.[36] On the other hand, it has also been realized that for carbonaceous anodes this formation process is not expected to start until the potential of this anode is cathodically polarized (the discharge process in Figure 11) to a certain level, because the intrinsic potentials of such anode materials are much higher than the reduction potential for most of the solvents and salts. Indeed, this potential polarization process causes one of the most fundamental differences between the SEI on lithium metal and that on a carbonaceous anode. For lithium metal, the SEI forms instantaneously upon its contact with electrolytes, and the reduction of electrolyte components should be indiscriminate to all species possible,[37,218,219] while, on a carbonaceous anode, the formation of the SEI should be stepwise and preferential reduction of certain electrolyte components is possible.

Endo et al. investigated the reductive decomposition of various electrolytes on graphite anode materials by electron spin resonance (ESR).[178] In all of the electrolyte compositions investigated, which included $LiClO_4$, $LiBF_4$, and $LiPF_6$ as salts and PC, DMC, and other esters or ethers as solvents, the solvent-related radical species, which were considered to be the intermediates of reductive decomposition,[55] were detected only after prolonged cathodic electrolysis. With the aid of molecular orbital calculation, they found that the reduction of salt anion species is very difficult, as indicated by their positive reduction enthalpy and that of free solvent ($\Delta H_r \approx -1$ kcal $mol^{-1}$). However, the coordination of lithium ions with these solvents dramatically reduces the corresponding reduction enthalpy ($\Delta H_r \approx -10^2$ kcal $mol^{-1}$) and renders the reaction thermodynamically favored. In other words, if no kinetic factors were to be considered, the SEI formed on carbonaceous anodes

would predominantly consist of the decomposition products of those solvents in the solvation sheath of lithium ion, which migrates toward the negatively charged anode surface. For state-of-the-art electrolytes, the reduction of cyclic carbonates such as EC and PC should provide the major species to build up the SEI while the participation of linear carbonates should be relatively inconsequential. A similar conclusion was drawn by Wang et al., who employed a high-level density functional theory to investigate the reductive decomposition mechanism for EC molecules in electrolyte solution and found that, while the reduction of a free EC molecule is very unlikely, the coordination of lithium ion to an EC molecule renders the one- or two-electron reduction processes thermodynamically possible in a supermolecular structure such as $Li^+(EC)_n$ ($n = 1-5$).[170]

In view of the possibility that certain electrolyte components could be preferentially reduced on carbonaceous anode, Peled and co-workers explored a means to manipulate the chemical nature of the SEI by deliberately using unstable electrolyte ingredients.[106] They argued that, since these components would be reduced at a higher potential, the SEI would be completed far before solvent cointercalation occurred, and the probability of cointercalation and its following exfoliation could be minimized. EC seems to be such a component due to its reactivity.[212–214] As a measure of the ease with which electrolyte components could be reduced, Peled and co-workers proposed using the vast data bank of the rate constant ($k_e$) of reduction in aqueous media, and a fair correlation was established between this constant and the SEI formation potential.[106] Thus, $k_e$ could be used as a tool for the selection of electrolyte solvents and salts. According to this model, ideal electrolytes should be formulated with the candidates of $k_e > 10^9$ $M^{-1}$ $s^{-1}$. By this standard, $AsF_6^-$, EC, vinylene carbonate (VC), and $CO_2$ are favored, while $BF_4^-$ and $ClO_4^-$ are not.

This model conceptually forms the theoretical basis for the later development of electrolyte additives, as evidenced by the success of $CO_2$ and VC in suppressing the irreversible capacity in the initial cyclings. But so far as major electrolyte components are concerned, this model is not widely applied, since many other properties such as ion conduction and phase diagrams must also be taken into account if the component is present in high concentrations.

*6.2.2.2. Besenhard Model: Ternary Graphite Intercalation Compound (GIC).* In addition to the indiscriminate versus selective reductions, another fundamental difference between graphite and lithium electrodes is the presence of the interlayer voids of the former that could accommodate both lithium ions and solvent molecules. Therefore, some researchers argued that the reductive decomposition of electrolytes in contact with the former might not be only a simple surface reaction as suggested in Peled's model. Instead, the solvent could cointercalate into graphene layers before they decompose therein, and the passivation film thus formed could penetrate into the structure of graphite.
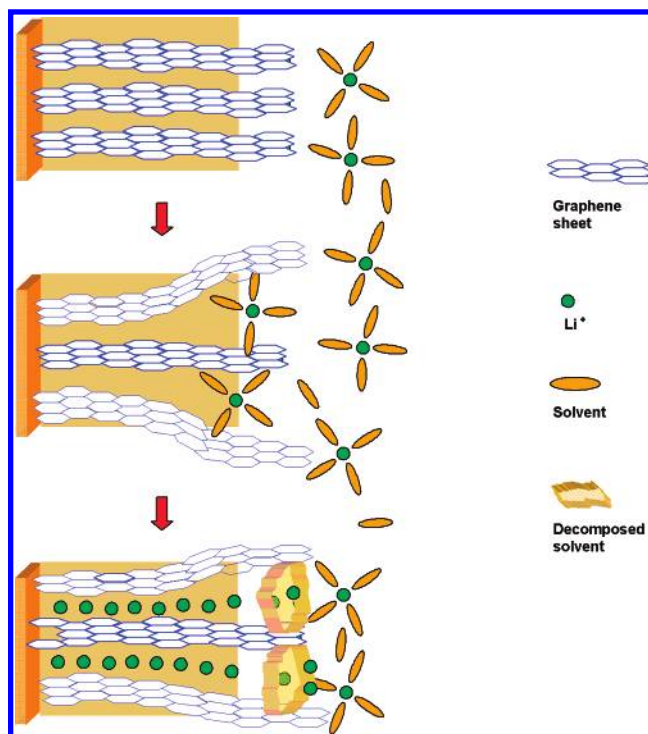


**Figure 12.** Schematic illustration of the SEI formation mechanism via the decomposition of Li(solv)$_x$C$_y$. Reconstructed based on ref 251.

The early studies have identified the existence of graphite intercalation compounds with solvent molecules.[239–243] On the basis of the knowledge about these compounds and their reactions, a mechanism for SEI formation was proposed later by Besenhard that involves the initial formation of a ternary GIC [Li(solvent)$_x$C$_y$] and its subsequent decomposition near the edge sites of the graphene planes to form the SEI.[251] Figure 12 schematically depicts the SEI formation process according to this mechanism. Upon cathodic polarization of the graphite anode, the solvated lithium ion migrates to the negatively charged surface of graphite and is intercalated into graphene layers at ~1.0–0.80 V before any reduction occurs. The ternary GIC thus formed, for example, Li(EC/DME)$_x$C$_y$, has a short lifetime and decomposes within the time scale of slow scan CV (~$10^4$ s), as indicated by the irreversible peak observed when the scanning rate is low; therefore, according to Besenhard et al., this process might easily be mistaken as an ordinary irreversible reduction of the electrolyte. However, at certain faster scan rates (e.g., 10 mV $s^{-1}$), part of the solvated ion could still be reversibly removed from graphene interlayer sites.[251] The reductive decomposition of these cointercalated solvents then renders an SEI that extends from the graphite surface at the edge sites into the interior of the interlayer voids.

The direct evidence that Besenhard et al. presented for the formation of a ternary GIC is the dilatometric measurement of the graphite electrode, which indicates a crystal expansion of 150% at the cointercalation potential.[251] However, this expansion due to solvent cointercalation was never confirmed on the microscopic level. All of the in situ X-ray diffraction (XRD) measurements conducted by different research-

ers on the cycling graphite failed to offer any evidence that a substantial change in the interlayer distance occurred around the cointercalation potential.[96,124,252,255] In these experiments, the maximal shift in $2\theta$ of the (002) diffraction peak during graphite cycling, which can reflect the size of the guest species, only corresponds to an expansion of 0.35 Å in the *c*-axis; hence, bare lithium ions seem to be the only species that can be accommodated.[252−254] It should be pointed out that the existence of ternary GICs is beyond question, and the doubt here is about whether they could be electrochemically formed under a similar situation in the forming of lithium ion cells.[256−260] So far, the chemical or electrochemical synthesis of ternary GICs has failed to produce any compositions based on carbonate solvents, despite the success of Ogumi and co-workers with various solvents such as ether or alkylsulfoxide,[257−260] casting more doubt on the Besenhard model.

In defense of the Besenhard model, Chung et al. argued that the lack of XRD evidence for ternary GICs might be simply due to either their rapid decomposition or the localized presence of them near the graphite edges.[255] Since XRD probing of the material is based on the averaged diffraction response of the sample lattice, these wider spacings of the ternary GICs might not be detected as an averaged bulk property.

In situ EQCM studies of graphite in various electrolytes also challenge the formation of ternary GICs with the real-time monitoring of the graphite electrode mass increase during cathodic polarization.[101] It was found that, between 0.8 and 0.5 V, where such GICs are supposed to be stable, the mass change per quantity of electricity ($\Delta m/\Delta Q$) was 27−35 g $F^{-1}$, corresponding well to $Li_2CO_3$ that has a $\Delta m/\Delta Q$ of 36.9 g $F^{-1}$. If solvents such as EC ($\Delta m/\Delta Q = 88.07$ g $F^{-1}$), PC ($\Delta m/\Delta Q = 102.1$ g $F^{-1}$), or the solvated lithium ion $[Li^+(PC)_n]$ ($\Delta m/\Delta Q > 300$ g $F^{-1}$ assuming a coordination number of 3) cointercalate into the graphene structure, the corresponding mass gain on the graphite anode, which is too conspicuous to miss, should have been well recorded by the quartz crystal sensor.

The thermodynamic stability of a ternary GIC is also questionable. Obviously, between a bare lithium ion and one solvated by molecular dipoles, the intercalation of the former between two giant graphene anions is far more favored thermodynamically than that of the latter. The fully lithiated GIC $LiC_6$, for example, does not solvate in nonaqueous electrolyte solvents, and the tendency of lithium to prefer binary (i.e., without solvent cointercalation) instead of ternary GICs has also been noticed in the solution syntheses.[257]

Despite the concerns raised by XRD, EQCM, and thermodynamics, the Besenhard model still received extensive support from various experimental observations as summarized below and soon became the prevalent model used by researchers in the lithium ion battery community.

It had been discovered earlier that when electrolyte solvents decompose reductively on graphite, one of the products is gaseous propylene.[237] Dey et al.
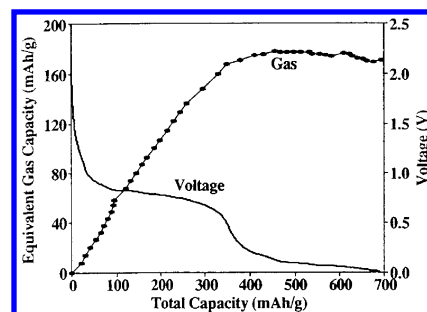


**Figure 13.** Correlation of gas evolution on a graphite electrode in 1.0 M $LiClO_4$/PC/EC (50:50) with the irreversible process at 0.80 V during the first discharge. Note the level off of gas volume as soon as reversible lithium ion intercalation starts. (Reproduced with permission from ref 261 (Figure 2). Copyright 1993 The Electrochemical Society).

**Scheme 9. Electrochemical Reduction of PC on Graphite: Ternary GIC Mechanism**
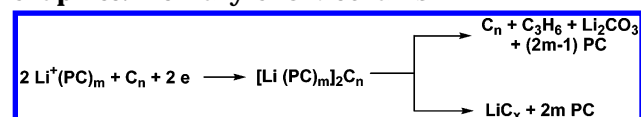


**Scheme 10. Electrochemical Reduction of PC on Graphite: Modified Ternary GIC Mechanism**
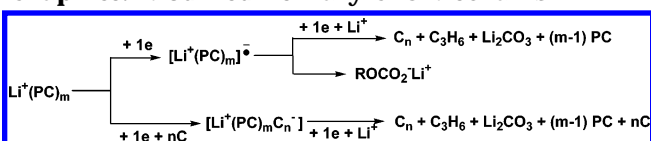


proposed a surface mechanism involving a two-electron process as shown in Scheme 8. Arakawa and Yamaki quantitatively analyzed the gas volume generated during the electrochemical decomposition of PC on a graphite electrode and found a mismatch between the Coulombic quantity and the equivalents of propylene gas generated, with an efficiency between 50% and 70%, depending on current density.[243] Apparently this result conflicts with Scheme 8, and other reaction processes must also exist simultaneously. Using a kinetic treatment, they suggested a mechanism (see Scheme 9) where a ternary GIC is the intermediate, which underwent two parallel but competitive paths to form either the gaseous product propylene and $Li_2CO_3$ or lithiated binary GICs. Using this mechanism, Arakawa and Yamaki successfully explained the relation between gas volume rate and time.[243]

Following a similar approach, Shu et al. used an EC/PC mixture instead of neat PC as electrolyte solvent, and their analysis of propylene gas volume corroborates the observations of Arakawa and Yamaki.[261] Furthermore, because EC was present in their electrolyte, the reversible lithium intercalation could occur after a long plateau at ~0.8 V (representing PC decomposition), therefore a correlation between the gas volume and this irreversible process was able to be established, as shown in Figure 13. Considering Aurbach's spectroscopic observations (to be discussed later), a modified mechanism (see Scheme 10) was proposed by Shu et al., wherein a competition exists between the surface reaction leading to radical anions and the formation of ternary

GICs, via the one-electron process in both cases. According to Shu et al., these intermediate species underwent further single-electron reduction and produce $Li_2CO_3$ and propylene gas, while alkyl carbonates are generated via radical termination as shown in Schemes 1 and 7[55,214] to become the major ingredients in the surface film.

In separate research, Matsumura et al. performed quantitative analyses of lithium content in graphite electrodes with plasma spectroscopy and correlated the results with the quantities of electricity associated with the reversible and irreversible processes.[262] With XPS, they found that after the graphite is delithiated, there is a certain amount of lithium remaining in the graphite that cannot be removed electrochemically. Depth profiles established by sputtering the graphite sample with $O_2^+$ confirmed that these lithium species are distributed rather evenly in the bulk of the graphite. The author ascribed the existence of these electrochemically nonremovable lithium ions as the result of lithium reaction with active sites on the carbon surface.[262] However, there is also the possibility that these lithium signals are from the lithium-containing ingredients in the three-dimensional SEI that exists in the graphite matrix.

Kim and Park investigated the mechanism of lithium ion intercalation in graphite anodes employing solid-state NMR.[263] Their results perhaps offer the most direct evidence in support of Besenhard's GIC model. By adding strongly coordinating additives for lithium ions, 12-crown-4 and 18-crown-6 ethers, into the electrolyte solution, they were able to observe an obvious Knight shift in the $^7Li$ signals of the graphite powder that was caused by the coordination. Separate $^{13}C$ NMR tests conducted on the same graphite sample also identified the signals of crown ether as well as carbonate (more likely its decomposition product) in the graphite powder following lithiation. Assuming that the adsorbed additives and solvents on the graphite surface have all been thoroughly removed during the washing procedure that preceded NMR measurements, the above observation should be considered as the first confirmation that solvent molecules indeed are found in the bulk of the graphite, and their cointercalation with lithium ions during the lithiation process would most likely be the path. However, since the author did not present any blank test to prove the effectiveness of the washing procedure, the possibility of surface contamination due to the remnant solvent molecules being trapped in the porous structure of the graphite electrode could not be completely excluded. Nevertheless, solid-state NMR proved to be an effective tool in studying the bulk structure of graphite anodes, and more efforts on SEI mechanisms should be done with this technique.

In situ Raman spectra studies performed on graphite anodes also seem to reveal a cointercalation occurrence that leads to exfoliation. Huang and Frech used solutions of $LiClO_4$ in EC/EMC and EC/DME as electrolytes and monitored the $E_{2g2}$ band at $\sim$1580 $cm^{-1}$ in the Raman spectra of the graphite that was cycled between 2.0 and 0.07 V.[264] Reversible lithium intercalation and deintercalation was indicated by
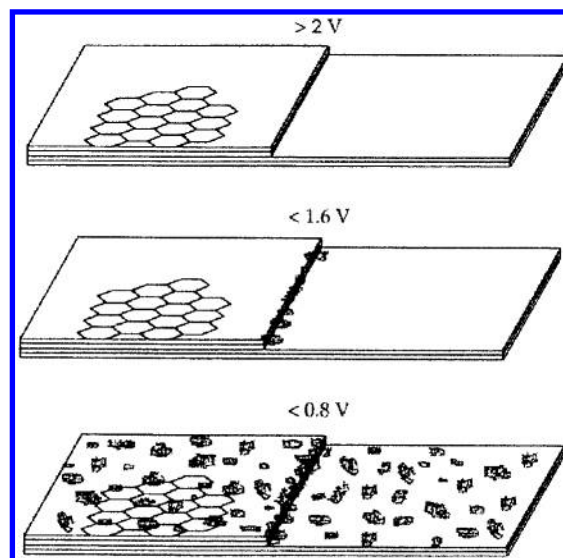


**Figure 14.** Schematic diagram summarizing the stepwise formation of the SEI on a graphite surface. (Reproduced with permission from ref 266 (Figure 10). Copyright 1997 The Electrochemical Society.)

the corresponding shift of this band in the EC/DMC-based electrolyte. But in the presence of DME, the graphite surface structure was detected to be irreversibly altered in the range between 0.9 and 0.5 V, as indicated by a shoulder on the $E_{2g2}$ band. Since no lithium ion intercalation is supposed to occur in this potential range, the authors attributed the Raman spectral changes to the extensive DME cointercalation. Interestingly enough, a DME-based ternary GIC was indeed electrochemically obtained and identified by Abe and Ogumi and co-workers with XRD.[257−260] As a matter of fact, the results from this Raman study support the Besenhard model but also cast doubt upon it simultaneously because no such irreversible $E_{2g2}$ band shift had been observed in the EC/DMC electrolytes, although obviously the SEI was formed in that case too.

Various microscopic means were also applied to study the SEI formation process, but the reproducibility of the results is highly dependent on the condition under which the observations were made and the pretreatment history of the samples. Even for the same observation, the interpretations could vary from author to author. For example, with a scanning tunnel microscope (STM), Inaba et al. observed the formation of some "blisters" on the graphite surface during its cathodic polarization and described them as the swelling of the graphene layer due to solvent cointercalation;[265] however, Farrington and co-workers, after observing the same phenomenon with an atomic force microscope (AFM), ascribed these island structures to the depositions of the decomposition products from the solvent.[266] One common phenomenon that was observed by all of these microscopic experiments is the stepwise formation of the surface species,[265−269] which appear first near the edge sites of the highly ordered graphite surface at potentials as high as 1.6 V and then grow and cover the whole electrode at potentials below 0.80 V, as shown in Figure 14. Since the intrinsic reduction potentials of the related solvents are much lower
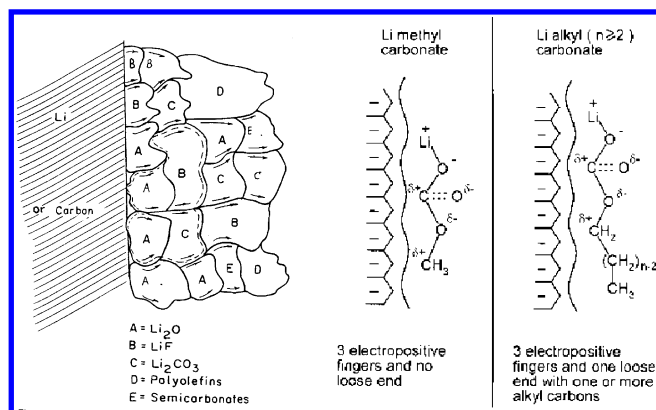
**Figure 15.** Schematic drawings of various models: (a, left) "mosaic" SEI model by Peled et al. (Reproduced with permission from ref 270 (Figure 1). Copyright 1997 The Electrochemical Society.) (b, right) Surface double layer capacitor model by Ein-Eli (Reproduced with permission from ref 272 (Figure 1). Copyright 1999 The Electrochemical Society.)

(Table 5), the edge-site process at the higher potentials might have been preceded by solvent cointercalation.

Recently, Chung et al. conducted EIS studies on a graphite electrode that had been previously exfoliated in a PC-based electrolyte and then reassembled in an EC-based electrolyte after washing.[255] They found that, compared with the fresh graphite electrode or the graphite anode that had been precycled in an EC-based electrolyte, the exfoliated graphite sample exhibited a much higher (>300%) double-layer capacitance, which was roughly proportional to the surface area that was accessible to the electrolyte. On the basis of this observation, Chung et al. postulated that the previous history exfoliation had resulted in a significant rupture of the graphite surface, as confirmed by the STM results obtained by Inaba et al. on the graphite exfoliation process.[269] Apparently, between a simple surface reaction model and Besenhard's model, the latter would more easily account for this surface area increase, because the direct consequence of ternary GIC formation is the creation of new surfaces.

*6.2.2.3. Other Models.* In addition to Besenhard's model, the other models were mainly modifications developed from the original Peled's concept for lithium electrode passivation, with surface reaction as the major process, and emphasis was placed upon the composition and structure of the precipitated film or the interaction between the precipitated products and the bulk electrolyte components.

On the basis of the results from XPS studies by Kanamura and co-workers that the SEI has a multilayered structure,[222,223] Peled and co-workers modified their lithium electrode passivation model to include carbonaceous anodes and proposed a so-called "mosaic model" to describe the SEI structure on the anode, as Figure 15a shows.[270] According to this model, multiple reductive decompositions occur between the negatively charged anode surface and the various electrolyte components simultaneously, depositing a mixture of insoluble products on the anode. This "heteropolymicrophase" SEI consists of many microregions that are of entirely different chemical

natures, ranging from thermodynamically stable anions such as $O^{2-}$, $S^{2-}$, and halides located in the immediate vicinity of the anode surface to partially reduced organic species such as alkyl carbonates and polyolefins located closer to the electrolyte solution. They suggested that, in the SEI of such a structure, the impedance to the intergrain lithium ion transport would be the rate-determining step. Apparently the pattern in which these "mosaic" pieces are arranged is decided by the order in which the electrolyte components are reduced. The reductions are considered to be surface processes, and the structural difference of the anode (lithium or graphite) is considered inconsequential.

In an attempt to explain why a linear methyl alkyl carbonate such as DMC and EMC can form a stable SEI on a graphite surface while ethyl or higher alkyl carbonates such as DEC cannot,[107,108,271] Ein-Eli proposed another surface model in which the decomposed electrolyte solvents are adhered to the negatively charged graphite anode surface through Coulombic interactions.[272] He argued that, during the cathodic polarization of the anode, the decomposition products, in the form of lithium organic salts, would be lined up in a model similar to that of a double-layer capacitor, as Figure 15b shows, and would attach themselves to the existing film via the positively charged lithium ion "head" and the partially positively charged carbons. According to this model, the effectiveness as well as the stability of the SEI would depend on these points of adhesion. The schematic drawing in Figure 15b shows that the decomposition products from methyl alkyl carbonate can form a tight adhesion without "loose ends", while a loose alkyl tail from DEC or higher alkyl carbonates prevents the formation of a compact film. Like Peled's original model[37,218,219] and its modification,[270] this model is still based on a two-dimensional surface reaction. It must be pointed out, though, that the graphic representation as shown in Figure 15b might be oversimplified and should only be understood as an empirical rule rather than an accurate picture on the molecular level, considering that the carbonyl bonds in the carbonate molecules have to be distorted out of the $sp^2$ plane of the carbonyl carbon to meet the contact points.

To investigate the failure mechanism of graphite electrodes in nonaqueous electrolytes, Aurbach and co-workers used various electrolyte solvents, salts, and graphite electrodes with varying structures and morphologies and attempted to correlate the SEI effectiveness with these parameters.[273–275] Their extensive studies led to the conclusions that the failure mechanism is solvent-dependent and exfoliation does not always happen to graphite anodes even if they physically disintegrate. For the reductively stable ether-based solvents (see Table 5), no massive surface film was observed above 0.30 V, and these solvents, coordinating with lithium ions, cointercalated into graphene and caused complete exfoliation of the latter. In this case, the evidence of destroyed crystallinity was obtained by XRD. However, for carbonates that are reductively active, such as EC or PC (Table 5), surface precipitations were observed

at potentials well above that of lithium ion intercalation, which prevented the complete exfoliation of the graphite anode, as indicated by its mainly intact crystallinity.[255,275] Rather, the physical disintegration in this case could only be caused by the electric isolation of graphite fragments on a macroscopic level, which is the result of both the solvent's chemical nature and the graphite's surface morphology.

On the basis of these conclusions, Aurbach and co-workers proposed a model for SEI formation that makes a compromise between solvent cointercalation (for ether-based solvents) and the surface reaction mechanism (for carbonates). According to the model, the graphite surface in electrolytes based on carbonate solvents including PC was covered with a surface film, and the balance between the kinetics of precipitation of highly cohesive surface films and the kinetics of overall surface reactions producing gaseous products determines whether the graphite is stabilized. In deep crevices that exist on the graphite surface, such gaseous products created sufficient strain and electrically disconnected the graphite fragments. Solvent cointercalation seems less probable with the existence of surface films. Obviously, this model would be able to account for the observed fact that surface area increases after the graphite is cycled in PC-based electrolytes, while the graphene crystal structure remains unchanged on a microscopic scale.[255]

The drastic difference between EC and PC concerning the stability of the graphite in them, despite their close structural similarity, was ascribed by Aurbach and co-workers to the effect of the methyl group from PC, which intervenes with good adhesion and cohesion of the formed product to the graphite surface,[275] in a very similar way, as described by Ein-Eli, to the "alkyl loose tails".[272] Thus, the gas evolution kinetics is faster than the buildup of the SEI on the graphite surface, and the electric disconnection and regional disintegration occur, starting at the deep crevices driven by the gas pressure therein.

*6.2.2.4. The Mystery of Exfoliation.* However, all of the above models that recognize surface reactions as the film formation path were strongly challenged by the results of the comparative studies carried out by Chung et al.[255,276] To explore the origin of graphite exfoliation, they used a series of model carbonates to study their cointercalation behavior with graphites and found a correlation between the stereo hindrance of the solvent molecules and the behavior of the graphite anodes in the electrolytes based on them. These model carbonates are all structural analogues of PC and include a pair of geometric isomer *trans*- and *cis*-butylene carbonates (*t*-BC and *c*-BC) as well as *trans*-2-pentylene carbonate (*t*-PC):
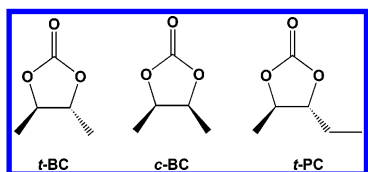


When the graphite anode was cycled in the electrolytes based on these carbonate solvents, it was found
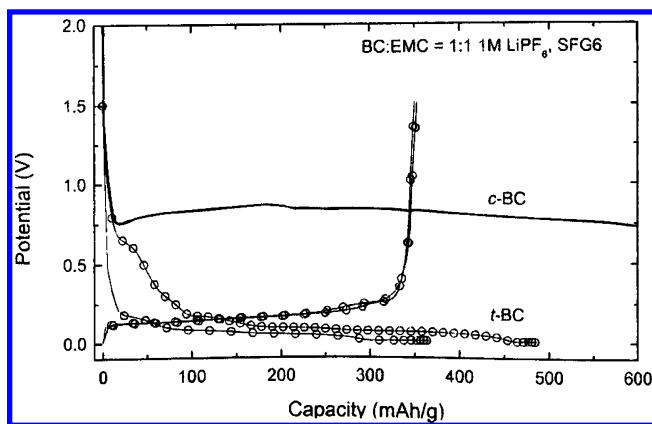


**Figure 16.** Voltage profiles for the first two lithium intercalation/deintercalation cycles realized on graphite anode in *t*-BC/EMC and *c*-BC/EMC solutions of 1.0 M LiPF$_6$. (Reproduced with permission from ref 255 (Figure 7). Copyright 2000 The Electrochemical Society.)

**Scheme 11. Nondifferentiation of Surface Reactions toward Diastereomers *t*-BC and *c*-BC**[a]
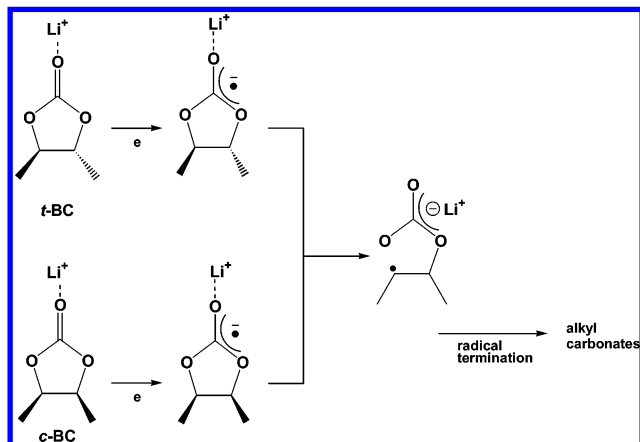


[a] An Identical Radical Anion Was Produced When the Ring-Opening Step Eliminated the Chirality of the Ether Carbon

that reversible lithium intercalation/deintercalation occurred with *t*- but not *c*-BC. The difference between *t*-BC and *c*-BC in terms of the graphite performance is a replica of the difference between EC and PC, as shown in Figure 16. Such different behaviors from geometric isomers *t*-BC and *c*-BC would not be expected if surface reactions dominated the formation of the SEI, as proposed in the models by Peled,[37,270] Ein-Eli,[272] and Aurbach,[273−275] because the chirality of the carbons would be eliminated once the ring opened to form the radical anion as the predecessor to lithium alkyl carbonates (Scheme 11). Thus, any reasonable model for SEI formation has to involve a mechanism in which the stereo difference between *t*-BC and *c*-BC could be recognized and play a role in determining the physicochemical nature of the resultant SEI. Chung et al. argued that the fundamental concept of the Besenhard model (i.e., the cointercalation of the solvent to form a ternary GIC before any reductive decomposition like the one in Scheme 11) would be able to explain the above stereo effect, since the graphene layer structure would serve as a sub-nanoscopic sieve (graphene interlayer distance ~ 0.35 nm) that could tell the difference in the strain introduced by these geometric isomers, as shown in a schematic drawing in Figure 17. Thus, PC and *c*-BC
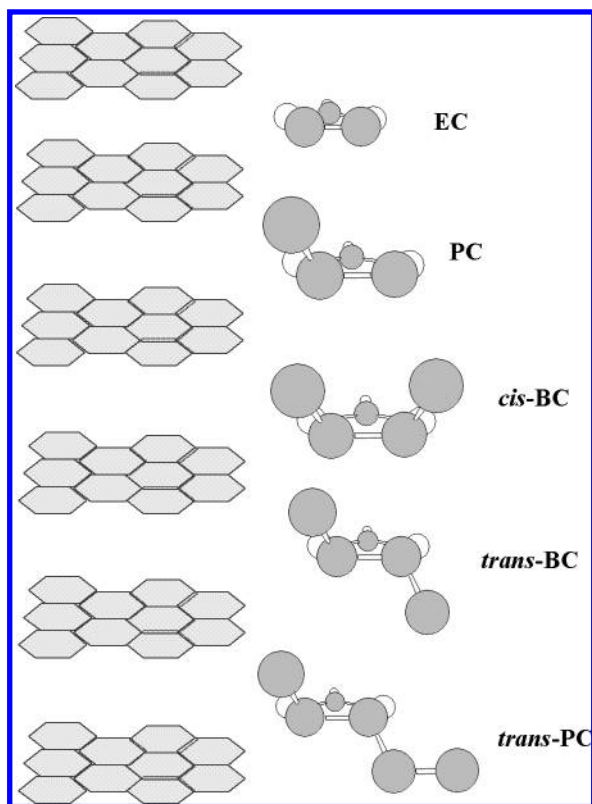
**Figure 17.** Schematic drawing of the GIC-exfoliation model. Differentiation of the stereo difference among EC, PC, and related carbonates by graphene structure.

have similar stereo hindrances and would exert similar strains into the graphene structure and cause exfoliation, while t-BC may experience severe geometric constraints for cointercalation. Hence, it can exhibit a reaction behavior on a graphite surface that is qualitatively different from that of PC.

Again, caution must be taken when using the graphic representation as shown in Figure 17 because such oversimplification might be misleading when a complex process such as the formation of an SEI on graphite is handled. For example, the graphic representation in Figure 17 suggests that cointercalation of solvent occurs without the assistance of lithium ions, while, in actual cointercalation, the solvents that coordinated with lithium ions in the solvation sheath would preferentially cointercalate. With the supermolecular structure of the solvation sheath in consideration, it would be more difficult to predict the effect of diastereomers on cointercalation by the analogue of Figure 17.

On the other hand, with an average solvation number of four, it would be hard to imagine that cointercalation would occur without breaking the solvation structure of the lithium ion, considering the required expansion in the graphite structure to accommodate such a gigantic guest. Most probably, at the edge sites of the graphite where cointercalation occurs, the solvated lithium ion is progressively stripped of its solvation sheath, and the free solvents would then insert into the graphite interior in a close way, as shown by Figure 17.

To summarize, various models have been proposed to depict the formation of an SEI on a graphite anode, based on the common knowledge that the reductive decomposition of electrolyte components leads to the formation of a protective film on the anode. However, these models differ in the mechanism by which the SEI is formed, especially concerning the issue of whether a ternary GIC is formed before the reductive decomposition occurs. Although each of these models can elegantly account for certain experimental observations, the Besenhard model that evolves around solvent cointercalation seems to be supported by the most experimental evidences, despite the fact that the electrochemical formation of a key species of this model, a metastable ternary GIC intermediate, has not been experimentally confirmed. Nevertheless, it is generally agreed nowadays that to a certain extent the solvent cointercalation does occur and is at least a part of the process related to the formation of the SEI. The complete clarification of the above controversy relies on obtaining more experimental evidence at a microscopic level from further studies.

### 6.2.3. Characterization of Surface Chemistry

Relative to the controversy associated with the mechanism of SEI formation, there is less uncertainty in the knowledge about the chemical composition of the SEI, due mainly to the exhaustive surface spectroscopic studies carried out by Aurbach and co-workers on carbonaceous anodes in various nonaqueous electrolytes, adopting both in situ and ex situ approaches.[104,108,123,124,249,250] Table 6 lists the chemical compounds as identified by these spectroscopic means and the proposed chemical reactions leading to those species.[27−284] As it has been pointed out, the solvents, especially the cyclic carbonates, play a more important role in the surface chemistry of the anode than the salt anions.[178]

Compared with the surface chemistry of nonactive electrodes[212−214] or lithium electrode,[55,117,118,209] similar chemical species were identified despite the differences in the electrode surfaces. A major modification of the previously accepted two-electron reductive pathway as suggested by Dey and Sullivan[237] was proposed by Aurbach and co-workers based on the identification of lithium alkyl carbonate by FT-IR.[108,124,249] They suggested that the surface reductive process for most carbonate molecules proceeds via a single-electron path leading to the intermediate, as shown in Schemes 1 and 7, and that $Li_2CO_3$ and alkylenes were formed through either the continued reduction of this intermediate or the secondary reaction between it and trace moisture in the system. Specifically, the following structures were assigned to the decomposition products from EC and PC, which supposedly constitute the main composition of the SEI layer:[102,104,117]
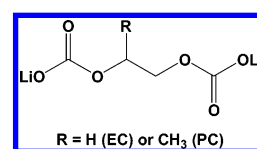


The predecessor of alkyl carbonate, a radical anion, has been experimentally observed by ESR, the life span of which depends on the carbonate structure and ranges from minutes to hours but is independent

of the salt species used.[178] Moreover, this one-electron reduction mechanism does seem to be strongly favored by the fact that the intermediate does not convert to alkylenes in 100% yield, reminiscent of the work by and Arakawa and Yamaki[243] and Shu et al.[261] who have already reported that the generation of gaseous products does not match the electric quantity injected into the anode.

A more quantitative confirmation of alkyl carbonate formation came from transmission electron microscopy (TEM), by which electron diffraction (ED), electron energy loss spectra (EELS), and imaging were conducted on disordered and graphitic carbonaceous anodes cycled in LiClO$_4$/EC, respectively.[280] Although the ED does not identify any crystalline phase other than the hexagonal structured graphite and Li$_2$CO$_3$ on the surface (probably suggesting that alkyl carbonates are noncrystalline), the atomic concentration ratio of oxygen and carbon (O/C) as determined by EELS ranges between 1 and 1.5, unequivocally indicating that the proposed alkyl carbonate formed from EC reduction. Interestingly, this O/C ratio was also found to vary with the potential to which the carbonaceous anodes were cathodically polarized: above 0.90 V an O/C ratio = 3.0 was obtained for the presence of Li$_2$CO$_3$, while below 0.80 V an O/C ratio = 1.0−1.5 was obtained. Thus, the authors proposed that the SEI was formed in a two-step process: (1) formation of Li$_2$CO$_3$ occurs at potentials between 1.0 and 0.80 V, and (2) formation of alkyl carbonates is favored at lower potentials below 0.80 V.

In retrospect, probably a more reasonable explanation could hereby be proposed concerning this potential-dependent reductive decomposition. Combining the observations from Shu et al. about the correlation of gas products with a 0.80 V plateau,[261] Farrington and co-workers about the deposition of the film onto the surface,[266] Aurbach and co-workers about the competition between single- and two-electron reductive paths,[108,124] and Kanamura et al. about the multilayered structure of the SEI,[222,223] one can conclude that, at potentials above 0.80 V, where the film has not completely covered the basal surface of graphite, the two-electron process as proposed in Scheme 8 is likely the predominant process because of the good electronic conductivity of the graphite surface, leading to Li$_2$CO$_3$ and ethylene; below 0.80 V the single-electron process prevails because of the much slower electron hopping kinetics, leaving the surface with alkyl carbonate depositions and rendering negligible gas evolution simultaneously. Therefore, the potential-dependence of the decomposition compounds as observed in a TEM study by Naji et al.[280] is actually the potential-dependence of the competition between one- and two-electron paths, as shown in Schemes 1 and 7.

In addition to FT-IR, XPS experiments performed on a graphite anode that had been cycled in various carbonate-based electrolytes also identified an alkyl carbonate species. Bar-Tow et al. characterized the surface of a highly oriented pyrolytic graphite (HOPG) that had been cycled in LiAsF$_6$/EC/DEC and found the C 1s signal located at 289 eV,[281] which had been
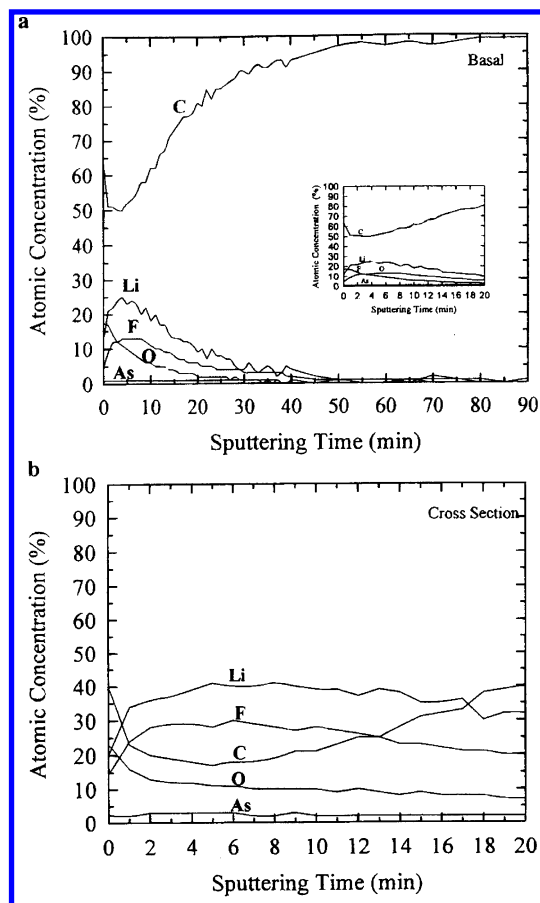


**Figure 18.** Depth profile of various chemical elements in the SEI formed on HOPG: (a) basal plane and (b) edge section. (Reproduced with permission from ref 281 (Figure 4). Copyright 1999 The Electrochemical Society.)

previously observed on a lithium surface and identified as alkyl carbonates by Kanamura et al.[222,223,282,283] after referencing with the C 1s signal of Li$_2$CO$_3$ at 290.5 eV. Surface sputtering with Ar$^+$ reduces the abundance of this species rapidly, suggesting that this species might only be stable on the top layer of the SEI.

Besides lithium alkyl carbonates, XPS also identified a wide variety of decomposition products from other electrolyte components, including polyether moieties as well as the lower valence As species. The depth profile of the SEI established by prolonged sputtering by Ar$^+$ reveals the multilayered structure of the SEI, as shown in Figure 18a, in which the organic species such as alkyl carbonate and Li$_2$CO$_3$ are present in predominant percentages on the solution side of the SEI while simple inorganic species such as Li$_2$O or As(0) are more stable on the graphite side of the SEI probably because of the more complete reduction facilitated by faster electron-tunneling kinetics.

Differences in chemical composition were also observed in the SEIs formed on basal planes and edge sites. The former were more enriched with organic species and the latter with inorganic species, especially with the decomposition products that obviously originated from salt anions. The authors thus concluded that, on the basal plane, the major contribution to SEI formation is from solvent reductive

**Scheme 12. Formation of Polymeric Species in the SEI**
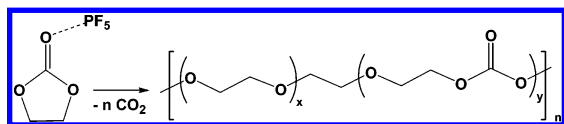


decomposition, whereas, at edge sites, the salt anion decomposition occurs on a larger scale.[281] This location-dependence of the SEI chemical composition strongly implies that the edge sites of the graphite are the main entrances for lithium ion intercalation.

XPS studies, carried out with $LiBF_4$- and $LiPF_6$-based electrolytes,[277] or with carbonaceous anodes with varying graphitic degrees,[125] or at different potentials after being fully cycled,[125] rendered quite similar results, except that the abundance of LiF increased in the SEI because of the higher sensitivity of $LiBF_4$ and $LiPF_6$ to moisture. Andersson and Edström observed a large amount of polymeric carbon on the cycled graphite surfaces that was linked with an ether-like oxygen, as evidenced by the signals located between 285.5 and 286.5 eV.[277] They attributed the formation of these polymeric species to the ring-opening polymerization of cyclic carbonates initiated by strong Lewis acids such as $PF_5$ (Scheme 12).

Aside from cyclic carbonates, the decomposition products from linear carbonates were also identified in the forms of either lithium alkyl carbonates or alkoxides, as shown by Scheme 7 and also in Table 6a.[125,271,279] Relatively, the reduction of linear carbonates was thought to be less consequential as compared to their cyclic counterparts, apparently due to their smaller presence in the solvation sheath of lithium cations.[170,171]

In accordance with these experimental results, Wang et al. employed density functional theory calculations to comprehensively examine the possible reduction pathways for EC molecules in supermolecular structures $Li^+-(EC)_n$ ($n = 1-5$) and found that, thermodynamically, both one- and two-electron reductive processes are possible.[170] A complete array of the possible reduction products from EC was listed in their paper considering the various competitive pathways, and they concluded that both $(CH_2OCO_2Li)_2$ and $(CH_2CH_2OCO_2Li)_2$ are the leading species in SEI, while minority species such as lithium alkoxide, lithium carbide, and the inorganic $Li_2CO_3$ coexist.[170]

A more recent XPS study by Ross and co-workers challenged the above general conclusion that lithium alkyl carbonates constitute the main composition of the SEI.[284] Using ultrahigh vacuum surface analytical methodology, they meticulously examined the reaction between a fully lithiated HOPG and DEC as a function of temperature and found that all carbonate signatures above 289 eV rapidly disappear in the room-temperature range, giving way to $Li_2O$, although alkyl carbonate as a metastable species did exist in the subambient temperature range briefly. Between 0 and 100 °C, the C/O stoichiometry ratio correspondingly changes from the known 1.6 for DEC to 1.0. Combining these observations, they suggested that oxalate species along with lithium methoxide
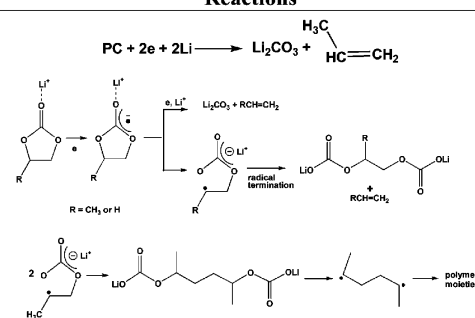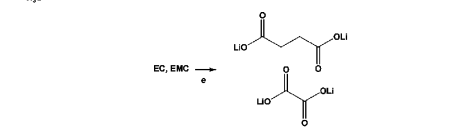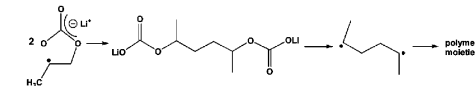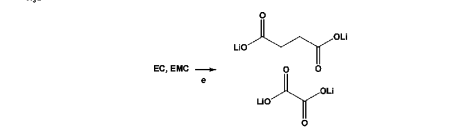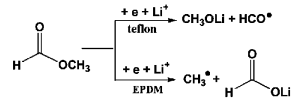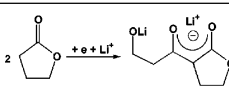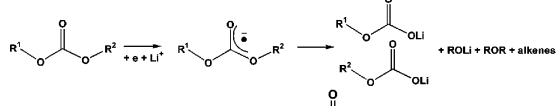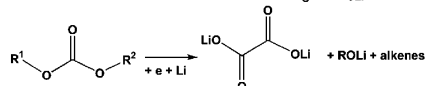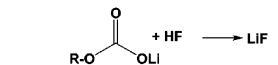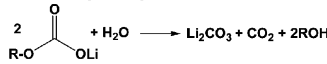
were formed in the SEI instead of an alkyl carbonate such as $C_2H_5OCO_2Li$.[271,279]

In the FT-IR analysis of an SEI on an anode surface, Ross and co-workers also disagreed with Aurbach and co-workers on the interpretation of the spectra.[285] The difference is mainly concentrated on the assignments of two absorption peaks at 838 and 1650 cm$^{-1}$, respectively, which were ascribed to the bending and stretching of carbonyls in lithium alkyl carbonate.[55,118] While the former was indeed observed by Ross and co-workers in their spectra, they excluded the possibility of it arising from lithium alkyl carbonate in view of its strong intensity. By comparing the IR spectra of an authentic sample of lithium monoethyl carbonate and propylene oxide, they suggested that the signal might originate from the asymmetric stretching of the O−C−O linkage from an epoxy structure, which was generated from the reductive decomposition of EC via an electrochemical−chemical process that involved the reduction of trace moisture in the electrolyte.[285] Considering the low bp of this compound (10.7 °C) and its strong tendency toward ring-opening polymerization by the catalysis of acids or cations, it is very unlikely that it would be a persistent ingredient of the SEI. Perhaps ethylene oxide was only detected as a transient species in the IR studies, which eventually polymerized into an oligoether species. On the other hand, the signature stretching mode of alkyl carbonate at 1650 cm$^{-1}$ was completely absent in IR spectra obtained by these authors.[278] By comparison with synthesized spectra based on authentic compound samples, the carbonyl stretching of high intensity was assigned to lithium oxalate ($Li_2C_2O_4$) and succinate ($LiO_2CCH_2CH_2CO_2Li$) (Table 6a). While the former was obviously formed from $CO_2$ through some reductive process, the source for the latter remains unclear. A likely mechanism is the recombination of radicals, which would explain the formation of new C−C bonds. At the same time, the presence of trace moisture complicates the surface chemistries by reacting with lithium alkoxides and renders the SEI with species such as LiOH, $CH_3OH$, and $LiHCO_3$.

Apparently, the above controversy regarding the identification of chemical species in the anode SEI will require further analytical work to resolve.

In addition to chemical compositions, another important aspect about SEI formation that is of practical significance to the forming of lithium ion cells is the potential range in which the above reactions occur leading to the formation of the SEI. Because of the earlier observation of the plateau near 0.80 V[36,237] and the concurrent gas evolution,[243,261] it was generally believed that the formation of the SEI occurred at this potential. An in situ analysis using a differential electrochemical mass spectrum (DEMS) performed on graphite as well as other electrode surfaces confirmed the above process by simultaneously recording voltammetry and analyzing the gaseous products from the electrode being cathodically polarized. It was found that hydrogen and ethylene were produced during the first cycle at about 1.50 and 0.80 V, respectively, as indicated by their molecular peaks as well as fragmentation patterns

**Table 6. Reductive Decompositions on Carbonaceous Anodes**

A. Electrolyte Solvents

| Solvents | Reactions | Refs. |
|---|---|---|
| PC, EC: |  PC + 2e + 2Li ⟶ Li$_2$CO$_3$ + | 237 |
| |  R = CH$_3$ or H | 55, 104, 125, 249, 250, 274, 277, 281 |
| |  | 262 |
| |  EC, EMC ⟶ | 278 |
| MF: |  | 249 |
| γBL: |  | 123 |
| Linear Carbonates: |  + ROLi + ROR + alkenes | 108, 123, 214, 271, 279 |
| |  + ROLi + alkenes | 284 |

B. Electrolyte Salts and Other Components

| | | | Refs. |
|---|---|---|---|
| Salt | LiClO$_4$: | LiClO$_4$ + ne + 2n Li$^+$ ⇌ Li$_2$O + LiClO$_3$, LiClO$_2$ + LiCl | 249 |
| | LiAsF$_6$: | LiAsF$_6$ + 2e + 2 Li$^+$ ⟶ AsF$_3$ + 3LiF | 120, 249, 250 |
| | | AsF$_3$ + 2ne + 2 nLi$^+$ ⟶ Li$_n$AsF$_{3-n}$ + nLi$^+$ | |
| | LiPF$_6$: | LiPF$_6$ + 2e + 2Li ⟶ PF$_3$ + 3LiF | 125, 250, 279 |
| | | LiPF$_6$ ⇌ LiF + PF$_5$ | |
| | | PF$_5$ + H$_2$O ⟶ 2HF + POF$_3$ | |
| | | PF$_5$ + 2ne +2 n Li$^+$ ⟶ LiPF$_{6-n}$ + nLiF | |
| Contaminants | H$_2$O: | H$_2$O + e + Li$^+$ ⟶ LiOH + H$_2$ | 249, 250 |
| | CO$_2$: | 2CO$_2$ + 2e + 2Li$^+$ ⟶ Li$_2$CO$_3$ + CO | 249, 250 |
| | O$_2$: | O$_2$ + 4e + 4Li$^+$ ⟶ 2Li$_2$O | 249, 250 |
| Secondary Reactions | | LiMF$_n$ + H$_2$O ⟶ LiM$_x$O$_y$ + nHF + MO$_z$F    M = P or B; n = 4, 6 | 125 |
| | |  + HF ⟶ LiF | 104 |
| | |  + H$_2$O ⟶ Li$_2$CO$_3$ + CO$_2$ + 2ROH | 104, 124, 249 |
| | | 2CO$_2$ + 2e + 2Li$^+$ ⟶ 2Li$_2$CO$_3$ + CO | 124 |
| | | Li$_2$CO$_3$ + 2HF ⟶ LiF + CO$_2$ + H$_2$O | 104, 124, 277 |

in the MS.[286] No sign of CO or CO$_2$ had been found, contradicting Schemes 1, 7, and 8. The production of H$_2$ was ascribed to the reduction of trace moisture contamination; thus, the SEI formation process seemed to start below ~0.80 V. However, since the MS can only detect gaseous species, another surface

spectroscopic means based on FT-IR was used as a complimentary analysis. It was concluded that, since the salt anion concentration near the electrode decreases rapidly at the same potential as $H_2$ is formed, the first electrolyte decomposition should occur at potentials near 1.50 V. Microscopic observations on the graphite surface cycling in nonaqueous electrolytes were in agreement with this conclusion; that is, surface deposits were visualized at potentials as high as 2.0−1.50 V near the edge sites, while basal planes would be completely covered at potentials below 0.80 V.[266,267] The combination of DEMS[286] and AFM[266,267] results perfectly echoed the conclusions drawn by Bar-Tow et al.[281] that the film at the edge sites was mainly formed by the reductive process of salt anions at higher potentials (∼1.50 V), while the film on basal planes that is formed at lower potentials (∼0.80 V) has the contribution mainly from solvent reductions.

A few other studies on the SEI placed the occurrence of SEI formation in lower potential ranges that overlap with those of the lithium intercalation process, that is, below 0.25 V. Using a plasma spectrometer, Matsumura et al. conducted quantitative chemical analyses on the lithium content in carbonaceous anodes that were electrochemically lithiated at different stages and correlated the irreversible lithium content (i.e., the electrochemically irremovable lithium that was consumed to form the SEI and then remained therein) with the cathodic polarization potential.[262] Unexpectedly, they found that a rather high portion (>80%) of the lithium was distributed in the potential range 0.50−0.01 V, with a relatively small percentage in the potential range above 0.80 V, where the formation of the SEI was thought to have occurred.

Similar results were obtained by Zhang et al., who analyzed the galvanostic cycling data of a graphite anode in LiPF$_6$/EC/PC/EMC and calculated the distribution of irreversibility in the first lithiation process in different potential ranges.[287] They found that, of the total 7% irreversible capacity in the first forming cycle, a majority (∼6%) was generated within the potential range between 0.25 and 0.04 V, where different stages of LiGIC were formed. The quantitative difference between the results of Zhang et al.[287] and Matsumura et al.[262] on the irreversible lithium at low potential ranges might be due to the different graphitic degrees of the carbon anode materials that were used in their investigations, but the common observation of these two experiments is that, concurrent with lithium intercalation, some other irreversible processes are also underway. A reasonable explanation would be that SEI formation is not completed above 0.80 V but continued deep within the potential range where lithium ion intercalation proceeds.

The electrochemical impedance analysis carried out in the same study by Zhang et al. seemed to confirm the above speculation with the change in the resistance of the SEI film as a function of the lithiation potential and corresponded well with the irreversible capacity analysis. Figure 19 shows the potential-dependence of the resistance for lithium ions in the
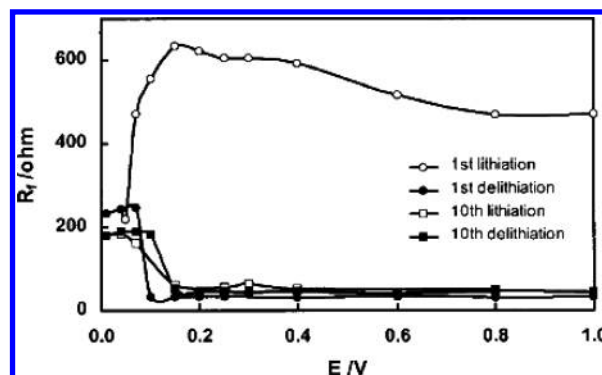


**Figure 19.** Dependence of the resistance ($R_f$) of the SEI film on the cell voltage for the lithium|graphite half-cell using LiPF$_6$/EC/EMC (3:7 wt) as electrolyte. Shown are the data for the 1st and the 10th cycles under galvonostatic conditions with the rate of 0.05 mA h cm$^{-2}$. (Reproduced with permission from ref 287 (Figure 4). Copyright 2001 The Electrochemical Society.)

SEI film when the graphite anode is repeatedly cycled in LiPF$_6$/EC/EMC (3:7 wt). In the potential range above 0.25 V, $R_f$ remains relatively stable at a high level, where solvent decomposition is believed to account for half of the irreversible lithium. The SEI film at this stage is incomplete and porous and, hence, unable to shield the graphite surface from further solvent reactions. A drastic decrease in $R_f$ within a narrow range of 0.20−0.04 V, which accounts for more than half of the irreversible capacity, probably represents a process in which the compact and conductive SEI film is formed and starts to protect the graphite surface.[287] Thus, the authors proposed that SEI formation on a graphite surface actually goes through two stages: (1) at potentials above 0.25 V, where solvent decomposition leaves a primitive surface deposition that is porous and also electronically conducting, and (2) at potentials below 0.25 V, where an insulating and compact SEI is formed. Once formed, this SEI film is protective of the graphite anode, and a reversible impedance response is expected, as shown by Figure 19 for all of the lithiation/delithiation processes after the first lithiation. The above potential-dependence of SEI resistance was reproducible when LiPF$_6$/PC/EC/EMC (1:1:3 wt) was used despite the higher irreversible capacity due to the presence of PC.[287]

The origin of these reductive processes in the lithiation potential range remains unclear, but it does not necessarily involve new components from bulk electrolytes. One possibility is that the radical intermediates, as shown in Schemes 1 and 7, undergo further single-electron reduction, leading to lithium salts with simple anions such as $CO_3^{2-}$, $O_2^-$, or $F^-$,[222,223] while reactions between intercalating lithium ions and the active sites of the graphite interior such as hydroxyls or carbene radicals are also possible.[262]

## 6.3. Electrolyte/Cathode Interface

Compared with the research interest in the passivation of anodes, especially materials with carbonaceous origins, there have been relatively few studies dedicated to the understanding of the interface formed between electrolytes and cathode surfaces. A

probable reason might be the stability of these cathode hosts against solvent cointercalation and exfoliation due to the layered structure being held together by Coulombic interactions between oppositely charged slabs composed of metal cations and oxide anions.[288] Nevertheless, irreversible decompositions, although oxidative in nature, do occur on cathode surfaces, and the decomposition products very likely form a passivation film that prevents any sustained solvent decomposition. In this sense, the interface between electrolyte and cathode should possess the same physicochemical fundaments of the SEI on anodes, that is, electronic insulator and lithium ion conductor. A number of authors have used the term "SEI" as well to describe the passivation of cathode surfaces in lithium/lithium ion cells; however, by the currently accepted convention the term is usually reserved for carbonaceous anodes. Instead, a more general reference of "passivation film" or "surface layer" has been used for electrolyte/cathode interfaces.

### 6.3.1. Passivation Film on a Cathode

The detection of protective films on cathode surfaces has not been as straightforward as that of the SEI on anodes, partially because a native surface film, mainly composed of $Li_2CO_3$, already exists on all transition metal oxide cathode materials based on manganese, cobalt, and nickel.[289−294] This surface component could arise from the precursors used to synthesize these metal oxides or, more likely, from the reaction between the metal oxides and the $CO_2$ in the atmosphere during the processing of these strongly oxidizing materials.[290] Upon contact with electrolytes, this native film is usually eroded by the acidic electrolyte salts currently employed by the lithium ion industry, and to make things more complicated, the active materials are usually involved in the subsequent oxidation of the electrolyte solvents on the exposed cathode surface. Proving the existence of a surface film on the cathodes has been difficult, and spectroscopic identification, which has been proven to be an effective tool in studying the SEI on anodes, often yields ambiguous results.

Goodenough and co-workers were perhaps the earliest authors to suggest that a film exists on the cathode/electrolyte interface.[295] In an attempt to simulate the ac impedance responses of an intercalation-type cathode in liquid electrolytes, they discovered that $Li_{1−x}CoO_2$ in PC cannot be described as a simple intracompound lithium ion diffusion; instead, a more complex electrochemical process, including the formation of a surface layer on the electrode due to the oxidation of the electrolyte, must be considered. They proposed an equivalent circuit, shown in Figure 20, for the lithium intercalation process into such cathodes, wherein $R_e$, $R_{sl}$ and $C_{sl}$, $R_{ct}$ and $C_{ct}$, and $Z_w$ represent the bulk resistance of electrolytes, the resistance and capacitance of the surface layer, the resistance and capacitance of the charge-transfer process, and the Warburg impedance, respectively. In such a model, lithium migration has to go through the surface layer because of its serial nature in order for the charge-transfer and further diffusion within
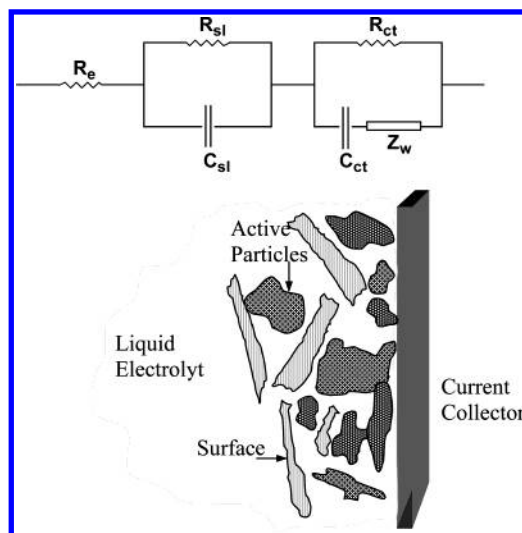


**Figure 20.** Equivalent circuit based on surface layer formation on cathode materials (a, top) and the electrolyte/cathode interface (b, bottom). (Reconstructed based on ref 295.)

the solid to occur. This equivalent circuit and its numerous variations have become a universally adopted model that simulates the behavior of both anode and cathode in nonaqueous electrolytes.

In formulating new electrolyte compositions that can withstand the high potentials of the cathode materials, Guyomard and Tarascon also realized that oxidative decomposition of electrolyte components occurred on cathode surfaces, and passivation of the surface prevented the bulk electrolytes from further decompositions.[93,98] Using $LiPF_6$/EC/DMC and the manganese spinel $LiMn_2O_4$, they systematically explored the origin of the oxidative decomposition by quantitatively analyzing the irreversible capacity associated with electrolyte oxidation and established a correlation between it and the surface area of the composite cathode. Thus, they concluded that the oxidative decomposition of electrolytes on cathodes is surface-catalyzed, and very likely the cathode surface would be covered evenly with a surface layer that is composed of the decomposition products.

Almost during the entire 1990s, the main interest of the lithium ion research community was focused on electrolyte/anode interfaces while its cathode counterpart was overlooked until various lithium ion systems, especially those based on manganese spinel cathodes, were found to suffer power loss and capacity fade upon prolonged cycling or storage at elevated temperatures.[296−302] Preliminary diagnostic studies pointed to electrolyte/cathode interfaces as the source of the degradation, and intensive research has been carried out to address this issue since the late 1990s.

Aurbach et al. studied the interfacial behavior of various cathode materials in $LiAsF_6$/EC/DMC using EIS and found that, for all of these cathodes, that is, $LiNiO_2$, $LiCoO_2$, and $Li_xMn_2O_4$, the impedance spectra obtained reflected several processes in series.[290] In other words, the overall lithium ion intercalation in and deintercalation from a variety of $LiMO_2$ bulk materials included the inevitable step of lithium ion migration through a certain surface layer in a manner very similar to that of the reversible lithium ion

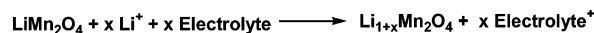intercalation/deintercalation process on carbonaceous materials.

Complementary to the EIS results, wide-line $^7$Li NMR research conducted by Greenbaum and co-workers also supported the existence of such a surface layer.[299] They reported that the lithiated (discharged) cathode $LiNi_{0.8}Co_{0.2}O_2$ showed two identifiable $^7$Li signals with a negligible difference in chemical shift, and these signals were characterized by vastly different spin−lattice relaxation times ($T_1$). The authors assigned the one with $T_1 < 10$ ms to the intercalated lithium ions in the bulk cathode and the other on the order of seconds to the lithium ions trapped in the surface layer. Corresponding $^{19}$F NMR also revealed the existence of a different F other than the binder PVdF; hence, the authors suggested that LiF constitutes the surface layer. However, the double-resonance ($^7$Li−$^{19}$F) measurements that would be sensitive to the presence of LiF were inconclusive.

Visual detection of surface layers on cathodes using microscopy techniques such as SEM seems to be supportive of the existence of LiF as a particulate-type deposition.[292,294] The current sensing atomic force microscope (CSAFM) technique was used by McLarnon and co-workers to observe the thin-film spinel cathode surface, and a thin, electronically insulating surface layer was detected when the electrode was exposed to either DMC or the mixture EC/DMC. The experiments were carried out at an elevated temperature (70 °C) to simulate the poor storage performance of manganese spinel-based cathodes, and degradation of the cathode in the form of disproportionation and $Mn^{2+}$ dissolution was observed.[300] This confirms the previous report by Tarascon and co-workers that the $Mn^{2+}$ dissolution is acid-induced and the electrolyte solute ($LiPF_6$) is mainly responsible.[301]

The speculation about LiF in the surface layer was supported by McBreen and co-workers, who detected the formation of a surface layer on well-cycled $LiNi_{0.85}Co_{0.15}O_2$ in $LiPF_6$/EC/DMC with soft X-ray absorption spectroscopy (XAS).[302] In the energy region between 500 and 950 eV, the cycled cathode demonstrated major changes at O and F K-edges as compared with the pristine powder or as-prepared cathode samples. By comparing with standard LiF XAS, the authors believed the signals to be arising from the mixture of PVdF (as binder) and LiF on the cathode surface. The source of LiF was believed to be generated by the decomposition of $LiPF_6$. Considering that the organic decomposition products are unstable on highly charged cathodes, the authors suggested that the surface layer on the cathode might be composed of a dense coating of LiF. This very resistive surface layer was believed to be responsible for the power loss of the lithium ion cell after prolonged storage.

Aurbach et al. and Andersson et al. also detected the presence of surface layers on cathodes with XPS. The former authors noted that the presence of salts ($LiPF_6$ and $LiAsF_6$) played a crucial role in changing the surface state of cathode materials due to their acidic nature, because pure solvents do not change th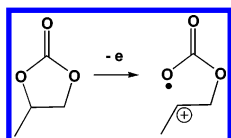e native surface layer, $Li_2CO_3$, when brought into contact with these cathodes.[292] They speculated that the hydrolysis products from the salts such as HF, $AsF_3$, or $AsF_5$ reacted with the native surface layer and led to its breakdown. Thus, it is this heavy involvement of salt anion that generates the detected LiF in the surface layer. By correlating with the EIS study, the effect of LiF on cell impedance was confirmed. During prolonged cycling, the surface layer on the cathode seemed to continue to grow; however, the chemical compositions did not experience qualitative changes. Through comparative studies, the latter authors confirmed Aurbach's observation that the pristine $Li_2CO_3$ surface layer on $LiNi_{0.80}Co_{0.20}O_2$ was changed, as evidenced by a wealth of new chemical components corresponding to the oxidations of both solvents and salt anions, with LiF being the dominant species.[293,294] In view of the highly oxidative nature of metal oxides, these authors suggested a spontaneous formation process for the new surface layer, in which the direct (hence, nonelectrochemical) redox reactions occur between the active materials of cathode and electrolyte components, leading to the lithiation of the former and the oxidation of the latter (Scheme 13). On a manganese spinel cathode, this spontaneous process was complicated by the coupling of the surface oxidations from electrolyte components with the concomitant $Mn_2O_4$ disproportionation and $Mn^{2+}$ dissolution.[293,300] Controversial results from the surface chemistries were obtained.

A few authors argued that the existence of surface layers on cathodes could also be confirmed by the irreversible capacity that only occurs in the first charge process.[303,304] By correlating this irreversible capacity with cell voltages during the forming process of a $LiNiO_2$-based cathode, they concluded that the surface layer was formed via a two-step process: (1) below 3.40 V, where a primitive and resistive film was formed, and (2) between 3.4 and 3.8 V, where a highly conductive film was built up through a further oxidative breakdown of the primitive layer. The EIS study that was carried out simultaneously showed an obvious potential-dependence of the resistance associated with the surface layer (Figure 20), which is characterized by a dramatic drop in the corresponding voltage regions.[303] The possibility of cathode structure reorganization should not be excluded for the irreversible stage between 3.6 and 3.8 V, though, and the authors suggested that probably both electrolyte oxidation and cathode structural transition are responsible.

Similar irreversible processes have been previously observed by Aurbach et al. on $LiNiO_2$[290] and Croce et al. on $LiNi_{0.75}Co_{0.25}O_2$[305] by slow scan cyclic voltammetric (SSCV) measurements. However, in their EIS studies the former authors did not observe any obvious potential-dependence for the resistance associated with the surface layer[290] but rather an invariant resistance in the range between 3.6 and 4.2 V. This latter observation is in direct disagreement

**Scheme 13. Self-Discharge of Spinel Cathode in Electrolyte**

$$LiMn_2O_4 + x\ Li^+ + x\ Electrolyte \longrightarrow Li_{1+x}Mn_2O_4 + x\ Electrolyte^+$$

**Scheme 14. Possible Electrochemical Oxidation Path for PC**



with the results of Zhang et al.[303,304] and Croce et al.,[305] where the change of surface-layer resistance with potential is obvious.

Some authors pointed out that the surface layer on the metal oxide cathodes might not be as stable as that on the carbonaceous anode, and the cell power loss and capacity fade are mainly caused by degradation of this electrolyte/cathode interface.[293] Their argument was supported by the increase in impedance with cycling, which very likely suggests a continued growth of surface layers on the cathode.[292] There was also one report revealing the complete absence of surface layers on cathodes after prolonged cycling, probably indicating that the electrolyte components or impurities react with the surface layer and leave the cathode surface with the IR-insensitive LiF.[298]

### 6.3.2. Characterization of Surface Chemistry

The overwhelming majority of the studies on the oxidative decompositions of solvents and salt anions were carried out on nonactive electrodes.[74,81,120,130,131,204,206,207,306−308] On the basis of the detection of ring-opening reactions by in situ FT-IR, a mechanism involving a single-electron process producing a radical cation was proposed for carbonate solvents (Scheme 14).[307] Subsequent decomposition of the intermediates leads to gaseous as well as solid products, which form a solid film on the electrode. The existence of such radical species during the oxidative decompositions of electrolyte components has been confirmed for a wide variety of electrolytes by ESR, and the surface of a charged cathode ($LiCoO_2$ at 4.3 V) is identified as the source of its generation, because a parallel blank test with electrolytes in the absence of a cathode produces no radical species.[309] The authors depict a picture of delocalized radical cation structures that are coordinated by the neighboring solvent molecules, whose half-life is on the order of minutes depending on the electrolytes. Thus, it is reasonable to believe that Scheme 14 represents the initial oxidative cleavage of the carbonate solvents.

The systematic surface characterization was conducted by Aurbach and co-workers using FT-IR spectroscopy for $LiCoO_2$, $LiNiO_2$, and $LiMn_2O_4$ spinel cathodes.[290] After cycling in electrolyte $LiAsF_6$/EC/DMC between 3.0 and 4.4 V, all of the cathode surfaces were found to be covered with a wealth of new chemical species, while the signals corresponding to the native $Li_2CO_3$ diminished. Preliminary interpretation of these spectra led the authors to conclude that the species very much resemble the lithium alkyl carbonates observed on various anode surfaces that have been formed, as supported by the signals around 1650 $cm^{-1}$. With further study, they confirmed that the electrolyte-related species were
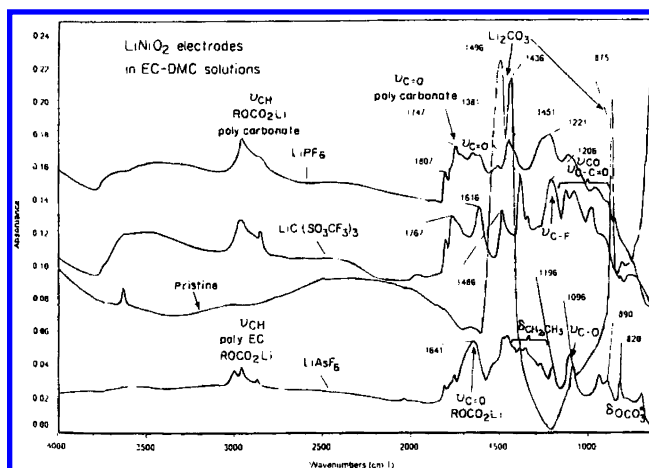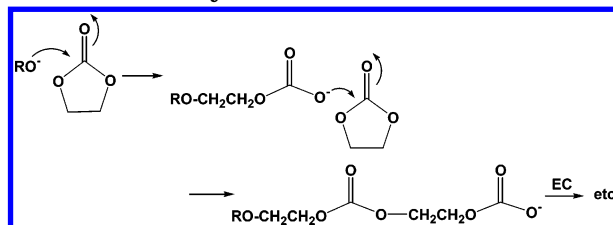


**Figure 21.** FTIR spectra (diffuse reflectance mode) measured from a pristine $LiNiO_2$ composite cathode and with a cathode after galvanostatic cycling in Li salt/EC/DMC solutions. (Reproduced with permission from ref 292 (Figure 1). Copyright 2000 The Electrochemical Society.)

**Scheme 15. Possible Mechanism for the Formation of Polycarbonates**



**Scheme 16. Surface Nucleophilic Reactions between $LiNiO_2$ and Electrolyte Solvents**
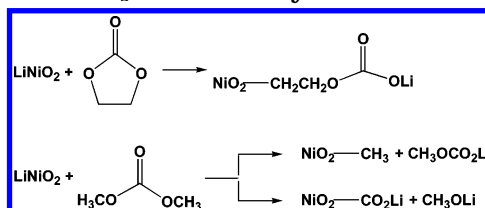


formed on the cathode surface upon storage or cycling but emphasized that, because of the complicated nature of the surface oxidation processes, it is impossible to obtain an unambiguous picture of the surface chemistry.[292] Since the native $Li_2CO_3$ does not change when in contact with pure (salt-free) solvents, the salt anions obviously played a crucial role in forming these new surface species. Cycling seems to facilitate the surface chemistry, as Figure 21 shows, since a variety of absorptions corresponding to C−H, C=O, and C−O bonds were identified. The carbonyl functionality around 1800−1700 $cm^{-1}$ was believed to be polycarbonate species, a possible source of which could be the oxidation of EC or the ring-opening polymerization of EC catalyzed by a nucleophilic mechanism (Scheme 15). The nucleophilic initiator $RO^-$, as evidenced by the absorptions near 1100 $cm^{-1}$, could be generated on the surface of the cathode because of the possible reactions between the active mass and the solvents (Scheme 16). Meanwhile, the signals around 1650 $cm^{-1}$ (asymmetric C=O), 1350−1300 $cm^{-1}$ (symmetric C=O), 1100 $cm^{-1}$ (C−O), and 850 $cm^{-1}$ ($OCO_2^-$) still suggest species with similar structure to alkyl carbonates. Since the mechanism
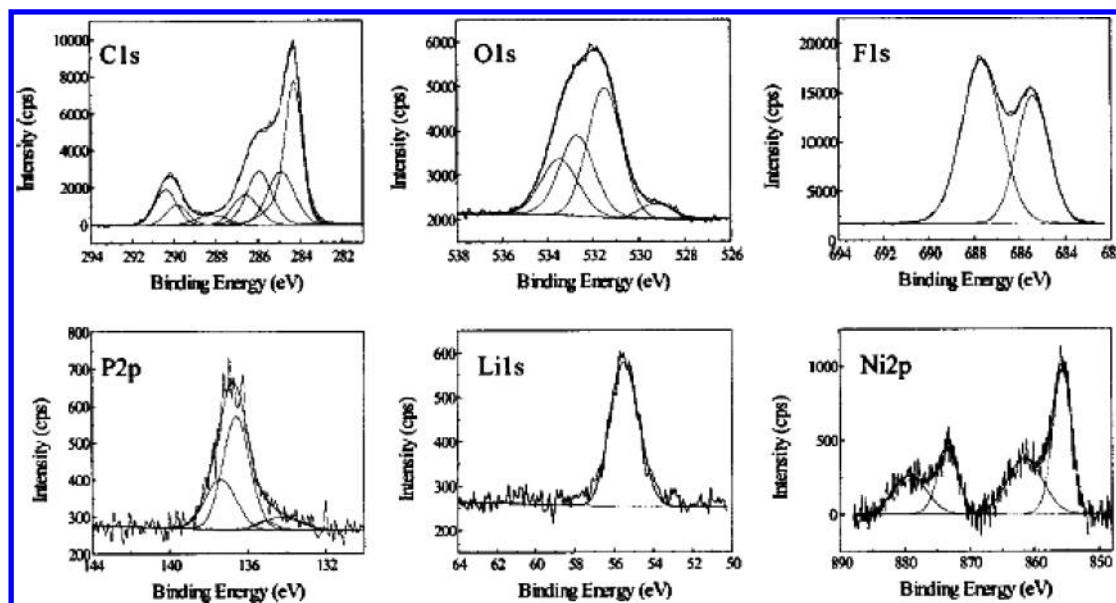
**Figure 22.** C 1s, O 1s, F 1s, P 2p, Li 1s, and Ni 2p XPS spectra for $LiNi_{0.8}Co_{0.2}O_2$ cycled in $LiPF_6$/EC/DEC. (Reproduced with permission from refs 294 (Figure 6). Copyright 2002 The Electrochemical Society.)

in Scheme 16 involves direct electron transfer from electrolyte solvents to electrode active mass, these reactions are spontaneous and do not require cell charging to initiate.

XPS and energy-dispersive X-ray analysis (EDAX) of the cathode surface chemistry clearly revealed that, in various electrolytes using different salts, the salt anions or the impurities related to them were also heavily involved in the surface layer formation.[292] EDAX detected a pronounced increase in the F content of the surface after the cathode was cycled in $LiPF_6$ or $LiAsF_6$ solutions, and appreciable amounts of As or P were also present on the surface. The surface chemistries of a cathode cycled in $LiAsF_6$ solution as detected by XPS correlated well with FT-IR, which confirmed the formation of organic and inorganic carbonates with signals at 285 and 290 eV as well as $RO^-$. The peak at 294 eV was ascribed to polycarbonate species, in accordance with the peaks around 1800−1700 cm$^{-1}$ in FT-IR. However, the cathode surface that had been cycled in $LiPF_6$ solutions lacked the signs of all carbonate or polycarbonate species, and the authors attributed the absence of these carbonyl-containing compounds to the role of HF, which reacts with carbonates and leaves LiF on the surface. This is supported by the F 1s spectra with a strong 685 eV signal, which is smaller for cathode surfaces cycled in $LiAsF_6$ solution. Further examination of F 1s spectra also points to other F-containing species with P−F and As−F bonds, which are evident in As 3d and P 2p spectra as well. Interestingly, Ni 2p signals of oxidation states for various Ni species were also detected in all of the cathode surfaces that were cycled in either $LiPF_6$ or $LiAsF_6$ solutions, as expected from the surface reactions involving $LiNiO_2$ as a nucleophilic agent (Scheme 16).

More recent XPS studies were conducted by Andersson et al. on a similar $LiNi_{0.8}Co_{0.2}O_2$ cathode cycled in $LiPF_6$/EC/DEC, and more detailed efforts were made to assign the signature signals for various surface species.[294] Figure 22 lists the XPS spectra generated from the cathode sample after the formation cycle. In C 1s spectra, three new peaks were ascribed to a polymeric moiety (285.1 eV), a carbon in ether linkage (286.8 eV), and a semi-carbonate such as an alkyl carbonate (290.0 eV). The polymeric moiety could be attributed to hydrocarbon species or polymers based on an ether linkage. On the other hand, quantitative analyses through peak devolution showed that a majority of the surface lithium content is accounted for by the presence of LiF, $LiPF_6$, and $Li_2CO_3$, and alkyl carbonates as well as polycarbonates are also likely. The F 1s spectrum corroborates the dominant presence of LiF by the peak at 684.9 eV, while the other F signal arises from the binder PVdF. P 2p spectra could be deconvoluted into a series of contributing components, which should include the oxidation products from $LiPF_6$ such as $Li_xPF_y$.

Obviously, the above compounds might result from several possible reactions. Since they did not find the transformation of the metastable alkyl carbonate into $Li_2CO_3$ upon high-temperature storage, as they had observed on carbonaceous anodes, Andersson et al. challenged the spontaneous reaction mechanism suggested in Scheme 16 and proposed that the carbonate species on cathode surfaces would be polycarbonates instead of simple alkyl carbonates.[294] Furthermore, self-discharge that leads to lithiation of the cathode host was observed during storage; hence, the authors argued that a mechanism similar to Scheme 13 would be more likely. Thus, the initiation for EC polymerization would be more likely realized by the electrophilic attack from the Lewis acid, $PF_5$, a decomposition product of $LiPF_6$, instead of a nucleophilic attack from $RO^-$. The fact that $PF_5$ reacts with cyclic carbonates, leading to polymerization of the latter, seems to favor this rationale.[298]

In a parallel study performed on the spinel cathode $LiMn_2O_4$, Eriksson et al. reported both XPS and FT-IR results[293] that conflicted with those by Aurbach

**Scheme 17. Mechanism for Electrolyte Oxidation Coupled with Spinel Disproportionation and $Mn^{2+}$ Dissolution**

$$LiMn_2O_4 + 3x\ Li^+ + x\ El \longrightarrow Li_{1+3x}Mn_{2-x}O_4 + xMn^{2+} + x\ El^+$$
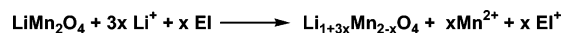
**Scheme 18. Mechanism for Electrolyte Oxidation on a Fully Charged Cathode Surface**

$$2\ \lambda-MnO_2 + x\ Li^+ + x\ El \longrightarrow Li_xMn_2O_4 + x\ El^+$$
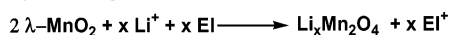
et al.[290,292] Besides polymeric species that were most likely polyethers, there was no sign of any carbonate-like species detected when the spinel was cycled in a $LiPF_6$-based electrolyte, as evidenced by both C 1s and O 1s XPS and FT-IR spectra. F 1s still identified LiF as the major surface species along with partially decomposed products from $LiPF_6$ as well as the $MnF_2$ species. When $LiPF_6$ was replaced by $LiBF_4$, semi-carbonate moieties began to appear in C 1s; therefore, the authors concluded that HF, which was more abundant in $LiPF_6$ solutions, removed the initially formed carbonate species. Meanwhile, a wealth of IR absorptions also indicated the formation of polyether structures for which the mechanism of formation from EC or linear carbonates remains unclear.

The formation of surface species on a spinel cathode surface is complicated by the coupling of electrolyte oxidation with the cathode structural disproportionation and the subsequent $Mn^{2+}$ dissolution.[296,300,310] Combining Scheme 13 with the latter considerations, a modified mechanism was proposed by Eriksson et al. (Scheme 17).[293] This mechanism only seems to apply when the cathode is not fully charged (<4.3 V). Since disproportionation can no longer occur at the fully delithiated potentials (4.3 V) where almost all manganese species are in the $Mn^{4+}$ state and $\lambda$-$MnO_2$ exists as the stable lattice, an alternative mechanism was also proposed by the same authors to account for the surface oxidation of electrolytes in this case (Scheme 18). Since similar surface layers have been observed on spinel cathodes in partially and fully charged states, their thickness and chemical composition do not seem to be dependent on the cathode potential, while thickness does increase with both storage time and temperature.

### 6.3.3. Breakdown of Surface Layer

While the low potential limit an electrolyte faces in lithium ion cells is set by the lithium metal deposition on carbonaceous anodes, the high limit is decided by the breakdown of the surface layer on cathode materials. At potentials above this limit, the protection against electron tunneling is lost and the decomposition of bulk electrolyte components occurs. Because of the limited amount of research carried out on cathode surfaces, there is no microscopic picture available for this breakdown mechanism and it remains unknown whether a global dissolution or physical disintegration of the surface layer is involved or, rather, following a similar mechanism of dielectric capacitor "breakdown", the surface layer remains largely intact but the high potential of the cathode "burns through" pathways for electron conduction at local sites on the surface.

The knowledge about this decomposition upper limit of potential is significant for practical applica-

tions of the electrolytes in actual lithium ion cells, because a number of factors related to the operation of the cell rely on it, such as the potential limit within which the cell can be cycled, the overcharge margin that a certain electrolyte formulation can provide, and the design and selection of cathode materials. Nevertheless, inadequate studies have been conducted so far on this issue, and most of the studies on the oxidative decomposition of electrolytes were carried out on nonactive electrodes on which the oxidative processes for carbonate-based solvents were generally believed to occur at potentials higher than 4.0 V despite the widely scattered data from the different electrode surfaces, salt species, and cutoff criteria employed in those investigations (Tables 4 and 5). However, considering the vast differences in surface areas as well as surface functionalities between the nonactive electrodes and composite cathode materials, there is sufficient reason to question whether the decomposition limits of electrolytes as determined on these nonactive electrodes would serve as reliable references when cathode composites of higher surface area and hence higher surface catalytic activity are in contact with electrolytes.

The discrepancies in stability limits caused by the differences in the surface areas of working electrodes had been noticed by Guyomard and Tarascon early on.[93] The solvent oxidation obviously proceeded with much slower kinetics on Pt electrodes than on composite cathode materials based on spinel manganese oxide. Cattaneo and Ruch[311] and Imhof and Novák[312] also recognized the importance of using the actual battery electrode materials instead of nonactive electrodes to obtain more relevant decomposition potentials of electrolyte components in lithium ion cells. They used manganese dioxide ($MnO_2$), $LiNiO_2$, $LiCoO_2$, and spinel $LiMn_2O_4$ as working electrodes, and they investigated the potential of cathode surface layer breakdown, which was found to vary in a pronounced way with each cathode surface: 4.2 V for $LiClO_4$/PC on $MnO_2$,[311] 4.2 V for LiIm/PC on $LiNiO_2$,[312] and 4.8 V for LiIm/PC on both $LiCoO_2$ and $LiMn_2O_4$.[312] By means of an in situ MS technique, these authors confirmed that the breakdown process was accompanied by the evolution of gas that consisted mainly of $CO_2$ and other species related to salt anions, an indication of bulk decomposition of electrolyte components that involve both salt and solvent.[311,312]

A more conspicuous example is the anodic stability of linear carbonate (Figure 23).[76] While the anodic limits for both DMC and EMC are above 5.0 V on GC, as observed by similar measurements,[313] the major decomposition current starts before 4.5 V for both solvents when a composite cathode based on spinel $LiMn_2O_4$ is used as working electrode.[76] Apparently, the enormous difference between GC and a composite cathode could not be explained solely by the larger surface area of the latter. It seems more likely that the irreversible oxidative processes were catalyzed by the active mass of the spinel surface, possibly involving spinel lattice disproportionation. Therefore, the stability limits as measured on all of these nonactive and nonporous electrodes can be
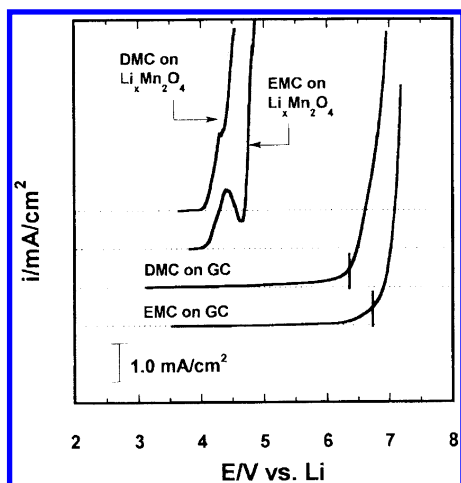
**Figure 23.** Anodic stability of linear dialkyl carbonates on GC and a composite cathode surface. Electrolytes: 1.0 LiPF$_6$ in DMC or EMC, respectively. (Reproduced with permission from ref 76 (Figure 2). Copyright 1999 The Electrochemical Society.)

**Table 7. Electrochemical Stability of Electrolyte Solvents: Active Electrodes**

| electrolyte | working electrode | $E_a{}^a$ | ref |
|---|---|---|---|
| 1.0 M LiClO$_4$/PC/DME (1:1) | LiV$_3$O$_8$ | 4.6 | 307 |
| 1.0 M LiAsF$_6$/PC/DME (1:1) | LiV$_3$O$_8$ | 4.7 | 307 |
| 1.0 M LiClO$_4$/EC/DEE (1:1) | LiMn$_2$O$_4$ | 4.55 | 93 |
| 1.0 M LiIm/EC/DEE (1:1) | LiMn$_2$O$_4$ | 4.4 | 99 |
| 1.0 M LiIm/EC/DME (1:1) | LiMn$_2$O$_4$ | 4.35 | 99 |
| 1.0 M LiPF$_6$/EC/DEE (1:1) | LiMn$_2$O$_4$ | 3.8 | 93 |
| 1.0 M LiBF$_4$/EC/DEE (1:1) | LiMn$_2$O$_4$ | 3.4 | 99 |
| 1.0 M LiClO$_4$/PC | LiMn$_2$O$_4$ | >5.1 | 99 |
| 1.0 M LiBF$_4$/EC/DMC (2:1) | LiMn$_2$O$_4$ | >5.1 | 98 |
| 1.0 M LiClO$_4$/EC/DMC (2:1) | LiMn$_2$O$_4$ | >5.1 | 99 |
| 1.0 M LiPF$_6$/EC/DMC (2:1) | LiMn$_2$O$_4$ | >5.1 | 44, 98 |
| 1.0 M LiClO$_4$/EMS | LiMn$_2$O$_4$ | 5.8 | 75, 314 |
| 1.0 M LiIm/EMS | LiMn$_2$O$_4$ | 5.8 | 75, 314 |
| 1.0 M LiPF$_6$/EMS | LiMn$_2$O$_4$ | 5.8 | 314 |
| 1.0 M LiPF$_6$/EiBS | LiMn$_2$O$_4$ | 5.8 | 314 |
| 1.0 M LiPF$_6$/DMC | LiMn$_2$O$_4$ | ~4.0 | 314 |
| 1.0 M LiPF$_6$/EMC | LiMn$_2$O$_4$ | 4.5 | 314 |
| 1.0 M LiPF$_6$/FPMS/DMC | LiMn$_2$O$_4$ | 5.55 | 314 |
| 1.0 M LiPF$_6$/FPMS/EMC | LiMn$_2$O$_4$ | 5.55 | 314 |
| 1.0 M LiPF$_6$/EC/PC/DMC (1:1:2) | LiNiVO$_4$ | >4.9 | 314 |

$^a$ Anodic limits, potential referred to Li$^+$/Li.

misleading, and the authentic anodic stability limits of any electrolyte component in an actual lithium ion device can only be evaluated on the surface of the electrode that is used in the device.

Unfortunately, this approach for electrochemical stability determination has not been widely adopted. The few exceptions include the seminal electrolyte work by Guyomard and Tarascon.[98,99] In the formulation of new electrolytes for lithium ion technology, the spinel composite electrode was used as the standard working surface in all of the voltammetric measurements. The oxidative decomposition limits of the new electrolytes thus determined are summarized in Table 7 along with a handful of stability data that were determined in a similar approach for other electrolyte systems.

Figure 24 shows the result of the voltammetry for EC/DMC- and EC/DEE-based electrolytes. The typical two-step process between 3.9 and 4.3 V corre-
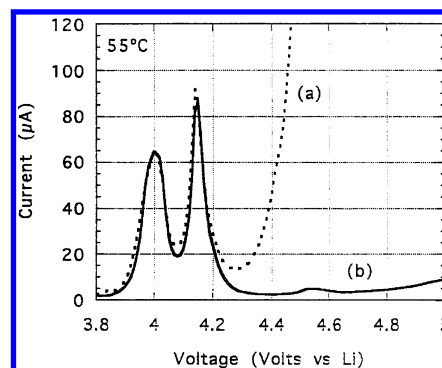


**Figure 24.** Voltammogram at 55 °C for the electrolytes (a) 1.0 M LiClO$_4$/EC/DEE and (b) 1.0 M LiPF$_6$/EC/DMC on spinel cathode LiMn$_2$O$_4$. (Reproduced with permission from ref 98 (Figure 1). Copyright 1993 The Electrochemical Society.)

sponds to the delithiation of the spinel structure, which is reversible. The oxidative decomposition of DEE occurs below 4.4 V almost immediately after the delithiation is completed. This proximity to the potential of the cathode electrochemistry leaves little tolerance for overcharge. On the other hand, the EC/DMC-based electrolyte only shows negligible background current before 5.1 V. After 4.3 V, the spinel lattice has actually turned into $\lambda$-MnO$_2$. On the surface of the $\lambda$-MnO$_2$, the low current of the EC/DMC exhibits the extreme stability of this mixed carbonate formulation. As already pointed out in earlier sections, the replacement of ether compounds by linear carbonate results in a significant expansion of the oxidative potential limits by ~0.80 V.

The anodic limit for the electrochemical stability of these carbonate mixtures has been determined to be around 5.5 V in numerous studies.[314–317] Thus, new electrolyte formulations are needed for any applications requiring >5.0 V potentials. For most of the state-of-the-art cathode materials based on the oxides of Ni, Mn, and Co, however, these carbonate mixtures can provide a sufficiently wide electrochemical stability window such that the reversible lithium ion chemistry with an upper potential limit of 4.30 V is practical.

When the poor anodic stability of DMC or EMC alone on a similar cathode surface is considered,[76] the role of EC in stabilizing the solvent system becomes obvious. A conclusion that could be extracted from these studies is that the existence of EC not only renders the electrolyte system with superior cathodic stability by forming an effective SEI on the carbonaceous anode but also acts as a key component in forming a surface layer on the cathode surface that is of high breakdown potential. It is for its unique abilities at both electrodes that EC has become an indispensable cosolvent for the electrolyte used in lithium ion cells.

### 6.3.4. Passivation of Current Collector

Another issue closely related with the anodic stability of electrolytes is the interaction between electrolyte components and the commonly used cathode substrate Al in lithium ion cells.

Al and Cu foils are used as current collectors for cathode and anode materials, respectively, in lithium

ion cells. In a working lithium ion cell that uses liquid electrolytes, the thin coating of active electrode materials is soaked with the liquid electrolytes and the interaction between the electrolyte components and the current collectors strongly affects the performance stability of the cell, especially at the cathode side, where Al is constantly held at high potentials. It has been confirmed by numerous observations that, in well-cycled lithium ion cells, the Al substrate suffers severe pitting-like corrosion at a fully charged state, which leads to a shortened calendar life and fading capacity.[298,318,319] Because very thin Al foils are used (down to 10 $\mu$m) in consideration of the energy density, the pitting could cause complete disintegration and fragmentation in some cases.

Few significant efforts were made on this issue before a new lithium salt (LiIm) was found to cause serious Al corrosion in nonaqueous electrolytes during the early 1990s.[141] Only in recent years has an in-depth understanding of this phenomenon been obtained, a direct result from the increased research interest driven by the expectation that this new salt may replace the thermally unstable LiPF$_6$.[153,154,320−323]

Al is thermodynamically unstable, with an oxidation potential at 1.39 V.[3] Its stability in various applications comes from the formation of a native passivation film, which is composed of Al$_2$O$_3$ or oxyhydroxide and hydroxide.[320] This protective layer, with a thickness of ~50 nm,[322] not only stabilizes Al in various nonaqueous electrolytes at high potentials but also renders the Al surface coating-friendly by enabling excellent adhesion of the electrode materials. It has been reported that with the native film intact Al could maintain anodic stability up to 5.0 V even in LiIm-based electrolytes.[147] Similar stability has also been observed with Al pretreated at 480 °C in air, which remains corrosion-free in LiClO$_4$/EC/ DME up to 4.2 V.[156] However, since mechanical damage of the native film (e.g., accidental abrasion) is often inevitable during electrode processing and cell assembly, the in situ re-forming of a protective surface layer in lithium ion cells depends strongly on the electrolytes.

In comparison with the surface layer chemistry on active cathode materials where both salt anions and solvents are involved, a general perception extracted from various studies is that the salt species has the determining influence on the stabilization of the Al substrate while the role of solvents does not seem to be pronounced, although individual reports have mentioned that EC/DMC seems to be more corrosive than PC/DEC.[321] Considering the fact that pitting corrosion occurs on Al in the polymer electrolytes LiIm/PEO[322] or LiTf/PEO,[323] where the reactivity of these macromolecular solvents is negligible at the potentials where the pitting appears, the salt appears to play the dominant role in Al corrosion.

Among the various lithium salts investigated, LiPF$_6$, LiAsF$_6$, and LiBF$_4$ were found to effectively passivate and stabilize Al at higher potentials (>4.2 V) than required by the operation range of common cathode materials based on LiNiO$_2$, LiCoO$_2$, and LiMn$_2$O$_4$, while LiIm, LiTf, and their derivatives



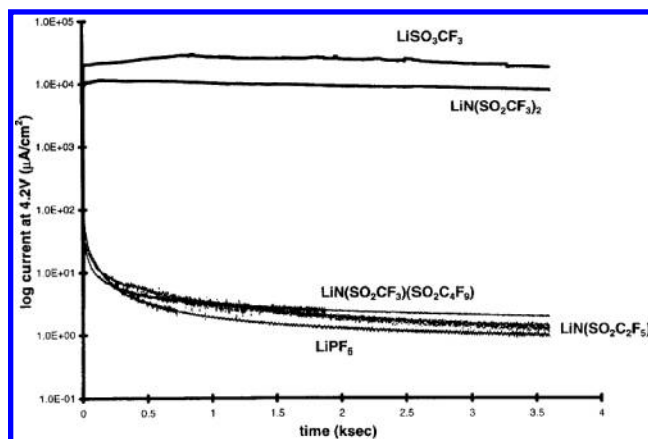**Figure 25.** Al corrosion current density at 4.20 V (vs Li$^+$/ Li) in 1.0 M PC solutions of various lithium salts showing a difference between Tf$^−$, Im$^−$, and other anions. (Reproduced with permission from ref 141 (Figure 1). Copyright 1997 Elsevier.)

usually caused severe corrosion on the Al surface, as indicated by the high anodic current at potentials as low as 3.0 V.[141,147,155,156] Figure 25 compares the ability of selected lithium salts to stabilize the Al surface in the electrolytes containing them. The passivating ability of the salt anion does not appear to depend on the solvent used, and in one solvent mixture, EC/DME, the following stability order is established:[156]

$$LiBF_4 > LiPF_6 > LiClO_4 > LiIm > LiTf$$

New synthetic efforts generated a few structural derivatives of LiIm with longer perfluorinated alkyls such as LiBeti and a lithium salt of an asymmetric imide anion, and the stability of Al in the electrolytes based on these salts was found to be much improved when compared with those in electrolytes based on LiIm and LiTf.[141,148]
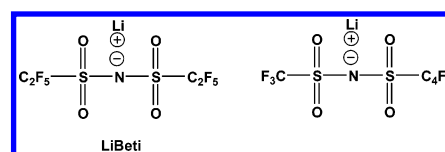


Krause et al. thus believed that a correlation existed between anion molecular weight and their protective abilities, although the complete mechanism is not clear.[141]

A distinctive dissimilarity between the passivation of Al and the formation of an SEI on a graphitic anode is the effectiveness of surface pre-formation: while it has been reported in numerous studies that an SEI formed in one electrolyte can continue to protect the graphite structure when the anode is transferred to another exfoliating electrolyte (such as PC),[250,255,324] Al that has been pretreated in LiPF$_6$- or LiBF$_4$-based electrolytes still suffers severe anodic corrosion when switched to LiTf- or LiIm-based electrolytes.[141,156] This observation provides additional evidence supporting the hypothesis that an oxidative decomposition of anions occurs at the Al surface.[141]
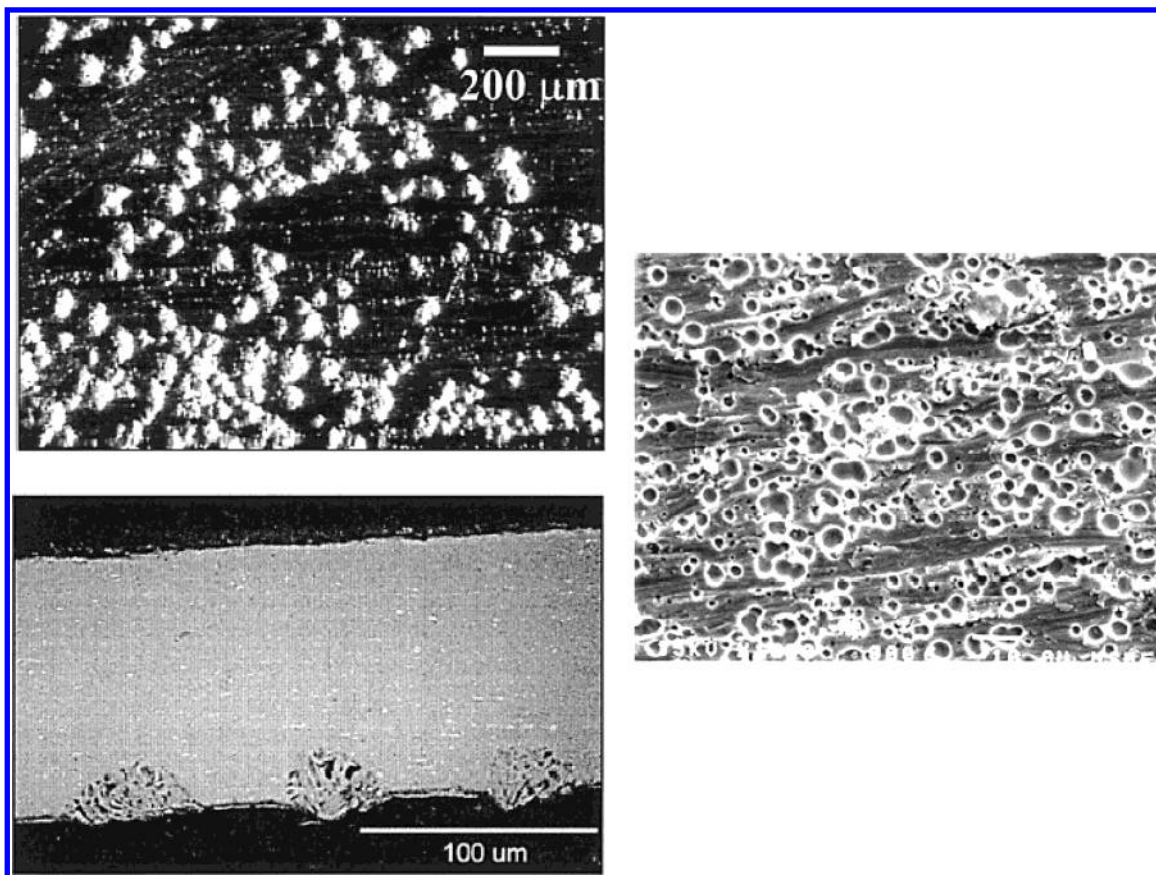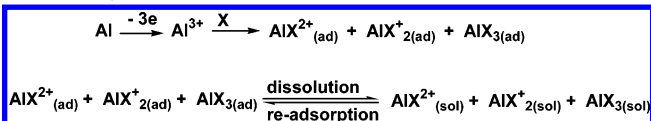
**Figure 26.** Micrographs of a corroded Al surface in various electrolytes. (a, top left) Micrograph in LiPF$_6$/EC/DMC electrolyte, after 150 electrical cycles. The light areas are mounds or nodules. (Reproduced with permission from ref 321 (Figure 7). Copyright 1999 The Electrochemical Society.) (b, bottom left) SEI image of the cross-sectional view of the mounds as shown in part a. (Reproduced with permission from ref 321 (Figure 8a). Copyright 1999 The Electrochemical Society.) (c, right) Micrograph in LiIm/PEO after 1 h of galvanostatic polarization at 100 $\mu$A cm$^{-2}$. (Reproduced with permission from ref 322 (Figure 14). Copyright 1999 The Electrochemical Society.)

Microscopic examination of the aged Al retrieved from well-cycled cells found that, even in electrolytes based on LiPF$_6$ or LiBF$_4$, localized pitting occurred on the Al (Figure 26a).[298,318,319] Closer examination of these corrosion sites under an SEM revealed that what had optically appeared to be a "pit" was actually a "mound" or "nodule" (Figure 26b) where both Al(0) and Al$_2$O$_3$ existed, according to XPS analysis.[321] Due to the anodic state of the Al during the electric cyclings in these cells, the presence of Al(0) practically suggests that the mounds were somehow electrically isolated from the foil. The authors presented two possible explanations for this situation: (1) corrosion and its associated reaction products undermined the surface of a developed pit and caused the overlying metal to bulge or break away or (2) a soluble Al(III) corrosion product was electrodeposited onto the poorly conductive solid corrosion products during the cathodic process (discharge) so that reduction actually occurred. The fact that the open circuit voltage (OCV) of Al lies between 3.2 and 3.6 V makes the latter reductive step possible in normal battery cyclings.

On the other hand, when the electrolyte salts were LiTf or LiIm, serious corrosions in the form of high-density pits were visible before any extensive cycling was conducted,[141,322] as shown by Figure 26c, where Al was merely polarized anodically in a LiIm-based electrolyte for a much smaller time scale than that of prolonged cycling in an actual rechargeable cell. The damage to Al in these cases was on a macroscopic scale.

Impedance analyses of the Al under corrosion were conducted via EIS. On the basis of the models previously established for the corrosion of other metals in both aqueous and nonaqueous electrolytes,[325,326] the corrosion process was proposed as a two-step adsorption/oxidation/desorption process (Scheme 19).[147,156]

The impedance response with frequency can be closely simulated by the equivalent circuit shown in Figure 27a, where $R_e$, $R_{ct}$, $C_{dl}$, $R_{ad}$, and $C_{ad}$ represent the resistance or capacitance for the electrolyte solution, charge-transfer, double layer, and adsorbed layer, respectively. An interesting correlation was found between the passivating ability of various anions and the resistances of the two impedance components $R_{ct}$ and $R_{ad}$, which are high for LiPF$_6$- and LiBF$_4$-based electrolytes and low for LiTf- or LiIm-based electrolytes.[156] Using the rationale proposed by the authors, the former component ($R_{ct}$) is

**Scheme 19.  Al Corrosion in Nonaqueous Electrolytes**

$$Al \xrightarrow{-3e} Al^{3+} \xrightarrow{X} AlX^{2+}_{(ad)} + AlX^{+}_{2(ad)} + AlX_{3(ad)}$$

$$AlX^{2+}_{(ad)} + AlX^{+}_{2(ad)} + AlX_{3(ad)} \underset{\text{re-adsorption}}{\overset{\text{dissolution}}{\rightleftharpoons}} AlX^{2+}_{(sol)} + AlX^{+}_{2(sol)} + AlX_{3(sol)}$$
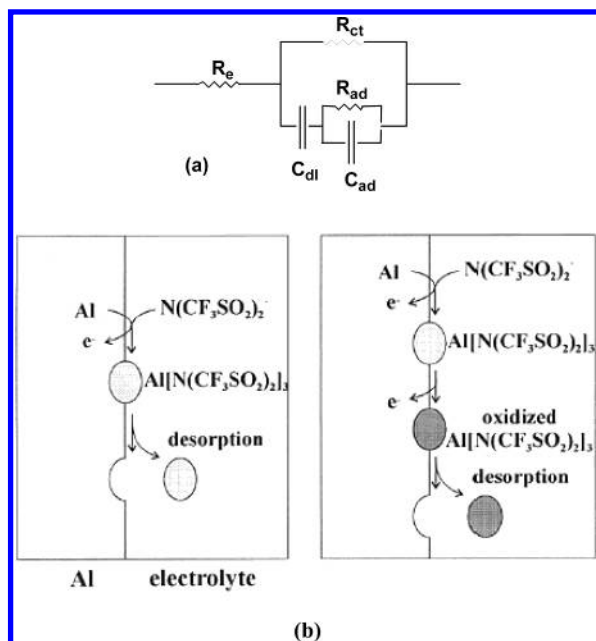
**Figure 27.** (a) Equivalent circuit used to express the corrosion process of Al. (b) Schematic representation of a possible mechanism for Al corrosion in LiIm-based electrolytes. (Reproduced with permission from ref 147 (Figure 14). Copyright 2000 The Electrochemical Society.)

related to the exchange current ($i^0$) at the electrolyte/Al surface:

$$R_{ct} = \frac{RT}{nFi^0} \tag{11}$$

while $R_{ad}$ indicates whether an adsorbed (passivation) layer could adhere to the surface of Al. Therefore, the physicochemical nature of the passivation layer is dictated by its chemical composition, which is in turn strongly affected by the anion oxidation chemistry.

Surface chemical characterization of the passivation layer on the Al surface has been performed mainly via XPS, and the interpretation of results generated by various researchers still remains controversial. Because salt anions with active fluorine (LiPF$_6$, LiAsF$_6$, and LiBF$_4$) are able to form stable surface layers on Al and protect it from corrosion, early studies had suggested that fluoride species such as LiF and AlF$_3$ are crucial to the protection.[141,153,154] The XPS study by Kanamura et al. seemed to support this speculation, having observed the F 1s signal at 686.5 eV on Al that had been passivated in LiPF$_6$/PC electrolyte.[148,327] Thus, they concluded that the surface species on Al after prolonged exposure to the above electrolyte consisted of a mixture of Al$_2$O$_3$ and AlF$_3$.

Krause et al. challenged this assignment of the F 1s signal.[141] In their XPS study of Al cycled in electrolytes based on LiIm, LiBeti, and LiPF$_6$, they also observed this F signal that is typical of metal fluoride, but they believed that LiF instead of AlF$_3$ would be responsible for it because of the detection of Li and the relative abundance of these two elements. Carbonate species as indicated by both C 1s and O 1s spectra were also present, which may exist in the forms of either Al$_2$(CO$_3$)$_3$ or Li$_2$CO$_3$. Thus, the authors postulated that oxidation of solvent also

occurs, probably by an Al$^+$-mediation mechanism. According to this mechanism, upon polarization of Al at high potentials, highly reductive intermediates of Al$^+$ were generated,[328,329] and they migrated to the vicinity of the passivation layer/electrolyte interface, where they subsequently reacted with adsorbed anions or solvents. Thus, the reaction kinetics depend on how readily the anions or solvents are adsorbed on the Al surface or surface layer.

The depth profile established by Ar$^+$ sputtering detects the distinct difference between the Al surfaces that are aged in various electrolytes, which suggests that a much thicker surface layer is formed in LiIm than in LiPF$_6$ or LiBeti electrolytes.[141] It appears that the high corrosion of Al in a LiIm-based electrolyte stems from a relatively porous and diffuse passivation layer where the high levels of LiF contribute to the disorder and porosity of the otherwise dense and protective Al$_2$O$_3$ or carbonate layer. The latter is found in Al surfaces passivated in LiBeti or LiPF$_6$.[141] Combining the above observations, Krause et al. explained the correlation between anion size and the passivating ability by referring to the ability to adsorb on the Al surface. Thus, small anions such as Tf$^-$ and Im$^-$ tend to adsorb to a high packing density, and their reduction by Al$^+$ predominates the surface process, with the product of LiF rendering the film nonprotective. Beti$^-$ anions adsorb poorly, and therefore, the reduction of solvent molecules prevails, with the surface layer consisting of a dense protective carbonate species. It must be pointed out that this mechanism remains to be confirmed with more direct evidence of the presence of Al$^+$ because the reductive process of solvents at a positively charged cathode does sound very unusual.

On the other hand, an XPS study by Braithwaite et al. on aged Al in LiPF$_6$/EC/DMC or LiPF$_6$/PC/DEC identified Li, F, and P as the major surface species, and the authors believed that the signals for these species were not simply from the adsorbed electrolytes because twice as much F was observed on the surface than would be associated with the PF$_6^-$ anion.[321] The existence of these nonstoichiometric compositions suggested that the oxidative decomposition of the salt anion had occurred. The high binding energy of Li as observed in Li 1s spectra indicates that such Li species exist in a very electron-deficient environment, as one similar to LiF. However, the observed binding energy for F is typical for the $-$CHF$_2$ species and distinctively different from that of a metal fluoride. Further attempts to analyze these pit nodules by XPS analysis proved to be inconclusive because of the high inhomogeneity of these areas, which exhibited complex chemistries that varied from nodule to nodule. In general, high concentrations of Li and F as well as Al$_2$O$_3$ were confirmed. On the basis of these seemingly conflicting results, the authors concluded that the role of these surface species formed in nonaqueous electrolytes could not be determined, and the protection against corrosion could simply have come from the native passivation film Al$_2$O$_3$.

More recently, Kanamura et al. studied the corrosion of an Al electrode that was anodically polarized

at a series of potentials in nonaqueous electrolytes based on LiIm, LiTf, and a new asymmetric imide, $Li(CF_3SO_2)(C_4F_9SO_2)N$, using both XPS and FT-IR.[148] These spectra confirmed the presence of organic species on the Al surface, and by monitoring the IR signature absorption for the carbonate functionality at 1710 cm$^{-1}$, they determined that these species appeared at ~3.6 V in LiIm- and LiTf-based electrolytes; however, when using $LiPF_6$, $LiBF_4$, and $LiClO_4$, this absorption was not found till 5.2, 4.4, and 4.6 V,[327] respectively. Hence, they argued that, while Al was well passivated by the native $Li_2CO_3$ film, such an oxidation by electrochemical means would not occur. In other words, the difference in the effect of the electrolyte components on Al stability is not in how they decompose to form a new protection layer—such as through the familiar mechanism of SEI formation—but in how inert they are to the existing native layer. This inertness depends on the cathode potential, and the occurrence of solvent oxidation is indicative of the breakdown of the native passivation film. Apparently, Tf$^-$ and Im$^-$ anion species are corrosive to the native film, so the breakdown potential of it is much lower in the electrolytes based on these salts. Therefore, it would be reasonable to believe that a reaction occurring between $Al_2O_3$ and electrolyte solutes at high potentials is responsible for the onset of major corrosion, during which the coordination ability of Im$^-$ and Tf$^-$ anions toward $Al^{3+}$ acts as the driving force that accelerates the anodic dissolution of Al substrate.

Large anion size was also found to favor Al stabilization, since the 1710 cm$^{-1}$ signature did not appear till a potential higher than 5.0 V was reached for the new, asymmetric imide. Unlike the interpretation of Krause et al.,[141] Kanamura et al. attributed its inertness to the well-distributed negative charge and the lower probability of these anions forming an ion pair with $Al^{3+}$.[148]

The only in situ and semiquantitative study on Al corrosion was carried out by Yang et al. using EQCM to monitor the mass change of an Al electrode in various electrolytes based on LiIm, LiTf, $LiPF_6$, $LiBF_4$, and $LiClO_4$.[147] The most interesting discovery was that, during the process of corrosion in all of the electrolytes, the mass change of Al was positive (i.e., the Al electrode gained net weight) instead of losing weight, as one would expect from a simple anodic dissolution of Al.

Furthermore, normalization of the weight gain against the corresponding charge quantity offered a semiquantitative method to identify the possible species formed, and in the case of $LiBF_4$- and $LiPF_6$-based electrolytes, $\Delta m/\Delta Q = 26-27$ was obtained, suggesting that essentially identical species were adsorbed on Al. Compounds with similar $\Delta m/\Delta Q$ values include $AlF_3$ ($\Delta m/\Delta Q = 19$) and $Al_2(CO_3)_3$ ($\Delta m/\Delta Q = 30$). On the other hand, LiTf- and LiIm-based electrolytes are characterized by very high $\Delta m/\Delta Q$ values. For example, in chronoamperometry stepped from 2.0 to 4.5 V, an Al electrode in LiIm/PC is accompanied by a $\Delta m/\Delta Q = 174$. It appears that the initial oxidation could be due to the formation of an Al compound of large molecular weight such as Al-

(Im)$_3$ ($\Delta m/\Delta Q = 280.2$) or a reaction intermediate of Al$^+$ or of a solution species,[141] but these compounds rapidly desorb from the Al surface, reducing the numerator in $\Delta m/\Delta Q$.

On the basis of the EQCM observations, the authors proposed an adsorption/oxidation/desorption mechanism for the severe pitting corrosion of Al in LiIm- and LiTf-based electrolytes, which is schematically shown in Scheme 19 and Figure 27b.[147] According to this mechanism, Al oxidizes to form adsorbed Al(Im)$_3$ that eventually desorbs from the surface because these species are soluble in the electrolyte solvents. It is the desorption of these oxidized products that leaves the otherwise smooth Al surface with pits. The possibility also exists that, before desorption occurs, the adsorbed species undergoes further oxidation; however, since the oxidation of Im$^-$ is insignificant below 4.5 V according to studies carried out on nonactive electrodes similar to Al,[81,130,131,206] it seems unlikely that further oxidation of the adsorbed Al-(Im)$_3$ would occur.

On the other hand, the oxidized products in $LiPF_4$ and $LiBF_4$ electrolytes could consist of less soluble species such as $AlF_3$ and $Al_2(CO_3)_3$, as suggested by $\Delta m/\Delta Q = 26-27$, indicating negligible desorption from the Al surface and therefore less corrosion of the Al substrate.

## 6.4. A Few Words on Surface Characterizations

Beyond any doubt, the electrode/electrolyte interfaces constitute the foundations for the state-of-the-art lithium ion chemistry and naturally have become the most active research topic during the past decade. However, the characterization of the key attributes of the corresponding surface chemistries proved rather difficult, and significant controversy has been generated. The elusive nature of these interfaces is believed to arise from the sensitivity of the major chemical compounds that originated from the decomposition of electrolyte components.

Hence, the presence of trace impurities, which either pre-exist in pristine electrode and bulk electrolyte or are introduced during the handling of the sample, could profoundly affect the spectroscopic images obtained after or during certain electrochemical experiments. This complication due to the impurities is especially serious when ex situ analytic means were employed, with moisture as the main perpetrator. For cathode/electrolyte interfaces, an additional complication comes from the structural degradation of the active mass, especially when over-delithiation occurs, wherein the decomposition of electrolyte components is so closely entangled with the phase transition of the active mass that differentiation is impossible. In such cases, caution should always be exercised when interpreting the conclusions presented.

On the other hand, when the chemical composition of the surface layer is discussed, distinction should be made regarding the conditions under which such characterizations were carried out and the history of the electrode surface. For example, an electrode surface that was subjected to long-term cycling is certainly different from the surface state of the same

electrode that only experienced the initial forming process. Unfortunately, this distinction was seldom made in the literature. Most work also failed to characterize the pre-existing film on the electrode surface prior to electrochemical studies, and this neglect could lead to significant misinterpretation of the surface chemistry, because organic species could pre-exist on cathode as well as anode surfaces as the result of various contaminations or processing. In this sense, to obtain insightful understanding about the interfacial chemistries in a lithium ion cell, close collaboration is still needed between electrochemcal and spectroscopic characterizations.

## 7. Chemical and Thermal Stability/Safety of Electrolytes

### 7.1. Long-Term Stability of Electrolytes at Elevated Temperatures

In most cases, the electrochemical stability of electrolyte components was studied at room temperature with various galvanostatic or voltammetric experimental techniques that were conducted within a certain time scale, usually $<10^5$ s. The stability thus determined should be considered relatively "transient" where the application in a longer time frame comparable to the cell lifetime is concerned, since the effect of those irreversible reactions of slow kinetics at room temperature, occurring either between the bulk electrolyte components (chemical) or between the electrodes and the electrolytes (electrochemical), cannot be factored in by such time-limited measurements. Only when stability of electrolytes is considered in a longer time frame ($t \sim 10^6$ s or up to months) can the impact of these reactions be visible. As a consequence of the slow irreversible processes, the performances of the lithium cells are often adversely affected, as typically evidenced by the persistent fade in capacity, loss in power rate, and increasing internal pressure within the cell, which can be attributed respectively to the irreversible consumption of the limited lithium ion sources, the depositions of high-impedance products on the electrode surface, and the generation of gaseous products by slow reactions.[152,277,297,309]

On the other hand, since most of these reactions are thermally activated, their kinetics are accelerated by the rise in temperature in an Arrhenius-like manner. Therefore, within a much shorter time scale, the adverse effect of these reactions could become rather significant during the storage or operation of the cells at elevated temperatures. In this sense, the long-term and the thermal stability of electrolytes can actually be considered as two independent issues that are closely intertwined. The study of temperature effects on electrolyte stability is made necessary by the concerns over the aging of electrolytes in lithium-based devices, which in practical applications are expected to tolerate certain high-temperature environments. The ability of an electrolyte to remain operative at elevated temperatures is especially important for applications that are military/space-related or traction-related (e.g., electric or hybrid electric vehicles). On the other hand, elevated tem-

**Scheme 20. Bulk Reaction between Electrolyte Components at Elevated Temperatures**
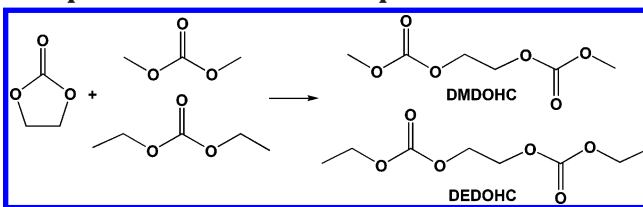


peratures are also often used as an accelerating tool to study the otherwise slow reactions at ambient conditions.

The intrinsic instability of the state-of-the-art electrolyte systems seems to arise mainly from the interaction between the cyclic carbonate and the Lewis acids, HF, $PF_5$, or $PO_xF_y$,[150,330] which are generated by the decomposition or the hydrolysis of $LiPF_6$ by trace moisture. While typical electrolyte compositions such as $LiPF_6$/EC/DMC could seem to be indefinitely stable at room temperature in the proper containers,[331] Kinoshita and co-workers found that significant decomposition occurred during storage under He atmosphere at 85 °C, as indicated by discoloration, gas production, and solid precipitation.[152] They estimated that at 85 °C the reactions were accelerated 10-fold as compared with the case of room temperature. Chemical analysis conducted on the stored electrolyte solution with a gas chromatograph detected the formation of a series of new species, among which the major component had a higher retention time (thus lower volatility) than EC. Through comparison with an authentic sample, the authors identified this species as dimethyl-2,5-dioxa-hexane carboxylate (DMDOHC), which was obviously formed from the ring-opening of EC and its subsequent transesterification with DMC (Scheme 20). Electrolytes based on an EC/DEC mixture rendered the corresponding product, DEDOHC, as shown in Scheme 20.[48a,298] The effect of such a transesterification species on the performance of electrolytes in lithium ion cells has not been described.

Other species with higher retention times were suggested to be the products formed through the coupling of two ring-opened EC or oligoether compounds. On the other hand, the $^1H$ NMR conducted on the reacted electrolyte showed broad singlet bands of equal intensity at 3.746 and 4.322 ppm vs TMS, which resembled those reported for the poly(ether carbonate) as polymerization products of EC.[332,333] The authors concluded that the polymerization and the transesterification were possibly initiated by $PF_5$. To confirm this hypothesis, they introduced newly generated $PF_5$ gas into the solvent mixture EC/DMC. After 10 h at room temperature, similar reaction patterns were observed by chromatography, with the above mixed carbonate as the major decomposition product, although its abundance was much lower. Minor differences unaccounted for between the two chromatographs were attributed to the presence of $Li^+$ as well as the high ambient temperature in the thermal reaction.

By monitoring the change in the ratio of EC/DMC over time, Kinoshita and co-workers also noticed that EC decreased at a more rapid rate than DMC,

**Scheme 21. Ester Exchange between Electrolyte Solvents**



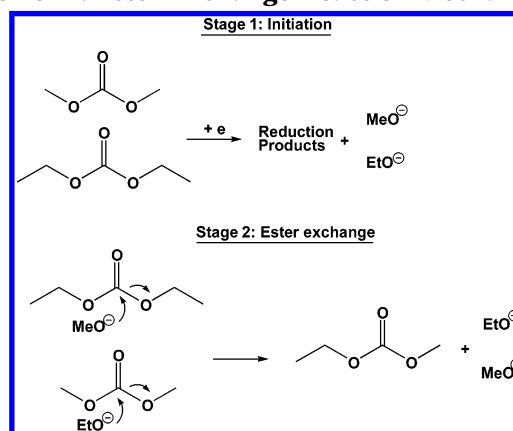**Scheme 22. Ester Exchange Reaction Mechanism**
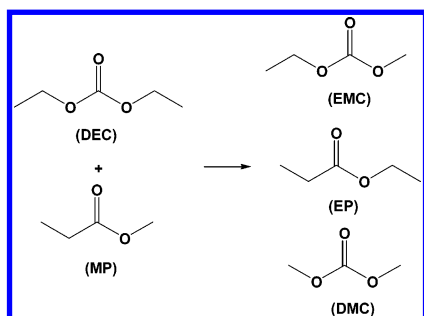


probably because $PF_5$ preferentially attacks the cyclic structure of EC. This hypothesis is consistent with the well-studied ring-opening polymerization of EC that is usually initiated by cationic species, as shown in Schemes 4, 12, and 15. The polymeric product could be a mixture of oligoether and polycarbonate structures.[332,333]

Besides salt/solvent interactions, the ester exchange between linear carbonates was also observed during the cycling of the cells. Terasaki et al. were the first to observe that a significant amount of EMC was formed in a solvent mixture of DMC and DEC and proposed a reductively initiated mechanism.[334] Interestingly, a corresponding oxidatively initiated mechanism was suggested by Ohta et al., when they observed that EMC, ethyl propionate, and DMC were generated from the original solvent mixture of DEC and methyl propionate (Scheme 21).[335] In both cases, EC was used as a cosolvent and $LiPF_6$ as an electrolyte salt, but no identification of any products that involved the participation of these two components was reported, probably because of the slow kinetics at room temperature or the insensitivity of the analytical method used to detect the new products.

Takeuchi et al. thoroughly investigated the ester-exchange reaction between DMC and DEC in the presence of PC and $LiPF_6$. By exposing the solvent mixture to individual cell components, including charged electrode materials at different potentials, salts, and acid impurities (HF), and monitoring the generated EMC content by means of a gas chromatograph, they conclusively proved that the ester-exchange process was reductively initiated by the lithiated carbon anode with potentials below 1.50 V and essentially negated the oxidative mechanism proposed by Ohta et al.[336] Since DMC and DEC could also be detected from the original PC/EMC mixture in the presence of the lithiated carbon, the exchange process should be reversible.

In a further effort to identify the active intermediate that initiates the reaction, they tested the effect of a few possible ingredients on the production of EMC based on the knowledge about the chemical composition of the SEI on carbonaceous anodes. These model compounds included $Li_2CO_3$, $LiOCH_3$, and LiOH, while lithium alkyl carbonate was not tested due to its instability and therefore rare availability.[337] The results unequivocally showed that $LiOCH_3$ effectively catalyzes the ester exchange.

A two-stage mechanism was proposed by Takeuchi et al. based on these observations, wherein the

generation of alkoxide anions is followed by the addition of them to the carbonyls of linear carbonates (Scheme 22). In other words, the ester-exchange reaction should start concurrently with the formation of the SEI, as shown in Scheme 7. According to the above mechanism, the alkoxide anions, once generated in the first stage, would continue to be produced in a chain reaction manner, and the above ester exchange would continue through the cell cyclings and be independent of the SEI formation. However, the authors found that the extent of the ester-exchange reaction was dependent on the anode surface passivation, and the complete formation of the SEI eventually prevented it. Therefore, a termination process had to exist at some stage, and the authors suggested that a cathode surface in a charged state would serve as such a terminator by quenching (oxidizing) the alkoxide anions. In view of the acidic nature of the electrolytes based on $LiPF_6$, neutralization of alkoxide anions by trace acid is another possible termination means.

The absence of EC in the discussions of all these reports[334−336] is interesting, since one would suspect that, based on the knowledge about EC reactivity, alkoxide could also attack its cyclic structure and cause irreversible reactions.[152,285,332,333] One possibility would be that, using gas chromatography, the identification of a high-volatility species such as linear carbonate is easy and reliable, while the formation of the polymeric species, which EC would most likely decompose into, is more difficult to detect.

Endo et al. studied the gradual degradation of electrolyte solutions in lithium or lithium ion cells by monitoring the production of active radical species with ESR.[337] To elongate the lifetime of the radicals so that their hyperfine structure could be analyzed, a spin-trapping technique was adopted to stabilize the original radicals generated from the reductive decompositions of electrolyte solvents on the anode surface. In this way, the authors were able to gain an insight into the structure of the radical species. The authors found that, even in the presence of a good, protective SEI, generation of active alkyl radicals, rather than radical anions, continued in the electrolyte and that a chain reaction initiated by cathodic polarization of the electrode was very likely responsible. In other words, once the radicals were produced in the initial cathodic polarization, the
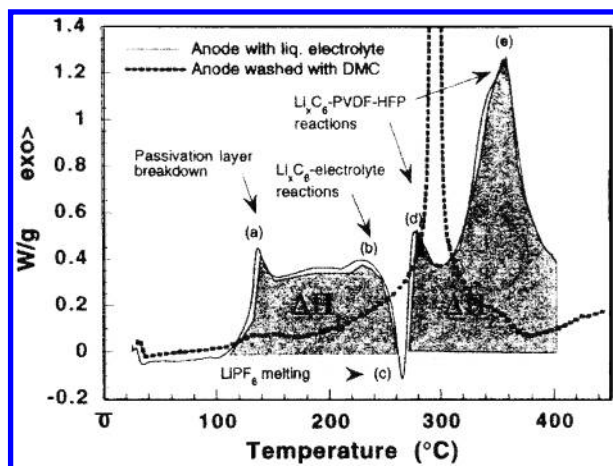
**Figure 28.** DSC trace of the reactions occurring between a fully lithiated graphitic anode and electrolyte. Anode surfaces both rinsed with DMC and unrinsed were studied. (Reproduced with permission from ref 338 (Figure 1). Copyright 1998 The Electrochemical Society.)

gradual decomposition of electrolyte solvents could occur in the bulk of the solution without involving electrodes. This propagation of radicals inevitably led to the polymerization of solvents. Using liquid chromatography, which is more sensitive to the detection of polymeric species, reductively induced polymerization of ester-based solvents was confirmed.

In the gradual degradation mechanism proposed by those authors, radical anions are first generated during SEI formation through a single-electron process, as proposed by Aurbach et al.,[108,124,249] and then polymerization proceeded gradually from these radical anions with subsequent and continuous production of more active alkyl radicals. In this sense, even a perfect SEI that insulates any electron transfer through it cannot prevent the continuous degradation of electrolyte solvents.

## 7.2. Stability of the SEI or Surface Layer at Elevated Temperatures

The presence of a protective SEI or surface layer prevents those irreversible reactions of electrolytes on anode/cathode surfaces that are otherwise favored by thermodynamics. Like the chemical process in the bulk electrolyte, the reactivity of the surface films formed in state-of-the-art electrolytes is negligible at room temperature. However, during long-term storage and cycling, their stability is still under question.

When conducting a differential scanning calorimetry (DSC) study on the stability of carbonaceous anodes in electrolytes, Tarascon and co-workers found that, before the major reaction between lithiated carbon and fluorinated polymers in the cell, there was a transition of smaller thermal effect at 120 °C, marked peak (a) in Figure 28.[338] They ascribed this process to the decomposition of SEI into $Li_2CO_3$, based on the previous understanding about the SEI chemical composition and the thermal stability of lithium alkyl carbonates.[102,117,249,281] Interestingly, those authors noticed that the above transition would disappear if the carbonaceous anode was rinsed in DMC before DSC was performed, while the other major processes remained (Figure 28). Thus,

they concluded that the components of the SEI layer are soluble in DMC.[338] Because of the similar physicochemical properties between various linear carbonate solvents, this dissolution of the SEI might very likely be universal in all state-of-the-art electrolytes.

This corrosion of the SEI by linear carbonate solvents would undoubtedly produce adverse effects on the performance of lithium ion cells. During long-term cycling, the damaged SEI has to be repaired constantly by the same electrochemical reactions that occurred in the initial formation process, which consumes the limited lithium ion source in the cell and increases the impedance at the electrode/electrolyte interface.

A more detailed study on the thermal stability of the SEI on lithiated and delithiated graphitic anodes was carried out by Amatucci and co-workers.[339] By storing the cells at 70 °C for 4 days and then resuming cycling at room temperature, they presented direct evidence that the SEI was damaged at the elevated storage temperature by successfully detecting the reappearance of the irreversible process at 0.75 V, which has been previously determined to be the formation of the SEI by reductive decomposition of the electrolyte. Furthermore, a correlation was also established between the capacity loss after such storages and the rebuilding of the SEI, with the latter being proportional to such factors as the storage temperature, the storage time, and the surface area of the anode. An Arrhenius behavior was actually observed for the dependence of capacity loss on the storage temperature, with an activation energy of 39.8 kJ mol$^{-1}$.[339]

As expected, the state-of-charge (SOC) of the anode also influences this rebuilding process, since the capacity loss due to the storage is much higher for the fully lithiated carbon anode than for the fully delithiated one. This fact was explained by the authors in terms of the reactivity of the carbon surfaces, which are partially exposed because of SEI corrosion, toward electrolyte components. Thus, intercalated lithium ions continuously diffuse from the interior of the graphitic structure through the imperfect SEI coverage and participate in the reaction with electrolyte solvents to re-form the SEI. Under stationary storage, an equilibrium would be reached between the SEI dissolution rate and the lithium ion diffusion rate. However, the net effect would be the irreversible consumption of electrolyte solvents as well as lithium ions.

The long-term deterioration of the SEI at elevated temperatures also was observed by McLarnon and co-workers, who conducted postmortem analyses on the electrodes from consumer lithium ion cells that were stored at various temperatures between 40 and 70 °C for weeks.[298] Using the IR absorption at 838 cm$^{-1}$ as the indicator of the SEI component, they quantitatively correlated the stability of the SEI on a carbonaceous anode against storage temperature and SOC. In an extreme situation where the cell was stored at 70 °C with 9% swing of SOC, no remaining SEI was found on the anode surface.
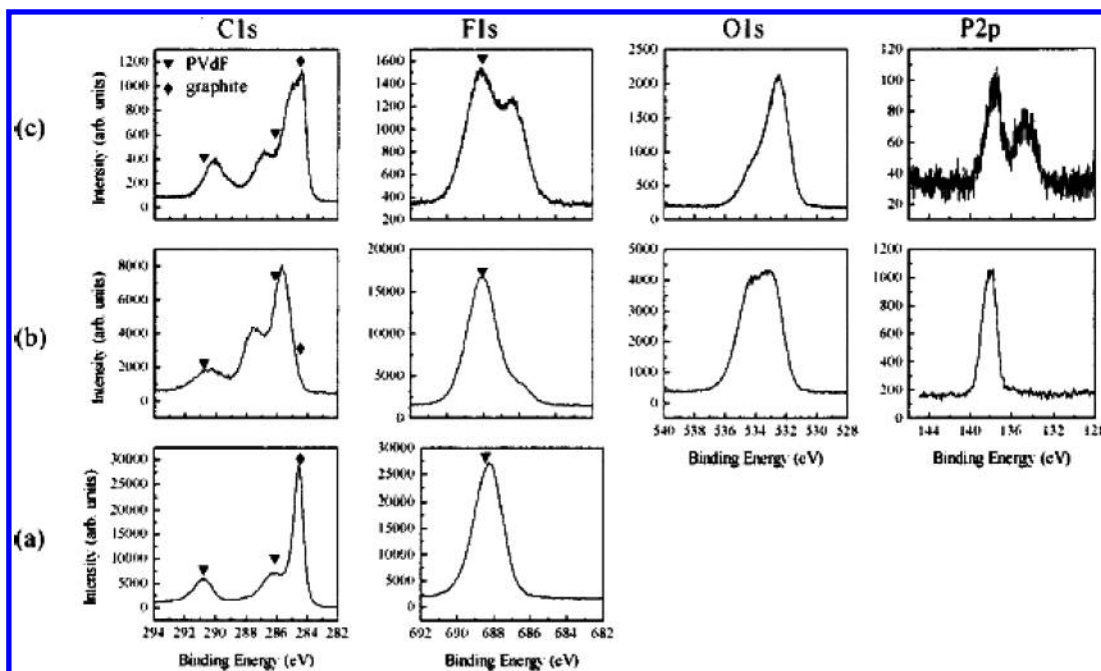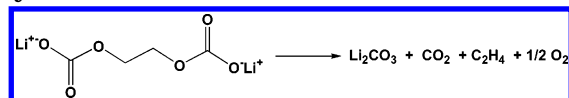
**Figure 29.** C 1s and O 1s XPS spectra for fresh, precycled, and stored graphite anodes. (Reproduced with permission from ref 294 (Figure 17). Copyright 2002 The Electrochemical Society.)

**Scheme 23. Thermal Decomposition of Lithium Alkyl Carbonate in the SEI**



Tarascon and co-workers proposed that the SEI on a carbonaceous anode is subject not only to simple dissolution but also to decomposition at elevated temperatures (>120 °C) into $Li_2CO_3$.[338] While the existence of some chemical process was generally agreed upon by various authors, they differed vastly on what the original SEI components had turned into through the process.[277,278,284,340]

In agreement with Tarascon and co-workers,[338] Dahn and co-workers proposed that the thermal decomposition of the SEI occurred via the transformation of the metastable lithium alkyl carbonate into stable $Li_2CO_3$ (Scheme 23).[340−342] This suggestion was supported by Amine and co-workers, who studied the change of surface chemistry on well-cycled carbonaceous anodes with elevated temperature storage by using XPS and observed the conspicuous presence of $Li_2CO_3$ on the graphite surface that was stored at 70 °C for prolonged durations (> weeks), as indicated by the C 1s signal at 290.4 eV in Figure 29.[294] Additional evidence came from the decreasing ether/ alkoxide signal at 287.4 eV in C 1s spectra and 534 eV in O 1s spectra. Furthermore, the elemental carbon signal at 284.5 eV was also clearly visible, indicating that the original SEI layer had been damaged, which left parts of the bulk graphene layers exposed.

However, $Li_2CO_3$ was not observed by Andersson and Edström in their XPS analysis of the graphitic anode that had been precycled and then stored at 60 °C for 7 days.[277] They found that, during the storage, the original SEI consisting of lithium alkyl carbonate was indeed unstable and disappeared with time, as indicated by the decreasing C 1s signal at 291 eV (corresponding to $ROCO_2Li$), but the new species did not seem to be $Li_2CO_3$, since the C 1s signal appeared at 290−290.5 eV instead of at 292 eV. These new species, still of a carbonyl nature, were thought by the authors to be polycarbonate formed from the ring-opening polymerization of EC. The discrepancy between the works of Amine et al. and Edström et al. could have arisen from the difference in the storage duration, which was much longer in the former case.

One common conclusion shared by both groups of researchers was the dramatic increase in LiF content as a result of the storage, which became the major species on the anode surface.[277,294] Because of the relatively low abundance of alkyl carbonate species in the original SEI and the large amount of LiF after storage, the authors disagreed with Kanamura et al., who attributed the formation of LiF to the reaction of lithium alkyl carbonate or $Li_2CO_3$ with HF.[282] Rather, they suggested that, the direct decomposition of fluorinated salt anions ($PF_6^-$ or $BF_4^-$) occurred at the elevated temperature and formed LiF through a variety of possible reactions.

A distinct difference between the behaviors of $LiBF_4$- and $LiPF_6$-based electrolytes must be pointed out. The recycling after storage at 60−80 °C revealed that lithium/graphite half-anode cells with $LiBF_4$-based electrolyte suffered serious capacity loss, while with $LiPF_6$-based electrolyte they maintained stable performance, as Figure 30 shows. A similar trend was found for a graphite anode with a different SOC, and a threshold value (60 °C) for the storage temperature seemed to exist for this performance degradation. Qualitatively the same surface species were detected by XPS analyses on graphitic anodes that were formed in $LiPF_6$- and $LiBF_4$-based electrolytes; therefore, the above difference could not be explained by chemistries. Andersson et al. speculated that the morphology of the major surface species, LiF, played
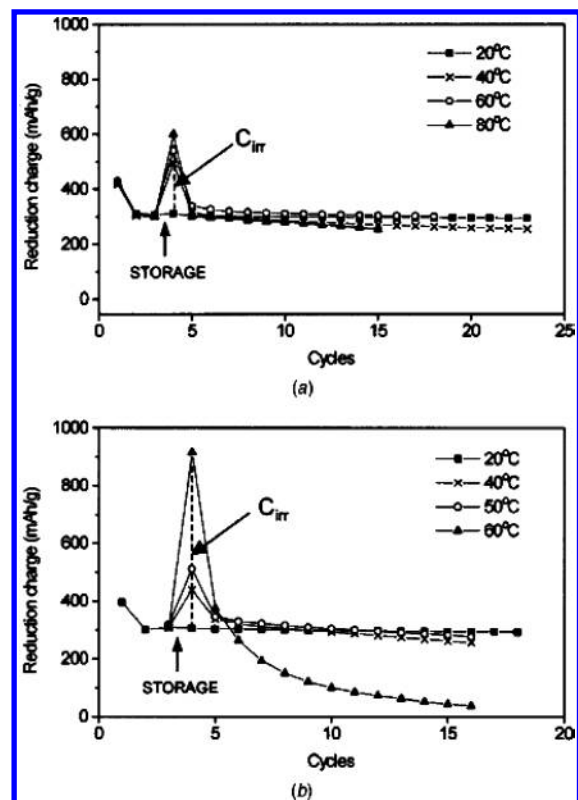
**Figure 30.** Capacity loss due to storage at elevated temperatures for Li/graphite half-cells. All cells were precycled at room temperature (cycles 1−3) prior to storage at indicated temperatures for 1 week, followed by continued cycling at room temperature. The electrolytes used were EC/DMC (2:1) and (a) 1.0 M LiPF$_6$ or (b) 1.0 M LiBF$_4$. The cells were stored in delithiated states. (Reproduced with permission from ref 277 (Figure 2). Copyright 2001 The Electrochemical Society.)

a critical role in defining the surface state of the anode. A highly speculative mechanism was proposed in accordance with this hypothesis in which the LiF formed at 60 °C from a LiBF$_4$-based electrolyte blocks the intercalation edge sites of the graphitic anode more effectively than the LiPF$_4$-based counterparts.[277]

The work by Ross and co-workers on the thermal stability of DEC on a lithiated graphitic anode further challenged the proposal that Li$_2$CO$_3$ was formed during the decomposition of the SEI.[284] By the well-controlled exposure of the fully lithiated graphite LiC$_6$ to DEC vapor in a vacuum and gradually heating the electrode, they used XPS to monitor the transformation of the SEI as the function of temperature. From 0 to 110 °C, the major surface species were believed to be oxalate anions as well as alkoxides, while, from 120 to 140 °C, obvious chemical reactions were observed. On the basis of the C/O stoichiometric change, it seemed that organic anions such as oxalate anions were converted into simple inorganic anions. The authors thus proposed that, in the exothermic process that was observed by Tarascon and co-workers in the DSC experiment,[338] the SEI most probably decomposed into simple inorganic species such as Li$_2$O and CO, instead of Li$_2$CO$_3$.[284]

On a cathode surface, the instability of electrolytes at elevated temperatures is also well studied, and it has been generally established that the continuous
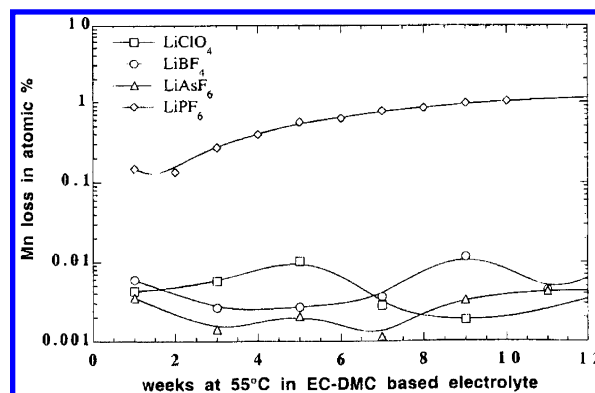


**Figure 31.** Effect of lithium salt on Mn$^{2+}$ dissolution from Li$_{1.05}$Mn$_{1.95}$O$_4$ stored in EC/DMC (2:1) electrolytes at 55 °C. The Mn$^{2+}$ concentrations in the electrolytes were determined by atomic absorption spectroscopy. (Reproduced with permission from ref 301 (Figure 4). Copyright 1999 The Electrochemical Society.)

decomposition and rebuilding of surface layers are responsible for the fade in capacity and loss in power.[296,297,343−346]

Using thermogravimetric analysis (TGA), Du Pasquier et al. studied the thermal breakdown of the surface layer on a spinel cathode that was aged in LiPF$_6$/EC/DMC at 100 °C for 8 h,[301] and they detected the presence of two distinct weight loss processes at 140 and 500 °C. While assigning the latter to the transformation of spinel into Mn$_2$O$_3$, they believed that the former process corresponded to the burning of the organic coating on the cathode surface and the concomitant release of CO$_2$, similar to the thermal transition that had been observed on the graphitic anode in the same temperature range.[338] Naturally, at room temperature, the above destructive process might only proceed with negligible kinetics.

For a spinel manganese cathode, the decomposition of the SEI is often entangled with the instability of the cathode structure in electrolytes at elevated temperatures, and the participation of electrolyte components in the Mn$^{2+}$ dissolution or the disproportionation of the spinel is already widely accepted.[293,301,343] The acidic nature of the electrolyte, originated from the moisture-sensitivity of PF$_6^-$ or BF$_4^-$ anions, is obviously the main cause, since a close correlation has been established by Du Pasquier et al. between the HF content and the Mn$^{2+}$ content in the electrolyte[301] and LiPF$_6$ has been identified as the salt species that causes the most severe Mn$^{2+}$ dissolution in state-of-the-art electrolytes[301,343] (Figure 31), apparently due to its higher tendency to hydrolyze. Elevated temperatures promote this dissolution process in a pronounced way, as Figure 32 shows. The continuous trend in Mn$^{2+}$ concentration implies that the dissolution process is kinetically governed, and there is no threshold temperature at which this process is switched on. However, acceleration does occur above 40 °C.[301] XRD analyses on the recovered spinel powder stored at 100 °C revealed the formation of a new phase, which the authors identified to be a protonated $\lambda$-MnO$_2$ that is partially inert with respect to electrochemistry. To account for the Mn$^{2+}$ concentration and the formation of a protonated $\lambda$-MnO$_2$ phase, the authors believed that
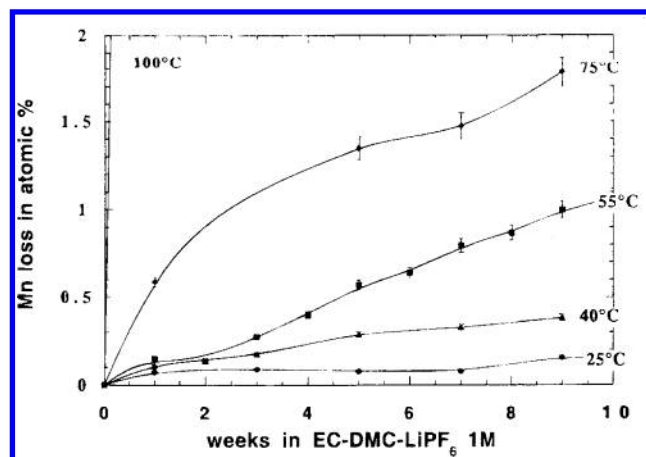
**Figure 32.** Effect of elevated temperatures on $Mn^{2+}$ dissolution from $Li_{1.05}Mn_{1.95}O_4$ stored in $LiPF_6$/EC/DMC (2:1). The $Mn^{2+}$ concentrations in the electrolytes were determined by atomic absorption spectroscopy. (Reproduced with permission from ref 301 (Figure 1). Copyright 1999 The Electrochemical Society.)

**Scheme 24. Structural Transformation of a Spinel Cathode at Elevated Temperatures Assisted by the Acidic Species in a $LiPF_6$-Based Electrolyte**
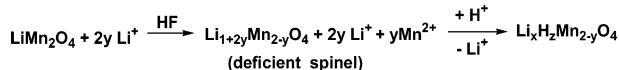


a proton–lithium ion-exchange process occurred instead of simple disproportionation (Scheme 24).[310] The structural transformation of spinel cathode materials is mainly responsible for the capacity fading of lithium ion cells based on them and $LiPF_6$-containing electrolytes. Although other authors differ on the mechanism by which the capacity loss is caused, they generally agree that the acidic nature of the electrolyte plays an influential role.[296,300,346] Thus, to make the advantages of spinel cathode materials feasible, the acidic nature of the electrolytes has to be mitigated, and the replacement of lithium salts based on anions with labile fluorine such as $PF_6^-$, $BF_4^-$, and $AsF_6^-$ seems to be a logical solution.

On the other hand, the adverse effect of HF on capacity seems to be much less significant to other cathode materials based on $LiNiO_2$ and $LiCoO_2$, which exhibit higher stability during storage at elevated temperatures, although an abundance of LiF found on cathode surfaces still indicates the reaction of a salt anion, most probably after its hydrolysis by trace moisture.[294,302] In the XPS analysis conducted on a $LiNi_{0.8}Co_{0.2}O_2$ cathode that had been stored at various temperatures up to 70 °C, Andersson et al. reported that the surface chemistry did not show any apparent dependence on storage temperature, storage duration, or SOC (i.e., the polycarbonates and various F-containing species in the surface layer remain stable regardless of storage temperature).[294] However, quantitative changes in the relative ratio of these species did occur during the storage, and it was believed that a thicker surface layer was formed as a result of longer storage at higher temperature. This conclusion was drawn from the simultaneous increase of C and O species during the storage despite the fact that F species actually decreased at the same
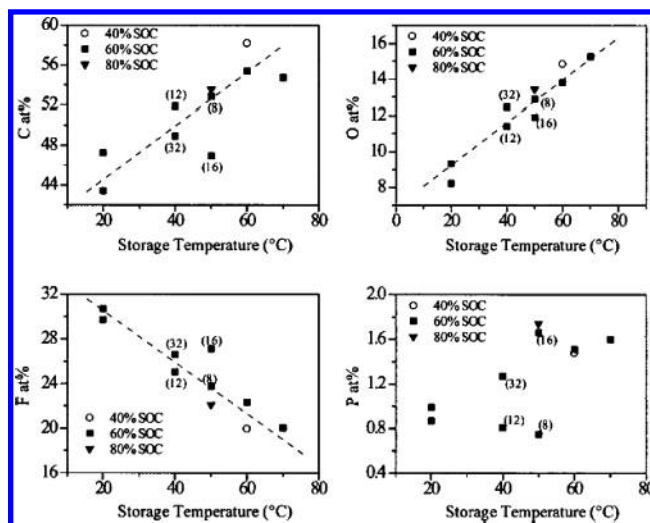


**Figure 33.** Relative amount (atom %) of surface species C, O, and F on cathode samples as a function of storage temperature. Numbers in parentheses indicate the storage duration in weeks. (Reproduced with permission from ref 294 (Figure 8). Copyright 2002 The Electrochemical Society.)

time, as Figure 33 shows. This unexpected trend in F abundance contradicts the knowledge about the instability of $LiPF_6$ salt at elevated temperatures as well as the results of LiF content on graphite[277,294] and spinel materials[301,343] during similar storage tests. To account for this abnormality, the authors argued that, while it would be impossible for the F content to actually decrease with temperature, the screening of the F 1s signal by an overlaying surface compound that is non-fluorine in nature could occur and would reduce the opportunity for the F 1s electron to escape.[294] In other words, the polymeric and inorganic moieties grown on a cathode surface camouflage the increased LiF content.

## 7.3. Thermal Safety of Electrolytes against Abuse

The catastrophic scenario for the thermal reaction between electrolytes and electrode materials in a lithium-based cell is called "thermal runaway",[347–351] whose onset temperature determines the safety limit of lithium-based cells. Thermal runaway occurs when the amplitude of an accidental temperature hike in the cell, usually initiated by local overheating, reaches a certain threshold value, and the heat thus generated can no longer be thermally dissipated but instead triggers a series of exothermic side reactions. Since the rate of heat generation is higher than that of heat dissipation, these exothermic processes proceed under an adiabatic-like condition and the global cell temperature experiences an uncontrollable rise. Figure 34a shows an example of a thermal runaway that was initiated in a well-cycled (25 times) lithium cell by a 140 °C hot box test.[348] Once initiated, thermal runaway apparently does not terminate until the reactive agents are completely consumed or, in most cases, the cell ruptures, venting with flames and smoke and sometimes even explodes.[348,351,352] For lithium or lithium ion batteries of industry sizes (i.e., a capacity of >10 A h), serious safety hazards would ensue from such a thermal breakdown.
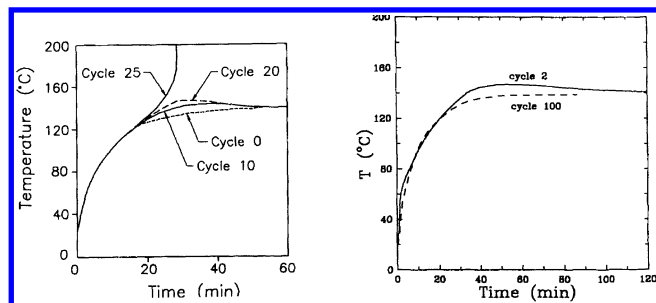
**Figure 34.** Temperature response of (a, left) cycled lithium (Li/MnO$_2$) and (b, right) lithium ion (coke/LiCoO$_2$) cells subjected to a 140 °C hot box test. These cells contain LiAsF$_6$/EC/PC and LiPF$_6$/PC/DEC as electrolytes, respectively, and were cycled at room temperature to the indicated cycle numbers. Note that the thermal runaway occurs for a lithium cell that has been cycled 25 times due to the formation of high surface area lithium, while extended cycling actually offers better safety to lithium ion cells (Reproduced with permission from ref 348 (Figures 1 and 4). Copyright 1994 Elsevier.)

The concern over the safety of lithium-based cells drew a great deal of attention after the unsuccessful commercialization of lithium cells.[353–358] The surface morphology of the well-cycled lithium electrode was believed to be the main source for thermal runaway, because the presence of high surface area dendritic lithium would greatly promote the exothermic reactions between lithium and electrolyte, thus lowering the threshold temperature at which self-heating occurred. As Figure 34a shows, the temperature of the fresh cell (cycle 0) under the same testing condition does not show any temperature overshoot but instead approaches 140 °C in an asymptotical manner, as would be expected from a thermally inert object. Temperature overshoot, a sign of self-heating within the cell, increases monotonically with cycle number until, after 25 cycles, the cell possesses a highly reactive lithium surface and undergoes thermal runaway, as characterized by the dramatic rise in temperature.[348] At the time, the role played by cathode materials in the safety of lithium cells seems to be overshadowed by the presence of lithium anodes because of the much higher reactivity of the latter.

The replacement of lithium by carbonaceous anode materials eliminated the highly reactive anode surface as a possible trigger for thermal runaway and led to the successful commercialization of lithium ion technology in the 1990s. However, safety remains an issue, since thermal runaway can be caused by mechanisms other than the formation of lithium dendrites. A general opinion is that the replacement of the metallic lithium by a carbonaceous anode does improve safety, as Figure 34b shows.[348,351,352,359] In contrast to a metallic lithium anode, a well-cycled carbonaceous anode offers additional self-heat suppression, as evidence by the absence of the temperature overshoot which was originally observed in a fresh cell. For most commercial lithium ion cells, the onset temperature that would trigger a thermal runaway is considered to be >150 °C.[351,352,360]

According to mathematic modeling and abuse tests, the normal operation for most lithium or lithium ion cells that use nonaqueous electrolytes should not induce sufficient heat to raise the cell temperature above the onset threshold. Instead, thermal runaway is often caused by various abuses, which could be thermal (overheating), electrical (accidental overcharge, high pulse power extraction), or mechanical (crushing, internal or external short circuit).[349,351,352] Various techniques have been employed to evaluate the safety of lithium ion cells, including hotbox[348,360] and accelerating rate calorimetry (ARC)[348,360,361] as well as abuse tests such as overcharging, shorting, crushing, and nail-penetration.[351,352] Profound differences in the abuse tolerance were found among the lithium ion cells from various manufacturers despite the common onset temperature of ~160 °C for nearly all these cells. In addition to the cell materials (electrolyte and electrode) that determine the amount of heat generation and the rate of heat release, the cell design and engineering was also found to be of vital importance for abuse tolerance by affecting the efficiency of heat dissipation.[349,355,360,361] The presence of excess electrolytes can increase the overall thermal conductivity of the cell by 55–70% and eliminate its dependence on OCV but cannot alter the anisotropy of heat flow within the cell. For example, in an electrolyte-filled cathode/separator/anode stack that simulates an actual lithium ion cell, the cross-plane thermal conductivity is ~10 times lower than the in-plane one.[360] In agreement with the above results, Leising et al. compared the internal and external temperatures of a prismatic 1500 mA h lithium ion cell during an external short, and they found a difference of 40 °C between the two.[352] The consequence of this anisotropy in thermal conductivity is especially serious for the popular spiral-wound cell design because it creates an adiabatic-like environment for any thermal perturbation occurring near the core of the cell and increases the opportunity for thermal runaway.

At elevated temperatures, there are five possible reactions that can occur between the cell components: (1) thermal decomposition of bulk electrolyte; (2) chemical reduction of electrolyte by the anode; (3) chemical oxidation of electrolyte by the cathode; (4) thermal decomposition of the cathode and anode; or (5) melting of the separator and the consequent internal short. To identify which of these contributes the decisive amount of heat that is critical in initiating the thermal runaway, it is necessary to study the thermal responses of these individual components or component couples separately.

The bulk electrolyte components do not seem to be such an initiation, since the thermal decomposition of the salts and the interactions between the salts and the solvents start as low as 70 °C,[150,152,330,337] and the thermal effect of these reactions is generally negligible as compared with the processes involving the fully charged anode and cathode materials.[361]

In early research efforts, attention was concentrated on carbonaceous anodes because of the earlier experiences with metallic lithium. Dahn and co-workers studied the thermal response of carbonaceous materials in the presence of electrolytes in an adiabatic environment created in a thermal analysis technique known as accelerating rate calorimetry (ARC). By choosing an arbitrary threshold value for

the self-heating rate (SHR) of 0.02 °C min$^{-1}$, they found that, besides the lithiation state of the anode, electrolyte composition had a critical effect on the onset temperature of thermal runaway, with the SHR increasing in the order

$$EC < DME < DEC < DMC$$

While the rationale for the above order remains to be well-understood, the authors speculated that the relative effectiveness and solubility of the SEI as well as the reactivity of these bulk solvents might be responsible.[348] Overall, this study showed that the reaction between the electrolyte and the lithiated carbon could trigger thermal runaway, except at much higher onset temperatures than those of lithium electrodes.

In their DSC studies on the SEI of carbonaceous anodes, Du Pasquier et al. identified the exothermic process at 120−140 °C as the transformation of the alkyl carbonate-dominated SEI into the more stable $Li_2CO_3$, and the heat generation associated with this process strongly depended on the surface area of the electrode. The reduction of electrolytes by lithiated carbon occurred between 210 and 230 °C, with comparable reaction heat to that of the transformation of an SEI.[338] According to the 140 °C hotbox test that was conducted with a lithium ion cell, it seemed that the breakdown of the SEI could be excluded as the cause for thermal runaway.[348] Works by other authors confirmed the occurrence of this SEI transformation process at >100 °C and the dependence of its heat generation on the carbonaceous anode surface,[359,362,363] but they disagreed on its role in initiating thermal runaway. For example, Joho et al. systematically measured the heat evolution of various graphitic anodes in the presence of $LiPF_6$/EC/DMC between 80 and 220 °C and evaluated the possibility that the graphitic anode was the source for thermal runaway in lithium ion cells. On the basis of the overall heat capacity data of the Sony 18650 lithium cell, they estimated that the temperature rise in the cell as the result of heat generation of those processes ranged between 30 and 90 °C, depending on the surface area as well as the irreversible capacity of the anode, and concluded that, while the transformation occurred at >100 °C, a temperature hike of this amplitude could place the cell well in the range of thermal runaway onset temperatures between 160 and 180 °C; therefore, the thermal decomposition of the SEI and the subsequent reduction of electrolyte components by lithiated carbon could be the source that initiates thermal runaway.[359]

In their further study on the thermal reaction between carbonaceous anodes and electrolytes, Richard and Dahn improved the ARC technique and miniaturized it for small sample amounts (<1.0 g) while retaining the sensitivity.[340,341] The self-heating was measured for MCMB in various electrolytes with different initial heating temperatures, and the SHR profile, characterized by a common initial peak, was obtained for nearly all of the tests, as shown in Figure 35. The authors speculated that the SHR profile represented in Figure 35 featured characteristics of three distinct reaction processes. The initial peak,
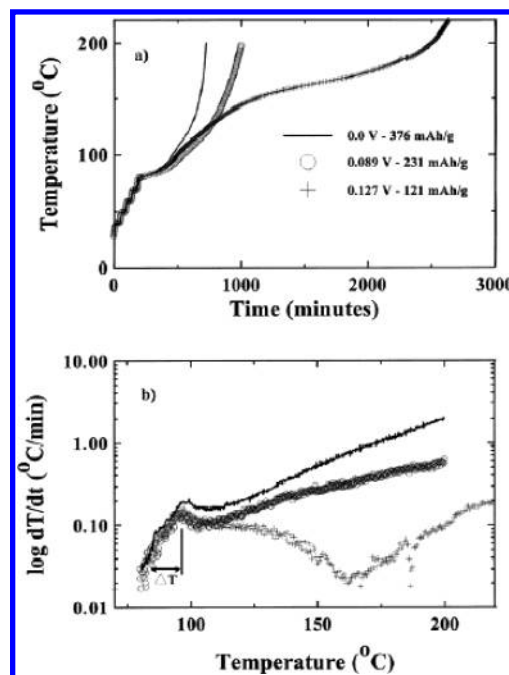


**Figure 35.** Temperature−time (a) and SHR (b) profiles measured for lithiated MCMB in LiPF6/EC/DEC (33:67). The MCMB electrodes were lithated to three compositions: $Li_{0.75}C_6$ (0.0 V), $Li_{0.45}C_6$ (0.089 V), and $Li_{0.25}C_6$ (0.127 V). (Reproduced with permission from ref 340 (Figure 8). Copyright 1999 The Electrochemical Society.)

which appears to be relatively independent of the lithiation degree of the carbonaceous anode, should represent a reaction that proceeds until one of the reactants is depleted. The decomposition of bulk electrolyte does not contribute to the SHR until 190 °C; therefore, there must be another exothermic process between 150 and 190 °C. During this temperature range, the SHR does depend on the lithiation degree of the anode, with the more lithiated anode generating a higher SHR. XRD analysis confirmed that this process does consume the intercalated lithium in the graphite interior.

On the basis of the above observation, Dahn and co-workers proposed a thermal reaction scheme for the coupling of carbonaceous anodes and electrolytes. The initial peak, which was almost identical for all of the anode samples and independent of lithiation degrees, should arise from the decomposition of the SEI because the amount of SEI chemicals was only proportional to the surface area. This could have been due to the transformation of the metastable lithium alkyl carbonate into the stable $Li_2CO_3$. After the depletion of the SEI, a second process between 150 and 190 °C was caused by the reduction of electrolyte components by the lithiated carbon to form a new SEI, and the autocatalyzed reaction proceeded until all of the intercalated lithium was consumed or the thickness of this new SEI was sufficient to suppress further reductions. The corresponding decrease in SHR created the dip in the least lithiated sample in Figure 35. Above 200 °C (beyond the ARC test range as shown in Figure 35), electrolyte decomposition occurred, which was also an exothermic process.

The tests with various electrolytes revealed that both electrolyte salts and solvent compositions affect

the initial SHR below 100 °C, which is of critical importance to the initiation of thermal runaway. For example, using the threshold value of the SHR at 0.02 °C min$^{-1}$ as the sign of onset, the self-heating for MCMB in LiPF$_6$/EC/DEC (33:67) starts at 80 °C, whereas it begins at 50 °C in LiBF$_4$/EC/DEC (50:50) and at 70 °C in LiPF$_6$/EC/DEC (50:50). The SHR profiles obtained for the MCMB anode in LiBF$_4$/EC/DEC did not show the initial peak that corresponds to the transformation of the SEI, suggesting that the SEI formed on the carbonaceous anode in LiBF$_4$-based electrolyte did not contain high amounts of metastable components such as lithium alkyl carbonate, as the SEI formed in LiPF$_6$- or LiAsF$_6$-based electrolytes would have. This inference was in agreement with the work by Aurbach et al.,[104,117] Kanamura et al.,[222,223] and Andersson and Edström.[277] On the basis of these ARC results, these authors believed that if a lithiated MCMB containing LiPF$_6$/EC/DEC (33:67) was heated directly to 150 °C, the known threshold for thermal runaway for most commercial lithium ion cells, the anode would self-heat at a rate of 100 °C min$^{-1}$. Hence, the universal self-heating behavior of a lithiated carbonaceous anode in the presence of electrolytes is very useful for predicting the initial self-heating in a practical lithium ion cell when combined with the overall heat capacity of the cell.[340]

The seminal work by Maleki et al. in 1999 seemed to provide a direct answer to the question about which of the five possible processes was responsible for the thermal runaway of a lithium ion cell.[361] Using ARC, they first determined the thermal runaway onset temperature in a lithium ion cell based on LiCoO$_2$/graphite with LiPF$_6$/EC/DMC/DEC to be 167 °C. The thermal reaction, however, was found to start at 123 °C and continued to self-heat the system to the above onset temperature. Using DSC and TGA, they further determined the heat evolution as well as the thermal profile for the individual components of the cell in the presence of electrolytes, which included cathode, anode, and anode binder (PVdF).

Thus, the total exothermic heat generation of 697 J g$^{-1}$ was recorded for the anode-related reactions, which included the major heat generated from anode/binder reactions starting at 210 °C and the anode/electrolyte reactions starting at 125 °C. The breakdown of the SEI on the anode occurred at 120 °C, as characterized by the distinct peak, which followed an endothermic process that was attributed by the authors to the bulk electrolyte decomposition below 100 °C. While the heat effect of the SEI breakdown seemed negligible as compared to those of the cathode/electrolyte and anode/electrolyte reactions, it contributed to the self-heating of the cell. For cathode-related processes, the total exothermic heat generation was 407 J g$^{-1}$, with the major thermal reaction starting at 167 °C. In other words, although the heats associated with anode-related reactions are higher, the heat from the cathode processes was released at a relatively lower temperature and was more likely responsible for the triggering of thermal runaway.

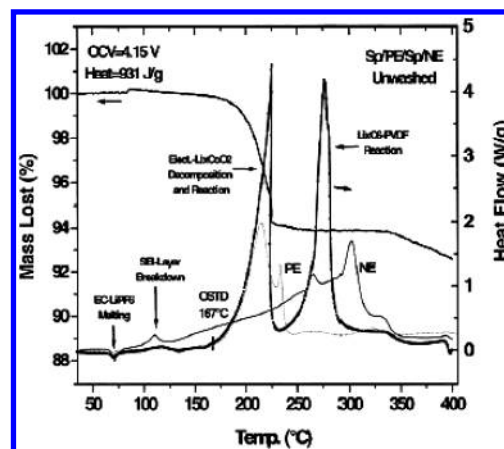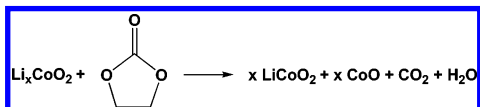A comparison was made between the profiles of heat evolution associated with the reactions of the



**Figure 36.** Comparison of DSC and TGA profiles for a cathode (PE), anode (NE), and separator (SP) composite with those of cathode/electrolyte and anode/electrolyte. Note the close match between the DSC/TGA profiles of the stack and the cathode/electrolyte couple. The OCV of the stack is 4.15 V. (Reproduced with permission from ref 361 (Figure 4). Copyright 1999 The Electrochemical Society.)

cathode/electrolyte and the anode/electrolyte, and a close match was identified between the DSC profile of the cathode/electrolyte couple and that of the cell stack, which consisted of cathode/separator/anode in the presence of electrolytes in a simulation of an actual lithium ion cell (Figure 36).[361] Therefore, the authors concluded that the thermal runaway was mainly caused by the heat generation from the cathode material, which decomposed to release oxygen, and the electrolyte components were oxidized subsequently. While the reaction of the anode/binder occurred at a relatively higher temperature, its substantial heat certainly contributed to the ultimate consequences of the thermal runaway. In a more comprehensive conclusion, the safety of a given lithium ion cell is dominated by the electrolyte reactions with the cathode and with the anode simultaneously.

The thermal decomposition of various cathode materials based on transition metal oxides has been known since the potential of these materials as rechargeable lithium-based batteries became realized, and the decomposition chemistry releasing oxygen has usually been thought to proceed at temperatures above 200 °C.[362,364−366] Interestingly, Maleki et al. found that the presence of a surface layer on the cathode, which was formed through the decomposition of electrolytes on the cathode during the cycling of the cell, actually promoted the thermal decomposition of the cathodes to occur at a lower temperature with higher heat generation and mass loss. The decomposition of the surface layer served as the thermal trigger for the major oxygen-releasing process.
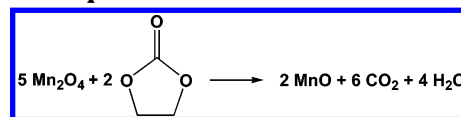
A direct result of the work by Maleki et al. is the gradual shift of safety research from carbonaceous anode to cathode materials. In the following years, Dahn and co-workers used an improved ARC technique to conduct a series of systematic investigations on the reaction between electrolyte and cathode materials based on LiCoO$_2$[367−369,371] and spinel LiMn$_2$O$_4$.[368,370] These studies have depicted a clear picture regarding the safety of lithium ion devices.

**Scheme 25.  Thermal Decomposition of LiCoO$_2$ in the Absence of Electrolyte**

$$Li_xCoO_2 \longrightarrow x\ LiCoO_2 + \frac{(1-x)}{3}\ Co_3O_4 + \frac{(1-x)}{3}\ O_2$$
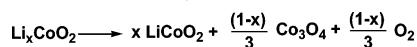
**Scheme 26.  Thermal Combustion of EC by the Cathode LiCoO$_2$**



**Scheme 27.  Thermal Combustion of EC by a Fully Delithiated Spinel Cathode**



In a standard electrolyte, LiPF$_6$/EC/DEC, the fully delithiated LiCoO$_2$ (OCV = 4.2 V) showed the threshold SHR of 0.02 °C min$^{-1}$ at ~130 °C that eventually led to thermal runaway at 160 °C. It had been found that the thermal decomposition of LiCoO$_2$ occurred at a much higher temperature (>200 °C) with oxygen generation (Scheme 25). The existence of Co$_3$O$_4$ had been confirmed by XRD analysis conducted on a cathode sample that was heated to 320 °C. However, MacNeil and Dahn found that the presence of electrolyte solvents catalyzed the decomposition of LiCoO$_2$ by reacting with the oxygen, thus greatly lowering the onset temperature at which oxygen was released. XRD analysis performed on the cathode after its reaction with EC/DEC showed that, when solvents were present, a new phase "CoO" was generated in addition to Co$_3$O$_4$ and the unreacted LiCoO$_2$.[369] The authors ascribed the formation of this Co(II) species to the reducing power of the organic solvents. In an ideal situation with full combustion of EC, the authors proposed the reaction scheme shown in Scheme 26. As a result, the presence of organic species as fuel not only reduced the onset temperature for the thermal decomposition of LiCoO$_2$ but also rendered the reaction more exothermic. This solvent effect, that is, lower onset temperature and higher reaction heat for thermal decomposition of cathode materials due to the participation of electrolyte solvents, has actually been observed previously by Maleki et al., who ascribed it to a complex synergistic mechanism among the electrolyte components and LiCoO$_2$ that catalyzed the reaction between electrolytes and the liberated oxygen.[361] Undoubtedly, as fuel in the adiabatic system, the presence of organic solvents in the electrolyte increases the chance of thermal disaster for lithium ion cells.

In contrast to that of solvents, the effect of the electrolyte solute, LiPF$_6$, on the thermal decomposition of the cathode, LiCoO$_2$, was found to be suppression instead of catalyzation.[369] The SHR of a partially delithiated cathode was measured in a series of electrolytes with various salt concentrations, and a strong suppression of the self-heating behavior was found as the concentration of LiPF$_6$ increased above 0.50 M. The mechanistic rationale behind this salt effect is still not well understood, but the authors speculated that the salt decomposition coated the cathode with a protective layer that acted as a combustion retardant. On the basis of these results, the authors recommended a higher salt concentration (>1.50 M) for LiCoO$_2$-based lithium ion cells is preferred in terms of thermal safety.

Parallel studies carried out on a manganese spinel LiMn$_2$O$_4$-based cathode showed that this cathode material could offer improved thermal safety as compared to LiCoO$_2$, but the SHR in this case was very sensitive to the relative amount of electrolyte compared to that of the cathode, while the corresponding dependence was not found with LiCoO$_2$/electrolyte.[368] Thus, only when the electrolyte/cathode ratio was in the vicinity of 1:6, which is close to the actual electrolyte/cathode ratio in lithium ion cells, would the LiMn$_2$O$_4$-based cathode show a lower SHR than LiCoO$_2$-based cells, in consistence with the hotbox data.[368]

Similar to the results obtained on the thermal reaction of LiCoO$_2$, the SHR of Li$_x$Mn$_2$O$_4$ in the presence of LiPF$_6$/EC/DEC reached the threshold value of 0.02 °C min$^{-1}$ at ~150 °C, indicating the beginning of exothermic events; then the system gradually self-heated to 275 °C. In comparative tests, LiMn$_2$O$_4$ in the absence of electrolytes showed a detectable thermal event at ~160 °C and converted from the $\lambda$-MnO$_2$ structure to $\beta$-MnO$_2$ one, while the oxidation of electrolyte solvent led to MnO with increased exothermic effect. Since MnCO$_3$ and Mn$_2$O$_3$ were also detected by XRD analysis, CO$_2$ and H$_2$O were suspected to be the combustion products of the solvents.[370] Assuming EC as the fuel to be fully combusted, 1 mol of delithiated spinel material can release 2 mol of oxygen and generate heat that is sufficient to raise the cell temperature over 300 °C, based on the heats of combustion for EC (1161.4 kJ mol$^{-1}$) and DEC (2715 kJ mol$^{-1}$) (see Scheme 27). In experiments, the actual rise in the ARC sample temperature was only 80 °C, most probably due to incomplete combustion or depletion of solvent.[370]

Therefore, the presence of the electrolyte solute, LiPF$_6$, added complexity to the thermal decomposition of the LiMn$_2$O$_4$-based cathode. Contrary to the salt effect found with the LiCoO$_2$ cathode,[369] the onset temperature of exothermic activity as represented by SHR > 0.02 °C min$^{-1}$ decreased as the concentration of LiPF$_6$ increased.[370] Apparently, LiCoO$_2$ and LiMn$_2$O$_4$ have fundamental differences in the way they react with solvent in the presence of salt. It seemed that the salt mainly contributes to an initial thermal instability, which increases with LiPF$_6$-concentration.[370]

Pointing out that the acidic nature of LiPF$_6$ assists the dissolution of Mn$^{2+}$ into electrolyte solution,[301,343] the authors speculated that HF in the electrolyte solution efficiently cleans up the spinel surface of MnO; therefore, the bulk electrolyte solvents can be continuously exposed to the fresh surface of Mn$_2$O$_4$ and be oxidized.[370] As a result, solvent oxidation would proceed more rapidly as compared with the case of an electrolyte that is less acidic. Therefore, for a spinel manganese-based lithium ion cell, a higher thermal safety would be obtained with lower salt concentration, and the authors suggested 0.5 M as the optimum concentration at which the ion

conductivity and thermal reactivity could be best balanced.[370]

A recent publication discussing the salt effect on the thermal safety of a LiCoO$_2$ cathode was entitled with an intriguing but seemingly paradoxical question: "Can an electrolyte for lithium ion batteries be too stable?", which revealed the relative importance of the interfacial stability arising from the passivation efficiency against that of the "intrinsic stability" with respect to the safety of cathode materials in lithium ion cells.[371] Using an improved DSC technique that enabled the direct analysis of electrolytes containing volatile components, the authors investigated the thermal stability of the LiCoO$_2$ cathode in the presence of the electrolytes based on LiPF$_6$, LiIm, and LiBeti. The latter two salts, which were based on an imide anion stabilized by two perfluorinated sulfonyl groups, had been developed in the early 1990s to replace the thermally unstable LiPF$_6$ and have been reported to be thermally stable till >300 °C.[146]

Surprisingly, when the cathode material, LiCoO$_2$, was in the presence of these "thermally stable" salts, LiIm and LiMe, much higher reactivity was detected than that in the presence of LiPF$_6$, as indicated by the total absence of any combustion suppression on SHR that had been observed with LiPF$_6$.[371] DSC results of LiCoO$_2$ in the presence of LiIm- or LiBeti-based electrolytes confirmed the above observation, which showed the onset thermal decomposition of LiCoO$_2$ to be at ~280 °C, whereas in LiPF$_6$-based electrolytes the same thermal event was much suppressed in terms of heat evolution as the concentration of LiPF$_6$ increased. In other words, the presence of LiIm and LiBeti did not introduce any increase in the thermal stability of the electrode, while LiPF$_6$, although believed to be thermally unstable, efficiently suppressed the thermal decomposition of the cathode.

The authors ascribed the above "abnormality" to the passivation of the cathode surface by the reaction products of the electrolyte solvent and salt. Since LiPF$_6$ readily decomposes organic solvents such as EC through a ring-opening mechanism at relatively low temperatures, the decomposition products, which were believed to consist of a wide variety of compounds, including a PEO-like polymer shown by Schemes 4, 12, and 15, deposited on the cathode surface and formed a protective layer between the highly oxidizing cathode materials and the bulk electrolyte solvents. According to the hypothesis of the authors, this polymeric coating on the cathode particles strongly delayed the thermal combustion of the solvents by hindering the release of oxygen, resulting in a more controlled thermal decomposition of LiCoO$_2$. On the other hand, similar polymer species were not formed from LiIm- or LiBeti-based electrolytes because of the stability of these salts, and the thermal combustion of electrolyte solvents in the presence of charged cathode materials proceeded unhindered, releasing heat that is sufficient to trigger thermal runaway.

Another well-studied salt, LiBF$_4$, was also believed to be more thermally and chemically stable than LiPF$_6$ in terms of its higher tolerance against trace moisture and lower tendency to react with cyclic carbonates in a manner similar to that shown by Schemes 4, 12, and 15.[132,133] However, a similar paradoxical conclusion was drawn about the thermal safety of LiCoO$_2$ in the presence of the electrolyte based on it, whose inability to produce polymeric coatings on the cathode is held responsible.[371] The above results from Dahn and co-workers suggested that the salts that were traditionally thought to be thermally stable, such as LiBF$_4$, LiIm, and LiBeti, should not be used in lithium ion cells if the thermal safety is the top concern in the application environment, which includes large size cells working under high-rate discharge, at elevated temperatures or at the risk of mechanic abuses and so forth, and that LiPF$_6$ remains the electrolyte solute of choice in terms of thermal safety.

## 8. Novel Electrolyte Systems

### 8.1. Problems Facing State-of-the-Art Electrolytes

Summarizing the materials reviewed in sections 2−7, one can immediately conclude that the current state-of-the-art electrolyte systems for lithium ion batteries are far from perfect and that, at least in the following four aspects, there is still room for possible improvement. Therefore, research and development efforts are continued in an attempt to reformulate new electrolyte systems or to modify the current state-of-the-art electrolyte systems.

**(1) Irreversible Capacity.** Because an SEI and surface film form on both the anode and cathode, a certain amount of electrolyte is permanently consumed. As has been shown in section 6, this irreversible process of SEI or surface layer formation is accompanied by the quantitative loss of lithium ions, which are immobilized in the form of insoluble salts such as Li$_2$O or lithium alkyl carbonate.[262] Since most lithium ion cells are built as cathode-limited in order to avoid the occurrence of lithium metal deposition on a carbonaceous anode at the end of charging, this consumption of the limited lithium ion source during the initial cycles results in permanent capacity loss of the cell. Eventually the cell energy density as well as the corresponding cost is compromised because of the irreversible capacities during the initial cycles.

The extent of the irreversible capacity depends on both the anode material and the electrolyte composition. Empirical knowledge indicates that the PC presence, which is well-known for its tendency to cause the exfoliation of the graphene structures, is especially apt to induce such irreversible capacities. On the other hand, reformulation of the electrolyte may lead to significant reduction in the irreversible capacity for given electrode materials.

**(2) Temperature Limits.** The two indispensable components of the present lithium ion electrolyte systems are LiPF$_6$ as salt and EC as solvent. Unfortunately, these two components also impart their sensitivity to extreme temperatures to the lithium ion technology, thus imposing temperature limits to the operation of lithium ion cells. In a somewhat oversimplified account, one can hold EC responsible

for the lower, and $LiPF_6$ for the higher, temperature instabilities.

Thus, at temperatures lower than the liquidus temperature (usually above $-20$ °C for most electrolyte compositions),[50e,159,160] EC precipitates and drastically reduces the conductivity of lithium ions both in the bulk electrolyte and through the interfacial films in the system. During discharge, this increase of cell impedance at low temperature leads to lower capacity utilization, which is normally recoverable when the temperature rises. However, permanent damage occurs if the cell is being charged at low temperatures because lithium deposition occurs, caused by the high interfacial impedance, and results in irreversible loss of lithium ions. An even worse possibility is the safety hazard if the lithium deposition continues to accumulate on the carbonaceous surface.

At temperatures higher than 60 °C, various decompositions occur among the electrolyte components, electrode materials, and SEI or surface layers, while $LiPF_6$ acts as a major initiator or catalyst for most of these reactions.[152,310,332,333] The damage caused by high-temperature operation is permanent. Because gaseous products accumulate, a safety hazard is also likely. Therefore, the specified temperature range for the normal operation of most commercial lithium ion cells is $-20$ °C to $+50$ °C. While sufficient for most consumer purposes, the above range severely restricts the applications of lithium ion technology for special areas such as military, space, and vehicle traction uses.

**(3) Safety and Hazards.** The linear carbonate solvents are highly flammable with flash points usually below 30 °C. When the lithium ion cell is subject to various abuses, thermal runaway occurs and causes safety hazards. Although electrode materials and their state-of-charge play a more important role in deciding the consequences of the hazard, the flammable electrolyte solvents are most certainly responsible for the fire when a lithium ion cell vents. The seriousness of the hazard is proportional to the size of the cell, so flame-retarded or nonflammable lithium ion electrolytes are of special interest for vehicle traction batteries.

**(4) Better Ion Transport.** In most nonaqueous electrolytes, the ion conductivity is much lower as compared with aqueous solutions, and the part of the current that is carried by the lithium ions is always less than half.[176] Although it has been found that, for actual cell operation, the impedances at the interfaces of anode/electrolyte and cathode/electrolyte weigh far more than the bulk ion conductivity does, there is a semiempirical rule with very few exceptions: the higher the bulk ion conductivity of an electrolyte is, the more conductive the SEI or surface films formed in this electrolyte can be. On the other hand, the improvement in lithium ion transference number is certainly welcome, although its significance in liquid electrolytes might not be as high as in polymer electrolytes.

Since the inception of lithium ion technology, there has been a great deal of research aimed at improving the state-of-the-art electrolyte systems via various approaches, including the development of new electrolyte solvents and salts and the application of functional additives. This section is dedicated to cover these efforts, most of which, although, have not been adopted in actual lithium ion electrolytes.
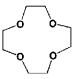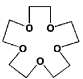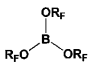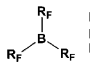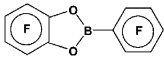
## 8.2. Functional Electrolytes: Additives

Instead of entirely replacing the major components of the current state-of-the-art electrolyte systems that cause problems, an efficient and economical alternative is to modify certain targeted functions of the electrolytes by incorporating a new component at small concentrations, known as an additive, so that its potential impact on the existing electrolyte can be minimized. In this way, the bulk properties of the electrolyte system can be maintained with the already proven merits such as cost and environmental concerns barely changed, since the presence of the new component in the bulk is negligible. On the other hand, the additive could significantly change the targeted property. This is especially pronounced in terms of interfacial properties because these additives are usually preferentially involved in interfacial redox processes before the main components of the bulk electrolyte are.

The additive approach has been used for lithium batteries to improve the surface morphology of a lithium electrode so that dendrite growth can be avoided.[10, 372–375] Since the concept of the SEI was proposed by Peled et al.,[37] the emphasis has been placed on the reductive decomposition of these additives and the effect of the decomposition products on the physicochemical properties of the SEI. Obviously, when carbonaceous materials replaced lithium metal as anodes, the same line of thought led to the attempts at controlling the SEI chemistry by means of using various additives.[376] During the past decade, this approach has been thoroughly studied, the focus of which has been placed at the SEI on the anodes, although additives targeting other cell components have also been developed. However, because of direct commercial interest, most of the work on additives has never been published in technical journals, especially the work that has eventually been accepted for use in commercial lithium ion cells. As an alternative, patent disclosures and conference abstracts did reveal scattered information about this aspect, although fundamental insight is usually unavailable in these forms of literature. In recent years, electrolytes containing additives have been named "functional electrolytes" by some researchers.[377]

According to the functions targeted, the numerous chemicals tested as electrolyte additives can be tentatively divided into the following three distinct categories: (1) those used for improving the ion conduction properties in the bulk electrolytes; (2) those used for SEI chemistry modifications; and (3) those used for preventing overcharging of the cells. Since the additives designed for the last purpose are usually compounds with oxidation potentials close to the operating potential of the cathode materials, the coverage of additive studies has included essentially

**Table 8. Performance-Enhancing Additives for Bulk Properties**

| Additive Structures | Host Electrolyte System | Remarks | Ref. |
|---|---|---|---|
| **12-crown-4** | $LiBF_4/PEO$, | Unhelpful with $t_{Li}$ negative effect on cycle life; toxic. | 379, 380, 382 |
| **15-crown-5** | $LiClO_4/PC$ | | 379 |
| **aza-ethers** R = CF$_3$SO$_2$ | $LiCl/THF$ or $LiBr/THF$ | Low solubility in polar solvents; instability with $LiPF_6$. | 384 385 |
| **borates** $R_F$ = perfluoro- or partially fluoro- alkyls, perfluorophenyls etc | $LiF/DME$; $CF_3CO_2Li/DME$ | Less electrochemically and thermally stable than borane. | 386~388 |
| **boranes** $R_F$ = perfluoro- or partially fluoro- alkyls, perfluorophenyls etc | $LiX/DME$ (X=F, Cl, Br, I); $LiX/PC/EC/DMC$; $LiF/DMC$; $CF_3CO_2Li/DME$; $C_2F_5CO_2Li/DME$ | Improves thermal stability of spinel. Improves thermal stability of $LiPF_6$. No negative effect on anode SEI. | 313, 386, 387, 389~391 |
| **boronates** | $LiF/DME$; $LiF/EC/DMC$; | Most significant effect on ion conductivity. Cycling stability on both $LiMn_2O_4$ and $LiNi_{0.8}Co_{0.2}O_2$. | 392 |

every major component of the lithium ion cell that interacts with the electrolytes.

### 8.2.1. Bulk Electrolyte: Ion Transport

The ability of crown ether to coordinate with lithium ion has long been recognized, and in terms of the cavity size, 12-crown-4 and 15-crown-5 have been identified as the most efficient ligands for lithium ion.[378] The idea of using these cyclic polyether compounds to promote the solvation of lithium salts in nonaqueous electrolytes was actively pursued when rechargeable cells based on lithium metal electrodes were still the commercial objective. It has been found that the presence of both 12-crown-4 and 15-crown-5 can effectively improve the solubility of the lithium salts and increase the ionic conductivity in the resultant electrolytes, especially when the solvents have low dielectric constants.[379−383] This improvement in bulk ion conductivity is also reflected in the interface properties, as the charge-transfer resistance on the $LiCoO_2$ cathode is also reported to be reduced because of the presence of 12-crown-4.[380,382] The electrochemical stability limits are not obviously influenced by crown ethers, but considering their ether-like structure, one should be concerned with their stability on the fully charged cathode surface in the long term. In polymer-based electrolytes, 12-crown-4 was also found to decrease the glass transition temperature of the system.[382] On the other hand, since the increase of ion conductivity is realized through the coordination of lithium ions by crown ether molecules, the lithium

transference number is lowered as a result of its presence. In other words, the addition of crown ethers in nonaqueous electrolytes actually promotes the undesired anion transport. The main barrier for the application of crown ethers in electrolyte, however, is their toxicity. The environmental concern over the processing and disposal of any materials containing these crown ethers makes it impossible for industry to adopt them in large-scale applications.

To develop an additive that selectively coordinates with salt anions and frees lithium ion for conduction, McBreen and co-workers pursued a molecular design and tailor-synthesis approach that yielded several families of novel compounds based on nitrogen or boron centers with strongly electron-withdrawing substituents.

The first family of the so-called anion receptors was aza-ethers that were based on cyclic or linear amides, where the nitrogen core was made electron-deficient by the perfluoroalkylsulfonyl substituents so that these amides would preferentially interact with the electron-rich anions through Coulombic attraction, contrary to how their unsubstituted counterparts would act.[384,385] Two selected representatives from the aza-ether family are shown in Table 8. When used as additives in solutions of various lithium halides LiX in THF, these novel compounds were found to increase both the solubility and the ion conductivity of these solutions. For example, the ion conductivity of the LiCl/THF solution was 0.0016 mS cm$^{-1}$, while the LiCl/THF solution with one of the linear aza-ethers containing eight perfluoroalkylsulfonyl substituents ($n$ = 5 for the linear aza-ether shown in
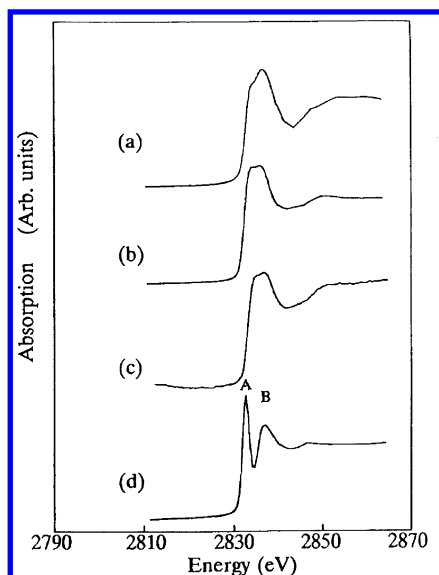
**Figure 37.** NEXAFS spectra at the K-edge of chloride for (a) LiCl crystal, (b) 0.2 M LiCl/THF, (c) 0.2 M LiCl/THF + 0.1 M aza-ether that does not have electron-withdrawing substituents on N, and (d) 0.2 M LiCl/THF + 0.1 M linear aza-ether with $n = 3$ in Table 8. Note the white line peak split when the electron-withdrawing substituents perfluoromethylsulfonyl are present. (Reproduced with permission from ref 384 (Figure 2). Copyright 1996 The Electrochemical Society.)

Table 8) exhibited an increase of ∼900 times at 1.4 mS cm$^{-1}$.[384] There was an obvious relationship between the ability of the aza-ether to coordinate the lithium cations and the extent by which ion conductivity was improved, since the latter proportionally increased with both the number of the electron-withdrawing substituents in the molecule and the electron-withdrawing ability of the substituents.[384,385] For example, tosylsulfonyl, a weaker electron-withdrawing group as compared with perfluoroalkylsulfonyl, proved to be a much less efficient additive.[385] On the basis of these dependences, it seemed that these aza-ethers did act as anion receptors in the nonaqueous solutions.

To further confirm that these aza-ethers actually coordinate with the salt anions, the authors used near X-ray absorption fine structure spectroscopy (NEXAFS) to study the coordination symmetry of the chloride anion in LiCl/THF solutions, in the absence or presence of aza-ether additives, and detected that the presence of the additives created a clear split in the Cl K-edge white line peak, as shown in Figure 37, indicative of the interaction between chloride and the electron-deficient nitrogen.[384] Further XRD studies conducted on complex crystals grown from the cosolutions of the cyclic aza-ether and lithium halide salts supported the above NEXAFS observations with new Bragg peaks representing a larger $d$ spacing (∼15 Å) in the crystal. Thus, the authors concluded that these new aza-ethers are indeed anion receptors, whose preference in coordinating ions was an exact opposite to that of the conventional crown ethers. With the addition of these molecules, the ion conductivity and the lithium transference number were enhanced simultaneously, a benefit that has rarely

been achieved thus far in nonaqueous lithium electrolytes.

Unfortunately, these aza-ethers showed limited solubility in the polar solvents that are typically preferred in nonaqueous electrolytes, and the electrochemical stability window of the LiCl-based electrolytes is not sufficient at the 4.0 V operation range required by the current state-of-the-art cathode materials. They were also found to be unstable with LiPF$_6$.[390] Hence, the significance of these aza-ether compounds in practical applications is rather limited, although their synthesis successfully proved that the concept of the anion receptor is achievable by means of substituting an appropriate core atom with strong electron-withdrawing moieties.

In their continued efforts, McBreen and co-workers selected boron, an electron-deficient atom, as the core to build a series of new anion receptors using the same tactics with electron-withdrawing substituents. These new additives can be classified roughly into these three subcategories: borate,[386–388] borane,[313,386,387,389–391] and boronate.[392] Selected representatives from each category are also listed in Table 8.

Basically, these boron-based anion receptors are much more efficient in coordinating anions, perhaps because of the electron-deficient nature of boron, since most of them can even effectively dissociate LiF up to 1.0 M, which is virtually insoluble in most organic solvents, and yield ion conductivities as high as 6.8 mS cm$^{-1}$ in DME.[313] Considering that the electrochemical oxidation potential for F$^-$ is ∼5.9 V, this new electrolyte does indeed seem attractive in providing a wide electrochemical stability window. On a GC electrode, the electrochemical stability limits were found to be in the range 4.05−5.50 V, usually set by the oxidation of electrolyte solvents,[388,392] while, on various cathode materials, stable cycling performance was observed with the upper voltage limit as high as 4.30−4.50 V.[313,387,390] Cycling tests at elevated temperature (55 °C) further showed that the electrolytes based on LiF coordinated by these additives were stable when compared with the state-of-the-art electrolytes based on LiPF$_6$.[389] Similar stability was also found on the carbonaceous anode surface, where the authors concluded that the presence of these anion receptors did not interfere with the formation of the SEI film, and the dissolution of the SEI was not detected even after heat treatment that would dissolve LiF salt.[391]

Among the three subcategories, boronate compounds seemed to be the most efficient in coordinating with anions and enhancing lithium ion stability, although the number of electron-withdrawing substituents in boronate is only two. The authors thus inferred that the ability of these anion receptors to capture an anion depends not only on the electron-deficiency of the core atom but perhaps also on the steric hindrance presented by these substituents on the core. With only two substituents, the core of the boronates is obviously more exposed and therefore more easily accessible for an anion. The higher ion conductivity achieved by boronate additive therefore comes from the better balance between the electron-deficiency and steric openness of this compound as

compared with boranes and borates.[392] On the other hand, in terms of ion conductivity enhancement, borates and boranes behave similarly,[386] though borates show less stability electrochemically and thermally than boranes.[387]

The solubility of these boron-based additives is also much higher than that of aza-ethers, and their effects on ion conductivity were studied in popular electrolyte solvent mixtures such as PC/EC/DMC[387] or EC/DMC.[388,389,392] Although for the salts such as $LiPF_6$, which are already well dissociated in these solvent mixtures, the enhancement in ion conductivity by the anion coordination might not be as pronounced as that for lithium halides, there is one advantage for $LiPF_6$ being used with these additives: the thermally unstable $LiPF_6$ is effectively stabilized by the presence of tris(pentafluorophenyl)borane (TPFPB), as indicated by the slow scan cyclic voltammetry experiments conducted on a spinel cathode surface after storage at 55 °C for 1 week.[390] The authors attributed this stabilization to the coordination of $PF_6$ anion, which elongated the interatomic distance between Li and F. This hypothesis was supported by the conclusion of a molecular dynamic simulation published earlier, wherein Tasaki and Nakamura postulated that the reactivity of lithium cation and F would be suppressed by the elongated distance between them if an effective anion coordination was achieved.[393]

Since these anion receptors based on boron offer a wide variety of merits, their application seems promising if the cost and toxicology do not constitute any serious barrier for industry-scale productions.

### 8.2.2. Anode: SEI Modification

Due to the core importance of the SEI formation on carbonaceous anodes, the majority of the research activities on additives thus far aim at controlling the chemistry of the anode/electrolyte interface, although the number of publications related to this topic is rather limited as compared with the actual scale of interest by the industry. Table 9 summarizes the additives that have been described in the open literature. In most cases, the concentration of these interface-targeted additives is expected to be kept at a minimum so that the bulk properties of the electrolytes such as ion conduction and liquid ranges would not be discernibly affected. In other words, for an ideal anode additive, its trace presence should be sufficient to decouple the interfacial from bulk properties. Since there is no official standard available concerning the upper limit on the additive concentration, the current review will use an arbitrary criterion of 10% by weight or volume, above which the added component will be treated as a cosolvent instead of an additive.

With few exceptions, the additives that are intended for the modification of the SEI usually have high reduction potentials, which ensure that these additives are reduced on the anode surface before the bulk electrolyte components are involved. In other words, during the first charging of a lithium ion cell, an SEI with the chemical signature from an additive would have been formed before the potential of the carbonaceous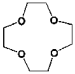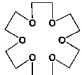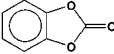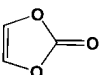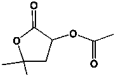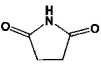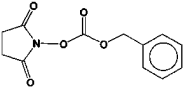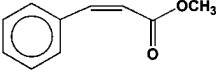 anode reached the onset reduction value for bulk electrolyte solvents, especially PC. Naturally, certain requirements have to be met by the decomposition products of the additives, such as insolubility in electrolytes, film compactness, and low impedance to lithium ion transport.
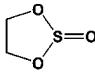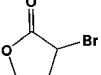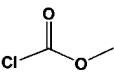
The search for potential SEI additives in the past decade has been carried out mainly on a trial-and-error basis until, recently, a semiempirical rule was developed to facilitate the screening process, which judges the readiness of a certain compound to be reduced on the anode by the energy level of its lowest unoccupied molecular orbital (LUMO).[377,394] The basis of this rule is the assumption that a molecule with a lower energy level of its LUMO should be a better electron acceptor and, therefore, more reactive on the negatively charged surface of the anode. Sharing the view that interfacial stability originates from the reactivity, this rule is conceptually related to the selecting tool for the SEI-forming electrolyte components as proposed by Peled et al.,[106] despite the fact that the latter was based on a kinetic consideration (exchange current) of the molecule instead of a thermodynamic one (LUMO energy level). Quantum calculations have yielded LUMO energy levels for most of the commonly used electrolyte solvents as well as some of the tested SEI additives, which are compiled in Table 10.[255,377,394,408] Apparently, the LUMO levels for all aliphatic cyclic carbonates are virtually identical, whereas structural modifications with an aromatic bond, double bond, or substitution of halogen atoms cause large decreases in the LUMO level.[255] This trend is in good agreement with the experimental findings, since most of the additives that demonstrated promising performances in electrolytes indeed possess one of the active functionalities. A fairly linear relationship has been established between the LUMO energy level and the reduction potential for these additives.[377]

The current efforts with SEI additives usually aim at one of these two distinct but closely interrelated goals: (1) to minimize the irreversible capacity needed in the first cycle to form the SEI and (2) to enable the use of PC at higher concentrations in the electrolyte. While the former would generally benefit a lithium ion cell in terms of a more stable SEI, the latter is of special significance to the purpose of adapting the electrolytes based on PC to the highly graphitic anode materials so that the operating temperature can be expanded toward the lower limit without sacrificing energy density.

In the early era of lithium ion cell research, Aurbach et al. noticed that the presence of $CO_2$ in the electrolyte had pronounced effects on the lithiation behavior of graphitic anodes. A number of electrolytes, which were thought to be incompatible with graphite because they are based on solvents such as methyl formate or THF, delivered much improved performance under 3−6 atm of $CO_2$.[250] They proposed that $CO_2$ participated in the formation of the SEI by a two-electron process, yielding $Li_2CO_3$, which assisted in the buildup of the protective surface film.[249] However, in PC-based electrolytes, $CO_2$ presence proved to be ineffective,[123] while, in electrolytes based on carbonate mixtures such as EC/DMC, the
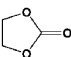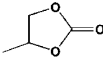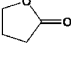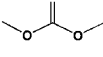
**Table 9. Anode SEI Additives**
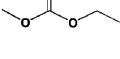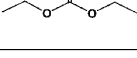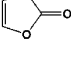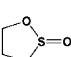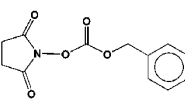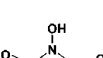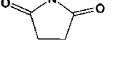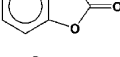
| Additive Structures | Host Electrolyte System | Remarks | Ref. |
|---|---|---|---|
| $CO_2$ | $LiAsF_6/MF$<br>$LiAsF_6/EC/DMC$ etc. | Non-effective for PC-suppression; internal pressure. | 104, 123, 249, 250, 272 |
| $SO_2$ | $LiClO_4/EC/DME$<br>$LiAsF_6/MF$<br>$LiAsF_6DMC$, $LiAsF_6/PC$ etc. | Effective for PC-suppression; anodic stability unknown; corrosive; safety hazard. | 251<br>395<br>396 |
| 12-crown-4 | $LiAsF_6/PC$<br>$LiClO_4/EC/PC$ | Effective for PC-suppression; preferential solvation of Li ion; high concentration needed; toxic. | 250, 261, 397, 398 |
| 18-crown-6 | $LiClO_4/EC/PC$ | Not as effective as 12-crown-4; high concentration needed; toxic. | 261 |
| catechole carbonate (CC) | $LiPF_6/PC/DEC$ | Effective for PC-suppression; anodically stable. | 377, 409 |
| vinylene carbonate (VC) | $LiIm/PC/EC/DMC$<br>$LiPF_6/PC$<br>$LiPF_6/DMC$<br>$LiAsF_6/EC/DMC$ | Effective for PC-suppression; increases SEI stability at high temp.; anodically stable. | 400<br>401<br>402<br>404 |
| ethylene sulfite (ES) | $LiClO_4/PC$ | Effective for PC-suppression; anodically stable. | 399 |
| α-bromo-γ-butyrolactone | $LiPF_6/PC$ | | 410 |
| methyl choloroformate | $LiPF_6/PC$ | | 410 |
| 2-acetyloxy-4,4-dimethyl-4-butanolide | $LiClO_4/PC$ | Preferential solvation of Li ion; Participation in SEI formation. | 411 |
| succinimide | $LiPF_6/PC/EMC$ | | 377 |
| N-benzyloxycarbonyloxysuccinimide | $LiPF_6/PC/EMC$ | | 377 |
| methyl cinnamate | | | 48b |

effect of $CO_2$ seemed to be negligible.[104] These efforts could be viewed as the first attempts of modifying the SEI with electrolyte additives.

$SO_2$, on the other hand, was found to be a much more efficient additive, as its presence at less than 20% effectively suppressed the cointercalation of PC and supported the reversible lithium intercalation/deintercalation of graphitic anodes at low potentials.[395,396] The reduction potential of $SO_2$ was found to be at ~2.7 V, far above that corresponding to the

**Table 10. LUMO Energy Level and Reduction Potentials of Solvents and Additives**

| Solvent/Additive | LUMO/eV | Reduction Potential (vs. Li$^+$/Li) | | Refs. |
|---|---|---|---|---|
| | | on GC | on GR | |
| EC | 1.175 | 0.9 | 0.8 | 212, 251, 377 |
| | 0.97 | | | 255 |
| PC | 1.235 | 1.0 | 0.78 | 214, 377 |
| | 1.02 | | | 255 |
| γBL | 1.049 | | | 377 |
| | 0.91 | | | 255 |
| DMC | 1.054 | 1.32 | | 214, 377 |
| EMC | 1.248 | | | 377 |
| | 1.17 | | | 255 |
| DEC | 1.288 | 1.32 | | 214, 377 |
| | 1.21 | | | 255 |
| VC | 0.10 | 1.4 | | 377 |
| | -0.14 | | | 255 |
| | | | | 214 |
| ES | 0.035 | 1.6 | 1.8~2.1 | 377, 399 |
| | 0.03 | | | 255 |
| BCSC | 0.234 | 1.52 | | 377 |
| N-hydroxysuccinimide (HSC) | 0.208 | 1.6 | | 377 |
| SC | 0.186 | 1.6 | | 377 |
| N-chlorosuccinimide (CSC) | -0.527 | 3.2 | > 2.5 | 377 |
| CC | 1.10 | | | 377, 409 |
| 2-acetyloxy-4,4-dimethyl-4-butanolide | 0.688 | | 1.3~1.1 | 411 |

cointercalation/decomposition process of PC.[251,395,396] Thus, Ein-Eli et al. believed that the SEI formation was initiated by the predominant decomposition of SO$_2$.[395,396] On the basis of the FT-IR analysis of the graphitic anode surface, they suggested that, in addition to the solvent decomposition products, lithium alkyl carbonate, the SEI also contained reduction products originated from SO$_2$ such as Li$_2$S and lithium oxysulfur species. An extra merit of SO$_2$ as an additive in electrolytes is the increase in ion conductivity, which is caused by its high dielectric constant and low viscosity.[396] However, the obvious
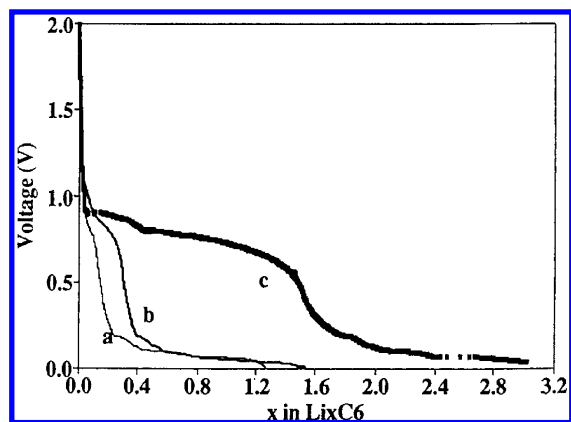
**Figure 38.** Effect of crown ethers on the irreversible capacity. Voltage profiles of a graphite anode in 1.0 M $LiClO_4$/EC/PC (1:1) electrolyte containing (a) 1.0 M 12-crown-4, (b) 1.0 M 18-crown-6, and (c) no crown ethers. (Reproduced with permission from ref 261 (Figure 3). Copyright 1993 The Electrochemical Society.)



**Figure 39.** Stabilization of a graphitic anode in 1.0 M $LiClO_4$/PC electrolyte by 5% ES. For comparison, the voltammograms of a graphitic anode in 1.0 M $LiClO_4$/PC electrolyte with 10% $SO_2$ were also shown. (Reproduced with permission from ref 399 (Figure 3). Copyright 1999 The Electrochemical Society.)

disadvantages of such an additive are the concerns over corrosion and the environmental and safety hazard issues related to the chemical nature of $SO_2$. Its instability on cathode materials has not been well addressed either, since most of the published results were obtained on lithium/graphite half-cells.

Besides $CO_2$ and $SO_2$, other gaseous species such as $N_2O$ were also considered as additives,[376] but none of these ideas seemed practical for the lithium ion industry, because the application of such approaches would certainly introduce an additional cost as well as safety concerns for the commercial cells, especially when increased internal pressure due to the gas production during prolonged cycling had already become a persistent problem for the manufacturers of industry-size lithium ion cells.

In the early 1990s, Wilkinson and Dahn realized that, in addition to enhancing ion conductivity, crown ethers could also reduce the irreversible capacity associated with the reduction process at 0.80 V when the electrolyte was based on high concentrations of PC.[397] Shu et al. studied the phenomenon by using 12-crown-4 and 18-crown-6 as additives in $LiClO_4$/EC/PC and established the direct connection between the decrease in gas evolution associated with the 0.80 V irreversible process and the addition of 12-crown-4.[398] As Figure 38 shows, the effectiveness of these crown ethers in suppressing the PC cointercalation/decomposition seems to be related to the cavity size,[261] knowing that 12-crown-4 serves as a better chelating agent for lithium ion than 18-crown-6.[378] The authors suggested that, unlike most of the additives that obey the empirical rule of the LUMO energy level, a crown ether might not be chemically involved in the formation of the SEI but rather affect this process indirectly by means of preferential solvation of lithium ions. Thus, the exclusion of PC molecules from the solvation sheath rather than the reductive decomposition of crown ethers is responsible for the reduced irreversible process at 0.80 V.[398]

Their hypothesis was confirmed by the work of Aurbach and co-workers, who performed detailed FT-IR investigations on the graphitic anode surface that
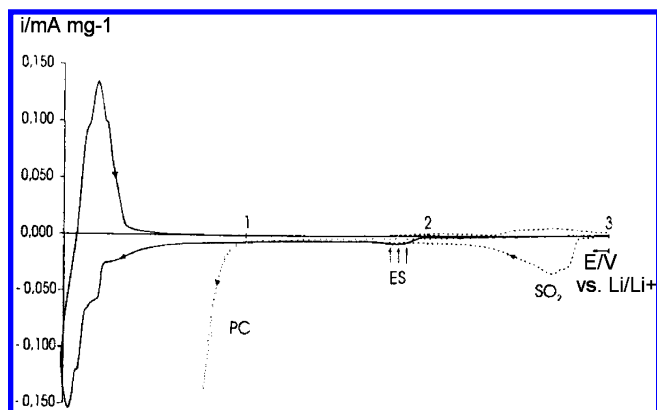
was cycled in electrolytes containing 12-crown-4.[250] Since the peaks corresponding to the possible reduction products of 12-crown-4 were absent in the spectra, they concluded that the effect of crown ether was not due to its participation in the buildup of the SEI. Instead, the prevention of graphene exfoliation was very likely due to the absence of PC molecules in graphene interlayers, a direct result of its expulsion from the lithium ion solvation sheath. This was even so when the concentration of 12-crown-4 was only one tenth of the salt concentration. The effectiveness of 12-crown-4 in suppressing PC cointercalation/decomposition is further demonstrated by the cycling of the graphitic anode in electrolytes based on neat PC.[250] Considering that the main signals collected from the anode surface during the experiment were at $\sim$1661 cm$^{-1}$, which is characteristic of the carbonyl stretching in lithium alkyl carbonate, the authors suggested that PC was forced to be reduced on the surface via a single-electron process. This seemed to be in good agreement with the previous report that only within graphene structures would PC likely undergo reduction via a two-electron process and result in exfoliation.

Despite the highly efficient performance of crown ethers in reducing the irreversible capacity at the anode side, especially when PC-based electrolytes were used, the toxic nature of these compounds still prevented their application in commercial lithium ion cells.

A sulfur analogue of EC, ethylene sulfite (ES), was proposed as an additive for PC-based electrolytes by Winter and co-workers,[399] apparently because of its structural similarity to EC and its potential, under reductive conditions, to release $SO_2$, a known additive that effectively suppresses PC decomposition.[395,396] As the voltammetry in Figure 39 shows, ES in only 5% presence successfully eliminated the exfoliation of the graphite anode, whereas 10% $SO_2$ failed. The irreversible process corresponding to the reduction of ES occurred at $\sim$2.0 V, lower than that of $SO_2$ by $\sim$0.80 V; however, the quantity of charge associated was much lower. According to the authors, the above apparent gap between the reduction potentials of ES

and SO$_2$ actually excluded the self-suggesting assumption that the SEI-forming ability of ES should stem from its tendency to release SO$_2$, which in turn participates chemically in the buildup of SEI in a mechanism suggested by Ein-Eli et al.[395,396] Furthermore, the reduction of SO$_2$ was reversible, whereas the reduction of ES did not seem to be, as evidenced by the absence of any anodic current in Figure 39.

On the other hand, the attempt to use ES as a bulk solvent proved to be unsuccessful because of the high irreversible capacity caused by the reduction of ES, although it looked like the reversible capacity associated with lithium intercalation was not affected by the irreversible process at 2.0 V. Considering that these results were obtained in an anode half-cell where lithium was the excess material, one should realize that the irreversible reduction of ES would cost the capacity of a full lithium ion cell. Therefore, ES should only be used as an additive at small concentrations.

The anodic stability of the electrolyte was not negatively affected by the presence of ES in LiClO$_4$/PC, as evidenced by the cyclic voltammetry carried out on the LiMn$_2$O$_4$ surface. The onset of major electrolyte decomposition, seemingly contributed by the oxidation of PC, occurs at ~4.8 V, which would allow the safe use of most state-of-the-art cathode materials based on LiCoO$_2$, LiMn$_2$O$_4$, or LiNiO$_2$. The first cycling of the cathode half-cell, Li/LiMn$_2$O$_4$, was shown in the report, but without the extended cycling of this cell or full lithium ion cells.[399]

Among the various additives tested, vinylene carbonate (VC) might be the most famous in the lithium ion research and development community, although the number of publications related to it seems to be rather small. Its importance can be evidenced by the number of companies that vied for the patent rights for it.[400−402]

The reactivity of VC apparently arises from its polymerizable vinyl functionality and its structure of high strain, which is caused by the sp$^2$-hybridized carbons on the ring (Tables 9 and 10).[403] The small concentration of VC can effectively reduce the irreversible capacity associated with the 0.80 V process in almost any PC-based electrolyte,[400] and its presence, even in bulk concentrations, does not constitute any instability on the charged surface of either anode or cathode materials. In the latter case, an electrolyte of 1.0 M LiPF$_6$/PC/VC performed reversibly up to 4.3 V with a LiMn$_2$O$_4$ cathode.[401] In a recent report Aurbach and co-workers thoroughly described the effect of VC as additive in electrolytes for lithium ion cells based on the graphitic anode and LiMn$_2$O$_4$ or LiNiO$_2$ cathode, using various techniques including EIS, EQCM, FT-IR, and XPS.[404] According to the voltammetry results of their work, there was no discernible characteristic reductive process in voltammetry that could be unambiguously assigned to the reduction of VC on the graphitic anode, in sharp contrast to the cases of other additives that showed distinctive reduction processes at high potentials. The only difference between VC-containing and VC-free electrolytes was the much-reduced irreversible capacity at 0.90−0.80 V. This visual absence of the VC

reduction process could be attributed either to the possibility that the passivation of the graphitic anode by the decomposition products was so efficient that the reduction of VC only occurred to a trace extent or to the possibility that the scan rate employed in the experiments (1.0 mV s$^{-1}$) was too fast for any quasi-equilibrium to be established between the additive VC and the anode surface, the result of which was the total drowning of the VC reduction peak by the main event occurring at the lower potentials. According to a separate voltammetry study carried out on inert electrodes (Au and GC), VC could be reduced irreversibly at 1.4 V.[214]

EIS results indicated that the impedance on a graphite surface was much lower in the presence of VC; however, at elevated temperatures (60 °C), it became higher than those of VC-free electrolytes. EQCM using a gold-plated quartz crystal detected that the mass accumulation in VC-containing electrolytes was higher by 50% as compared with the cases of VC-free electrolytes during voltammetric scanning between 3.0 and 0.5 V, indicating that the reactive VC might be profoundly involved in the formation of the SEI. The comparison between the FT-IR spectra collected on both gold mirror and graphite electrodes for VC-free and VC-containing electrolytes further confirmed the participation of VC with characteristic absorptions at ~3000 cm$^{-1}$, representing the possible existence of polymeric moieties in addition to the alkyl carbonates observed commonly on a graphitic anode that was cycled in carbonate-based solvents.

The surface chemistry of VC on graphite was also semiquantitatively investigated by C 1s and F 1s spectra in XPS analyses,[404] as shown by Figure 40. Apparently, the presence of VC drastically reduced the content of LiF in the SEI, as indicated by the LiF signal at 685 eV, which only appeared as a shoulder for that of PVdF (anode binder) at 687 eV while it was the predominant species in VC-free electrolyte. On the other hand, the abundance of lithium alkyl carbonate in the SEI as represented by the signal at 289 eV was increased with VC concentration. This improvement of the SEI chemistry with higher lithium alkyl carbonate content and lower LiF content was reflected in the increased stability of a VC-containing electrolyte, which demonstrated a more stable performance in a lithium/graphite anode half-cell at an elevated temperature of 60 °C, while the identical cell based on VC-free electrolyte suffered constant capacity loss.[404]

The possible impact of VC on the stability of an electrolyte at a cathode surface was also investigated and no obvious negative effect of VC on either LiNiO$_2$ (Figure 41) or LiMn$_2$O$_4$ was observed at up to 4.2 V. A slight kinetic improvement due to the presence of VC, as indicated by the better resolved peaks and higher current response, was observed in the slow scan voltammetry, as shown in Figure 41.[404] FT-IR studies on the cycled cathode surface indicated the formation of surface species that were probably oligomeric VC, originating from the cationic polymerization on the delithiated cathode surfaces.
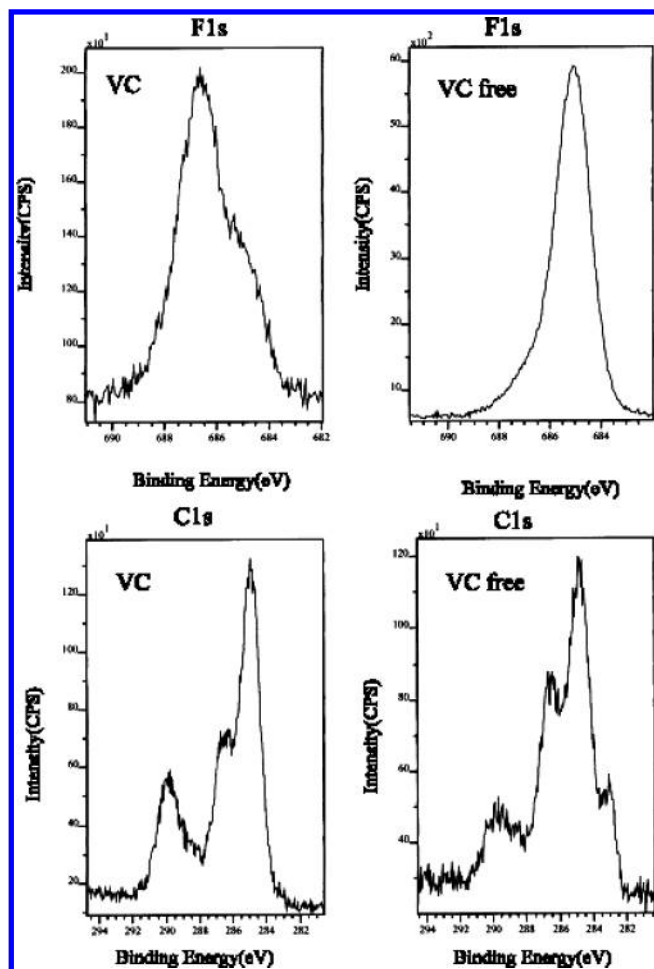
**Figure 40.** XPS C 1s and F 1s spectra of graphitic anodes cycled in 1.0 M LiAsF$_6$/EC/DMC electrolyte. 5% VC was used as additive in the left spectra. Note the different scales for the two F 1s spectra. (Reproduced with permission from ref 404 (Figure 10). Copyright 2002 Elsevier.)



**Figure 41.** Cyclic voltammograms of a LiNiO$_2$ cathode in VC-free and VC-containing 1.0 M LiAsF$_6$/EC/DMC electrolyte at scan rates of (a) 0.50 mV s$^{-1}$ and (b) 0.1 mV s$^{-1}$. (Reproduced with permission from ref 404 (Figure 11). Copyright 2002 Elsevier.)

In conclusion, many authors believed that VC was a rather effective additive for chemical modification of the anode SEI. It not only reduced the irreversible capacity during the initial charging process of lithium ion cells, but it also improved the stability of the SEI at elevated temperatures. Because of VC participation, the new SEI chemistry contained polymeric species that stemmed from the reductive polymerization of VC, which was characterized by a high content of alkyl carbonate functionalities. Comparative studies of this additive in commercial lithium ion cells proved that VC presence improved cycle life performance.[405−407]

It should be mentioned that the commercially available VC usually contained a small percentage (<2%) of prohibitors that stabilized the reactive VC from polymerizing upon storage. These compounds were usually radical scavengers such as 2,6-di-*tert*-butyl-*p*-cresol (DBC) or butylated hydroxytoluene (BHT). Recently, reports pointed out that the presence of these prohibitors actually had a negative impact on the anodic stability of VC on various cathode materials, and VC of high purity was of vital importance in obtaining reproducible performance in lithium ion cells.[404,408]
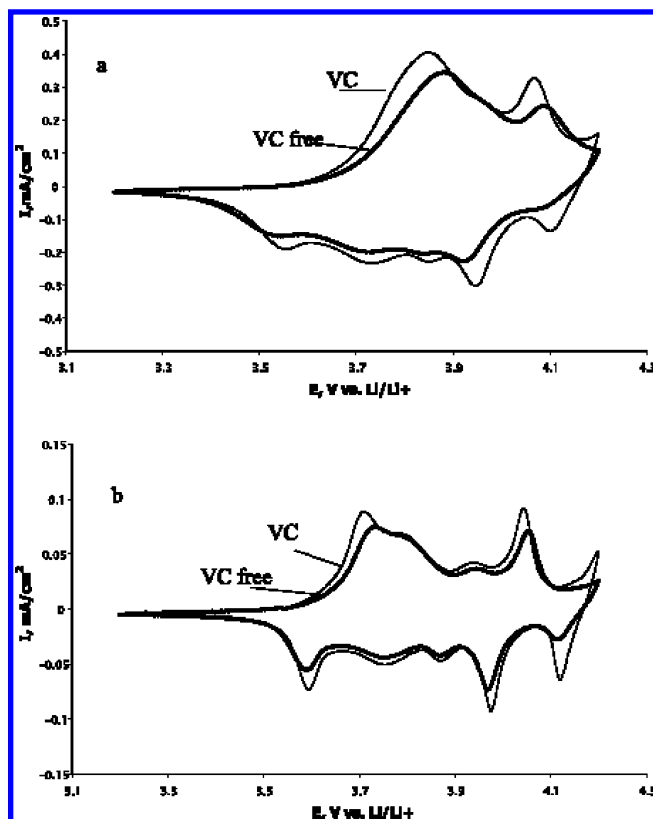
Another highly efficient additive for the anode SEI is catechole carbonate (CC), reported by Wang et al., which has a benzene ring fused with a functionality structurally similar to EC (Tables 9 and 10).[377,409] Like VC, in small percentage (∼2%), it suppresses the irreversible capacity due to PC decomposition/cointercalation at 0.80 V and supports extended cycling of the graphitic anode in LiPF$_6$/PC/DEC. A study on the concentration-dependence of this irreversible capacity indicated that the optimum content of CC lies between 0.5% and 2%. The authors postulated that the mechanism through which CC stabilized the graphitic anode against exfoliation by PC should involve the direct participation of CC in the formation of the SEI, since its small concentration does not allow for preferential solvation as crown ether does. They further proposed that in electrolyte solutions CC served as a radical scavenger and quenched PC radical anions so that the continued reduction of PC via a two-electron process was inhibited.

The anodic stability of the electrolyte containing 2% CC was tested on a LiCoO$_2$ cathode, and no obvious oxidative decomposition was observed. It must be noted, though, that the above conclusion was based on a voltammetry experiment conducted with a relatively high scanning rate (15 mV s$^{-1}$). The performance test of the electrolyte LiPF$_6$/PC/DEC with 2% CC in a full lithium ion cell was shown to deliver a slightly fading capacity when cycling between 2.75 and 4.10 V.

The continued efforts in this area in recent years generated a series of reactive compounds as potential candidates, which include halogenated species such as bromo-$\gamma$-$\gamma$BL,[410] other $\gamma$BL derivatives,[411] compounds containing vinyl groups,[412,413] and compounds that belong to the succinimide family[377] (Tables 9 and 10). Most of these additives were reported to be effective in reducing the irreversible capacities in the first charge process, while some also successfully eliminated the cointercalation of PC and avoided the exfoliation of graphitic anodes. Among these works, one interesting mechanistic study was carried out by Matsuo et al., who employed a $^{13}$C NMR technique to investigate the effect of $\gamma$BL derivatives on lithium solvation and found that PC molecule was excluded from the solvation sheath of lithium ions by these additives.[411] Thus, these authors suggested that $\gamma$BL derivatives might suppress PC decomposition via a mechanism that combines both preferential solvation as crown ethers do and direct chemical participation as most of the other additives do, although the preferential solvation effect would be negligible when the concentration of these additives is far below 1.0 M.

The work on SEI-modification additives is currently carried out throughout the lithium ion research community, and candidates of new structure are being tested in large numbers. As a result, the major lithium ion manufacturers have applied various additives in their electrolyte formulations. However, the lack of information in the open literature makes the in depth and comprehensive review of this new branch of electrolyte chemistry difficult.

### 8.2.3. Cathode: Overcharge Protection

Unlike the anode-targeted additives discussed in the preceding part, the additives intended for cathode protection have a much longer history than lithium ion technology itself and were originally developed for rechargeable cells based on lithium metal anodes and various 3.0 V class cathode materials.

It has been long recognized that the accidental overcharge of lithium cells would lead to irreversible decomposition of electrolyte components, which is mainly the oxidative decomposition of solvents on a cathode surface and whose reaction heat and gaseous products are responsible for the hazardous thermal runaway. Since the overwhelming majority of the charging protocols are based on cell voltage as the indicator for the end-of-charge, such accidents are especially likely to occur for multicell battery packs in which cells with mismatched capacities are put in series. To avoid the cell degradation or hazards related to overcharging, cells for battery packs must be handpicked to match a nominal capacity or each individual cell within the pack must be regulated externally with electronic devices, such as positive temperature coefficient (PTC) resistors or integrated circuits (IC). However, both remedies add to the manufacturing cost and lead to a lower energy density of the cells.

As an alternative, Abraham and co-workers proposed an electrochemical mechanism built in the electrolyte that is able to shunt the excess charge
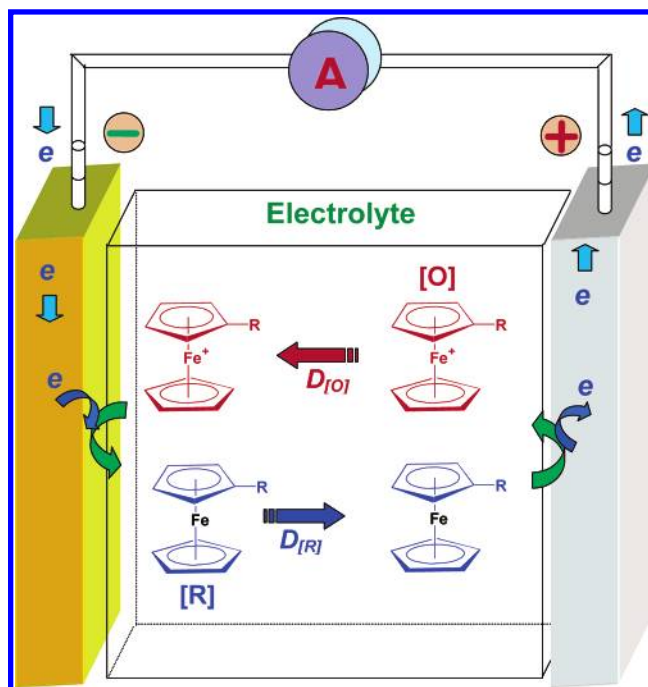


**Figure 42.** Schematic representation of the shuttling occurring in an overcharged cell that is based on electrolytes containing redox additive as protection.

injected into the cell when overcharge occurs.[414,415] The mechanism, intended to prevent the oxidative decomposition of electrolyte solvents at the cathode surface, was based on a redox additive that has an oxidation potential slightly lower than that of the electrolyte anodic decomposition and would serve as a current shuttle under the condition of overcharge, as Figure 42 shows. On an overcharged cathode surface, the redox additive would be transformed into its oxidized form [O], which, via diffusion across the cell electrolyte, would be reduced back to its original (reduced) state [R] on the surface of a negatively charged anode. Thus, the reversible nature of the redox couple [R]/[O] would maintain the above cycle of "oxidation−diffusion−reduction−diffusion" indefinitely and hence lock the cathode potential at the oxidation potential of [R] until termination of the charge. Ideally, no permanent damage would be done to the cell capacity during the redox shuttling, since the Faradaic current was only carried by the reversible redox reactions, while, energetically, the excess charge injected would be neither stored in the cathode nor consumed in reversible decompositions but rather dissipated in the form of heat associated with the shuttling current. Therefore, the net result of the above redox shuttling mechanism during overcharging could be viewed as a controlled internal short, and the effectiveness of a certain redox additive could be evaluated in terms of the maximum overcharge current it can shuttle.

Narayanan et al. conducted a theoretical analysis on the cell parameters that determined this maximum shuttling current.[416] By assuming that the mass transport of the redox couple [R]/[O] is mainly realized by means of diffusion—which is reasonable because the low concentration of [R]/[O] at the additive level makes the field-assisted migration negligible—they applied the finite linear diffusion

approximation to gain the diffusion-limited steady-state overcharge current $i$ as

$$i = \frac{nFADC}{l} \frac{\exp\left\{nF\left(\dfrac{E_c - E_c^0}{RT}\right)\right\}}{1 + \exp\left\{nF\left(\dfrac{E_c - E_c^0}{RT}\right)\right\}} \qquad (12)$$

where $F$, $A$, $D$, $l$, $C$, $E_c$, and $E_c^\circ$ are the Faraday constant, electrode area, diffusion coefficient for [R] or [O], interelectrode spacing, total concentration of the additive ([R] + [O]), single electrode potential of the cathode, and formal potential of the redox couple [R]/[O], respectively.

Obviously, when no overcharging exists (i.e., $E_c - E_c^\circ \ll 0$), the shuttle current is negligible, while the redox reaction remains not activated.

On the other hand, when overcharge does occur, eq 12 could be much simplified on the condition that $E_c - E_c^\circ \gg RT/nF$, and eq 12 is transformed into

$$i = \frac{nFADC}{l} = i_d \qquad (13)$$

The applied condition represents a relatively large positive deviation of the single-electrode potential for a cathode from the oxidation potential of the redox couple [R]/[O]. For a single-electron reaction at room temperature, the above criterion for the deviation $E_c - E_c^\circ$ corresponds to $RT/nF = 0.026$ V, and one would therefore expect the simplification that leads to eq 13 to hold true for most of the overcharge situations encountered in practical applications.

Thus, eq 13 expresses the limiting overcharge current that can be sustained by a particular choice of redox additive and electrochemical conditions, and it suggests that this maximum diffusion current $i_d$ is independent of the cell potential or the formal potential of the redox couple but is solely determined by its concentration and diffusion coefficient in the electrolyte. In the case that the overcharge current becomes too high for the redox couple to shuttle, as would happen when a large terminal voltage is mistakenly set during constant potential charge, any excess current over the maximal limit specified by eq 13 would continue to delithiate the cathode material and cause irreversible decompositions, and safety hazards would eventually be caused by this overflowing charge.

To maximize the current limit that could be shunted by redox additives so that the occurrence of such irreversible processes due to overflowing current could be more efficiently suppressed, the redox additive apparently should be present in the electrolyte at high concentrations, and both its oxidized and reduced forms should be very mobile species. Where the criteria for selecting potential redox additives are concerned, these requirements can be translated into higher solubility in nonaqueous media and lower molecular weight. In addition to solubility and diffusion coefficients, the following requirements should also be met by the potential redox additives: (1) the formal potential of the redox couple [R]/[O] should be lower than the onset potential for major decom-position of electrolyte solvents but high enough to ensure a full utilization of cathode active mass; (2) the electrochemical reversibility of the redox reactions should not degrade discernibly within the time frame of cell life; (3) the additive should be inert before and after activation by overcharging (i.e., both oxidized and reduced forms of the additive must not react with any electrolyte components).
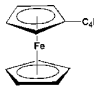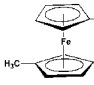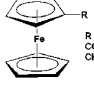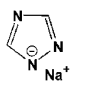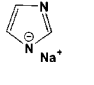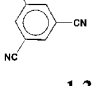
During the past two decades, the redox shuttle mechanism has been influencing researchers as the most promising solution to the challenge of cathode overcharge, and among the limited number of publications, most of the additives were selected based on their redox potentials.

The cathode materials employed for the early lithium-based systems were 3.0 V class oxides or sulfides; thus, the redox potential for the additive should be located in the neighborhood of 3.2−3.5 V. Accordingly, the first generation redox additive proposed by Abraham et al. was based on the iodine/iodide couple,[415] which could be oxidatively activated at the cathode surface at 3.20 V and then reduced at the lithium surface.[414,415,417−420] For most of the ether-based solvents such as THF or DME that were used at the time, the oxidation potential of iodide or triiodide occurred below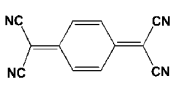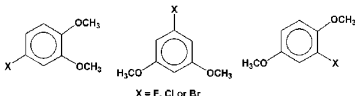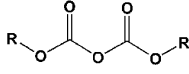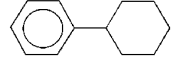 that of their major decom-positions, while the high diffusion coefficients of both iodine and iodide in these electrolyte systems ($\sim 3 \times 10^{-6}$ cm$^2$ s$^{-1}$) offered rapid kinetics to shuttle the overcharge current. Similarly, bromides were also proposed.[418−420] However, this class of halide-based additives were deemed impractical due to the volatil-ity and reactivity of their oxidized forms (halogen).

The well-known redox compounds based on the metallocene family, which are much more amicable than halide/halogen couples, were also first investi-gated by Abraham and co-workers as redox shut-tles.[421,422−426] These organometallic complexes consist of a metal core—usually Fe or Co—coordinated by two cyclopentadienyl ligands, as Table 11 shows, and they are able to undergo reversible redox reactions in the neighborhood of 3.2−3.5 V.[421] The electron exchange occurs through the change of valence orders of the metal core; however, the formal potential of this redox process not only varies with the metal core but also is sensitive to the substitution on the cyclopentadienyl rings.[424] The number as well as the chemical nature of the substituents (electron-donat-ing or -withdrawing) could affect the potential by as much as $\pm 0.30$ V.[427] Theoretically, this substitution-sensitivity offers a convenient tool to tailor the redox potential of these metallocenes for various cathode materials.[422,425]

Abraham et al. tested the performance of an $n$-butyl-substituted ferrocene in a lithium/TiS$_2$ cell, where LiAsF$_6$/THF or LiAsF$_6$/2MeTHF was used as an electrolyte. They found that, under overcharge conditions, the voltage of the cell containing ferrocene as an additive leveled off at 3.25 V, corresponding well to its redox potential of 3.18−3.50 V, while the reference cell without additive was overcharged up to 5.0 V, corresponding to the decomposition of THF.[422] No capacity loss was observed in successive cyclings after the overcharge test, thus confirming

**Table 11. Cathode Surface Layer Additives: Overcharge Protection**

| Additive Structures | Host Electrolyte System | Type | $E_{onset}$/V | Ref. |
|---|---|---|---|---|
| $I^-/I_2$ | LiAsF$_6$/THF | Redox | 3.2~3.5 | 414, 415, 417~420 |
| *n*-butylferrocene | | Rodox | 3.18 | 421, 422, 423 |
| 1,1'-dimethylferrocene | LiAsF$_6$/EC/2-Me-THF | Rodox | ~3.0 | 416 |
| ferrocene derivatives | LiAsF$_6$/EC/PC | Rodox | 3.09~3.55 | 429 |
| *1,2,4*-Triazole, Na salt | LiIm/PEO | Rodox | 3.1 | 431 |
| imidazole, Na salt | LiIm/PEO | Rodox | 2.5 | 431 |
| 1,3,5-tricyanobenzene (TCB) | LiIm/PEO | Rodox | 2.9 | 431 |
| tetracyanoquinodimethane (TCNQ) | LiIm/PEO | Rodox | 3.5 | 431 |
| substituted benzenes | LiPF$_6$/PC/DMC | Rodox | 3.93~4.27 | 432, 434 |
| pyrocarbonate | | Gas/CID[a] | > 4.0 | 48b, 440 |
| cyclohexylbenzene | | Gas/CID | > 4.0 | 48b, 440 |

CID: current interrupter device activated by internal pressure.

that the additive based on ferrocene had little deleterious effect on the stability of the cell components. These promising results initiated a new round of research activities based on structural modifications on the cyclopentadienyl rings.[425−429]

In a systematical study, Golovin et al. investigated a series of metallocene derivatives in terms of their redox potentials, mass transport properties, and chemical and electrochemical stabilities in both electrochemical test cells and commercial-size AA rechargeable cells.[429] Figure 43 shows the complete voltammetric scan of the ferrocene-containing electrolyte on a GC working electrode, where the peaks indicated as O2 and O3 represent the oxidation of cyclopentadienyl rings and electrolyte solvents, respectively, while R2 and R3 stand for the reductive decomposition of electrolyte solvents and the deposition of lithium from solution. Obviously, on the anode side, the limit was set by the lithium deposition, as the reduction of solvents only occurs in the first charging cycle in a lithium-based cell. The anodic limit, on the other hand, was imposed by the O2. The redox potential of the shuttle agent ferrocene was indicated by a pair of closely located peaks [R1]/[O1]
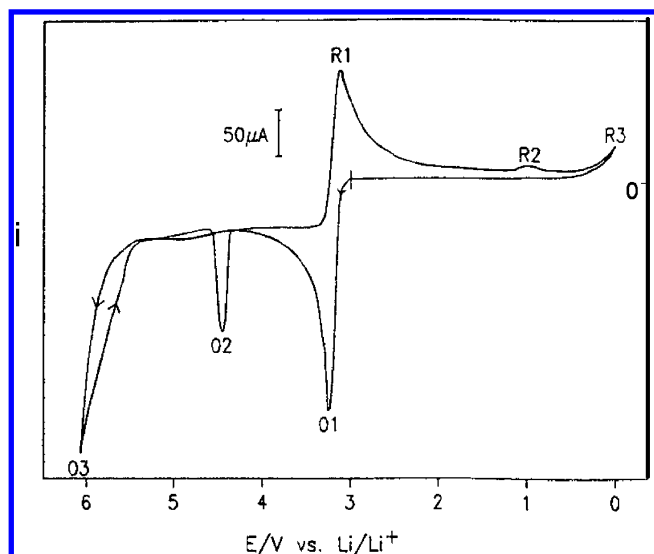
**Figure 43.** Cyclic voltammograms of 0.08 M ferrocene in 1.0 M LiAsF$_6$/EC/PC conducted at 20 mV s$^{-1}$. (Reproduced with permission from ref 429 (Figure 2). Copyright 1992 The Electrochemical Society.)
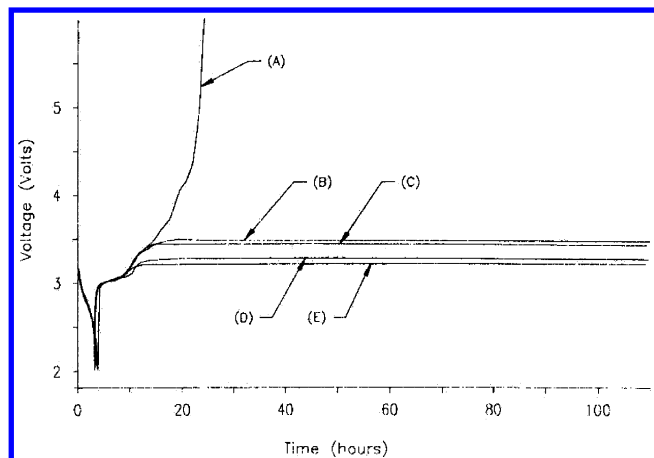


**Figure 44.** Voltage profile of overcharged Li/Li$_x$MnO$_2$ AA cells containing different substituted ferrocenes as redox additives in 1.0 M LiAsF$_6$/EC/PC: (A) reference; (B) ferrocenyl ketone; (C) dimethylaminomethylferrocene; (D) ferrocene; (E) n-butylferrocene. (Reproduced with permission from ref 429 (Figure 6). Copyright 1992 The Electrochemical Society.)

at ~3.25 V, which occurred reversibly. With various substitutions on the cyclopentadieneyl rings (Table 11), the redox potential could be adjusted to occur in the range 3.09−3.55 V. For cathode materials based on Li$_x$MnO$_2$, whose potential at full charge is 3.50 V, these substituted ferrocenes could make feasible candidates as redox additives, since their redox potentials can be adjusted to be between those of the major oxidative decomposition of electrolytes (>4.0 V) and the cathode full utilization (3.50 V).

The effect of these ferrocene-based additives on overcharge protection is shown in Figure 44, where AA cells based on lithium, Li$_x$MnO$_2$, and electrolytes with or without additives were overcharged. In the absence of these redox shuttles (A), the cell voltage continues to rise, indicating the occurrence of major irreversible decompositions within the cell whereas the presence of shuttle agents (B−E) locks the cell potential in the vicinity of their redox potentials

indefinitely. The successive cyclings of these over-charged cells showed that no adverse effect was caused by these ferrocene additives on cycle life. Furthermore, the reversibility of the redox reactions and the long-term stability of them with respect to other cell components were also tested. The authors had observed over a hundred "turnovers" of these ferrocene shuttles in the cell while demonstrating a reversible shuttle effect, and prolonged cyclings of these cells showed excellent cycle life, indicating the good compatibility between ferrocene additives and the bulk electrolytes.

The practical importance of overcharge protection by these ferrocene additives was further confirmed with a battery pack in which cells with mismatched capacity were intentionally connected in series and subjected to overcharge.[427] As expected, the added ferrocene acted to prevent the cell with low capacity from being overcharged as the other cell continued to charge. At the end of the charge, all cells had attained essentially the same state-of-charge, and successive discharge and recharge showed excellent cycling characteristics, despite the mismatched capacities in the pack. If no redox additives were used, such mismatch in capacity would result in poor cycle life or even hazards.

The ability of these ferrocenes as carriers for shuttling current through the cell was determined by charging the cell with a constant current at the fully charged state (3.5 V). When the interelectrode spacing was between 25 and 50 μm, the limiting shuttle current of these ferrocenes was found to be as high as 2.0 mA cm$^{-2}$.[429]

One adverse effect of these additives on cell performance seemed to be related to their blocking of ionic paths on the surface of cathode materials, as indicated by the reduced power capabilities in the presence of ferrocenes. Analysis on the concentration changes of ferrocene additives in the electrolyte solutions before and after their exposure to cathode materials established that an adsorption of ferrocene species occurred on the cathode surface, 93% of which would be covered when as low as 0.3 M ferrocenes were present in the electrolyte solution.[429] This surface deactivation resulted in the loss of both rate capability and capacity.

Redox shuttles based on aromatic species were also tested. Halpert et al. reported the use of tetracyanoethylene and tetramethylphenylenediamine as shuttle additives to prevent overcharge in TiS$_2$-based lithium cells and stated that the concept of these built-in overcharge prevention mechanisms was feasible.[430] Richardson and Ross investigated a series of substituted aromatic or heterocyclic compounds as redox shuttle additives (Table 11) for polymer electrolytes that operated on a Li$_2$Mn$_4$O$_9$ cathode at elevated temperatures (85 °C).[431] The redox potentials of these compounds ranged between 2.8 and 3.5 V, and like ferrocene-based additives, they are only suitable for cathode materials of low voltage.

Accompanying the commercialization of lithium ion technology, the emergence of 4.0 V class cathode materials based on spinel, LiCoO$_2$, and LiNiO$_2$ presents a more stringent requirement for the selection

of shuttle additives, since few redox couples could undergo reversible turnover at such high potentials near 4.0 V. Among those few were some organometallic complex compounds with Fe, Ru, Ir, or Ce as metal cores and phenanthroline or bipyridine as ligands. Their redox potentials were found to be in the vicinity of 4.0 V, and like ferrocenes, fine adjustment in the redox potential could be realized by varying the chemical nature, number, and relative positions of the substituents on the aromatic rings.[432] However, these complexes had very limited solubilities (<50 mM) in nonaqueous media, which, in combination with their large molecular weight and size (hence, low diffusion coefficient), contributed to a low shuttle current limit. Tests in a cathode half-cell using $LiPF_6$/PC/DMC showed that under overcharge the hike in cell voltage was only delayed, but not locked, at the level of the redox potential, apparently due to the low limiting diffusion current that these organometallic redox additives can carry.[432]

Inspired by earlier reports that some substituted aromatic compounds can be reversibly reduced and oxidized in the neighborhood of 4.0 V,[433] Adachi et al. focued their attention on a series of anisole-based compounds, which have two methoxy substituents and one halogen substituent on the benzene ring (Table 11).[432] The high solubility of this class of organic compounds in carbonate-based electrolytes makes them a family of more promising candidates than the metal complexes. The cyclic voltammetry of one of those potential redox additives, 4-fluoro-1,2-dimethoxybenzene, was shown in Figure 45a. Of the two electrochemical processes, as represented by the two pairs of peaks located between 4.0 and 4.75 V, the one on the positive side is similar to the characteristic profile of a reversible redox couple as judged by the separation of the anodic and cathodic peaks as well as their shape. Similar behavior was also observed for bromo-substituted counterparts with higher shuttle voltage.

A correlation was found between the reversibility of these redox couples and the relative positions of the two methoxy groups. Among the various anisole compounds investigated, only those with the two methoxy groups at 1,2- (ortho-) and 1,4- (para-) positions showed reversibility at the 4.0 V region, while 1,3- (meta-) counterparts were oxidized irreversibly, as indicated by the absence of the corresponding reduction process in Figure 45b. The authors proposed that the stabilization of the oxidized product by methoxy substituents plays an important role in determining whether the reaction is reversible. Similar to the rationale for the aromatic electrophilic substitution that is familiar to organic chemists, the canonical structures of the possible oxidized states with the largest contribution are used to explain this stabilization effect by substitutes, as shown in Scheme 28.

It was assumed that, during an oxidation of these aromatic moieties, an electron would be removed from the aromatic ring at the location where the electron-donating methoxy is positioned. Whether this oxidation is reversible critically depends on the stability of the produced cationic product. On the
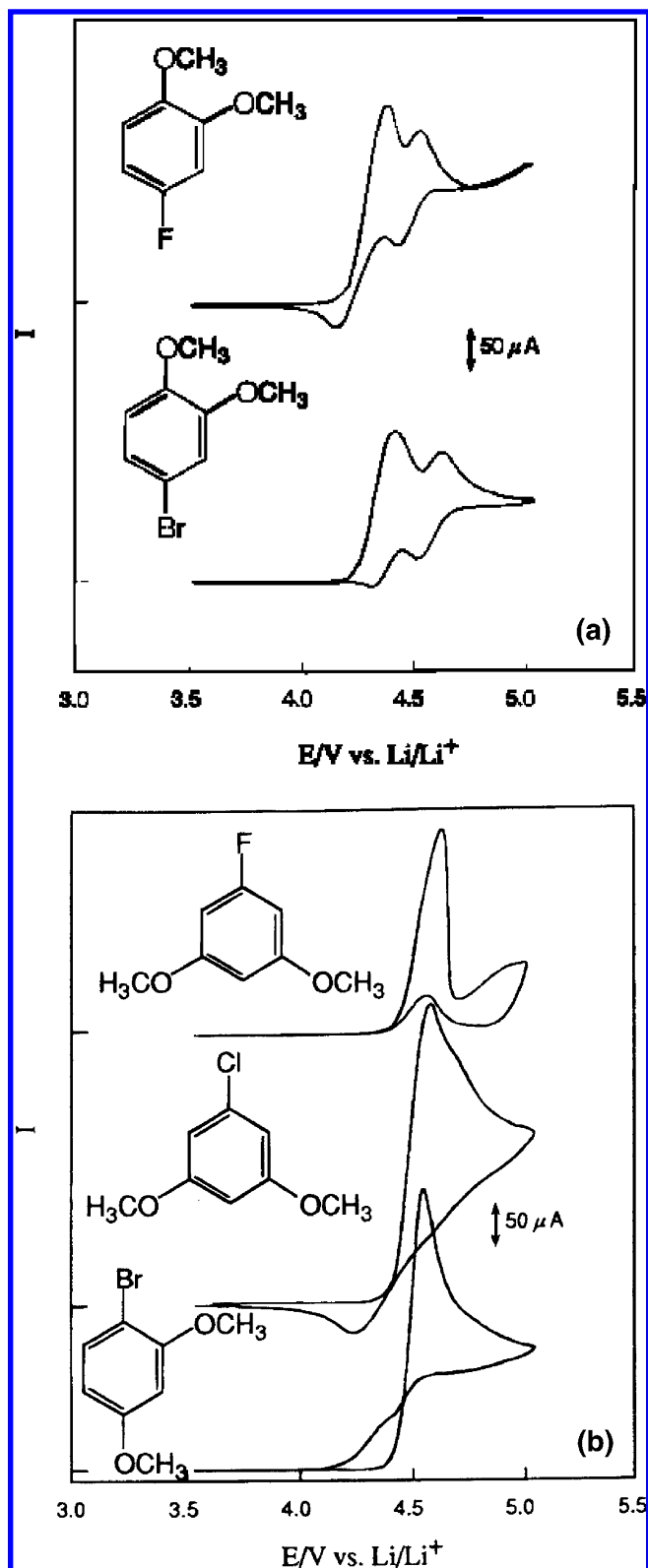


**Figure 45.** Cyclic voltammetry of (a) 4-halo-1,2-dimethoxybenzenes (Reproduced with permission from ref 432 (Figure 8). Copyright 1999 The Electrochemical Society.) and (b) 1,3-dimethoxybenzenes in $LiPF_6$/PC/DMC on Pt (Reproduced with permission from ref 432 (Figure 9). Copyright 1999 The Electrochemical Society.)

other hand, the stability of this cationic product relies on the effectiveness of the delocalization of the formal charge. Apparently, the lone pair of electrons on the methoxy oxygen can effectively contribute to this

**Scheme 28. Effect of Methoxy Relative Position on the Stabilization of the Oxidized State of Anisole Redox Additives: (a) 1,2-Methoxybenzene, Whose Oxidized Product Was Stabilized by the Neighboring Methoxy; (b) 1,3-Methoxybenzene, in Which the Meta Methoxy Fails To Stabilize the Dianion**
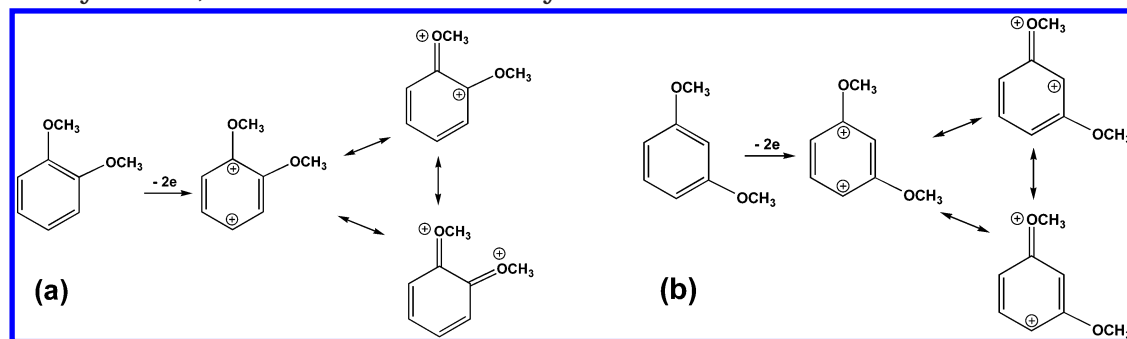


delocalization if the methoxy is at either ortho- (Scheme 28a) or para-positions (not shown in Scheme 28), while the methoxy at the meta-position (Scheme 28b) cannot. In this sense, the unstable oxidized product from the meta-substituted compounds would act like an intermediate and readily undergo further side reactions, thus rendering the original oxidation irreversible. The position of the halogen does not seem to be important, as long as the two methoxy groups are either para or ortho to each other; however, its presence is critical, since 1,4-dimethoxybenzene itself shows no reversible redox behavior. Thus, the role of the halogen in affecting the stability of the cationic species remains unclear. Nevertheless, the empirical structure−property relationship discovered by the authors for the anisole family could serve as a useful guideline for the future selection of redox additives.

Overcharge tests were carried out in $LiCoO_2$ cathode half-cells that contained these additives, and a redox shuttle effect was observed between 4.20 and 4.30 V, close to the redox potentials of these additives. The same shuttling effect was observed even after 2 months of storage for these cells, indicating the stability and redox reversibility of these additives. A closer examination of the capacity retention revealed that 4-bromo-1,2-dimethoxybenzene seemed to have the best shuttle-voltage performance for the 4.0 V lithium cell used.[432] The stability of these additives against reductive decomposition was also tested by the authors on metallic lithium as well as on carbonaceous anodes, and no deterioration was detected.

A convincing analysis carried out in this work established a direct connection between the shuttle current and the thermal effect in the cell, and it helps us to understand energetically the mechanism by which redox additives worked as shuttle carriers. As Figure 46 shows, calorimetric measurement was performed on cells that were being overcharged simultaneously, while the voltage profiles and heat flows were plotted together to reveal the correlation. In the reference cell, where no additive was present, there was no heat flow until the very end of the charge, where electrochemical decomposition of the electrolyte solvents and the thermal reaction between cathode and electrolyte would occur. On the other hand, the obvious thermal effect could be detected for the test cell containing 4-bromo-1,2-dimethoxy-

benzene as soon as the cell voltage leveled off because redox shuttling started. This suggests that the current supplied over 4.3 V (or after 60 h) is neither stored in the cathode nor consumed by irreversible decompositions. Rather, the shuttling redox couples convert this part of the current into heat during their repeated movement across the cell. In other words, during the course of shuttling, no work is done by the current to change the state-of-charge in the cathode, and all of the current supplied is dissipated by the diffusion of [O] and [R] species of the redox additive.
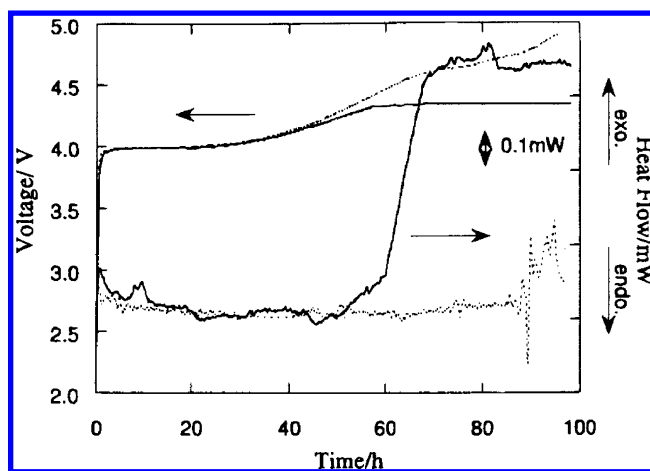


**Figure 46.** Correlation between the voltage profiles and heat flow of a cell under overcharge: cells with 100 mM 4-bromo-1,2-dimethoxybenzene (solid lines) and reference cell (dashed lines) (Reproduced with permission from ref 432 (Figure 17). Copyright 1999 The Electrochemical Society.)

Following Adachi et al., aromatic compounds with similar functionalities were proposed for polymer electrolytes as redox shuttle additives, which included bipyridyl and biphenyl carbonates and difluoroanisoles.[48b,434] All these additives could protect the cathode from overcharging in the vicinity of 4.1 V.[434]

Other less prominent types of additives, also intended for overcharge protection, were termed "shutdown additives" in the battery industry based on their tendency at high potentials to release gas, which in turn would activate a current interrupter device (CID), or to polymerize and block the ion passage in the electrolyte. The former included such

compounds as pyrocarbonates,[48b] biphenyl,[48b,435,436] cyclohexylbenzene,[48b] and phenyl-*tert*-butyl carbonate,[437] while the latter include biphenyl and other substituted aromatic compounds.[438,439] Related publications on these additives have been absent except for patent disclosures and conference presentations. However, according to Yoshino et al., some of these additives have been used in commercial lithium ion cells for several years.[48b,440] The major difference between these additives and the redox shuttles is that, once activated by the cathode potential, the gassing or polymerizing of these additives terminates the cell permanently, while the operation of redox additives is nondestructive, at least theoretically. Since the redox additives have a maximal current limit defined by their diffusion coefficient and concentration, the presence of the gassing- and polymerizing-type additives would serve as a more reliable line of defense against catastrophic failure from overcharging. Therefore, the integration of multiple additives of different types into a single electrolyte seems to be a feasible approach on the condition that the destructive additives should have higher activation potential.

## 8.3. New Electrolyte Components

The modification of electrolytes via additives is attractive to industry as an economical approach; however, its impact on electrolyte performance is mainly restricted to tuning interfacial-related properties because of their small concentration in the electrolyte, while other challenges for the state-of-the-art electrolytes such as temperature limits, ion conductivity, and inflammability are still determined by the physical properties of the bulk components. Improvements in these bulk-related properties can only be realized by replacing the bulk components of the electrolytes with new solvents and salts, but such efforts have been met with difficulty, since more often than not the improvement in the individually targeted properties is achieved at the expense of other properties that are also of vital importance to the performance of electrolytes. Such "collateral damage" undermines the significance of the improvements achieved and, in some cases, even renders the entire effort unworthy.

Nevertheless, research activities in this arena continue to be driven by the potential commercial interest that might arise from any possible replacement of the state-of-the-art electrolyte components. Realizing that the probability of success is rather limited with any radical change of the entire electrolyte system, an increasing number of researchers on novel electrolytes are adopting the current state-of-the-art electrolytes as the platforms for innovation and attempting to approach the targeted improvements without serious sacrifices in the well-established merits, which at least should include (1) facile ion transport as characterized by ion conductivities above 5 mS cm$^{-1}$ at room temperature, (2) electrochemical stability on both carbonaceous anode and metal oxide cathode materials in the range 0−5 V, (3) inertness to other cell parts such as packaging materials and anode and cathode current collectors,

(4) wettability toward porous separators as well as electrode materials, (5) relatively low toxicity, and (6) relatively low cost.

This section reviews these research efforts in the past decade on developing new solvents and lithium salts for nonaqueous electrolytes of lithium ion cells, but the cosolvents or additives developed for nonflammable electrolytes, most of which are phosphorus or fluorinated molecules, are not included, since their presence is intended for improvement in safety rather than performance. They will be reviewed in section 8.5.

With few exceptions, these new electrolyte solvents focus on possible improvements in low-temperature performance, while new salts are intended to offer higher thermal stability. This divided directions of pursuit after the targeted improvements is apparently created by the fact that solvent and salt, respectively, impose the upper and lower temperature limits of the current state-of-the-art electrolytes.
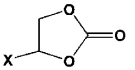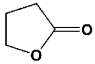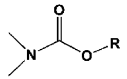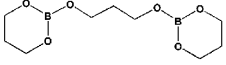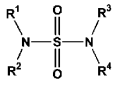
### 8.3.1. Nonaqueous Solvents

The state-of-the-art electrolytes use mixtures of cyclic and acyclic carbonates as solvents, whose functions are to solvate lithium salts and to facilitate lithium ion transport, respectively. The key cyclic solvent, EC, is also responsible for forming a protective SEI on graphitic anodes and probably a similar surface layer on metal oxide cathodes. However, this indispensable solvent simultaneously sets the narrow range of service temperature for these electrolytes with its high melting point, while its replacement by other low-melting solvents such as its structural analogue PC is often rendered difficult by the requirement for SEI-forming ability. The attempts at solving this dilemma have been directed at the structural modification of either EC or PC so that a balance between low melting point and favorable interfacial chemistry could be reached.

On the other hand, the linear carbonates used in the state-of-the art electrolytes, DMC, DEC, and EMC, serve as diluents to the high-melting and viscous EC. They have been known to be unsuitable as single solvents because of their inability to solvate lithium salts as well as their instability on the oxidizing surface of cathode materials, while the gassing of lithium ion cells during long-term cycling is also believed to arise from them. However, any possible replacements for linear carbonates to serve as cosolvents with EC or PC should at least possess the major prerequisites of lower viscosity and lower melting point.

Preferably, the new solvents are also expected to possess better stability or ability in interfacial chemistry on both anode and cathode materials so that the new electrolyte formulation can rely less on EC; or they are expected to be less inflammable, as a major shortcoming of the linear carbonates is their low flash points ($T_f$) (Table 1). In the search for new solvents, fluorination has been adopted as a favorable approach to achieve improvements in these two aspects because the presence of C−F bonds in organic molecules is found to affect interfacial chemistry on carbonaceous anodes in a positive manner,[441−443] and

**Table 12. Novel Nonaqueous Solvents and Their Major Properties**

| Solvent Structures | Remarks | Ref. |
|---|---|---|
| **cyclic carbonates** (X = Cl, F, CF$_3$) | Halogen-substitution lowers m.p. and improves SEI-formation ability; high self-discharge rate from ClEC; toxicity remains unknown. | 446, 447, 449 442, 452 443, 453 |
| **$\gamma$BL** | Unique match with LiBF$_4$. | 123, 208, 133, 458~460 |
| **linear esters** (n = 0~7, m = 1~4) | Better low-temperature performance. | 406, 461~463 |
| **fluorinated esters** (n = 1~7, m = 1~2, X = F or H) | Better low-temperature performance; better SEI-formation ability; lower inflammability. | 464, 465 |
| **fluorinated carbonates** (R$^1$ = CH$_3$, CH$_2$CH$_3$, CH$_2$CH$_2$CH$_3$, CH$_2$CF$_3$; R$^2$ = CH$_2$CF$_3$, CH(CF$_3$)$_2$) | Better low-temperature performance; better SEI-formation ability; lower inflammability. | 466 |
| **fluorinated carbamates** (R = CH$_2$CF$_3$, CH(CF$_3$)$_2$) | Resistive SEI; low capacity. | 466 |
| **fluorinated ethers** (R = alkyl, X = F or R$_F$) | Improved SEI chemistry; increased safety under thermal abuse. | 441 |
| **glycol borate ester (BEG)** | Moderate ion conductivity; higher t$_{Li}$; good anodic stability on Pt. | 467 |
| **sulfones** (R$^1$ = Me, R$^2$ = Et, Pr, iBu, R$_F$) | High ion conductivity; good anodic stability on cathode materials; alkyl fluorination improves SEI chemistry on graphite. | 75, 314 |
| **sulfamides** (R$^{1-4}$ = alkyls, alkoxyls, alkyoxyalkyls) | Moderate ion conductivity; poor anodic stability on Pt. | 468 |

many organofluorine compounds act as flame-retardants.[444,445] Table 12 summarizes the novel electrolyte solvents according to their structural cyclicity.

**8.3.1.1. Cyclic Solvents.** Halogen substitution on the carbonate ring of EC and PC is postulated to serve the dual purpose of lowering melting temperature by breaking the molecular symmetry and improving the SEI-forming ability. Shu et al. used chloroethylene carbonate (ClEC) as a cosolvent for PC and found that an effective and protective SEI could be formed on a graphitic anode, with the Coulombic efficiency in the first charging cycle comparable to that of the commercial electrolytes for lithium ion cells.[446,447] The potential plateau at 0.80 V, characteristic of the reductive decomposition of PC, was completely eliminated due to the presence of ClEC, while a new process was observed at 1.70 V. When taking the irreversible capacity in the first cycle as a metric, the optimum concentration of ClEC was determined to be 30 vol %,[448] although in a ternary solvent system containing EC, its concentration could be minimized to 5%.[447] Further electro-

chemical studies confirmed that ClEC forms a compact and uniform SEI on the surface of the graphitic anode that can prevent the cointercalation of PC and the subsequent exfoliation of graphene even in PC-rich electrolytes,[449,450,451] and the origin of this effective interfacial chemistry seems to be the reductive decomposition of ClEC at 1.70 V, which generates $CO_2$ as a major intermediate, as indicated by the conspicuous absorption at 2341 cm$^{-1}$ in in situ FT-IR spectra.[449] The fate of $CO_2$ is yet unclear, but a strong possibility is its further reduction into lithium alkyl carbonate as a major component of the new SEI. Since this process occurs at a potential far above that of PC cointercalation, graphitic materials could successfully be used in ClEC/PC mixed solvents. Naturally, such a formulation without EC should offer much better performance at subzero temperatures.

The tests in full lithium ion cells, however, yielded less than satisfactory results.[447] Despite the stable cell life observed during the test of >800 cycles, only 92% Coulombic efficiency was achieved, as compared with the 98+% Coulombic efficiency for the corresponding anode half-cells. Initial suspicion about the anodic instability of ClEC was excluded, because this less-than-ideal efficiency did not lead to obvious capacity fading, and cyclic voltammetry carried at high potentials up to 4.2 V showed no discernible oxidation of ClEC, suggesting that ClEC is at least as stable as EC on the cathode surface. Therefore, the above loss in charge efficiency should come from the combined presence of both anode and cathode materials. Shu et al. thus proposed a shuttle-like mechanism in which ClEC was reductively cleaved on a carbonaceous anode, yielding the organic products related to alkyl carbonates and LiCl. Since LiCl is weakly soluble in nonaqueous media, chloride would diffuse to the cathode surface and be oxidized into $Cl_2$. This internal chemical shuttling process between the anode and cathode surfaces consumes charges, and its reversibility accounts for the constantly low Coulombic efficiency during long-term cycling tests. This internal self-discharge mechanism is obviously undesirable and eventually rendered ClEC an impractical cosolvent.

Considering the virtually zero solubility of LiF in nonaqueous media, McMillan et al. synthesized the fluorinated counterpart of ClEC.[442] As expected, the shuttle phenomenon was eliminated because of the fluorination, as evidenced by the quantitative Coulombic efficiency, while a similar SEI effect was maintained, since FEC/PC mixed solvent can support reversible lithiation/delithiation of the graphitic anode materials. However, capacity was observed to fade by 37% in 200 cycles. Follow-up work on this solvent has been minimal.[452]

Similar structural modification was also performed on PC. Trifluoropropylene carbonate (TFPC) was synthesized in the hope that a novel electrolyte free of linear carbonates could be formulated with improved safety in the case of fire.[443,453] Like ClEC and FEC, it is liquid at room temperature with a high flash point (134 °C), but its high viscosity results in slower ion transport within the electrolytes, because the maximum ion conductivity at room temperature

achieved by these cyclic-only electrolytes is 6.6 mS cm$^{-1}$ (for LiPF$_6$ in TFPC/EC 1:3) and in neat TFPC it is only ~3.0 mS cm$^{-1}$. On the other hand, EIS studies carried on anode half-cells found that the ClEC/TFPC couple forms the least resistive SEI film. While the electrochemical behavior of neat TFPC was not described, the cathodic stability of the electrolytes based on mixed solvents, TFPC/ClEC and TFPC/EC, was tested with a graphitic anode, and no reductive processes characteristic of TFPC were visible, in addition to those of ClEC (1.70 V) and EC (0.60 V). Similar to the cases of ClEC and FEC, its presence did prevent PC cointercalation, but the irreversible capacity associated with PC decomposition still accounted for ~132 mA h g$^{-1}$ of the irreversible capacity in the anode half-cell, which was ~40% of the total charge. Spectroscopic means, including XPS and FT-IR, were used to analyze the SEI chemistry on the anode, and the presence of a C−F bond was identified, indicating the decomposition products of TFPC do constitute part of the SEI. Cycling performance of these electrolytes was tested in anode and cathode half-cells, but no data on full lithium ion cells were shown.[453]

Among the limited choices of candidates intended to replace cyclic carbonates, $\gamma$-butyrolactone ($\gamma$BL) seemed to be the most promising and therefore closest to practical application. $\gamma$BL has long been considered a possible component for electrolytes in lithium/lithium ion cells due to its moderately high dielectric constant, relatively low viscosity, EC-like structure, and excellent solvating ability.[454−456] Its reductive behavior has been studied on inert electrode surfaces,[208,209] lithium surfaces,[222,457] and graphite surfaces.[123] Unfortunately, in the early era of lithium ion technology, Aurbach and co-workers had found that $\gamma$BL/LiAsF$_6$ solution failed to perform satisfactorily in lithium ion cells based on the graphite anode unless under an atmosphere of $CO_2$, thus diminishing its possible application.[123] Detailed mechanistic studies attributed the failure to metallic lithium deposition on the carbonaceous anode surface and the subsequent reaction with $\gamma$BL, which was made possible by the high resistance of the SEI formed in $\gamma$BL-based electrolytes.[177]

The publications related to the use of $\gamma$BL as an electrolyte solvent for lithium ion cells have been scarce until recently, when a Japanese group from Toshiba reported the electrolyte based on a solution of LiBF$_4$ in $\gamma$BL/EC mixtures for laminated thin lithium ion cells.[133,458] This new formulation, when used in combination with a graphitic carbon fiber, exhibited stable cell performance with 94% Coulombic efficiency in the first cycle. Most importantly, it afforded much higher thermal stability than the electrolytes based on LiPF$_6$ solutions, since storage of the cell at full state-of-charge (4.20 V) at 85 °C only led to negligible capacity loss. The low-temperature performance was also much improved as compared to the cases of state-of-the-art electrolytes, with 88% of the nominal capacity retained at −20 °C at the drain rate of 0.5 C. Since the new formulation is free of linear carbonates, its tolerance against thermal abuse should be superior to that of the current
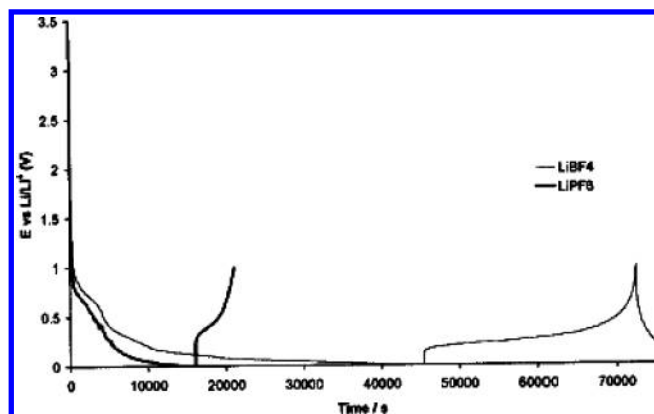
**Figure 47.** Voltage profile of graphitic anode in LiPF$_6$ and LiBF$_4$ solutions in $\gamma$BL/EC (1:1). (Reproduced with permission from ref 460 (Figure 1). Copyright 2003 The Electrochemical Society.)

commercial lithium ion cells. Preliminary results showed that the gassing of this new electrolyte is much less severe, and an independent study employing the in situ DEMS technique confirmed that the dominant participation of $\gamma$BL in SEI formation reduced the gas evolution by forming a $\gamma$-alkoxy-$\beta$-keto ester:[459]
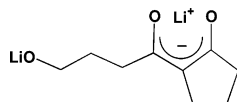
The spectroscopic identification of the $\beta$-keto ester and the reduction mechanism leading to it have been previously described by Aurbach and co-workers when studying the surface chemistry of $\gamma$BL-based electrolytes on various electrodes polarized to low potentials.[123,208,209]

Interestingly, all the above improvements seemed to be unexpectedly achieved from components (LiBF$_4$ and $\gamma$BL) that were already tested individually and considered inferior in performance to the commonly used LiPF$_6$ and various carbonates. According to a more recent publication, this unique match between LiBF$_4$ and $\gamma$BL originates from some interactions between the two that are not yet understood.[460] For example, among the five salts investigated that included LiBF$_4$, LiPF$_6$, LiAsF$_6$, LiIm, and LiClO$_4$, only LiBF$_4$ in $\gamma$BL/EC supported reversible lithium intercalation/deintercalation with capacities close to the theoretical value, as Figure 47 shows. Other salts seemed to suffer from a highly resistive surface film on the graphite surface, which worsened with cycling number. Although extensive characterizations were carried out with techniques such as XRD, SEM, and XPS, the nature of this interaction remains unclear.

**8.3.1.2. Linear Solvents.** For novel solvents that are intended to replace linear carbonates, the emphasis was placed on such properties as melting temperature, viscosity, and inflammability of the solvents. As Table 12 shows, these solvents can be roughly classified into four groups: (1) linear esters or carbonates,[406,461−463] (2) fluorinated esters,[464,465] (3) fluorinated carbonates,[466] and (4) fluorinated ethers.[441]

Like linear carbonates, none of these linear esters were used as single solvents but rather as cosolvents

with cyclic components including EC and PC. Binary, ternary, and even quaternary compositions were formulated with these esters, and improvements of low-temperature performance were described.[406,461−463] According to Herreyre et al., ternary compositions based on ethyl acetate (EA) and methyl butyrate (MB) demonstrated electrochemical stability up to 4.85 V on the cathode surface at 60 °C, while the compositions containing lower molecular weight methyl acetate (MA) deteriorated.[406] Similar conclusions were drawn by Smart et al., who investigated a series of linear esters and carbonates as low-temperature electrolyte components and found that a desirable SEI (i.e., less resistive and protective) could only be formed when esters of higher molecular weight were used, although esters of lower molecular weight could afford higher bulk ion conductivity at low temperatures because of their lower viscosities.[462] Judged on the basis of the reversible capacity in the first charge cycle achieved by a graphite anode in quaternary electrolytes, LiPF$_6$/EC/DEC/DMC/ester, the esters with longer alkyl chains were obviously superior to the ones of lower molecular weight:

ethyl propionate (EP, 340.75 mA h g$^{-1}$) >

ethyl butyrate (EB, 309.46 mA h g$^{-1}$) >

MA (236.5 mA h g$^{-1}$) > EA (214.2 mA h g$^{-1}$)

The above cell performance order is almost the reversal of that for the low-temperature ion conductivity, which clearly shows the decoupling of interfacial properties from bulk properties. Thus, Smart et al. concluded that the nature of the SEI instead of bulk ion conductivity plays the key role when new solvents are selected.

To improve the thermal stability of electrolytes against lithium metal electrodes, various fluorinated organic solvents were tested as electrolyte solvents (Table 12).[441,464−466] For example, Yamaki et al. introduced a series of partially fluorinated esters in which the fluorination was conducted on the carboxylic acid section and used them as single solvents for electrolytes,[465] while Smart et al. synthesized a series of partially fluorinated carbonates for similar purposes.[466] When compared with their nonfluorinated counterparts, the presence of fluorination in these molecules was reported to result in lower melting points, higher anodic stability, increased safety, and favorable SEI-forming characteristics on metallic lithium or graphitic anodes. For fluorinated carbonates a number of electrochemical techniques such as Tafel polarization and micropolarization confirmed that facile kinetics of lithium ion intercalation were made possible because of the new SEI chemistry imparted by those fluorinated solvents. In terms of interfacial resistance and utilized capacity, fluorinated carbonates are generally superior to the fluorinated carbamates studied (Table 12).[466]

**8.3.1.3. Other Novel Solvents.** In addition to molecules based on carboxylic and carbonic esters, other types of organic polar compounds were also explored as possible solvent candidates but with limited success. Zhang and Angell synthesized a dimeric glycol ester of boric ester (BEG, Table 12) in

the hope that the electron-deficient boron of the molecule would assist in dissociating lithium salts and coordinating with anions.[467] The solvent, despite its high viscosity, can dissolve various lithium salts to appreciable concentrations, and it exhibited particular stabilization of metallic lithium at elevated temperatures up to 100 °C. With EC as cosolvent, the electrolytic solution of LiClO$_4$ and LiIm showed moderate ion conductivities on the level of 10$^{-3}$ S cm$^{-1}$. The anodic stability of the electrolytes based on this borate ester was measured on a Pt electrode, and a wide electrochemical stability window of ~5.8 V was reported. The cathodic stability of the borate ester on graphitic anode material was also confirmed by cycling an MCMB electrode in an electrolyte LiClO$_4$ in BEG/EC, which yielded stable cycles. Considering the high viscosity of both solvent components used in the study, the above cell test results appear to be promising, but better results could be achieved if conventional diluents such as linear carbonate were used. However, no further work has been reported on this interesting solvent.

Choquette et al. investigated the possibilities of using a series of substituted sulfamides as possible electrolyte solvents (Table 12).[468] These compounds are polar but viscous liquids at ambient temperature, with viscosities and dielectric constants ranging between 3 and 5 mPa s and 30 and 60, respectively, depending on the alkyl substituents on amide nitrogens. The ion conductivities that could be achieved from the neat solutions of LiIm in these sulfamides are similar to that for BEG, that is, in the vicinity of 10$^{-3}$ S cm$^{-1}$. Like BEG, it should be suitable as a polar cosolvent used in a mixed solvent system, though the less-than-satisfactory anodic stability of the sulfamide family might become a drawback that prevents their application as electrolyte solvents, because usually the polar components in an electrolyte system are responsible for the stabilization of the cathode material surface. As measured on a GC electrode, the oxidative decomposition of these compounds occurs around 4.3−4.6 V when 100 $\mu$A cm$^{-2}$ was used as the cutoff criterion, far below that for cyclic carbonate-based solvents.

Another class of organic compounds that could make promising electrolyte solvents for lithium-based rechargeable cells is based on alkyl sulfones. Since most of these compounds are solids with melting points above ambient temperature, interest was rarely invested in them when possible candidates for electrolyte solvents are considered. One exception is the cyclic member, tetramethylene sulfone (also known as sulfolane), whose melting temperature is close to room temperature (27 °C) and whose dielectric constant is close to that of PC (60 at 25 °C). The electrolyte based on the salt solutions of this cyclic sulfone remains liquid till subzero temperatures because of the freezing-depression effect of the solute. Matsuda et al.[469] and Morita et al.[470] have individually tested it as a cosolvent for lithium cells, and focus was placed on the lithium cycling efficiencies. Generally decent ion conductivity could be achieved either with sulfolane as a single solvent or with mixed solvents based on it. For example, 15 mS cm$^{-1}$ at
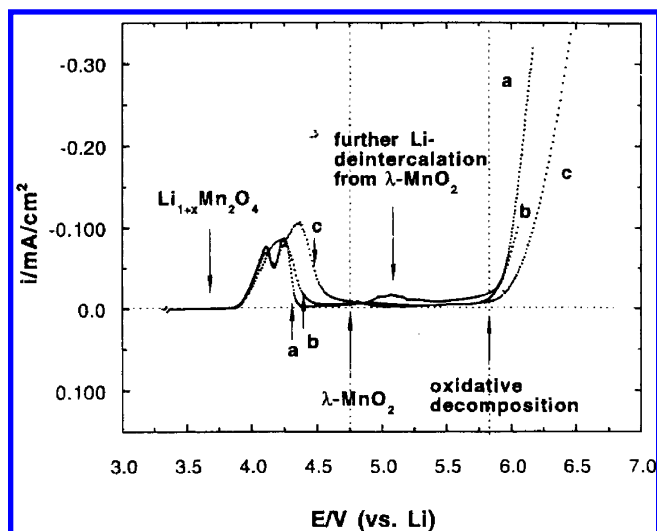


**Figure 48.** Anodic stability as measured on a spinel Li$_x$-Mn$_2$O$_4$ cathode surface for EMS-based electrolytes: (a) LiIm; (b) LiClO$_4$; (c) LiTf. In all cases, 1.0 m lithium salt solutions were used, and slow scan voltammetry was conducted at 0.1 mV s$^{-1}$, with lithium as counter and reference electrodes and spinel Li$_x$Mn$_2$O$_4$ as working electrode. (Reproduced with permission from ref 75 (Figure 3). Copyright 1998 The Electrochemical Society.)

room temperature has been measured for LiPF$_6$ in a sulfolane/DME mixture, which should obviously be attributed to the combined effect of the high dielectric constant of sulfolane and the low viscosity of DME. On the other hand, the higher melting temperatures of the linear counterparts of sulfolane excluded them from being considered as room-temperature electrolyte solvents. For example, the lithium cell based on the simplest member of the linear sulfone family, dimethyl sulfone (DMS, mp 110 °C), has to operate at 150 °C, although, surprisingly, high Coulombic efficiency and stable performance could be achieved even at that high temperature.[471]

With the introduction of structural asymmetry, Xu and Angell attempted to reduce the lattice energy of the sulfone molecules so that the melting temperature of linear sulfones could be lowered to the level that allowed room-temperature application.[75] They synthesized five linear sulfones with asymmetric alkyl substituents and found that all of these compounds were liquids or solids that melt in the vicinity of room temperature. They were able to dissolve various lithium salts up to 3.0 M and yield moderate ion conductivity, and the most interesting solvent candidate from the family was the simplest member, ethylmethyl sulfone (EMS), which has an extraordinarily high dielectric constant (95 at 20 °C, as compared with 89 of EC).[314] When tested on the surface of a spinel-based composite cathode material, this solvent showed an electrochemical stability window of approximately 5.80 V, as Figure 48 shows. This high anodic stability limit, which remains the highest ever known on the surface of a composite cathode material (versus an inert electrode), is significant, since it would allow the various applications of high potential requirements such as a energy storage device with 5.0 V class cathode materials or electrolytic and electroanalytic devices that need an inert supporting medium. The usefulness of this
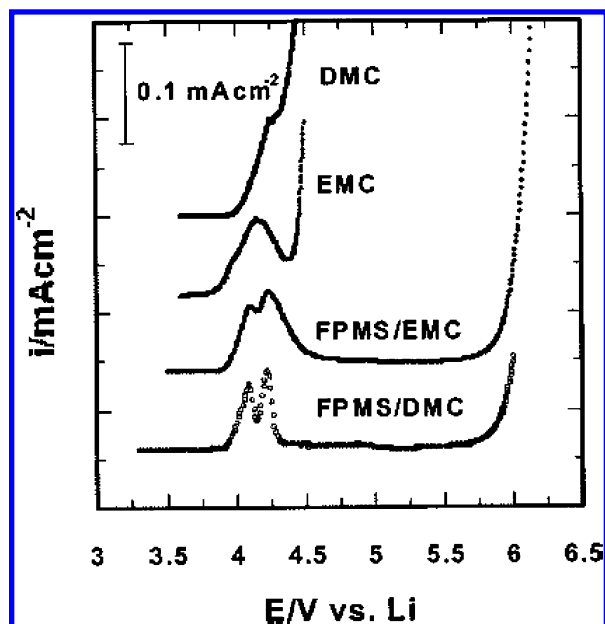
**Figure 49.** Effect of cosolvent FPMS on the anodic stability of the mixed solvents. Also shown for comparison are the neat linear carbonates. In all cases, 1.0 m $LiPF_6$ solutions were used, and slow scan voltammetry was conducted at 0.1 mV s$^{-1}$, with lithium as counter and reference electrodes and spinel $Li_xMn_2O_4$ as working electrode. (Reproduced with permission from ref 314 (Figure 6). Copyright 2002 The Electrochemical Society.)



**Figure 50.** Galvonostatic cycling of anode (Li/graphite) and cathode (Li/$Li_xMn_2O_4$) half-cells using 1.0 m $LiPF_6$ in FPMS/EMC 1:1 and 1:2 mixture solvents, respectively. $i = 0.001$ mA cm$^{-2}$. (Reproduced with permission from ref 314 (Figure 8). Copyright 2002 The Electrochemical Society.)

anodically stable solvent has been confirmed by the various applications that followed the report of Xu and Angell.[316,317,472,473] For example, Seel and Dahn have successfully used EMS as the nonaqueous electrolyte for an anion intercalation cell, which enables the otherwise impossible staging of graphene layers with $PF_6^-$ anions at 5.60 V,[316] and the electrolyte based on the same sulfone also supported the complete delithiation of a new cathode material at ~5.4 V.[317]

Unfortunately, EMS cannot form an effective SEI on graphitic anode materials, thus undermining the possibility of its use in lithium ion cells. In their further work, Xu and Angell partially fluorinated the alkyl of an asymmetric linear sulfone, inspired by the reports that fluorinated alkyl could improve the SEI chemistry on a graphitic anode.[441−443] The fluorinated sulfone, 3,3,3-trifluoropropylmethyl sulfone (FPMS), has a melting point at 56 °C and could only be used as cosolvent with other diluents such as DMC and EMC.[314] The anodic stability of sulfone compounds seemed to be maintained, despite the presence of fluorination and the mixing with linear carbonates, as evidenced by the oxidative limits at ~5.70 V observed in Figure 49 for the mixed solvents. The SEI-forming ability, however, was indeed improved due to the fluorination, as shown by Figure 50, wherein the electrolytes based on these mixed solvents supported reversible lithium ion intercalation/deintercalation of the graphite anodes. The cycling tests in the longer term confirmed that the surface of a graphitic anode was well protected because close-to-unity Coulombic efficiency was obtained, and the authors suggested that FPMS might be a promising
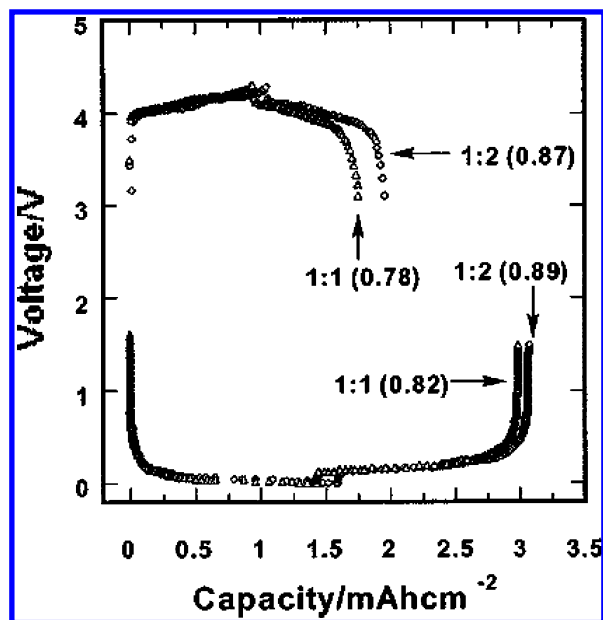
candidate for the lithium ion cell if the manufacturing cost of it could be reduced.

### 8.3.2. Lithium Salts

The pursuit of new lithium salts has been driven by the thermal instability of the current state-of-the-art lithium salts that were based on perfluorinated anions, and the thermal as well as chemical inertness has been taken as the main metric to evaluate any potential candidates to replace those salts, although, similar to the new solvent efforts, often the improvement in these properties comes at the price of other properties that are equally important for the operation of a lithium ion cell.

**8.3.2.1. Lithium Tris(trifluoromethanesulfonyl)methide (LiMe).** Following the development of LiIm, Dominey invented a new lithium salt based on a carbanion that is stabilized by three perfluorinated methanesulfonyl groups.[474] Because of the effective delocalization of the formal charge on the anion, the salt LiMe (Table 13) could be dissolved in various nonaqueous media and showed better ion conductivities than LiIm.[146] Its stability at high temperature is confirmed by TGA studies, which detected no sign of decomposition before 340 °C, while accordingly the electrolyte solution based on the salt remained stable at 100 °C. The electrochemical stability of the salt was studied in THF solution, and the cyclic voltammetry conducted on GC showed major anodic decomposition process at ~4.0 V. Although, on the basis of the previously published data this decomposition seemed to be caused by the solvent THF rather than by the salt anion,[64,74,177] the authors did not report further electrochemical measurements in other more stable solvents.[146] Initially the salt was reported to be inert toward an Al current collector,[116,153] but a more detailed study later found that corrosion of Al

**Table 13. Novel Lithium Salts and Their Major Properties**

| Salt | Structure | M. Wt | $T_d$ / $^\circ$C [a] | $E_a$ /V [b] (solvent -electrode) | $\sigma$ /mScm$^{-1}$ (0.7~1.0 M, 25 $^\circ$C/ solvent) | Ref. |
|---|---|---|---|---|---|---|
| LiMe | $F_3CO_2S$, $SO_2CF_3$, $F_3CO_2S$ C$^-$ Li$^+$ | 417.9 | 340 | 4.4 (THF-GC) 4.0 (EC/DMC-GC) | 7.1 (EC/DMC) 12 (EC/MF/DMC) | 116, 146, 474 |
| aromatic Li borates | $F_n$ B $F_n$ Li$^+$, n = 0, 1, 4 | 233.4~ 305.4 | 250 (n=0) | 3.6 (PC-SS $^c$, n=0 $^d$) 3.7 (PC-Au, n=1) 4.1 (PC-Au, n=4) | 0.6 (PC, n=0) 5.6 (EC/DME, n=0) 0.77 (PC, n=1) 11.07 (DME, n=4) 1.22 (PC) | 475~477, 481 |
|  | (naphthalene borate) Li$^+$ | 334.1 | 320 | 3.75 (PC-Pt) | 3.84 (PC/DME) 1.39 (PC/EC) | 478, 482 |
|  | $R^3$, $R^4$, $R^2$, $R^1$ borate, $R^3$=H or CH$_3$, $R^4$=H or Cl | 290.0~ 427.7 | 260 ($R^{1\sim3}$=Cl) 290 ($R^{1\sim3}$=H) 310 ($R^{1\sim2}$=Cl) 320 ($R^1$=CH$_3$) | 4.0 (PC-SS, $R^{1\sim3}$=H) 4.4 (PC-Pt, $R^{1\sim3}$=Cl) 4.4 (PC-Pt, $R^{1\sim3}$=H) 4.3 (PC-Pt, $R^{1\sim2}$=Cl) 4.1 (PC-Pt, $R^1$=CH$_3$) |  | 477, 481 |
|  | (diphenyl borate) Li$^+$ | 386.1 |  |  |  | 478, 481 |
|  | (disulfonyl borate) Li$^+$ | 293.9 |  | 4.6 (EC/DMC-Pt) |  | 479 |
|  | (pyridyl borate) Li$^+$ | 219.9 |  | 3.95 (PC/DMC-Pt) |  | 480 |
| non-aromatic Li borates | $R_F$ B $R_F$ Li$^+$, $R_F$ = CF$_3$ | 681.9 | 280 | 5.4 (DME-Pt) 5.0 (PC-Pt) | 11.1 (DME) | 483 |
|  | (malonato borate) Li$^+$ | 221.9 | 245 |  | 5.6 (DMSO) | 113 |
|  | LiBOB | 193.9 | ~300 (d) | 4.5 (PC-Pt) | 3.1 (PC) 9.0 (DME) 7.5 (EC/DMC) | 113, 155, 324, 483~486, 488, 489 |
|  | $R_x$ B $R_x$ Li$^+$, $R_x$ = CF$_3$, C$_2$F$_5$, CClF$_2$, CCl$_3$ | 469.9~667.9 | 100 | 4.5 (PC-Pt) | 8.0 (PC/DMC) | 493 |
| chelated Li phosphates | $F_n$ P $F_n$ $F_n$ Li$^+$ | 361.9 (n=0) 577.9 (n=4) | 150 (n=0) | 3.7 (PC-Ni, n=0) 3.95 (EC/DMC-Pt, n=1) 4.3 (EC/DEC-Pt, n=4) | 3.89 (EC/THF, n=0) 2.09 (EC/DEC, n=4) | 494 (n=0) 495 (n=4) |
| Li FAP | $R_F^1$, $R_F^4$, $R_F^3$, $R_F^5$, $R_F^6$, $R_F^2$ P$^-$ Li$^+$, $R_F$ = perfluorinated alkyl or F | 451.9~433.9 |  | 5.0 (DME-Pt) 5.0 (EC/DMC-Pt) | 8.17 (PC/EC/DMC, $R^{1\sim2}$ = i-C$_3$F$_7$, $R^{3\sim6}$=F) 8.2 (EC/DMC, $R^{1\sim3}$ = C$_2$F$_5$, $R^{4\sim6}$=F) | 496 498 499 500 |
| Li azolate | NC, CN pyrazolate N N $^-$ Li$^+$ | 124.9 |  |  |  | 501 |
| Li imidazolide | $F_3B$ N N $BF_3$ $^-$ Li$^+$ | 209.9 |  | 4.85 (DMC-Pt) | 5.06 (EC/EMC) | 502 |

$^a$ Thermal decomposition temperature determined by TGA. $^b$ Anodic stability limit determined by cyclic voltammetry. $^c$ Stainless steel working electrode. $^d$ Number of fluorine substituents on the aromatic ring.

does occur in various LiMe-based electrolytes at potentials above 4.5 V, though somehow it is less severe than that for the case of LiIm.[147] Therefore, its application in high-potential lithium ion cells

seems unlikely because Al is universally adopted as the current collector for the cathode materials.

**8.3.2.2. Lithium Borates with Aromatic Ligands.** A new class of lithium salts was developed

by Barthel et al. in the mid 1990s based on a borate anion chelated by various aromatic ligands.[475−480] Table 13 summarizes the representative members from this class along with their selected physical and electrochemical properties. The authors described the synthesis and chemical or physical characterizations of these salts in detail but only provided limited electrochemical data. Generally speaking, this class of salts is rather stable thermally and decomposes only at very high temperatures without melting, although moisture can still decompose them through hydrolysis.[481] The solubilities of most of these salts in nonaqueous media seemed to be dependent on the substitution of aromatic ligands, and moderate to good ion conductivities have been reported, ranging from 0.6 to 11.1 mS cm$^{-1}$ depending on the solvents used.

The stabilities of these salts against oxidation were studied with cyclic voltammetry on various inert electrodes, and an interesting correlation was established between the number of electron-withdrawing substituents on aromatic rings and the anodic stabilities (i.e., higher oxidation potentials were found for the better stabilized borate anions with more electron-withdrawing groups). This correlation could be well explained by the order of the HOMO energy levels obtained by quantum chemical calculations.[477,479] Thus, the anodic decomposition potential ranges from 3.6 V for the unsubstituted borate[475] to 4.60 V for the borate with fluorinated and sulfonated aromatic ligands.[479] A similar relationship was reported by Sasaki et al., who listed the following order of oxidation potential limits according to the voltammetry results obtained on a Pt electrode, and revealed the obvious dependence of the anodic stability of these anions on the electron density of the aromatic rings:[481]
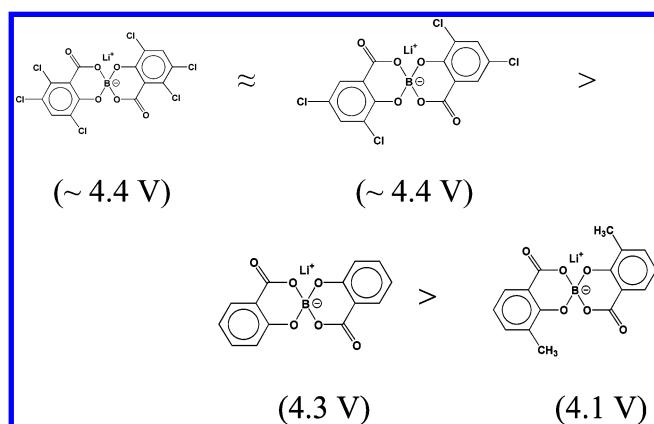


In addition to the above thermodynamic consideration, kinetics also play an important role in determining the anodic stability of these salts. For example, some salts whose decomposition products are polymeric moieties were found to passivate the electrode surface effectively.[478] Therefore, although the intrinsic oxidation potentials for these anions were not as high ($\sim$4.0 V), they showed stability up to 4.50 V in subsequent scans. It should be cautioned here, though, as the passivation was only observed on an inert electrode surface, whether similar passivations would occur on an actual cathode surface

and act to extend the potential range of application for these salts remains to be tested. Al was reported to be stable in the electrolytes based on at least two of these salts.[479,480]

The cycling test for one of the salts was conducted by Handa et al. in lithium cells using a low-potential cathode material, V$_2$O$_5$.[482] OCV and initial discharging behavior similar to those of other nonaqueous electrolytes were reported, although no data concerning extended performance were given. The key property that would decide whether these salts could be used in lithium ion technology (i.e., the ability of forming a protective SEI on the surface of graphitic materials) has not been reported for any of these salts.

**8.3.2.3. Lithium Borates with Nonaromatic Ligands.** The presence of aromatic ligands in Barthel's salts was believed to be responsible for the high melting points and basicity of the borate anions, which in turn translate into moderate or poor solubilities and ion conductivities as well as low anodic stabilities. To avoid use of these bulky aromatic substituents, Xu and Angell synthesized a series of borate anions that are chelated by various alkyl-based bidentate ligands, which serve as electron-withdrawing moieties by the presence of fluorine or carbonyl functionalities.[113,483,484] Table 13 lists the selected members of this aromatic-free borate family. Compared with their aromatic counterparts, these novel salts showed much higher ion conductivity and anodic stability, while maintaining comparable thermal stability. Detailed studies of ionics indicated that these salts could well dissociate in the media of moderate dielectric constants and yield ion conductivities slightly lower than those for state-of-the-art electrolyte solvents.[485,486] As an example, in EC/DMC solutions of lithium bis(oxalato)borate (LiBOB) and LiPF$_6$, the ion conductivities are 7.5 and 10 mS cm$^{-1}$, respectively. For at least one of these salts, the lithium ion transport number seemed to be higher than 0.50 because of the large anions size.[485,486] The dependence of ion conductivity on salt concentration is also different from the familiar bell-shaped dependences observed for LiPF$_6$- or LiBF$_4$-based solutions: the isothermal ion conductivity of these lithium borate solutions remains almost independent of salt concentration in the range 0.5−1.0 M, which could be advantageous for practical applications.

Among these new borates, particular attention should be paid to a salt based on oxalato ligands, which has aroused intense interest recently in the lithium ion research and development community. This salt was invented by Lischka et al.[487] and independently synthesized and investigated by Xu and Angell, who also gave it the popular name LiBOB. Following these extensive physical characterizations, a rather comprehensive electrochemical evaluation was conducted on this salt by Xu et al.,[155,324,488,489] who found that the solutions of LiBOB in mixed carbonate solvents met the complete set of stringent requirements for electrolyte solute intended for lithium ion cell applications: (1) it is anodically stable on the surface of composite cathode materials up to 4.3 V, (2) it can form a protective SEI on the
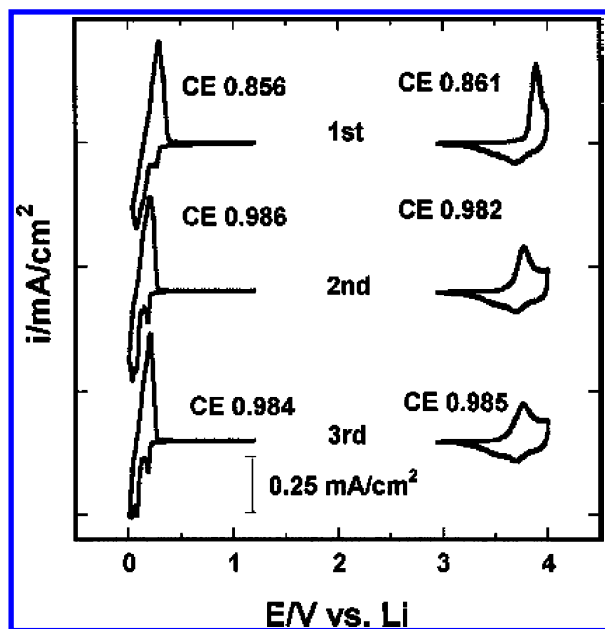
**Figure 51.** Cathodic and anodic stability of LiBOB-based electrolytes on metal oxide cathode and graphitic anode materials: Slow scan cyclic voltammetry of these electrode materials in LiBOB/EC/EMC electrolyte. The scan number and Coulombic efficiency (CE) for each scan are indicated in the graph. (Reproduced with permission from ref 155 (Figure 2). Copyright 2002 The Electrochemical Society.)
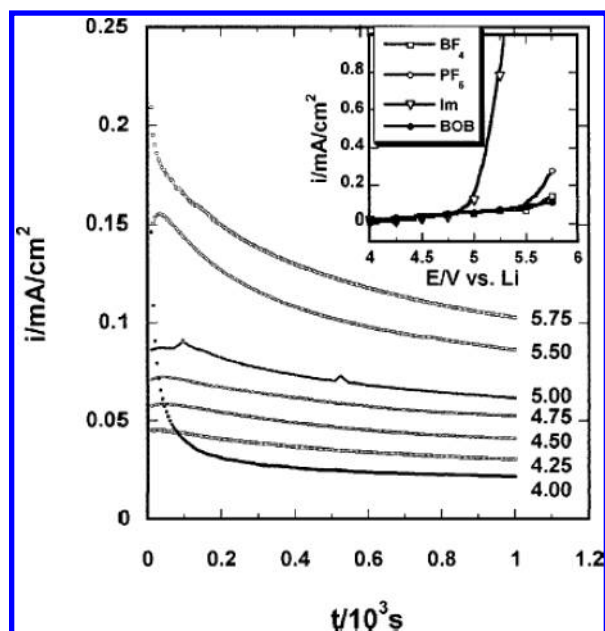


**Figure 52.** Passivation of Al substrate in LiBOB-based electrolytes: Time-decaying current observed on an Al electrode at various potentials containing 1.0 M LiBOB in EC/EMC. Inset: the dependence of steady-state current density (at $t = 10^3$ s) on applied potential as obtained on an Al electrode in electrolytes based on various salts in the same mixed solvent. (Reproduced with permission from ref 155 (Figure 1). Copyright 2002 The Electrochemical Society.)

surface of graphitic anode materials that supports reversible lithium ion intercalation/deintercalation, and (3) it stabilizes an Al current-collector at high potentials up to 6.0 V. Figures 51 and 52 present a brief summary of these qualifications, by all of which LiBOB showed performances comparable with or
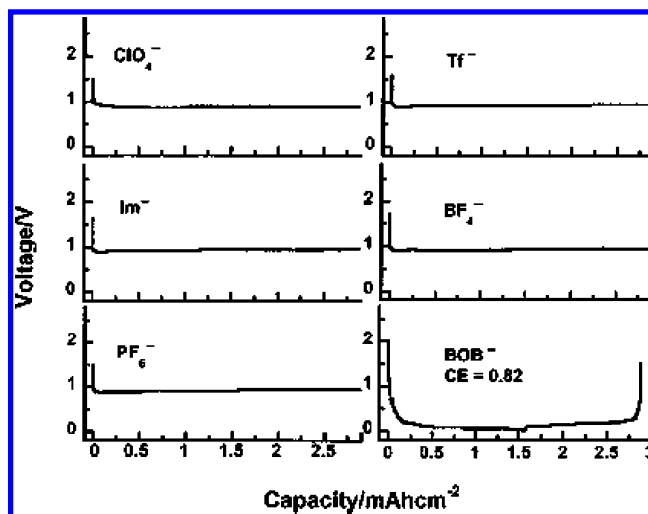


**Figure 53.** Stabilization of graphite in PC by LiBOB. Voltage profiles of lithium/graphite half-cells containing 1.0 m lithium salts in neat PC as electrolytes. Only for LiBOB/PC was the complete lithiation/delithiation cycle achieved. (Reproduced with permission from ref 324 (Figure 1). Copyright 2002 The Electrochemical Society.)

even superior to those of $LiBF_4$, $LiClO_4$, and $LiPF_6$. Especially, compared with the industry standard, $LiPF_6$, this salt also offers the additional advantages of being thermally stable, being economical in terms of manufacturing cost, being more environmentally friendly by decomposing into less corrosive products in the presence of moisture. The combination of these merits has not been found in other novel salts thus far investigated and has certainly made LiBOB a hopeful contender for lithium ion technology applications. The stable performance of LiBOB-based electrolytes was confirmed by the extended cycling of the full lithium ion cells using such electrolytes, where no capacity fading was detected during the operation of ~200 cycles.[155]

An unexpected but certainly welcomed discovery on LiBOB is its peculiar cathodic chemistry.[324] As has been pointed out in the preceding sections, the cornerstone of lithium ion technology is the formation of a protective SEI on the carbonaceous materials, and the conventional wisdom in this technology is that PC cannot be used in combination with graphitic anode materials because of its strong tendency to cointercalate and exfoliate the graphene structure. Prior to LiBOB, the presence of electrolyte solutes alone has never been able to challenge this wisdom, as Figure 53 shows. As an exception, however, LiBOB in neat PC solution successfully enables the reversible lithium ion intercalation/deintercalation on various graphitic anode materials, with capacity utilization and Coulombic efficiencies comparable with those of the state-of-the-art electrolytes. Considering that similar stabilization of graphene structure in PC was only able to be achieved by molecular additives before, the authors postulated that the BOB anion must have participated in the SEI formation during the initial lithiation process of the graphite, most likely through a single-electron reductive process.[324] The durability of such a protective SEI was put to a stringent test by cycling a full lithium ion cell based on LiBOB/PC or other EC-free formulations as elec-

trolytes. As the result, stable capacity and quantitative Coulombic efficiency were obtained for up to 100 cycles, similar to the case of the state-of-art electrolytes.[324] Since these formulations are EC-free, the lower temperature limit that has been plaguing EC-centered electrolytes should be much improved.

Xu et al. emphasized that the significance of the above serendipity lies not only in the fact that PC-rich solvents could be used with graphitic anode materials because of LiBOB but more in the perspective that the unofficial law governing the selection of electrolyte solvents could be revised, and unprecedented flexibility is offered by LiBOB to the reformulating of lithium ion electrolytes, where the displacement of the high-melting-point component EC is no longer restricted by the concern over the stability of the graphitic anode.

In the subsequent investigations, these authors adopted a preformation technique to differentiate the steps for the formation of an effectively protective SEI by LiBOB.[488] They systematically interrupted the lithiation of a graphite anode in LiBOB/PC at a series of potentials and then tested the survivability of these preformed anodes in LiPF$_6$/PC, which would have severely exfoliated the graphene structure had there been no protective SEI present. The results confirmed the critical role of BOB anion in the protection of graphitic anodes and, perhaps more importantly, found that an SEI sufficiently effective in protecting graphite against PC cointercalation and exfoliation was not completely formed till ∼0.60 V. They thus concluded that a 1.60 V reduction process that was universally observed for all LiBOB-based electrolytes might not have a direct relation with the formation of this effective SEI.[488]

XPS analysis was also conducted by Xu et al. to characterize the surface chemistry of a graphitic anode resulted from LiBOB electrolyte, which yielded an entirely different image of the SEI in terms of the relative abundances of the chemical species, as Figure 54 shows.[489] With BOB-anion participation, the content of chemical species similar to lithium alkyl carbonate became the major components of the SEI, as evidenced by the prominent peak at ∼289 eV. The authors believed that these alkyl carbonate-like species are originated from the oxalate moiety of the BOB anion and are mainly responsible for the effective protection of graphitic anodes. A tentative mechanism was proposed accordingly in Scheme 29.[489] Qualitatively, the chemical species present in the SEI formed by a LiBOB-based electrolyte seemed to be identical to those formed by LiPF$_6$ counterparts, since the comparison between the XPS C 1s spectra indicated that essentially the same peak locations for hydrocarbon, ether-containing species, and semicarbonates were found in both spectra (Figure 54). This fact could suggest that similar active agents originated from the state-of-the art electrolytes are present in the LiBOB-originated SEI, despite the fact that these species are much more populated due to the involvement of BOB anion in SEI formation.

Further studies on LiBOB as a potential replacement for LiPF$_6$ were carried out by Liu et al., who reported that, due to the absence of HF and the much
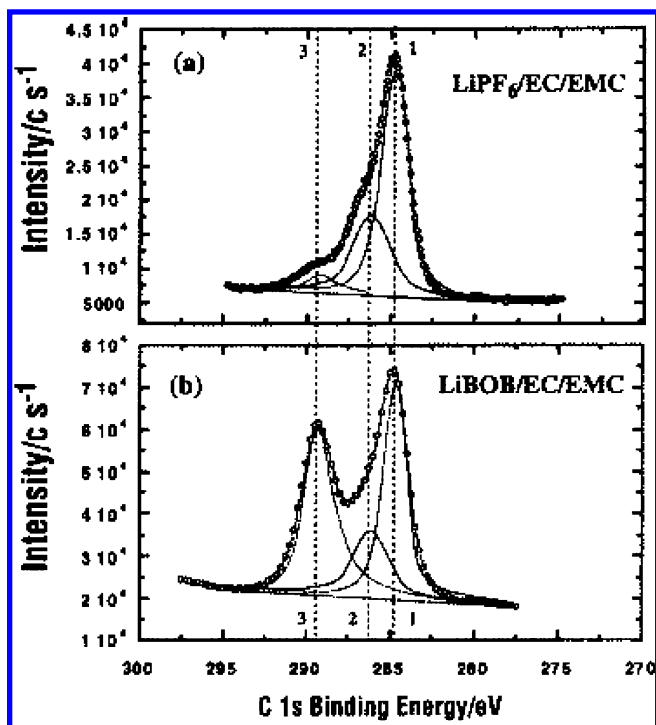
**Figure 54.** Peculiar surface chemistry of BOB anion on graphitic anode material: XPS C 1s spectra for a graphitic anode surface cycled in LiBOB- and LiPF6-based electrolytes. The peaks were resolved into three major contributions representing (1) hydrocarbon at 284.5 eV, (2) oligo-ether linkages at 286.5 eV, and (3) lithium alkyl carbonates at 289.37 eV, respectively. (Reproduced with permission from ref 489 (Figure 3). Copyright 2003 The Electrochemical Society.)

**Scheme 29. Proposed Mechanism for BOB Reductive Decomposition on a Graphitic Surface at Low Potentials**
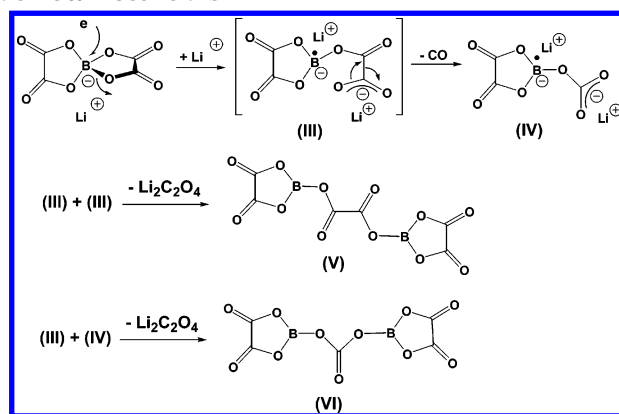
weakened acidity of the LiBOB electrolyte, cathode materials based on spinel LiMn$_2$O$_4$ were well stabilized, and the dissolution of Mn$^{2+}$ species, which had been considered a main cause of the capacity fading of this class of cathode materials, was nearly eliminated.[490] The thermal safety of LiBOB-based electrolytes against reductive decompositions was also compared with that of the LiPF$_6$ counterpart by Jiang and Dahn, who concluded that LiBOB is a much safer electrolyte solute as compared with LiPF$_6$ on a graphitic anode because its exothermic reaction with the fully lithiated MCMB was delayed by 90 °C due to the presence of LiBOB.[491] However, considering the conclusions by Maleki et al.[361] and especially

MacNeil and Dahn,[371] whether the LiBOB-based electrolytes are safer against thermal runaway would still depend on their interaction with the cathode materials.

On the basis of the findings on LiBOB performance in nonaqueous solvents and other advances made to improve the low-temperature performance of lithium ion electrolytes, Jow and co-workers proposed that an electrolyte with a much wider temperature range could be formulated using LiBOB alone or in combination with other salts.[492] The following section (8.4) will be dedicated to this topic.

Another series of lithium borates with nonchelating alkyl ligands were briefly reported by Yamaguchi et al. recently, where perhalogenated carbonyls were used to make the ligands electron-withdrawing.[493] Their solubilities in linear carbonates are obviously superior to that of LiBOB, as solutions of these salts could be made in neat DMC or DEC with concentrations higher than 1.0 m. The anodic stabilities of the electrolytes based on these salts were measured on Pt and found to be comparable with those of electrolytes based on LiBOB, while Al substrates were not corroded in these electrolytes at potentials up to 4.8 V. However, the thermal stability of these salts seemed to be inferior to that of the chelated borates with either aromatic or alkyl ligands, although their decomposition temperatures, ranging between 94 and 135 °C, were still higher than that of $LiPF_6$. Among these salts, the one with the perfluorinated carbonyl ligands was considered to be the best-performing, and the cycling of a graphitic anode half-cell containing a solution of this salt in EC/EMC showed that stable capacity could be obtained during 50 cycles. With the exceptions of the initial cycles, quantitative Coulombic efficiency was observed, indicating this salt is stable against cathodic reductions on graphitic anode materials. However, no data of full lithium ion cells were reported.

**8.3.2.4. Lithium Chelatophosphates.** If the work of Barthel et al. and Angell et al. on various borate-based salts could be viewed as the structural modification of a perhalogenated borate salt ($LiBF_4$) that was already used in commercial lithium ion cells, then similar modifications were also carried out on the more popular salt $LiPF_6$, the industry standard of lithium ion cell electrolytes.

Handa et al. reported the synthesis of a phosphorus equivalent of Barthel's salts in which the hexavalent phosphorus(V) was coordinated by three bidentate ligands, 1,2-benzenediolato-$O,O'$.[494] Its thermal stability is similar to that of its boron counterparts, and moderate ion conductivity was achieved in nonaqueous media. The authors attributed the less-than-satisfactory ion conduction to the large size of the anions, which increased the viscosity of the resultant electrolyte solutions. The anodic stability limit, as measured by voltammetry on a Ni electrode, was below 3.7 V. A preliminary test of this salt in EC/THF was conducted in a lithium cell using the low potential cathode, $V_2O_5$, and the authors believed that this salt could be a superior electrolyte solute, judging from the utilized cell capacity that was close to the theoretical value.

On the basis of their previous experiences with lithium borates coordinated by substituted ligands, Barthel and co-workers modified the chelatophosphate anion by placing various numbers of fluorines on the aromatic ligands.[495] Table 13 lists these modified salts and their major physical properties. As expected, the introduction of the electron-withdrawing fluorines did promote the salt dissociation and reduce the basicity of phosphate anion, resulting in increased ion conductivity and anodic stability. The phosphate with the perfluorinated aromatic ligands showed an anodic decomposition limit of 4.3 V on Pt in EC/DEC solution. So far, these modified lithium phosphates have attracted only academic interest, and their future in lithium ion cell applications remains to be determined by more detailed studies.

**8.3.2.5. Lithium Fluoroalkyl Phosphates (LiFAP).** Since the P–F bonds in $PF_6^-$ anion are labile toward the attack of moisture and other nucleophiles such as the organic solvents with high electron-donicity, they are believed to be the source for the instability of the state-of-the-art electrolytes. Recent structural modification of $PF_6^-$ anion was conducted by Satori et al. via the partial replacement of fluorine substituents with perfluoroalkyls in the hope that chemical as well as thermal stability of the resultant salts (LiFAP) could be improved due to the inert nature of the P–C bonds.[496,497] Since the new substituents are also strong electron-withdrawing groups, the main merits of $LiPF_6$, such as good solubility and ion conductivity, are expected to be maintained.

In their patent disclosure, Satori et al. described eight such salts with different perfluorinated alkyls,[497] the representatives of which are listed in Table 13 along with the main physical and electrochemical properties. Among these salts, the most thoroughly investigated is the lithium salt based on an anion with three pentafluoroethyl groups. Hydrolysis studies confirmed that, due to the replacement of fluorine by the much bulkier perfluorinated alkyls, the sensitivity of the anion toward moisture is much reduced, as evidenced by the almost negligible amount of $H_2O$ consumption during 70 h of storage (Figure 55) and, correspondingly, the negligible HF level in the electrolyte.[498] The much lower reactivity of LiFAP should be the result of the combined effects of the lower chemical activity of the P–C bond and the spatial hindrance to the attack of $H_2O$. Ion conductivities of LiFAP in mixed carbonate solvents were slightly lower as compared with $LiPF_6$, obviously due to the larger anion size; however, comparable anodic stability was observed for LiFAP in the voltammetry scan conducted on a Pt electrode; that is, the major oxidative event occurred at ~5.0 V, although a higher background current level at potentials above 4.0 V was observed. Preliminary cycling tests were conducted in cathode half-cells based on $LiMn_2O_4$ using LiFAP/EC/DMC as electrolyte, and higher capacity was obtained than with $LiPF_6$ despite the fact that the capacity of the cells based on both electrolytes faded in a similar manner.
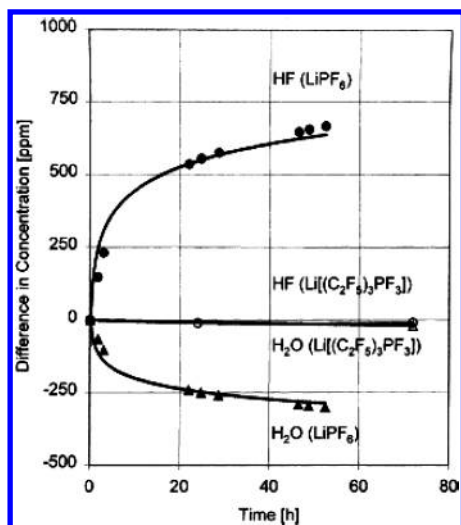
**Figure 55.** Presence of fluoroalkyls enhancing the anion stability against moisture. Consumption of $H_2O$ and the generation of HF in 1.0 M salt solutions of EC/DMC with added $H_2O$ at 500 ppm (for $LiPF_6$) and 1000 ppm (for LiFAP), respectively: triangle, $H_2O$ concentration; circle, HF concentration. (Reproduced with permission from ref 498 (Figure 2). Copyright 2001 Elsevier.)

More stringent electrochemical characterizations were carried by Aurbach and co-workers, who comparatively investigated the interfacial properties of the electrolytes based on LiFAP on anode and cathode materials against the benchmark salts $LiPF_6$ and LiBeti through various instrumental means, including voltammetry, EIS, FT-IR, and XPS.[499,500] They found that, while on both the graphitic anode and the spinel cathode the LiFAP-based electrolyte showed higher capacity utilization and better capacity retention, slower kinetics for lithium ion intercalation/deintercalation were found in both cases. The cause for the slow kinetics seemed to be related to the resistive SEI and surface films on each electrode, which was unexpected because there should have been little LiF present in the SEI, due to the stability of LiFAP, and it was concluded that LiF was mainly responsible for the high-impedance interfaces on either the anode or the cathode with $LiPF_6$ as the electrolyte solute. FT-IR and XPS indicated that LiFAP-based electrolytes generated higher amounts of lithium alkyl carbonate on the inert electrode (Pt and Au) surfaces that were cathodically polarized to simulate the surface chemistry on a cycled graphitic anode, but these spectroscopic means failed to identify any direct involvement of FAP anion in SEI formation. Nevertheless, it is apparent that in LiFAP-based electrolytes the surface species are mainly reduction products from solvents, while in $LiPF_6$-based electrolytes the anion is apparently more involved in the reductive decompositions, as evidenced by the XPS C 1s and F 1s spectra.[499] The higher stability of LiFAP is shown clearly by Figure 56, wherein two sets of CV were measured for LiFAP- and $LiPF_6$-based electrolytes after stabilization of the electrode and after 1 week of cyclings, respectively. In all the voltammetric profiles, four distinct stages of lithium intercalation are visible, but a very significant difference exists between LiFAP and $LiPF_6$: nearly identical current responses for LiFAP but an
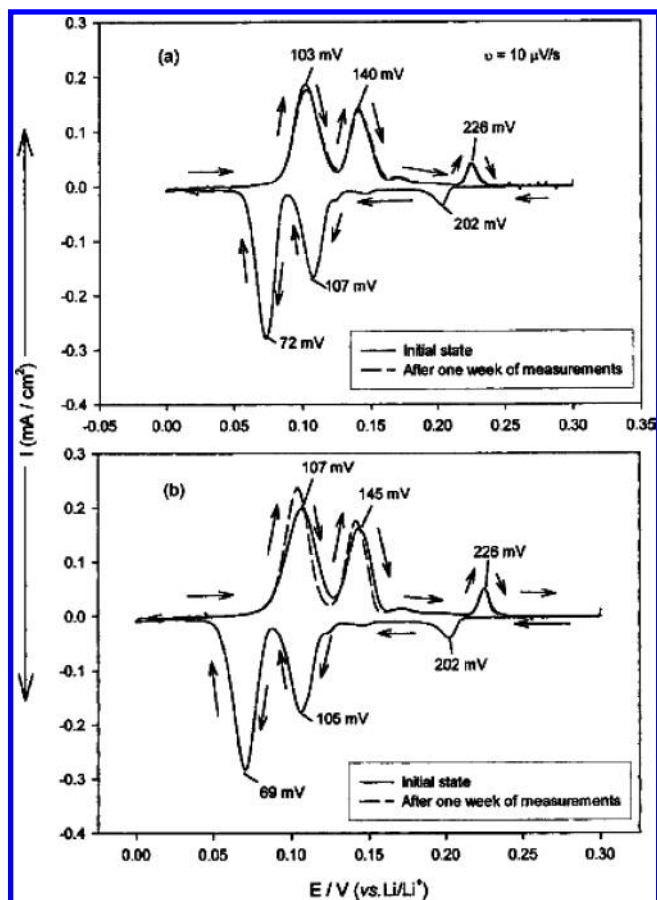


**Figure 56.** Slow scan (10 $\mu V\ s^{-1}$) voltammetry on a graphite working electrode: (a) 1.0 M LiFAP in EC/DEC/DMC; (b) $LiPF_6$ in EC/DEC/DMC. Solid line: pristine graphite. Dashed line: after 1 week of cycling. (Reproduced with permission from ref 499a (Figure 4). Copyright 2003 The Electrochemical Society.)

obvious gap for $LiPF_6$ in the anodic section were observed. In other words, there were long-term secondary processes in the $LiPF_6$-based electrolyte that affected the electrode kinetics, while the graphitic anode in the LiFAP-based electrolyte was under better protection from such undesirable processes.

Therefore, the authors concluded that, although direct identification was not available through spectroscopic means, the FAP anion must have participated in the formation of surface layers, which served as protection against sustained decompositions on one hand but were also responsible for the high impedance across the interfaces on the other. These robust surface films might exist on both anode and cathode surfaces and consist mainly of lithium alkyl carbonates because of the low level of HF in the solution.

The thermal stability of LiFAP was also studied by Aurbach and co-workers in EC/DEC/DMC solution using ARC. As compared with $LiPF_6$, LiFAP delayed the onset thermal decomposition of the electrolyte by ~10 °C; however, the self-heating became much more severe once the reactions started.[500] The above ARC was conducted in the absence of electrode materials.

In brief summary, LiFAP as a potential replacement for $LiPF_6$ would result in a stable performance in lithium ion cells with possibly increased thermal

stability, but the power rate of such cells would probably be inferior to that of the state-of-the-art electrolytes. If the manufacturing cost of producing these perfluorinated anions could be reduced, LiFAP or its derivatives might be a competitive electrolyte solute for lithium ion electrolytes.

**8.3.2.6. Lithium Salts Based on Heterocyclic Anions.** Lithium salts based on organic anions where the formal charge is delocalized throughout substituted heterocyclic moieties were also reported sporadically, which included, for example, lithium 4,5-dicyano-1,2,3-triazolate[501] and lithium bis(trifluoroborane)imidazolide (LiId).[502] The former was developed as a salt to be used for polymer electrolytes such as PEO, and no detailed data with respect to electrochemistry were provided, while the latter, which could be viewed as a Lewis acid−base adduct between $LiBF_4$ and a weak organic base, was intended for lithium ion applications (Table 13).

Because of the organic presence in these anions, the corresponding lithium salts are highly soluble in media of low or medium dielectric constants and could provide ion conductivities comparable to those of $LiPF_6$. LiId was reported to have high anodic stability as compared with $LiPF_6$, although the background current of the electrolytes based on it was higher than those for $LiPF_6$ counterparts at potentials above 4.0 V, as measured by cyclic voltammetry on Pt. The compatibility of this salt with $LiNi_{0.8}Co_{0.2}O_2$ cathode material was investigated by testing the corresponding half-cells, and performances comparable with or better than those of $LiPF_6$-based electrolytes were reported. However, in the case of MCMB, it took longer for LiId-based electrolyte to reach full utilization of the capacity, and it was only after ~10 cycles when the difference between LiId and $LiPF_6$ vanished. A higher irreversible capacity was also associated with LiId in the first cycle, where the Coulombic efficiency was 10.2% versus 6.2% for $LiPF_6$, suggesting that more charges were consumed in building up an SEI when LiId was the electrolyte solute. On the other hand, the authors argued that this capacity loss was negligible in terms of the total capacity. Considering the presence of B−F bonds in the anion of LiId, its thermal and chemical stability should be similar to that of $LiBF_4$, and its potential applications to replace $LiPF_6$ remain to be confirmed by further studies.

## 8.4. Novel Electrolytes with a Wide Temperature Range

### 8.4.1. Low-Temperature Performance

Following its rapid rise to dominance in the consumer cell market intended for portable electronics, lithium ion technology was actively considered for special applications such as those in military and space missions.[503−505] However, the poor performance of the state-of-the-art lithium ion cells at temperatures below −20 °C remained a major obstacle to enabling the normal operations in harsh environments that are frequently encountered in those missions. For example, according to a comprehensive survey of the commercial lithium ion cells made by major manufacturers in the late 1990s, the power rate and energy density that can be delivered at −40 °C averaged only 1.25% and 5% of those achievable at room temperatures, respectively.[506] A similar survey conducted a few years later showed that significant progress had been made, where as much as 30% of the rated capacity was deliverable at −40 °C by the best cells tested.[507] However, the deteriorated performance still plagued the reliable operations of this technology. Despite the sharp differences among the cells from various manufacturers, a common observation concerning their low-temperature behavior is that the major deterioration in performance occurs below −20 °C, while above this threshold temperature at least 80% of the rated capacity is deliverable.[505,507]

This sharp decline in cell output at subzero temperatures is the combined consequence of the decreased capacity utilization and depressed cell potential at a given drain rate, and the possible causes have been attributed so far, under various conditions, to the retarded ion transport in bulk electrolyte solutions,[503,508,509,510] the increased resistance of the surface films at either the cathode/electrolyte interface[506,507] or the anode/electrolyte interface,[461,504,511] the resistance associated with charge-transfer processes at both cathode and anode interfaces,[134,135,512] and the retarded diffusion coefficients of lithium ion in lithiated graphite anodes.[165,513] The efforts by different research teams have targeted those individual electrolyte-related properties to widen the temperature range of service for lithium ion cells.

**8.4.1.1. Solvent Approach.** Since the high-melting EC constitutes 30−50% of the bulk electrolyte in most of the commercial lithium ion cells, it has been the primary blame for the poor performances of such electrolytes at low temperatures, and its mixing with other lower melting cosolvents has been the most favorable approach so far adopted by the researchers with the aim to develop an electrolyte for subambient applications. As a pioneering attempt to develop a low temperature for lithium ion chemistry, Ein-Eli et al. used methyl formate (MF, mp −99 °C) and reported the ion conductivity at −40 °C for LiMe in EC/MF (1:3) to be 5.4 mS cm$^{-1}$.[102] The authors concluded that the depression effect of MF rendered the electrolyte liquid at such low temperatures. However, the performance of the anode half-cell was not improved ideally as expected, since only 50% deliverable capacity was achieved at −2 °C, which far exceeded the extent by which the bulk ion conductivity dropped. The possible origin for this discrepancy might arise from the elimination of supercooling at temperatures below −20 °C due to the presence of electrode particles in the anode half-cell, which are absent in conductivity cells, but more likely, it indicates that the bulk ion conductivity may not dictate the performance of the electrolytes in an actual lithium ion device. Since electrolytes based on neat MF failed to form an effective SEI on graphite and the stability of a graphite anode in the above EC/MF mixture solvents was clearly dependent on the EC presence, it appears that reductive decomposition
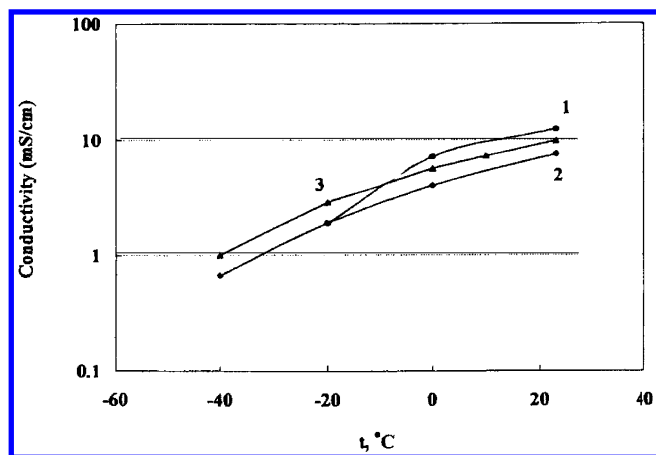
**Figure 57.** Ion conductivity of electrolytes containing 1.0 M LiPF$_6$ in (1) EC/DMC (3:7), (2) EC/DEC (3:7), and (3) EC/DMC/DEC (1:1:1). (Reproduced with permission from ref 508 (Figure 1). Copyright 1999 The Electrochemical Society.)



**Figure 58.** Comparison of the discharge profiles of graphite-based AA-size lithium ion cells at −20 °C among the various electrolytes. (Reproduced with permission from ref 508 (Figure 7). Copyright 1999 The Electrochemical Society.)

of MF made it an unfavorable candidate despite its low melting temperature.

An important contribution to the search for a low-temperature electrolyte was made by Smart et al. in late 1990s, apparently driven by the needs of NASA for the application of lithium ion devices in space missions.[461,462,466,508,515] The basic strategy of the team was to minimize the concentration of EC in the ternary or quaternary electrolyte formulations so that a synergistic effect could be reached by the various components based on either linear carbonates or esters. In an ideal scenario of role assignment, less than 30% EC would suffice for the effective solvation of lithium salts and ensure the formation of an effective SEI on electrode surfaces, while the majority components such as the low-melting DEC and the less viscous DMC would confer upon the mixture solvents a low liquidus temperature and facile ion transport at low temperatures. Figure 57 shows this synergistic effect achieved in a ternary electrolyte through the comparison of the temperature-dependence of ion conductivities against the corresponding binary electrolytes.[508] The discharge characteristics of the cells based on these electrolytes were also compared at −20 °C, as Figure 58 shows. An apparent gap exists among the electrolytes in terms of the delivered cell capacity, although at room temperature all of the electrolyte compositions behave similarly. In an extensive characterization of the irreversible capacity during the initial cycle, the durability and resistance of the SEI, the self-discharge rate, and so forth, the ternary electrolyte was shown to possess a series of intermediary qualities as compared with the binary baselines. The authors believed that it was these well-balanced properties of the ternary composition that made it an excellent candidate for subzero applications.

An important conclusion that these authors drew based on their polarization and EIS studies is that the properties of the SEI film on a graphite anode surface play a far more decisive role in determining the kinetics of the lithiation/delithiation at low temperatures than does the bulk ion conductivity, although it is necessary for the latter to achieve a
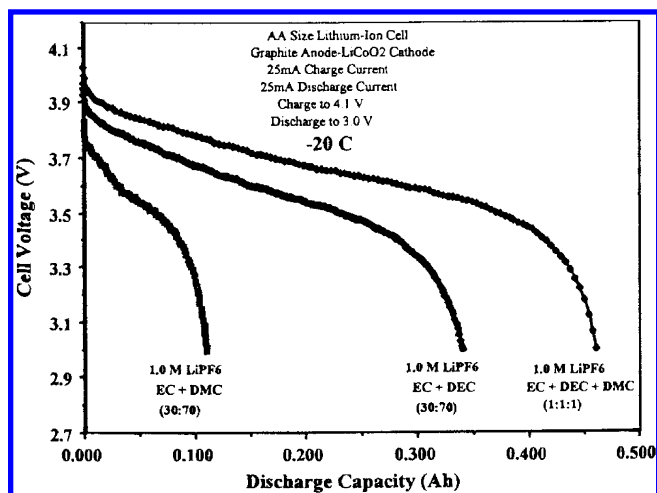
thresdhold value.[461,462] In other words, the reformulation of these low-temperature electrolytes has to consider the surface chemistry of the new cosolvents in addition to their positive effects on ion conductivity. This conclusion, now well accepted as a basic guideline, has been confirmed by the numerous examples found later, where the most conductive electrolytes do not necessarily provide the best improvement at low temperatures.[134,168,511,512]

Following the initial work by Smart et al., similar efforts were reported based on various binary and ternary compositions, such as EC/DMC/EMC (1:1:1),[503,505,509] EC/DMC/DEC (2:2:1),[505] EC/EMC (1:3),[505] EC/DMC/methylpropyl carbonate (MPC) and EC/DMC/isopropyl carbonate (iPC) at a series of varying compositions.[514] Unfortunately, below −30 °C the above compositions still failed to function well.[515]

In view of the limited improvements, Smart et al. sought to use linear alkyl esters, which are lower melting than the common alkyl carbonates by an average of 20−30 °C (Table 1). On the basis of the experience that MF was incompatible with graphitic anodes, they chose alkyl esters of higher carboxylic acids so that carboxylate connected with an alkyl instead of H as in MF. Thus, acetates such as MA and EA and higher carboxylates such as EP and EB were used to formulate quaternary electrolytes on the basis of the ternary compositions EC/DMC/DEC (T).[461,462] As expected, due to the introduction of these esters, the ion conductivity was obviously improved, while both anodic and cathodic stability as measured on a Pt surface were negatively affected. In terms of compatibility with a graphite anode, there exists an apparent distinction between the acetates (MA and EA) and the esters of higher carboxylic acids (EP and EB), since the reversible capacities that can be utilized by the electrolytes containing the acetates are much lower, and EP− or EB-based electrolytes yield comparable performances with the ternary baseline. Therefore, the authors speculated that the SEI formed in the presence of low molecular weight esters appeared to be resistive and inadequately protective, whereas, in the presence of esters of
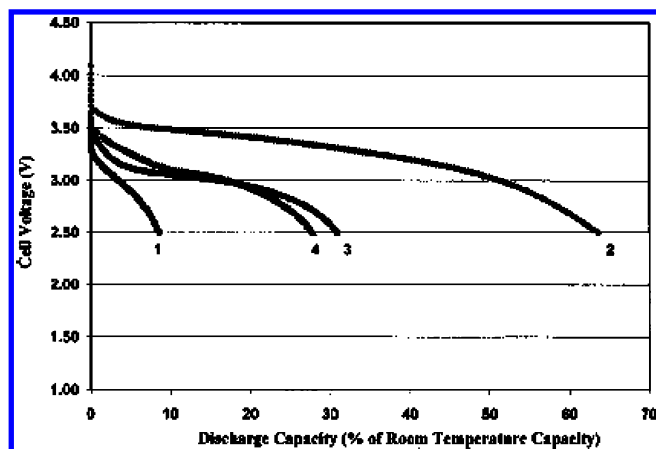
**Figure 59.** Effect of ester-containing quaternary electrolytes on the discharge capacity of AA-size lithium ion cells (0.4−0.5 A h) at −40 °C under the drain rate of 25 mA. The electrolytes are (1) 1.0 M LiPF$_6$/EC/DEC/DMC (1:1:1), (2) 0.75 M LiPF$_6$/EC/DEC/DMC/MA (1:1:1:1), (3) 0.75 M LiPF$_6$/EC/DEC/DMC/EA (1:1:1:1), and (4) 0.75 M LiPF$_6$/EC/DMC/MA (1:1:1). (Reproduced with permission from ref 462 (Figure 12). Copyright 2002 The Electrochemical Society.)



**Figure 60.** Discharge capacities of LiNiCoO$_2$/MCMB lithium ion cells at −20 °C with different carbonate-based electrolytes. Cells are charged at room temperature and discharged using a C/15 rate. (Reproduced with permission from ref 515 (Figure 4). Copyright 2003 Elsevier.)

higher molecular weight, the SEI could be formed with more desirable attributes. Combining the observations of Ein-Eli et al.,[102] Smart et al.,[461,462] and Herreyre et al.,[406] it could be tentatively concluded that longer alkyl chains in the carboxylic acid section of the esters play a critical role in determining the cathodic stability of this component on a graphite anode. The tests in AA-size full lithium ion cells were only reported for EA- and MA-based quaternary electrolytes, and Figure 59 shows the discharging profiles of these cells at −40 °C. Despite their negative effect on anode capacity utilization at room temperature, MA and EA still improved the capacity significantly.

On the other hand, the presence of these esters in the electrolyte solutions raised concern over the long-term performance at room temperatures, because EIS studies indicated that the resistance associated with the SEI film increased at a much higher rate for ester-based electrolytes as compared with the compositions that were merely based on carbonates. The authors attributed this rising cell impedance to the reactivity of these esters toward the electrode active material, which resulted in the continued growth of the SEI film in the long term and suggested that alkyl esters, especially those of acetic acid, might not be appropriate cosolvents for low-temperature application electrolytes.[461]

The work of Herreyre et al., however, took a much more optimistic tone on the use of linear esters EA and MB.[406] In LiCoO$_2$/graphite cells, the ternary electrolyte compositions such as 1.0 M LiPF$_6$ in EC/DMC/EA, EC/DMC/MB, and PC/EC/MB were reported to be able to deliver as much as 88−95% of the rated capacity at −30 °C with a C/2 rate or 81−87% at −40 °C, while at room temperature the capacity fading rate (0.05% per cycle for MB and 0.09% per cycle for EA) and capacity retention with high-temperature storage (60 °C, 14 days at full state-of-charge) of these cells were comparable with those of the state-of-the-art electrolytes (0.05% per
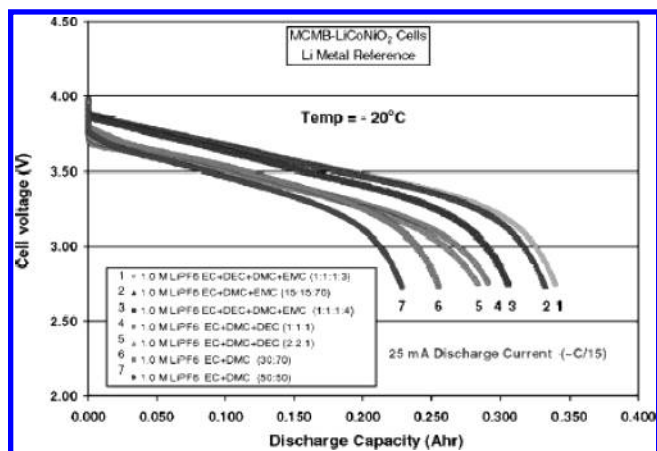
cycle). Thus, the authors concluded that these new electrolytes could be used as cosolvents for low-temperature electrolytes. Considering that Smart et al. and Herreyre et al. used entirely different cells as their testing vehicles, the above discrepancy might not be too incomprehensible, since similar discrepancies had been encountered when the trends observed in anode half-cells did not correlate well with that of prototype cells with a different cell design.[462] It actually indicated the complexity in the operation of lithium ion chemistry, during which various factors including chemistry as well as engineering exert their influences.

Besides the Coulombic capacity, Herreyre et al. also pointed out that the depression in cell voltage at low temperatures could be mitigated by EA and MB as cosolvents because of the reduced resistance in both bulk electrolyte and electrolyte/electrode interfaces. Moreover, they found that this cell voltage depression was also related to the salt concentration; using 1.5 M instead of 1.0 M LiPF$_6$ in the electrolyte enabled the increase of the cell working range from −30 to −40 °C, as, in most cases, the cell cycling is regulated by a preset cutoff potential.

Out of the belief that the alkyl esters are reactive in a lithium ion cell during the long-term operation, Smart et al. proposed a "carbonate-only" guideline and formulated a series of quaternary compositions consisting of EC/DEC/DMC/EMC, in which the EC concentration remained under 25%.[515] The solution of 1.0 M LiPF$_6$ in EC/DEC/DMC/EMC (1:1:1:3) was reported to be the best composition, whose ion conductivity at −40 °C was 1.32 mS cm$^{-1}$, and its cycling in LiNiCoO$_2$/MCMB lithium ion cells was comparable to that of the baseline electrolyte 1.0 M LiPF$_6$ in EC/DMC (3:7) or (1:1) at room temperatures. At −20 °C, the superiority of these quaternary electrolytes became pronounced, as compared with the ternary and binary baselines shown in Figure 60.

More importantly, these electrolytes also allowed the lithium ion cells based on them to be charged at low temperatures at reasonable rates, as shown by Figure 61, which had been impossible for most of the lithium ion cells because the high impedance of the
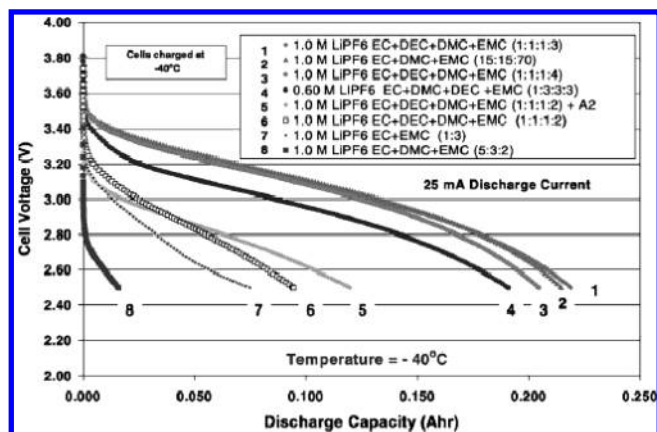
**Figure 61.** Discharge capacities of LiNiCoO₂/MCMB lithium ion cells at −40 °C with different carbonate-based electrolytes. Cells are charged at −40 °C and discharged using a *C*/4 rate. (Reproduced with permission from ref 515 (Figure 6). Copyright 2003 Elsevier.)



**Figure 62.** Cycle life performance of SAFT DD-size lithium ion cells containing 1.0 M LiPF₆/EC/DEC/DMC/EMC (1:1:1:3) at various temperatures. Cutoff voltages for low-temperature charge were indicated in the graph. (Reproduced with permission from ref 515 (Figure 11). Copyright 2003 Elsevier.)



**Figure 63.** Delithiation capacity of an MCMB anode at −20 °C in various electrolytes following charge (lithiation) at −20 °C. The drain rate is 50 mA (~*C*/12). (Reproduced with permission from ref 466 (Figure 4). Copyright 2003 Elsevier.)

cells at a discharged state would result in lithium deposition on a graphite surface due to the high overpotential.[515] Using a three-electrode cell, Smart et al. monitored the potential of the cathode and anode of a LiNiCoO₂/MCMB lithium ion cell during its cycling at −20 °C, and they confirmed that, although the potential of the graphite anode was indeed driven to negative regions in the charge process, no lithium deposition occurred, as evidenced by the absence of a potential plateau at 0.0 V corresponding to lithium stripping in the following discharge process, which had been observed previously in a similar cell using LiPF₆/EC/EMC (1:3) as the electrolyte.[165] They attributed this to the facile kinetics of lithium ions in the bulk electrolyte as well as in the SEI film on the graphite anode. The cycling tests of SAFT prototype lithium ion cells carried out in a wide temperature range between −70 and 40 °C confirmed that the above quaternary composition is an excellent low-temperature electrolyte. As illustrated in Figure 62, when the cell is continuously cycled at −20 °C using a *C*/10 charge rate and a *C*/5 discharge rate, stable capacity retention can be obtained with 80% of the rated capacity delivered. Using lower rates (*C*/15 charge and *C*/10 discharge), 70% of the rated capacity can be accessed even when cycled at −40 °C.

Fluorinated carbonates were also used by Smart et al. as low-temperature cosolvents (Table 12), in the hope that better low-temperature performances could be imparted by their lower melting points and favorable effects on SEI chemistry.[466] Cycling tests with anode half-cells showed that, compared with the ternary composition with nonfluorinated carbonates, these fluorinated solvents showed comparable and slightly better capacity utilizations at room temperature or −20 °C, if the cells were charged at room temperature; however, pronounced differences in discharge (delithiation) capacity could be observed if the cells were charged (lithiated) at −20 °C, where one of these solvents, ethyl-2,2,2-trifluoroethyl carbonate (ETFEC), allowed the cell to deliver far superior capacity, as Figure 63 shows. Only 50% of the capacity deliverable at room temperature was
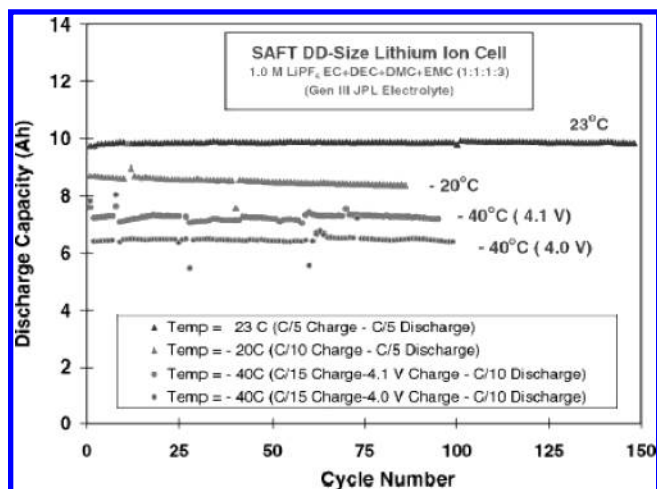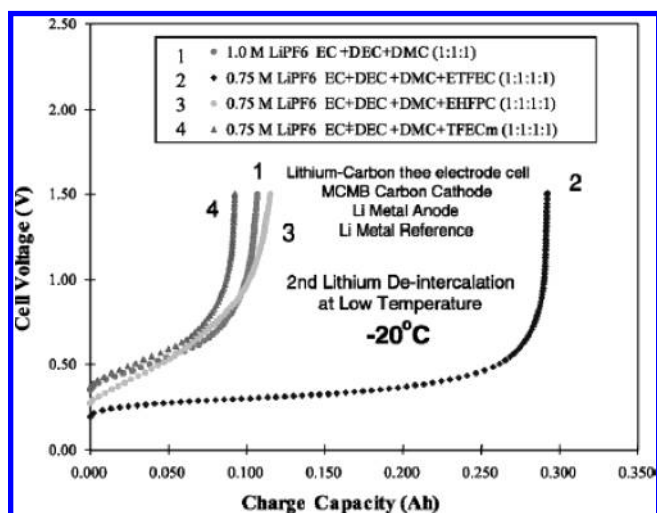
achieved in the best case, however. EIS and polarization studies on the interface between the electrolyte and the graphitic anode showed that these fluorinated cosolvents in general created less resistive surface films and more rapid charge-transfer kinetics when compared with nonfluorinated carbonates, and the difference increased with decreasing temperature. Full lithium ion cells based on LiNi$_x$Co$_{1-x}$O₂ and MCMB were also assembled with one of these novel solvents, and good reversibility was observed, although no data on subzero temperature tests were reported.

According to the authors, additional merits of such fluorinated carbonates would include their lower flammability and higher stability against storage at elevated temperatures as compared with their nonfluorinated counterparts; therefore, the incorporation of these novel solvents into the current commercial

lithium ion cells seems promising if the manufacturing costs and environmental requirements do not constitute any obstacle.

In addition to linear carbonates, PC was also considered as a cosolvent that could help to improve the low-temperature performance of the electrolytes, mainly due to its wide liquid range and solvation ability to lithium salts. This latter property seems to be a merit relative to the linear carbonates, whose dielectric constants are generally below 10 and whose displacement of EC usually causes the solubility of lithium salts to decrease in such mixed solvents, especially at low temperatures.

To characterize the effect of PC addition on the related properties of the electrolytes, Zhang et al. carried out a comparative study on PC/EC/EMC (1:1:3) and EC/EMC (3:7).[168] They found that, because of the higher viscosity of PC, the ion conductivity of the former formulation was lower at subzero temperatures, and its declination accelerated with decreasing temperature. Nevertheless, due to the large portion of linear carbonates in the formulation, the compromise in ion conductivity was marginal. Discharge tests in $LiNiO_2$/graphite lithium ion cells were carried out down to −30 °C, and PC-containing electrolytes was found to outperform the baseline. According to the authors, this improvement could not be attributed to the bulk ion conductivity of the PC-based electrolyte but to the lower cell impedances associated with the films on both cathode and anode surfaces. No cycling tests below −20 °C were described. Considering that PC would induce higher irreversible capacities in the initial cycles and eventually result in lower capacity in cathode-limit lithium ion cells, the use of it as a low-temperature electrolyte cosolvent is possible only if one of the following measures is adopted to suppress the cointercalation and decomposition of PC: (1) the use of SEI-modifying additives, (2) the use of special salts that can help form a more protective SEI (such as LiBOB), or (3) the surface modification of the graphite anode.

**8.4.1.2. Salt Approach.** Another less expected approach aimed at low-temperature electrolytes was also proposed by Zhang et al., who reported that the replacement of $LiPF_6$ by $LiBF_4$ would result in improved discharge capacity of lithium ion cells.[134,135]

$LiBF_4$ had been considered an inferior electrolyte solute to $LiPF_6$ due to its lower ion conductivity in nonaqueous solvents and the less protective SEI formed by these electrolytes, and its application in commercial lithium ion cells seemed to be possible only in the unique solutions containing γBL. As Figure 64 shows, in the entire temperature range from 60 to −60 °C, $LiBF_4$ exhibited a lower ion conductivity than $LiPF_6$ in PC/EC/EMC (1:1:3) solutions,[134] while a similar trend was found for EC/DMC/DEC solutions as well.[135] However, all the $LiBF_4$-containing lithium ion cells obviously outperformed their $LiPF_6$ counterparts in discharge capacity at temperatures below 0 °C, and as Figure 65 shows, at −40 °C, its PC/EC/EMC solution was still able to deliver up to 86% of the rated capacity, while the $LiPF_6$ counterpart could only access 72%. These results once again confirmed that ion conductivity in
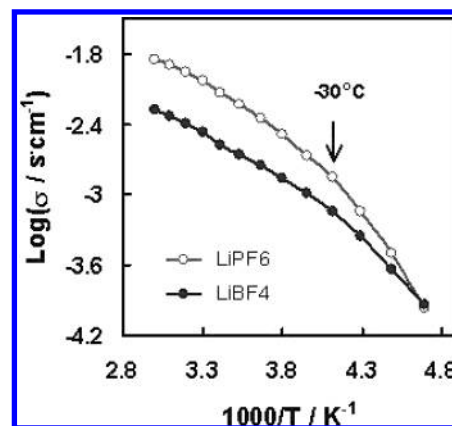


**Figure 64.** Arrhenius plots of the ion conductivities for the electrolytes composed of 1.0 m lithium salts in PC/EC/EMC (1:1:3). (Reproduced with permission from ref 134 (Figure 1). Copyright 2002 Elsevier.)
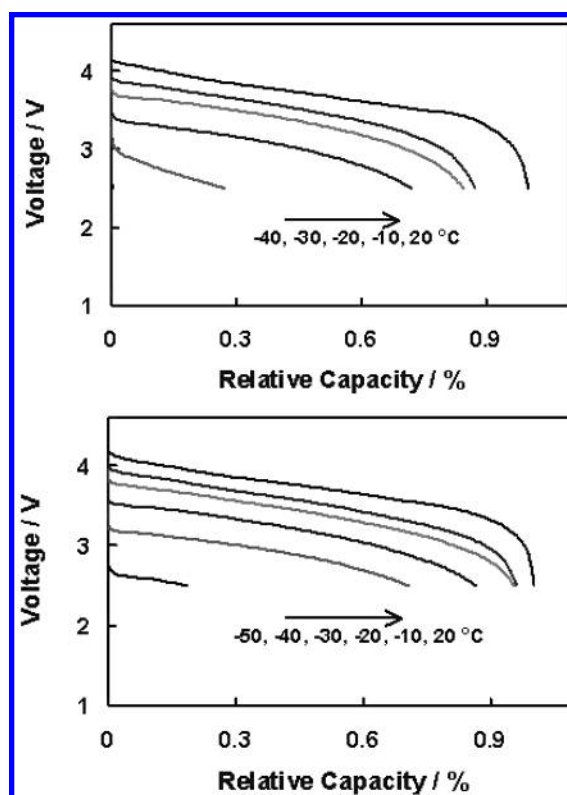


**Figure 65.** Comparison between the discharge capacities for lithium ion cells at various temperatures. Relative capacity was defined as the ratio of the capacity at the specified temperature to the one obtained at 20 °C: (a, top) $LiPF_6$/EC/PC/EMC (1:1:3); (b, bottom) $LiBF_4$/EC/PC/EMC (1:1:3). (Reproduced with permission from ref 134 (Figure 2). Copyright 2002 Elsevier.)

the bulk electrolytes does not dictate low-temperature performance.

By EIS analysis of the corresponding lithium ion cells, Zhang et al. showed that the impact of SEI resistance on total cell impedance was rather negligible, and hence, they attributed the superior low-temperature behavior of $LiBF_4$-based electrolytes to the lower resistance associated with the so-called "charge-transfer processes", which are usually represented in impedance spectra by the semicircle at the lower frequency region.[516] This suggestion could be viewed as a further extension of the conclusion

**Figure 66.** Nyquist plots of the impedance spectra as measured for the fully charged lithium ion cells at −30 °C in which the inset shows the magnified view of the high-frequency part. Electrolytes are 1.0 m $LiPF_6$ (hollow) and $LiBF_4$ (solid) in PC/EC/EMC (1:1:3). Note that the semicircles in the inset are almost invisible in the scale of the whole spectra. (Reproduced with permission from ref 134 (Figure 4). Copyright 2002 Elsevier.)
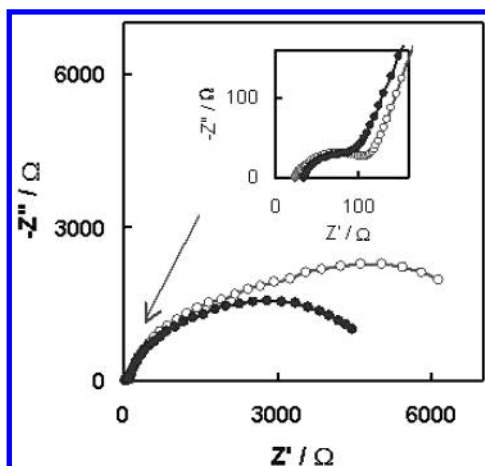
drawn by Smart et al., who had identified $R_{SEI}$ as the limiting resistance in the lithium cell operation at low temperatures.[462] In fact, Smart et al. had already realized the effect of $R_{ct}$ on low-temperature behavior, since they also used an effective exchange current density to represent the lithium ion intercalation kinetics. This latter quantity should reflect the overall effect of $R_{SEI}$ and $R_{ct}$.[462,508]

Thus, by comparing the impedance spectra of the lithium ion cells, Zhang et al. showed that the resistance corresponding to the charge-transfer process ($R_{ct}$) dominates the total cell resistance at low temperatures. For example, at −30 °C (Figure 66), the semicircle and the interception corresponding to $R_f$ and $R_b$ have to be magnified in the inset to be visible. Considering the huge difference between the magnitudes of $R_b$ or $R_f$ and $R_{ct}$, the authors concluded that the poor low-temperature performance of lithium ion cells is caused by the slow kinetics of charge-transfer at these temperatures. The decoupling of the bulk resistance ($R_b$, related to the ion conductivity in the bulk electrolytes) from the charge-transfer process and film resistances ($R_{ct}$ and $R_f$, related to the ion transport in the surface film and the Faradaic process, respectively) can also be clearly seen in Figure 66 (at −30 °C): that is, although the cell based on $LiBF_4$ has higher $R_b$ (the inset), its $R_{ct}$ is much lower than that of the cell with $LiPF_6$.[134] Similar observations were also made with EC/DMC/DEC formulations.[135] It should be noted that, since full lithium ion cells were used in these EIS studies, $R_{ct}$ and $R_f$ mentioned above should reflect the combination of these corresponding processes on both anode/electrolyte and cathode/electrolyte interfaces.

In another work unrelated to the low-temperature electrolytes, Mohamedi et al. characterized the spray-deposited thin film of spinel cathode material by means of EIS and studied the correlation between electrolyte composition and the impedance components. Among the three lithium salts investigated, the lowest $R_{ct}$ and $R_f$ were obtained in a $LiBF_4$-based

electrolyte.[517] This observation indirectly corroborated the conclusions of Zhang et al. and seemed to indicate that $LiBF_4$ possessed certain qualities of an electrolyte solute for low-temperature-oriented applications. In combination with the advances obtained in the solvents approach, further improvement in the performance at extreme temperatures might be a probable perspective.

**8.4.1.3. Limiting Factors for Low-Temperature Operation.** One controversial topic that has raised wide attention relates to the limiting factors of the low temperature of lithium ion cells. The researchers not only debated about whether the anode or cathode controls the overall low-temperature performance of a full lithium ion cell but also disagree upon the rate-determining steps that govern the low-temperature kinetics of lithium ion intercalation at the graphitic anode.

Due to the contributions from Smart et al.,[462] the emphasis of low-temperature study on electrolytes has been placed on the anode side, and the SEI film on the graphitic surface has generally been recognized as the most resistive component in the journey of the lithium ions during the cell operation, which must travel across the electrolyte and intercalate into or deintercalate from the bulk graphite structure. This hypothesis was mainly established on the basis of two observations made in the EIS studies of the lithium/graphite half-cells: (1) the resistance corresponding to the surface film component ($R_{SEI}$) far outweighs the component representing electrolyte bulk resistance, and (2) the steep temperature-dependence of $R_{SEI}$ in the low-temperature ranges below −20 °C matches the rapid deterioration of the half-cell performance, while the ion conductivities do not suffer any dramatic drop in this range.[164,168] These two phenomena have been repeatedly observed in various electrolyte systems in which novel cosolvents were added to depress the liquidus temperature and to improve solution transport properties, and complementary evidence was also obtained from various electrochemical polarization techniques.[466,511,512]

The above hypothesis was questioned by Huang et al., who suggested that the critical factor that limits the anode capacity accessible at the low temperatures is the kinetics of the lithium ion in the bulk carbonaceous anode instead of the surface film.[513] Their argument was based on the universally observed asymmetric behavior of graphitic anodes toward lithiation and delithiation at low temperatures; that is, while the fully charged graphite can release the intercalated lithium ions at temperatures below −20 °C with relative readiness, the attempt to lithiate a fully discharged graphite anode at the same temperature is severely hampered by the high resistance at the surface. Considering the electrolyte nature of the SEI, which serves as an electronic insulator but an ionic conductor, the authors pointed out that it should neither behave like a diode that only impedes lithium insertion but allows extraction nor vary in its resistance depending on the state-of-charge of the graphite. Therefore, the above asymmetric behavior should not be attributed to the SEI, whose resistance should
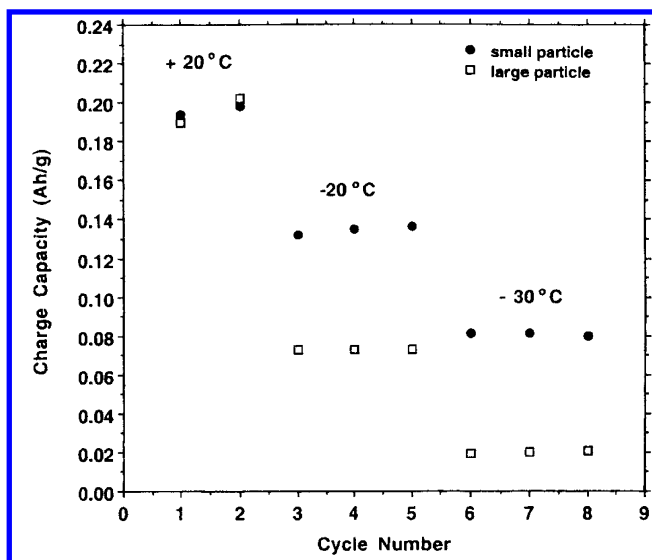
**Figure 67.** Effect of coke particle size on the charge capacity at various temperatures. (Reproduced with permission from ref 513 (Figure 8). Copyright 2000 The Electrochemical Society.)

be independent of the lithiation degree in the graphite, but rather to the lithium ion diffusion within the carbonaceous anode structure, which has directionality due to the concentration polarization. Thus, the diffusion coefficient of lithium ion within the carbonaceous anode ($D_{Li}$) would always be higher for lithium deintercalation but lower for intercalation, and the gap between the two processes becomes more prominent as temperature goes down.[513]

To further support their argument that low-temperature lithium ion intercalation is governed by lithium diffusion instead of the SEI, the authors investigated the effect of carbon particle size on its specific capacity by choosing two carbonaceous anodes of the same capacity at room temperature but different particle sizes (6 and 25 $\mu$m). They found that, when cycling at temperatures below $-20$ °C, the anode with fine particles outperformed the one with coarse particles in the charge capacity, as Figure 67 shows. The authors believed that this particle size effect was consistent with their contention that lithium diffusion is the rate-determining step that limits the low-temperature performance of carbonaceous anodes, because the large diameter of the 25 $\mu$m particle would require longer lithium diffusion lengths and, consequently, a lower lithiation degree would be realized in this case, with the assumption that $D_{Li}$ is the same for both anode materials.

Combining the above evidences, Huang et al. further concluded that the improvement in the low-temperature performances of lithium ion cells would eventually rely on the effort to develop anode materials of high lithium diffusion coefficients instead of the electrolytes and SEI that were less resistant.

The conclusion of Huang et al. was supported by Lin et al., who used a three-electrode cell design to monitor the voltage profile of both the anode and cathode in a full lithium ion cell during cycling at low temperatures and found that these cyclings resulted in the deposition of metallic lithium on the graphite surface and the subsequent permanent capacity loss when an unusual cycling regulation was applied to deal with the reduced capacity accessible at low temperatures.[165] These authors attributed the lithium deposition to the excessive concentration polarization on the graphite surface.

However, more recent work by Wang et al.[511] and Zhang et al.[512] seemed to present convincing evidence challenging the suggestion by Huang et al. that electrolyte and the SEI resistances do not affect the low-temperature performance of graphitic anodes. The former authors used the combination of the galvanostatic intermittent titration (GITT) technique and EIS to analyze the individual impedance components that simulate graphite in the quaternary electrolyte composition LiPF$_6$/EC/PC/DMC/EMC (4:1:3:2). Since the reaction resistance as measured by GITT is the sum of the electrolyte bulk resistance, $R_{SEI}$, $R_{ct}$, stage transformation, and the resistance that corresponds to lithium diffusion in graphite, it is possible to distinguish the impact of their temperature-dependences on the overall electrode kinetics. They found that, during the low-temperature cyclings, the diffusional resistances were similar during charge and discharge, thus contradicting the hypothesis by Huang et al. that the concentration-dependence of lithium diffusion would result in higher concentration polarization to lithiation than to delithiation. Furthermore, in a quantitative manner, they also found that the magnitude of $R_{SEI}$ makes it the dominating component at the low temperatures when compared with the other impedance components and, hence, concluded that at $-30$ °C the limiting factor for the lithium intercalation is $R_{SEI}$.

The latter authors used anode and cathode symmetrical cells in EIS analysis in order to simplify the complication that often arises from asymmetrical half-cells so that the contributions from anode/electrolyte and cathode/electrolyte interfaces could be isolated, and consequently, the temperature-dependences of these components could be established. This is an extension of their earlier work, in which the overall impedances of full lithium ion cells were studied and $R_{ct}$ was identified as the controlling factor.[134,135] As Figure 68 shows, for each of the two interfaces, $R_{ct}$ dominates the overall impedance in the symmetrical cells as in a full lithium ion cell, indicating that, even at room temperature, the electrodic reaction kinetics at both the cathode and anode surfaces dictate the overall lithium ion chemistry. At lower temperature, this determining role of $R_{ct}$ becomes more pronounced, as Figure 69c shows, in which "relative resistance", defined as the ratio of a certain resistance at a specific temperature to that at 20 °C, is used to compare the temperature-dependences of bulk resistance ($R_b$), surface layer resistance ($R_{sl}$), and $R_{ct}$. For the convenience of comparison, the temperature-dependence of the ion conductivity measured for the bulk electrolyte is also included in Figure 69 as a benchmark. Apparently, both $R_b$ and $R_{sl}$ vary with temperature at a similar pace to what ion conductivity adopts, as expected, but a significant deviation was observed in the temperature dependence of $R_{ct}$ below $-10$ °C. Thus, one
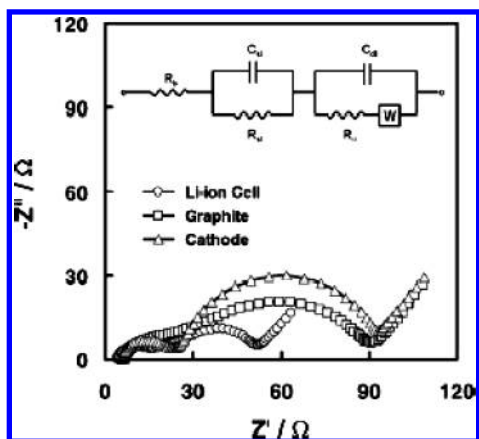
**Figure 68.** Nyquist plots of a charged lithium ion cell, a lithiated graphite/graphite cell, and a delithiated cathode/cathode symmetrical cell. The inset is an equivalent circuit used for the interpretation of the impedance spectra. (Reproduced with permission from ref 512 (Figure 3). Copyright 2003 Elsevier.)

could conclude that the rate-determining factor that limits the capacity utilization of the graphitic anode as well as the cathode should most likely be $R_{ct}$.

Perhaps a more important finding by these authors is the "concentration-dependence" of $R_{ct}$. As Huang et al. has pointed out, $R_{SEI}$ should be independent of state-of-charge,[513] and the authors proved that $R_{SEI}$ remains relatively constant on both charged and discharged anode and cathode surfaces, as shown by the insets of Figure 70. However, $R_{ct}$ showed a strong dependence on the lithiation degree of both the anode and cathode. Two extreme situations were simulated in Figure 70, which correspond to a fully charged lithium ion cell, wherein the cathode is delithiated and the anode is lithiated, and a fully discharged lithium ion cell, wherein the cathode is lithiated and the anode is delithiated. Apparently, in the former case, $R_{ct}$ on both the anode and cathode is substantially high, indicating a high polarization for the lithiation of the anode and delithiation of the cathode, while the reverse processes for each electrode are much easier in a fully charged lithium ion cell. Hence, these authors proposed that the asymmetrical behavior of lithium ion cells at low temperature most likely originated from the concentration-dependence of $R_{ct}$ instead of the directionality of lithium diffusion within the bulk graphite anode.[512] Since in numerous reports $R_{ct}$ has been shown to be closely related to SEI or surface film properties, although its physical significance remains ambiguous,[516] a fact beyond doubt is that this rate-determining component is under the influence of electrolyte composition, as evidenced by Smart et al.'s success.[515] On the other hand, the suggestion by Huang et al. that the electrolyte and SEI do not control the low-temperature performance of lithium ion cells seems to be challenged in these electrode/electrolyte systems.

It must be noted here that the observation made by Zhang et al. about the dominating magnitude of $R_{ct}$ could be electrode-specific because $R_{ct}$ is not always higher than $R_{SEI}$ in all systems and at all temperatures. At least in the works by Smart et al.[461,462] and Wang et al.,[511] $R_{ct}$ in magnitude is comparable with or even smaller than $R_{SEI}$. Certainly,
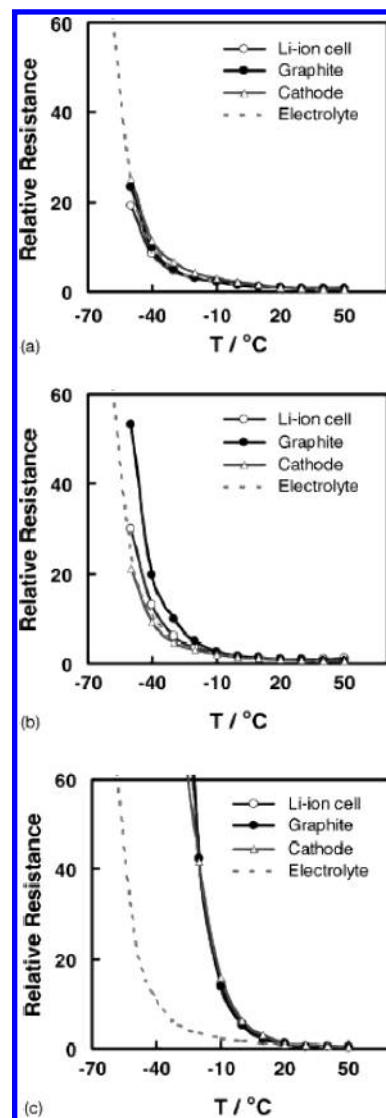


**Figure 69.** Comparison for temperature-dependence of the relative resistances of a charged lithium ion cell, a lithiated graphite/graphite cell, and a delithiated cathode/cathode cell. The dashed curves show the "relative resistance" of the electrolyte, which was taken as the ratio of the electrolytic conductivity at a specific temperature to the conductivity at 20 °C: (a) $R_b$; (b) $R_{sl}$; (c) $R_{ct}$. (Reproduced with permission from ref 512 (Figure 4). Copyright 2003 Elsevier.)

as long as the temperature-dependence and "concentration-dependence" of $R_{ct}$ remain unchanged, the relative magnitude of $R_{ct}$ versus $R_{SEI}$ should not reverse the conclusion by Zhang et al. Nevertheless, in such situations it seems to be necessary to define a new quantity that would more accurately describe the overall kinetics of lithium ion intercalation/deintercalation in the surface film. The interface exchange current derived from various polarization techniques that has been used by Smart et al. could be such a quantity, because both $R_{SEI}$ and $R_{ct}$ are taken into account.

In most of the situations discussed above, the graphite anode was investigated as the single and isolated component, while no or little consideration was given to the other components where simultaneous electrochemical processes occurred. In a full

**Figure 70.** Asymmetrical behavior of $R_{ct}$ toward lithiation and delithiation. Comparison between the Nyquist plots of the anode and cathode symmetrical cells at different state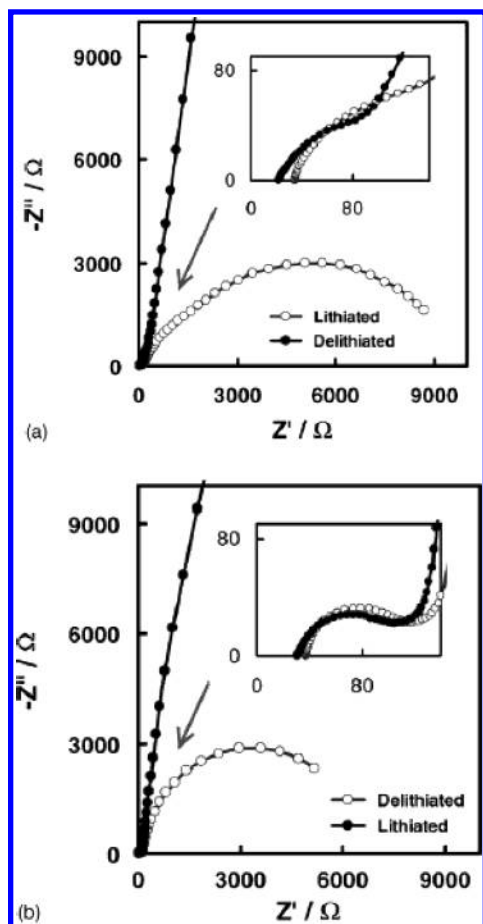s-of-charge: (a) graphite/graphite; (b) cathode/cathode. (Reproduced with permission from ref 512 (Figure 5). Copyright 2003 Elsevier.)

lithium ion cell, which integrates all of those components, including electrolyte, separator, cathode, and anode, the identification of the limiting factor for low-temperature performance becomes more complicated, and conflicting conclusions have been reported from various authors. Clearly, these conclusions are highly conditional and most likely system-specific; therefore, caution should always be taken when interpreting the results of these studies.

Conceptually, besides SEI and charge-transfer resistance in the interfaces as well as lithium diffusion coefficients in the electrodes, the possible limiting factors that might affect the kinetics of lithium ion chemistry could also be electrode surface area and porosity, electrode density and loading, affinity of binder toward electrolyte, and separator porosity and lipophilicity. Any material or engineering flaw could make any of these factors the rate-determining step of the kinetics; hence, it is not strange that different limiting factors have been identified for different lithium ion systems when low-temperature performance was investigated.

Ozawa was perhaps the first author who tried to determine whether the anode or cathode acts as the kinetic bottleneck in a full lithium ion cell, although the purpose at the time was not intended for low-temperature considerations.[157] In interpreting the

Nyquist plots obtained in the EIS analysis of the first generation of Sony 18650 cells, he assigned the larger semicircle at lower frequency to the anode/electrolyte interface and the smaller at medium frequency to the cathode/electrolyte interface on the basis that the diameter of the former relies on the state-of-charge of the anode, while the latter becomes larger in diameter when the surface area of the $LiCoO_2$ cathode decreases. Thus, he concluded that the charge-transfer process occurring at the anode/electrolyte interface is the slowest step for the whole cell chemistry. However, since the EIS study was conducted on the lithium ion cell without an independent reference electrode, the attempt to separate the contribution from each individual electrode to the overall cell impedance is deemed unreliable. His way of assigning the two semicircles to individual electrodes was also questionable, since it is well accepted that these semicircles correspond to different processes rather than different electrode interfaces.[134,462] As has been shown in Figure 68, since the time constants for these two electrochemical components, $R_{SEI}$ and $R_{ct}$, are comparable at anode/electrolyte and cathode/electrolyte interfaces, respectively, the impedance spectra of a full lithium ion could have similar features in which the higher frequency semicircle corresponds to the surface films on both the anode and the cathode, and the other at lower frequency corresponds to the charge-transfer processes occurring at both the anode and the cathode.[512]

By incorporating an independent lithium reference electrode in a commercial lithium ion cell from A&T, Nagasubramanian managed to separate the contributions from the anode and cathode to cell impedance and established their individual temperature profiles.[506] He found that the increase in cell impedance with decreasing temperature mostly came from the cathode/electrolyte interface, while the contributions from the anode/electrolyte interface or the bulk resistance were negligible. Similar impedance behavior was also observed in commercial cells from Moli and Panasonic.[506] Thus, he concluded that the interfacial resistance at the cathode, which should include both $R_{SEI}$ and $R_{ct}$, is mainly responsible for the poor cell performance at low temperatures. This conclusion was supported by Chen et al., who investigated the 18650 lithium ion cell assembled by Polystor using EIS and identified charge-transfer resistance at the $LiNi_{0.8}Co_{0.2}O_2$ cathode/electrolyte interface as the main contributor of overall cell impedance, although the study was only carried out at room temperatures.[518] An indirect evidence for this conclusion came from the XPS studies conducted by Andersson et al. on the cathode and anode surface from the same lithium ion cell, which showed that the surface film on the cathode is much thicker compared with the anode SEI.[294]

The opposite conclusion was reported by Lin et al.,[165] who used a three-electrode configuration to study the electrode polarization of the MCMB anode and $LiCoO_2$ cathode under galvanostatic conditions. They found that in all cases the polarization at the MCMB anode surface far outweighs that at the cathode to such an extent that the potential profile
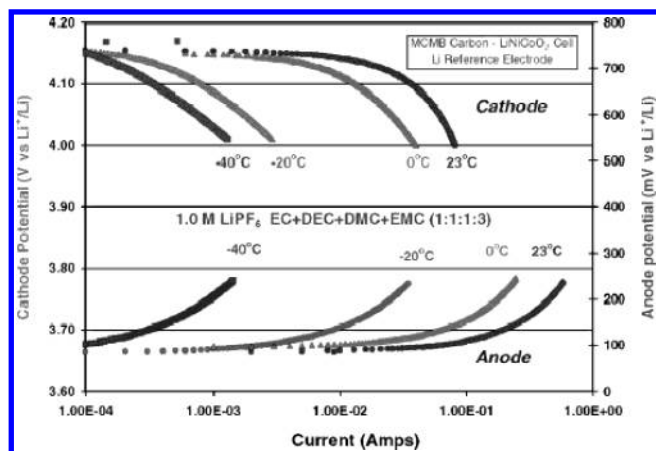
**Figure 71.** Tafel polarization measurement at different temperatures performed on MCMB and $LiNiCoO_2$ electrodes in 1.0 M $LiPF_6$/EC/DEC/DMC/EMC (1:1:1:3). (Reproduced with permission from ref 515 (Figure 8). Copyright 2003 Elsevier.)

of the full lithium ion cell actually mirrors that of the anode. This dominance of anode polarization becomes even more severe at low temperatures, and the logical conclusion should be that the kinetics at the graphitic anode are the rate-determining step.

In a more recent survey of the commercial lithium ion cells, Fan believed that the resistance of the cathode surface layer was the factor limiting the low-temperature performance of the cell chemistry.[507] Unlike the previous researchers who also believed that the cathode acted as the limiting factor,[462,506,512] Fan specifically excluded the role of $R_{ct}$ when he made the identification, and his major arguments were based on the summary and interpretation of the previously published data on lithium diffusion coefficients in both the cathode and anode and the fact that the surface area of the cathode is normally only a fraction of the anode. Without data from direct measurement, the above speculation seems to be premature; hence, further experimental confirmation is needed.

With the aim of gaining insight into the kinetics of lithium intercalation/deintercalation of both anodes and cathodes in novel low-temperature electrolytes, Smart et al. carried out the Tafel polarization experiments on MCMB and $LiNiCoO_2$ electrodes as a function of temperature in a three-electrode cell, and the results are summarized in Figure 71. In the temperature range from ambient to $-40$ °C, the limiting current densities observed on the anode remained higher than those observed on the cathode. In other words, under the condition of galvanostatic cycling at low temperatures, the cathode would be preferentially polarized and very likely serves as the bottleneck for the kinetics of lithium ion chemistry. As pointed out earlier, these polarization current densities reflect the resistances of both the surface film and charge-transfer on anodes and cathodes, respectively. Interestingly, the temperature-dependences established for the limiting current densities on anodes and cathodes showed that, as temperature decreases, the gap between the polarizations at anode/electrolyte and cathode/electrolyte interfaces rapidly closes (Figure 71), predicting a switch of rate-

determining step in the temperature ranges below $-40$ °C if other factors such as the precipitation of bulk electrolyte components do not intervene.

The EIS studies using symmetrical cells by Zhang et al. presented a third answer to the question about whether the cathode or the anode is the limiting factor.[512] They showed that the controlling factor for each electrode, $R_{ct}$, is comparable in magnitude at room temperature for a graphite as well as a $LiNiO_2$ electrode (Figure 68); and with decreasing temperatures down to $-20$ °C, these charge-transfer quantities also decline following a matching profile (Figure 69c). Therefore, merely on the basis of the impedance measurement, it would be difficult to tell which interface is rate-determining. Thus, the authors concluded that charge-transfer processes in both the anode and the cathode limit the capacity utilization at subambient temperatures.

### 8.4.2. High-Temperature Performance

Compared with the efforts spent on the low-temperature performance, less attention has been paid to the applications of lithium ion technology at elevated temperatures, with perhaps storage stability as the only exception. Cycling tests at temperatures above 50 °C have been rarely reported in the literature, most likely owing to the chemical instability of $LiPF_6$ in the organic solvents at elevated temperature and the difficulty of replacing it with new lithium salts.

Using the thermally stable salt LiBOB, Xu et al. showed that a full lithium ion cell can operate at temperatures up to 70 °C with limited capacity fading, while $LiPF_6$-based cells suffer obvious permanent capacity loss, as shown in Figure 72.[155,492] The authors believed that the chemical stability of BOB anion and the absence of reactive decomposition products such as HF and $PF_5$ confer upon the electrolyte stable performance at elevated temperatures. Liu et al. also reported the improved cycling performance of lithium ion cells based on the spinel cathode and LiBOB-containing electrolyte at elevated temperatures.[490] Since $Mn^{2+}$-dissolution caused by the HF from $LiPF_6$ has resulted in a severe capacity fading problem for spinel-based cathode materials, especially at elevated temperatures, the application of this promising cathode material has been prevented; therefore, the thermal and chemical stability of it in the presence of LiBOB might have special significance.

Another salt that is less sensitive to moisture than $LiPF_6$, $LiBF_4$, was also tested as an electrolyte solute intended for high-temperature applications. Zhang et al. reported that electrolytes based on this salt could allow the lithium ion cells to cycle at temperatures up to 70 °C.[132] Irreversible reactions occurred at temperatures above 80 °C, and the cells lost capacity rapidly, which was accompanied by the rise of cell impedance simultaneously.

As the structurally modified version of $LiPF_6$, LiFAP has also been reported to be less chemically sensitive due to the partial replacement of fluorine with the more stable perfluorinated alkyls.[496,497] Aurbach and co-workers investigated the stability of
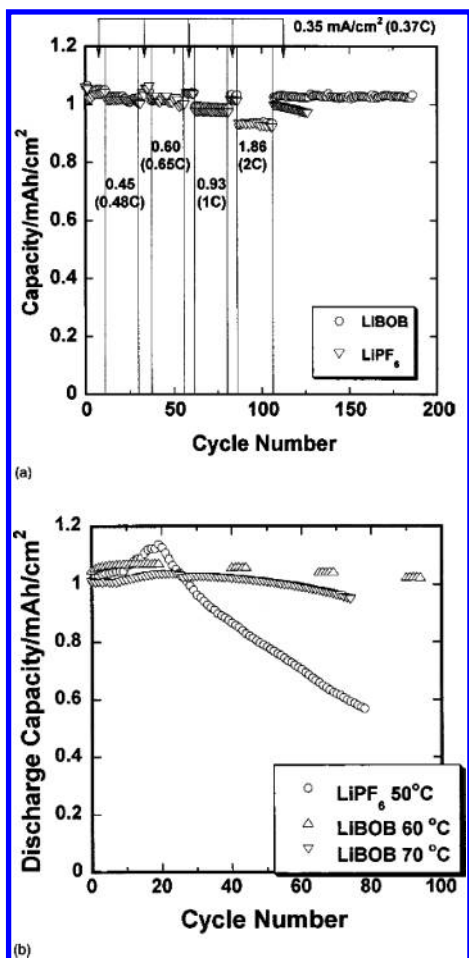
**Figure 72.** Capacity and capacity retention of the full lithium ion cells based on graphite as anode, $LiNiO_2$ as cathode, and $LiPF_6$ or LiBOB in EC/EMC as electrolytes: (a) room temperature; (b) elevated temperatures. (Reproduced with permission from ref 155 (Figure 5). Copyright 2002 The Electrochemical Society.)

the electrolytes based on this salt at elevated temperatures in anode half-cells.[499a] To ensure the complete formation of the SEI on the graphitic anode, all cells subjected to high-temperature testing were preconditioned by cycling at room temperature. As the inset of Figure 73 shows, the half-cell containing baseline electrolyte with $LiPF_6$ as salt suffers an immediate capacity loss at 60 °C, while the half-cells based on LiFAP solutions could be cycled at this temperature for 50 times before deterioration happened. Surprisingly, the most stable behavior was demonstrated by the electrolyte based on the mixed salt 0.50 M LiFAP/0.50 M $LiPF_6$, which not only delivered stable performance at 60 °C (Figure 73) but also showed higher capacity and lower fading rate even at 80 °C. As a rationale for the mixed salt effect, these authors in their more recent work proposed that some possible bulk reactions occurred between the two salts, one of which is the nucleophilic substitution of the fluorinated alkyl by $F^-$, forming new P−F bonds and $HCF_2CF_3$.[499b] Since the $FAP^-$ anion in this reaction actually serves as HF-scavenger, it should have a positive effect on both the performance of the Li−graphite electrodes and the thermal behavior of the solutions.
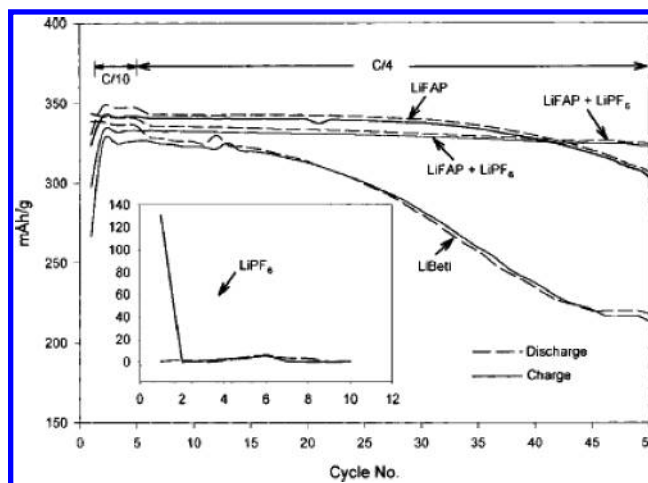


**Figure 73.** Cycling of graphite anode half-cells at 60 °C after extended cycling at room temperatures. 1.0 M LiFAP, 0.50 M LiFAP/0.50 M $LiPF_6$, and 1.0 M $LiPF_6$ (inset) in EC/DEC/DMC (2:1:2) were used as electrolytes. (Reproduced with permission from ref 499a (Figure 6). Copyright 2003 The Electrochemical Society.)

## 8.5. Electrolytes of Low Flammability

As diluents of low viscosity for the electrolyte solutions, the linear carbonates or esters were used at high concentrations along with EC, and their high flammability, as indicated by the low flash points (Tables 1 and 2), has imparted the state-of-the-art electrolyte systems with potential fire hazards in the situations of various types of accidents and abuses. Hence, these organic solvents serve as fuel for the various combustion processes, whether in open air when cells are ruptured and accidental sparks ignite their vapors[351] or under hermetic conditions where overcharge or overheating trigger thermal runaway.[340,341,360]

The efforts aiming to improve the thermal safety of electrolytes under these abuse conditions have intensified in recent years, partially driven by the more stringent safety requirements for large industry lithium ion cells intended for electric vehicle (EV) or hybrid electric vehicle (HEV) applications. Unlike consumer-size lithium ion cells with capacities below 2 A h, the battery packs for the above applications are usually based on individual cells of 10 A h or higher in capacity, and the dangerous combination of flammable solvents with the highly energetic electrodes in such scaled-up systems would be severely magnified by the amount of materials contained in the cell. For example, a recent test, which was designed as a close simulation of a car accident in real life, showed that violent fire and explosion ensued from the ignition of electrolyte vapors by an externally generated spark when a fully charged lithium ion cell vented.[519]

Since any compromise in cell energy density for the sake of safety would be undesired, most of the research efforts were concentrated on the reformulation of the electrolytes by using a flame-retarding additive or cosolvent, with the goal that its presence, kept at a minimum, could result in nonflammability or at least retarded flammability of the whole electrolyte system.
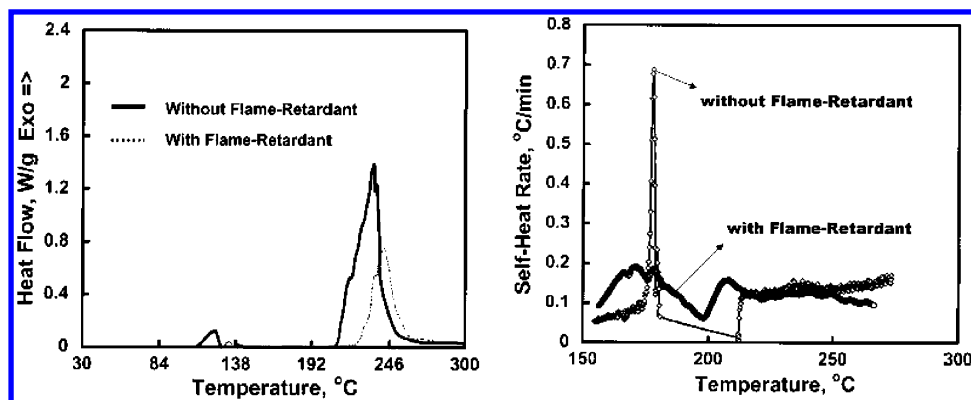
**Figure 74.** Improved thermal stability of an electrolyte by flame retardant HMPN: (a, left) DSC traces for baseline electrolyte with (1.68%) and without HMPN in the presence of a fully lithiated graphite anode (Reproduced with permission from ref 523 (Figure 5). Copyright 2000 The Electrochemical Society.); (b, right) SHR of baseline electrolyte with (10.0%) and without HMPN in the presence of metallic lithium. (Reproduced with permission from ref 523 (Figure 6). Copyright 2000 The Electrochemical Society.)

The early patent disclosures have claimed the application of a wide spectrum of gas-evolving ingredients and phosphorus-based organic molecules as flame retarding additives in the electrolytes.[520] Pyrocarbonates and phosphate esters were typical examples of such compounds. The former have a strong tendency to release $CO_2$, which hopefully could serve as both flame suppressant and SEI formation additive, while the latter represent the major candidates that have been well-known to the polymer material and fireproofing industries.[521,522] The electrochemical properties of these flame retardants in lithium ion environments were not described in these disclosures, but a close correlation was established between the low flammability and low reactivity toward metallic lithium electrodes for some of these compounds. Further research published later confirmed that any reduction of flammability almost always leads to an improvement in thermal stability on a graphitic anode or metal oxide cathode.
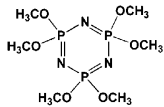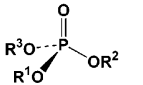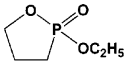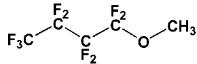
Prakash and co-workers described the first application of a flame retardant additive in an electrolyte solution that has been commonly used for lithium ion technology.[523] By using a substituted cyclic phosphorimide, hexamethoxycyclophosphazene (HMPN), at additive levels (<10%), they investigated the improvement in thermal stability of the baseline electrolyte $LiPF_6$/EC/DMC by means of DSC and ARC, respectively. As Figure 74a shows, the presence of HMPN at concentrations below 2% resulted in a dramatic reduction in the thermal reactivity of the electrolyte toward the fully lithiated graphite anode, as indicated by the much lower heat generation as well as the much delayed onset temperature of the major exothermic process. The improved stability was also found in the self-heating of the electrolyte under adiabatic conditions in the presence of metallic lithium, as Figure 74b shows. The maximum SHR of the baseline electrolyte at 178 °C was apparently triggered by the melting of lithium (mp 180 °C), which induced a high rate of self-heating at 0.68 °C min$^{-1}$, while the presence of 10% HMPN effectively suppressed this self-heating process, with a maximum SHR of 0.16 °C min$^{-1}$ at 170 °C. The authors attributed these improvements in thermal stability

to the nonflammability of HMPN with a mechanism of passivating the surface of lithium. Because of its small presence, HMPN does not show any negative impact on the electrochemical stabilities of the baseline electrolyte, as indicated by the cyclic voltammetry experiments as well as the preliminary cycling results in a cathode half-cell based on $LiNi_{0.8}Co_{0.2}O_2$.

Similar improvements in thermal stability were also made with a series of partially fluorinated esters by Yamaki et al.,[465] who used these fluorinated esters shown in Table 12 as the single solvents for electrolytes intended for the application of rechargeable metallic lithium cells. Compared with their nonfluorinated counterparts, the thermal stability of these electrolytes against both metallic lithium and $LiCoO_2$ cathode materials was significantly improved, and in both cases, the onset temperatures for the major exothermic reactions were postponed to above 300 °C. The authors believed that the higher stability of the fluorinated esters against metallic lithium was related to their chemical reactivity at room temperature with lithium, the reaction products of which coated the surface of lithium with a thick SEI film that delayed the reaction of the molten lithium at higher temperatures. On the other hand, since the intrinsic decomposition of $LiCoO_2$ cathode materials occurred at ~300 °C, the authors attributed the thermal event observed in the temperature range between 300 and 350 °C to the combination of the individual thermal decompositions of $LiCoO_2$ and electrolyte. The cycling efficiencies of metallic lithium in those fluorinated esters were also studied, based on which the authors proposed that rechargeable cells using metallic lithium as anode might be practical due to the stabilization effects of those solvents on both the lithium anode and $LiCoO_2$ cathode. No data were reported on the reduction behavior of those solvents on graphitic anodes; therefore, the application of these novel solvents in lithium ion cells remains to be investigated.

Following the pioneering work by Prakash and co-workers,[523] the researchers of the electrolytes for lithium ion cells started to concentrate their attention on the organophosphorus(V) compounds, and a number of publications since 2001 marked this renewed

**Table 14. Flame-Retarding Additives or Solvents**

| Solvent Structures | $T_m/$ °C | $T_b/$ °C | $\varepsilon$ (20 °C) | Remarks | Ref. |
|---|---|---|---|---|---|
| HMPN | 49 | > 250 | | Solid with m.p. at 49 °C; miscible with carbonates; improve thermal stability with graphite or Li (DSC, ARC) at additive level. | 523 526 |
| alkyl phosphates ($R^{1-3}=CH_3$) ($R^{1-3}=C_2H_5$) ($R^{1-3}=CF_3$) ($R^{1-2}=CF_3, R^3=CH_3$) ($R^1=CF_3, R^{2-3}=C_2H_5$) ($R^{1-3}=C_6H_5$) ($R^{1-3}=C_4H_9$) | -46 -56.4 -19.6 -22.5 | 197 215 178 203 210 | 20.7 13 10.5 12 15 | Viscous liquids; miscible with carbonates; render nonflammability at 20% if fluorinated; improve SEI stability on anode. | 524, 525 526~530 531 |
| EEP | | | | Used as additive with TMP; improves SEI stability on anode. | 532 |
| MFE | -135 | 60 | | Used with EMC as co-solvent; no flash point; improves thermal stability. | 534, 535 |

interest in nonflammability of electrolytes.[524−532] The overwhelming choice of these compounds has certainly originated from the in-depth knowledge about the combustion of organic materials accumulated in the polymer industry, where halogenated and organophosphorus compounds have been identified as the most effective flame retardants.[521,522,533] Traditionally, two major models have been proposed to explain the flame retardation achieved by these compounds: (1) char-formation, which builds up a thermal barrier between the condensed and gaseous phases, and (2) radical-scavenging, by which the chain reaction is inhibited in the gaseous phase due to the radical traps formed by the decomposition products of these additives.[533]

Wang et al. seemed to favor the second mechanism when the effectiveness of organophosphate in flame retardation was discussed in their work.[524] Using trimethyl phosphate (TMP, $R^{1-3} = CH_3$ in Table 14) as the flame retardant additive/cosolvent, they confirmed that when TMP content was higher than a certain threshold value, which depends on the flammability of the baseline solvents, the electrolyte could be rendered nonflammable. On the basis of the previous findings that the radical species containing phosphate have been detected in the MS, they proposed that such radicals act like a trap to scavenge the main active agent for flame propagation, H• radicals. To estimate the minimum amount ($N_{limit}$) of TMP needed in any binary electrolyte composition to achieve nonflammability, they even derived an empirical equation:

$$\log N_{limit} = 2.6 - 9.3 \left[ \frac{C_P T_H}{C_H T_P} \right] \quad (14)$$

The unitless quantity in eq 14, $C_P T_H / C_H T_P$, is the so-called "nonflammability index" defined by the authors using the atom content of H or P in the two electrolyte components and their boiling points, respectively. Qualitatively, this equation is of general significance in that the effectiveness of a certain flame retardant is proportional to the percentage of P in its molecule and inversely to its bp, while, for the baseline components, their flammability is proportional to their bp and inversely to the H content in their molecule. The lower flammability of the electrolyte formulated with TMP was also confirmed to yield higher thermal stability by calorimetry tests, in which the thermal reaction between $LiPF_6/EC/DEC$ and the $LiCoO_2$ cathode was apparently suppressed due to the presence of 20% TMP.

Unfortunately, TMP was found to be cathodically unstable on a graphitic anode surface, where, in a manner very similar to PC, it cointercalated into the graphene structure at 1.20 V and then decomposed to exfoliate the latter, although its anodic stability did not seem to be a problem. For this reason, TMP has to be used in amounts less than 10% with EC and other carbonates in high concentration in order to achieve decent performance in lithium ion cells. However, capacity fading caused by the increase of cell impedance cast doubt on the application of this flame retardant in a lithium ion cell.[524] To avoid the poor cathodic stability of TMP on graphitic anodes, the possibility of using it with other amorphous carbon electrodes was also explored by the authors.[525]

The above flame retardants, HMPN and TMP, along with another commercially available alkyl phosphate, triethyl phosphate (TEP), were systematically characterized by Xu et al.[526] To quantify the flammability of the electrolytes so that the effectiveness of these flame retardants could be compared on a more reliable basis, these authors modified a standard test UL 94 HB, intended for solid polymer samples, and measured the self-extinguishing time (SET) instead of the universally used flame propagation rate.[520a] Compared with the UL 94 HB, this new quantity is more appropriate for the evaluation of the electrolytes of low flammability, since the electrolytes that are determined to be "retarded" or "nonflammable" by this method all showed zero flame propaga-
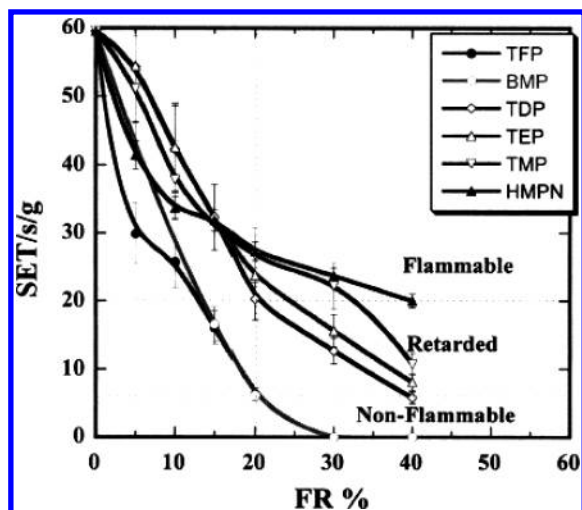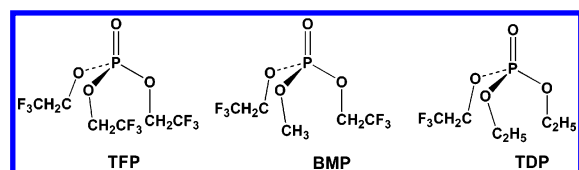
**Figure 75.** Flammability of the electrolytes containing various phosphorus-based flame retardants (FR). All electrolytes are composed of these flame retardants in 1.0 m LiPF$_6$/EC/EMC. (Reproduced with permission from ref 529 (Figure 1). Copyright 2003 The Electrochemical Society.)

gation rate. Since the SET thus obtained could be normalized against the amount of electrolytes, the reproducibility of flammability data was also improved, and comparison between these different flame retardants was made possible.

Figure 75 shows the dependence of the normalized SET on the concentration of different additives/cosolvents in a baseline electrolyte 1.0 M LiPF$_6$/EC/EMC (1:1). Apparently, the flammability decreases steadily with the concentration of TMP, TEP, and HMPN, but even in high concentrations, they fail to render the electrolytes completely nonflammable.

In their further work, Xu et al. combined the effects of the two different groups of flame retardants, halogens and phosphates, into one molecule in the hope that the integration would result in the improvement of flame retarding efficiency.[527−530] For this purpose, they synthesized a series of organophosphates with partially fluorinated alkyls, which included TFP, BMP, and TDP.



A brief summary of their physical properties is provided in Table 14. Their effects on the flammability of the baseline electrolyte are also compared in Figure 75. Apparently, the combination of fluorination with phosphate structure has brought the expected higher efficiency in suppressing burning. For example, with 20% TFP the electrolyte was rendered nonflammable.

While all these phosphate-based cosolvents were shown to be rather stable on various cathode materials, Xu et al. concentrated the evaluation effort on the reduction behavior of these flame retardants at the surface of graphitic anode materials. Figure 76 shows the results obtained with electrolytes containing high concentrations of TMP, TEP, and HMPN.
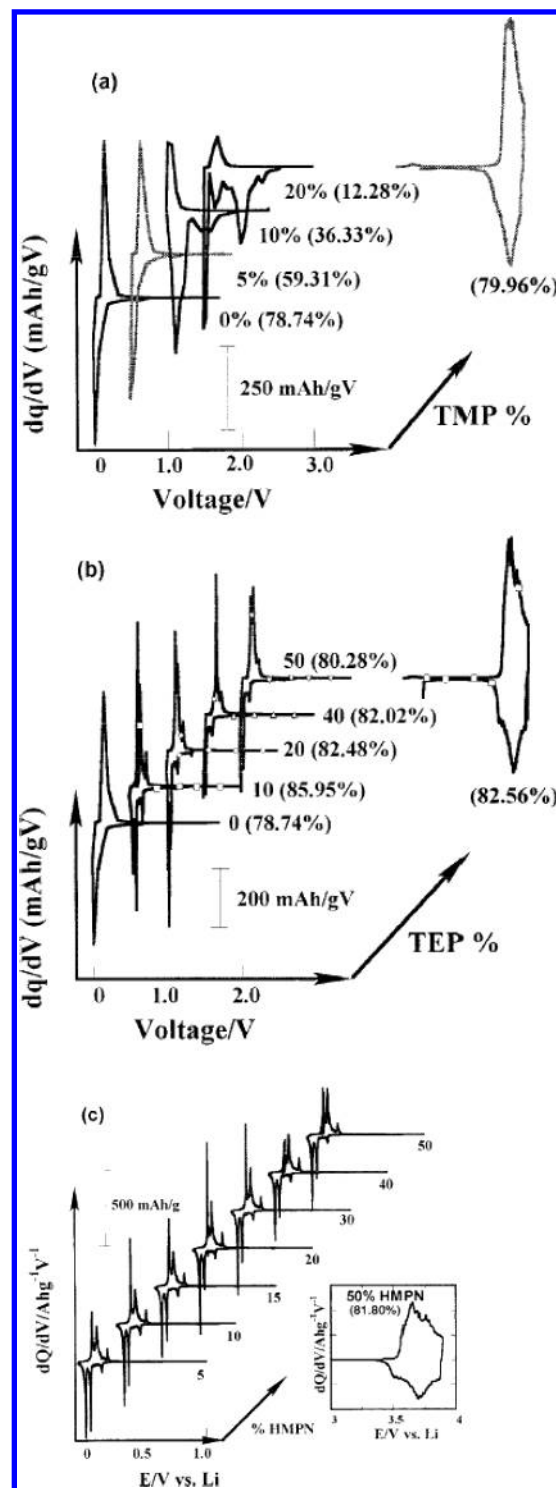


**Figure 76.** Cathodic stability on graphitic anode: Differential capacity vs voltage plots for anode and cathode half-cells containing different concentrations of (a) TMP, (b) TEP, and (c) HMPN. Only the first cycles are shown. Concentrations are indicated in the graph with the Coulombic efficiency for each cycle in the parentheses. (Reproduced with permission from ref 526 (Figure 2). Copyright 2002 The Electrochemical Society.)

While confirming the results reported by Wang et al. that TMP is cathodically instable, the authors also showed that longer alkyl substituents (as in TEP) improved cathodic stability, although, in long-term cycling or storage at elevated temperatures, the reductive decomposition of TEP still caused poor cell

performances. Among the three nonfluorinated co-solvents, HMPN was the only exception: its presence up to 40% did not have any negative impact on the cathodic stability of the electrolyte on the graphitic anode. Whether it also participated in the formation of the SEI remained to be investigated.

The fluorinated phosphates, on the other hand, showed generally improved cathodic stability, the extent of which seemed to be proportional to the content of fluorine in the molecule. The stability was further confirmed by the storage test of these electrolytes in a fully charged lithium ion cell at 60 °C. The cycling of the lithium ion cells with these electrolytes containing up to 40% TFP and BMP showed little difference from the baseline electrolyte at room temperature and at moderate drain rate, while the extended cycling up to 300 times delivered stable capacity with negligible fading. Like HMPN, these flame retardants also seemed to be involved in the formation of a more effective SEI on carbonaceous anode materials because higher concentrations of them always resulted in higher capacity retention in the extended cycle life tests.

However, as Figure 77 shows, the presence of TFP did render the lithium ion cells with lower rate capability, although reformulation of the baseline electrolyte with a higher content of the low viscosity solvent could alleviate the loss in rate performance. A similar trend was found with HMPN, which was more viscous than TFP. Studies on ion conductivity and EIS corresponded well with the above findings; that is, the resistances associated with the ion transport in both bulk electrolyte[528] and the electrode/electrolyte interfaces[530] increased with the presence of these flame retardants. In other words, even with the electrochemically stable TFP and HMPN, the improvement in low flammability has to be realized at the expense of cell performance because the flammability of a system is mainly a bulk property and the reduction of it requires the use of flame retardants in high concentrations. On the other hand, if the stringent standard of "nonflammability" set by Xu et al. is abandoned and thermal stability with respect to electrode materials as measured by DSC or ARC is adopted as the criterion, then these flame retardants could be used at much lower concentrations, that is, as additives instead of cosolvents. This difference has been shown by the work of Wang et al. and Xu et al.

While the consideration of nonflammability and SEI stability favors a high concentration of these organophosphorus compounds in electrolytes, the capacity utilization, rate capabilities, and low-temperature operation require that they be used at minimal concentrations. A compromise would be reached between 15 and 20% TFP or BMP in a binary 1.0 M LiPF₆ in EC/EMC (1:1) system or at higher than 30% in a ternary 1.0 M LiPF₆ in PC/EC/EMC (1:1:3) system. Such electrolytes are completely or at least nearly nonflammable. To further alleviate the above tradeoff, Xu et al. suggested that new cosolvents of higher flame retarding ability should be tailor-made.[530]
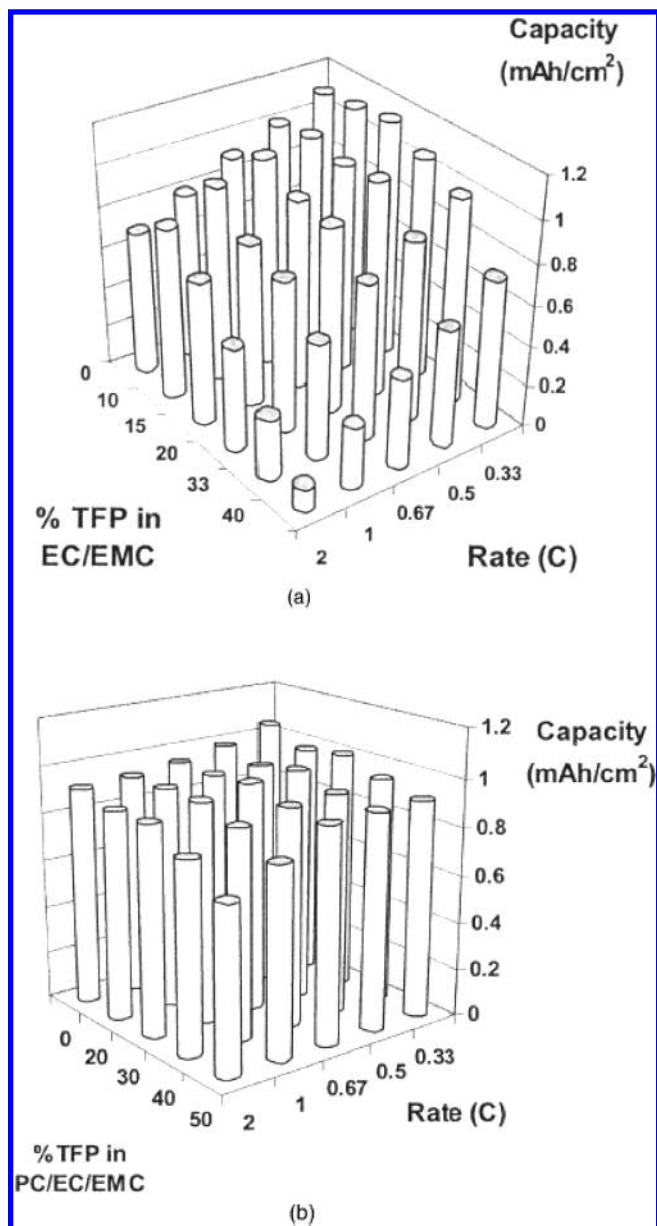


**Figure 77.** Effect of TFP concentration in different baseline electrolytes on the rate performance of the lithium ion cells: (a) 1.0 m LiPF₆/EC/EMC (1:1); (b) 1.0 m LiPF₆/ PC/EC/EMC (3:3:4). (Reproduced with permission from ref 530 (Figure 5). Copyright 2003 The Electrochemical Society.)

Amine and co-workers reported similar organophosphates with larger alkyl (TBP) or aromatic (TPP) substituents, as Table 14 shows.[531] They adopted an improved UL 94 vertical burning technique to evaluate the efficiency of these flame retardants in the baseline 1.0 M LiPF₆/EC/DEC (1:1) and tried to correlate the flammability of the resultant electrolytes with their thermal stability against a lithiated graphite anode under adiabatic conditions. They found that the flame propagation rate was significantly reduced even with only 1% TPP, while the optimum content of it was 5%. The exothermic reactions of the electrolytes with the fully lithiated graphite were effectively suppressed, as indicated by the lower SHR, lower heat generation, and higher onset temperature, similar to the observations of Prakash et al. and Wang et al. These authors

believed that the char-formation mechanism was responsible for the delayed thermal decomposition.

Like all the phosphates investigated as cosolvents, TBP and TPP showed higher anodic stability, as confirmed by their cycling in lithium ion cells based on a $LiNi_{0.8}Co_{0.2}O_2$ cathode up to 4.2 V, and separate cyclic voltammetry tests also showed that they would not decompose anodically below 5.0 V on an inert working electrode. Little capacity fading was detected during the extended tests of TPP or TBP in full lithium ion cells up to 150 cycles.

In view of the poor cathodic stability of TMP on a graphitic anode, Ota et al. recently described a cyclic phosphate ethylene ethyl phosphate (EEP) (Table 14) to be used with TMP as the additive for the modification of the SEI.[532] They found that 5% EEP could render the electrolyte 1.0 M $LiPF_6$/EC/DEC/TMP (6: 2:2) stable on the graphite surface down to low potentials and support the reversible intercalation/deintercalation of lithium ions, while the electrolyte 1.0 M $LiPF_6$/EC/DEC/TMP (6:2:2) without EEP steadily decomposed at 0.40 V in a manner similar to that for PC. The decomposition plateau at a much lower potential as compared with the case of neat TMP solution, as reported by Wang et al.,[524] should be attributed to the high EC content used by Ota et al. in their electrolyte composition. The evidence from XPS and FT-IR seemed to confirm that EEP was directly involved in the formation of the SEI, as both spectra detected the signature stretching of P−O bonds that did not exist in EEP-free electrolyte. The authors suggested that EEP underwent a ring-opening decomposition while participating in the surface chemistry on the graphite surface during charge. In temperature-programmed decomposition mass spectra (TPD-MS), such an SEI was shown to be more thermally stable even than the SEI formed by the baseline electrolyte 1.0 M $LiPF_6$/EC/DEC (1: 1): the former decomposes at 125 °C and the latter at 110 °C. The authors summarized that EEP should be a promising additive for lithium ion electrolyte because it showed the simultaneous merits of being flame retardant and an SEI modifier.

Another non-phosphorus cosolvent was recently described as the bulk component for a nonflammable electrolyte by Arai, who used a partially fluorinated ether, methyl nonafluorobutyl ether (MFE), to form a binary mixture solvent with the linear carbonate EMC and reported the complete elimination of the flash point of the electrolyte thus-based (Table 14).[534,535] The 18650 lithium ion cells using graphite/ $LiCoO_2$ and 1.0 M LiBeti/MFE/EMC (8:2) delivered the same capacity at low drain rates (0.1 C) as the baseline electrolyte 1.0 M $LiPF_6$/EC/EMC (3:7) but showed no thermal runaway under the abusive conditions of nail-penetration of an overcharged cell; however, the rate capability of this nonflammable electrolyte is very low. Galvanostatic and EIS studies on the corresponding cathode and anode half-cells identified that the highly resistive anode/electrolyte interface was the source for this problem. With 0.5 M EC and 0.1 M $LiPF_6$ salt as additives in the MFE-based bulk electrolyte, the polarization was significantly reduced, as shown in Figure 78. The presence
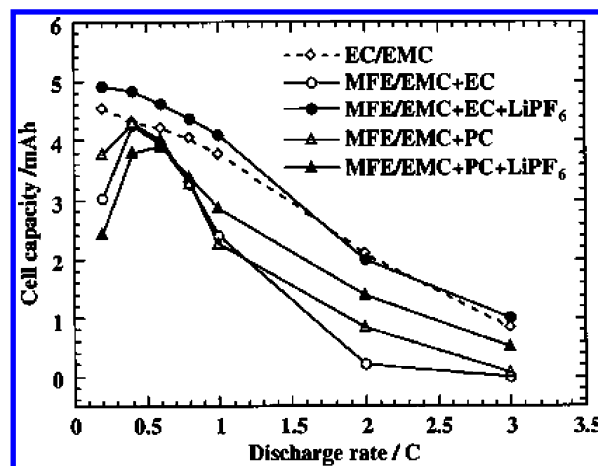


**Figure 78.** Rate capability of graphite/$LiCoO_2$ lithium ion cells using nonflammable MFE-based electrolytes and EC/EMC baseline. (Reproduced with permission from ref 534 (Figure 6). Copyright 2003 The Electrochemical Society.)

of EC and $LiPF_6$ led to the significant reductions in not only $R_{ct}$ but also $R_{SEI}$, while XPS and FT-IR confirmed that an increase in the amount of lithium alkyl carbonate was simultaneously observed on the graphite surface. In other words, the newly formulated nonflammable electrolyte based on MFE remained dependent on the use of EC and $LiPF_6$. This probably showed from another angle why EC and $LiPF_6$ are indispensable components in the state-of-the-art electrolytes.

One surprise in Arai's results is perhaps the anodic stability of the ether-based solvent MFE, which remained stable anodically at up to 4.2 V on the $LiCoO_2$ surface. Considering the numerous previous reports that the ether linkage is oxidatively decomposed near 4.0 V,[74,75,78,93] one might attribute this additional stability of MFE to the fluorination of the molecule.

The MFE-based nonflammable electrolyte was also tested in lithium ion cells using a spinel cathode.[535] The effects of EC and $LiPF_6$ seemed to be distinguished: while the presence of EC improved the rate capability of these lithium ion cells, longer cycle life with higher capacity retention could only be achieved by further addition of $LiPF_6$. On the basis of the above results, the authors believed that MFE-based bulk electrolyte provided a better baseline in terms of safety and nonflammability, although further optimization should be carried out on this new baseline.

## 8.6. Polymer and Polymer Gel Electrolytes

Polymer electrolytes intended for applications in lithium-based cells could be roughly divided into two major classifications: (1) those based on neat high polymers, which serve as both solvent to dissolve lithium salts and mechanical matrix to support processability,[536−540] and (2) those based on polymers gelled by conventional electrolyte solutions, wherein the small organic molecules serve as the major solvents, while the low percentage of high polymer, fully swollen by these solvents, acts only to provide dimensional stability.[541,542] In recent literature the former is usually referred to as solid polymer elec-

trolytes (SPEs), and the latter as gel polymer electrolytes (GPEs). Due to the poor ion conductivities, SPEs remain materials of mere academic interest, with only remote prospects for their applications. On the other hand, GPEs have shown much higher feasibility, and second generation lithium ion cells from the major manufacturers have incorporated these novel electrolytes. Apparently the proximity of GPEs to the conventional nonaqueous electrolytic solutions, in physical chemistry and electrochemistry, is the main reason.

The current section does not intend to comprehensively review SPE and GPE materials, as the preceding sections do to liquid electrolytes, mainly because of the fact that a number of recent reviews have covered this field thoroughly,[41–48,536–542] the latest of which was published in 2003,[48b] and also the fact that the most promising systems, that is, GPEs, are similar in many ways to the conventional liquid electrolytes, including their electrochemical stabilities on various electrodes and the corresponding interfacial chemistries. Rather, a more general overview will be given on both systems with little detailed discussion on any individual electrolyte, although exceptions apply to a few selected systems that are of special significance.

### 8.6.1. Solid Polymer Electrolyte

While Wright and co-workers were the first group of researchers to discover that the ether-based polymer poly(ethylene oxide) (PEO) was able to dissolve inorganic salts and exhibit ion conduction at room temperature,[543] it was the suggestion from Armand et al. that placed these novel materials at the center stage of lithium electrolyte research for more than a decade.[544] The number of comprehensive reviews on this subject could serve as an indicator of the general enthusiasm for these materials during the period.[41,47,536–542]

At the time, the targeted device was the rechargeable cell using a metallic lithium anode, and the worldwide interest was mainly stimulated by the following projected advantages that these polymer electrolytes could potentially offer when compared to their liquid counterparts: (1) excellent processability and flexibility that could enable the fabrication of ultrathin lithium cells of various geometric shapes so that high energy and power density could be achieved for versatile applications, (2) higher safety due to the absence of flammable organic solvents and the much lower reactivity of macromolecules toward lithium, (3) the possible prevention of the growth of lithium dendrite crystals upon cycling, and (4) the high dimensional stability that could lead to the elimination of a separator, so further improvement in both energy density and manufacturing cost could be achieved due to the simplified cell configuration and enhanced packing efficiency.

Despite the initial misinterpretation in the ion conduction mechanism, it was soon realized that the ion conduction in PEO and other similar polyether-based media mainly occurred in the amorphous phases. Increasing evidences were obtained that ionic motion in these polymer ion conductors was closely

**Scheme 30. Schematic Illustration of Lithium Ion Transport in Polyether Media (Redrawn from Ref 536)**
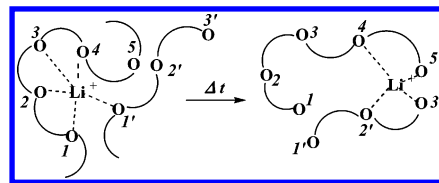


associated with certain local structural relaxations related to the glass transition of the polymer.[538] A generally accepted model described a microscopic sequence in which lithium ions were coordinated by the ether oxygen atoms on the segments of a polymeric chain in a similar way to their complexation by crown ethers or other oligoether-based solvents. A continuous segmental rearrangement accompanied by the gradual replacement of the ligands in the solvation sheath of lithium ions, hence, resulted in the long-range net displacement of lithium ions, as Scheme 30 shows.[539] Thus, these polymer-salt complexes may exhibit mechanical properties which are similar in most ways to those of true solids due to chain entanglement of the polymer host, while the microscopic environment that a lithium ion sees remains liquidlike and the ion conductivity is "coupled" to the local segmental motion of the polymer. The latter property is often characterized by the glass transition temperature ($T_g$) of the polymer, which to a great extent determines the mechanical strength and hence processability of a polymer material.

The above coupling between ion transport and mechanical properties has created a perpetual dilemma concerning the prospect of using these polymer ion conductors, since the efforts to improve their ion conductivities—typically between 0.01 and 0.001 mS cm$^{-1}$ at room temperatures and far short of supporting normal operation in lithium (ion) cells—were always met by sacrificing dimensional stability. Various new host polymers with low $T_g$ were investigated, which included the more flexible polypropylene oxide (PPO) hosts that remain completely amorphous at room temperatures, the siloxane- or phosphazene-based polymers whose low $T_g$ renders the polymer host more flexible and facilitates faster ion conduction, the comb-type polyethers in which ether linkages are attached as side-chains to the backbone so that more flexible segmental motion is possible, the polymer composite electrolytes that have incorporated inorganic additives to eliminate the crystallinity of polyether segments, and so forth. However, almost always before the ion conductivities reach the coveted goal of the "liquidlike" level (i.e., >1.0 mS cm$^{-1}$), the mechanical strength of these polymers approaches "liquidlike" state, thus conflicting with the fundamental reason polymer electrolytes are desired. The introduction of chemical cross-linking or the preparation of various interpenetrating networks (IPNs) indeed improves the dimensional stability of polymer electrolytes, but the ion conductivity swings back to levels < 0.01 mS cm$^{-1}$.

During the two decades following the initial proposal by Armand, essentially little progress was made concerning the actual application of SPEs, where the

poor ion conduction exists as a seemingly insurmountable barrier. Due to the low level ion conductivity, little has been known about the electrochemical stability of these polymer electrolytes on various intercalation-type electrode materials, and even less about their cycling in actual lithium and lithium ion cells. On the basis of a general survey of the most solid polymer electrolyte systems developed so far, an upper limit in ambient-temperature ion conductivity seems to exist at 0.1 mS cm$^{-1}$ for any polymer host whose mechanical strength could afford the formation of a free-standing film.[538–541] Applications at high temperature seem to be a solution to the poor ion conductivities, but a high rate of degradation often deters the efforts, as indicated by the fading capacities of such cells.

Various attempts have been made to break the coupling of ion transport from the polymeric segmental relaxation. Combining the projected merits of SPEs and superionic glass electrolytes that have been the subject of intensive study in solid-state ionics since the late 1970s, Angell and co-workers proposed an innovative approach of "polymer-in-salt" to bypass the poor ion conductivity of the "salt-in-polymer" SPEs.[545] In the proposed "ionic rubber", a polymer material of high molecular weight is used only at additive levels as a sheer provider of mechanical strength and filming processability, whereas the bulk of the electrolytes consist of the highly conductive ionic liquid. Ideally, these materials should have a $T_g$ low enough to remain rubbery at room temperature while preserving the lithium ion conductivities similar to those of the typical ionic liquid systems because most of the ions would be free of coordination with polymer segments due to the small presence of the latter. Unfortunately, although the initial results with simple lithium salts confirmed the conceptual feasibility of the approach, exceeding difficulties were encountered in the attempts to formulate a practical system, which should be based on an ionic liquid or such mixtures that not only have low melting and glass-transition temperatures but also are inert to the polymer additives at these temperatures as well as retain electrochemical stability in a wide potential range.[546,547]

More recently, Ingram et al.[548] and Wright et al.[549] independently tried to develop new polymer hosts with secondary structures similar to that of a liquid crystalline state, so that ion transport could occur with a higher degree of freedom in the highly oriented environments and become at least partially decoupled from the polymer segmental relaxations. Ion conductivities approaching "liquidlike" values have been obtained on the condition that the liquid crystalline state could be maintained.[549] However, the incorporation of these novel polymer materials in electrochemical devices remains to be tested.

On the other hand, ion conductivity is not the only obstacle that prevents the application of SPEs. In 1994, Anderman published a review highly critical of the prospects for the application of SPEs in electrochemical devices, in which he questioned almost all of the previously projected advantages from the viewpoint of cell design and engineering.[550]

He argued that (1) the flexibility that a polymer electrolyte could offer presents no true advantage to cell design, since the current cell components (i.e., electrodes coated on substrates and a separator based on polyolefin films) already possess sufficient flexibility, and limitations on the geometric shapes of lithium cells do not come from the rigidity of electrolytes but rather from the terminals/connectors as well as economical considerations; (2) the low reactivity of a polymer toward an electrode would very likely be counteracted by the micrometer thickness of such polymer materials, since the chances of an internal short increase significantly (the necessity for thin films arises from the poor ion conductivities of such electrolyte materials and the need to provide sufficient ion flux for the normal cell operation); (3) the safety of polymer electrolyte-based cells would be further challenged by technical difficulties, since it would be almost impossible to manufacture a polymer film of micrometer thickness in large scale and pinhole free; and (4) there would be hardly any improvement in the tolerance against mechanical abuse for the polymer electrolytes, since they do not offer superior mechanical strength to that of the presently used polyolefin separators.

In addition to the criticisms from Anderman, a further challenge to the application of SPEs comes from their interfacial contact with the electrode materials, which presents a far more severe problem to the ion transport than the bulk ion conduction does. In liquid electrolytes, the electrodes are well wetted and soaked, so that the electrode/electrolyte interface is well extended into the porosity structure of the electrode; hence, the ion path is little affected by the tortuosity of the electrode materials. However, the solid nature of the polymer would make it impossible to fill these voids with SPEs that would have been accessible to the liquid electrolytes, even if the polymer film is cast on the electrode surface from a solution. Hence, the actual area of the interface could be close to the geometric area of the electrode, that is, only a fraction of the actual surface area. The high interfacial impedance frequently encountered in the electrochemical characterization of SPEs should originate at least partially from this reduced surface contact between electrode and electrolyte. Since the porous structure is present in both electrodes in a lithium ion cell, the effect of interfacial impedances associated with SPEs would become more pronounced as compared with the case of lithium cells in which only the cathode material is porous.

Even after all the above issues, that is, mechanical strength, ion conductivity, and interfacial resistance, have been resolved, SPEs still have to face the crucial issue of surface chemistry on each electrode if the application is intended for lithium ion technology, and there is no reason to be optimistic about their prospects.

Despite the wide variety of polymer hosts that have been synthesized and tested, the fundamental chemical structures adopted for SPEs remain strictly ether-based and are variations of the original oligo(ethylene oxide) structure, primarily due to the fact that no

other chemical linkages are able to possess sufficient solvation power for inorganic salts while remaining amorphous and flexible at room temperature. The inability of ether-based solvents, such as DME and DEE, to form an effective SEI on carbonaceous anodes has been reported in numerous reports, where porous and highly resistive SEIs originating from these solvents have been described. Moreover, the anodic stability of these ethers on cathode materials does not offer relief, since their oxidative decomposition potentials have been reported to be well below 4.0 V, which falls in the reversible lithiation/delithiation range for most of the metal oxide cathode materials and far below the oxidation limits of $\sim$5.5 V set by carbonate-based solvents. Although the reduction in the reactivity of ether linkages could be expected because of the giant molecular size of the polymer solvent, the long-term stability of such polyether materials sandwiched between a graphite anode and a metal oxide cathode does raise concern. This concern is indirectly supported by the fact that, among the few rare publications wherein the cycling behavior of SPEs was tested under either galvanostatic or voltammertic conditions, decent cycle life was obtained only when low-potential cathodes such as $V_2O_5$, $TiS_2$, or polymeric electroactive materials were used, while the industry standard $LiCoO_2$ or other 4.0 V class cathode materials always rendered poor cycling performances.

In a brief summary, although the studies on SPEs remain of academic interest in the areas of materials science and solid state ionics, their immediate application in any commercial electrochemical devices, especially in the state-of-the-art lithium ion industry, seems to be remote. Considering the multilateral challenges that SPE materials are facing, any isolated breakthrough in an individual property might not be sufficient to justify replacement of the current electrolytes used in lithium ion cells. However, it must be cautioned that the above judgment is strictly based on the *status quo* of lithium ion technology, which could change with the improvement of electrode materials. Hence, one should not draw premature conclusions about the fate of SPEs because, after all, science development is full of unexpected. Recent advances made by Scrosati and co-workers have shed a light of hope on the SPE applications in lithium/lithium ion cells intended for elevated-temperature environments, where the disadvantage of low ion conductivity could be avoided.[501,551−555]

### 8.6.2. Gel Polymer Electrolyte

Compared with SPEs, GPEs are much closer to actual applications because they inherited the major properties from the bulk liquid electrolytes, including ion conduction, electrochemical stability on both carbonaceous anode and various metal oxide cathode materials, safety, and tolerance against mechanical and electric abuses. Moreover, since the polymer at additive levels only serves as the skeleton providing dimensional integrity, the ether linkage is no longer the sole choice of building block for its chemical structure, thus eliminating potential concerns over the electrochemical stability that might arise from the oxidative or reductive degradations of polymer segments in a lithium or lithium ion cell environment. Certainly, the concomitant consequence of the low polymer presence in GPEs is the poorer mechanical strength as compared with the cases of the pure SPEs, and either chemical or physical cross-linking is frequently necessary for the dimensional stability of such gel materials.

The recent advances of GPE materials have been exhaustively covered in two general review articles up to 2000.[541,542] Especially in the review by Song et al., a rather systematical coverage was given on the most popular GPE systems that were based on PEO, poly(acrylonitrile) (PAN), poly(methyl methacrylate) (PMMA), and poly(vinylidene fluoride) (PVdF), along with an excellent discussion of the fundamental aspects concerning the formation, morphological structure, and physical stability of GPE.[541] Because of the wide variety of polymer and copolymer hosts available in the market, the number of new GPE systems reported in the literature is ever increasing, especially in recent years, while the bulk electrolyte compositions and hence the fundamental electrochemistry associated remain relatively constant. It is not the objective of the current section to review those individual systems in detail.

On the application front, GPE technology has been used by most of the major manufacturers of lithium ion cells following the third generation lithium ion cells of Sony, and an energy density of 180 W h K g$^{-1}$ was reported.[2] The specific polymer hosts used in commercial lithium ion cells were seldom reported in the open literature for obvious reasons. It should be mentioned here that, in marketing terms, these cells are often confusingly referred to as "polymer lithium ion cells", giving the wrong impression that solvent-free SPEs are in use.

The only commercial GPE cell that had been described in the open literature was perhaps the Bellcore/Telcordia technology based on a fluorinated polymer, PVdF, from which one could readily sense that the key factor controlling the success of certain polymer hosts in lithium ion cells is no longer material chemistry only, and that more often than not the processing and fabrication of the GPE plays the decisive role.[556]

As pointed out by Song et al.,[541] the significance of the Bellcore technology rested with its technical innovation rather than scientific discovery because PVdF-based polymers as a host for GPE had been investigated by Feuillade et al.[557] and Tsuchida et al.[558,559] as early as two decades ago. However, what distinguished Bellcore technology not only from those early studies but more generally from all of the previous research in polymer electrolytes was that the traditional approach of preparing a homogeneous GPE film was abandoned and replaced by a two-step process, in which PVdF−hexafluoropropylene (HFP) copolymer was first processed into a microporous film that could be assembled with cathode and anode films in an ambient atmosphere, and then the whole cell assembly could be activated by liquid electrolytes in a similar manner, where the traditional polyolefin separator was wetted by liquid electrolyte. After

activation, the liquid electrolyte swells the originally microporous film and eventually forms a GPE. Since the only step that must be conducted in a moisture-controlled environment is the electrolyte injection, the advantages of this technology in terms of manufacturing cost and operational ease are apparent.

Perhaps more important than cost is the solution to the crucial problem of interfacial contacts that always plagues homogeneous GPE films prepared from traditional approaches. Since both cathode and anode composite materials are coated on their substrates with the same PVdF−HFP copolymer as the binder, the "in situ gellification" following the electrolyte activation effectively fuses the three cell components into an integrated multilayer wafer without physical boundaries, so that the interfaces between anode and electrolyte or cathode and electrolyte are well extended into the porous structures of these electrodes, with close similarity to the interfaces that a liquid electrolyte would access.

Another important merit of the "in situ gellification", rarely mentioned by various authors in the literature, is that the limitation on electrolyte composition can be relaxed. In the traditional process of making a GPE, the liquid electrolyte has to be heated with the polymer host to form the gel, during which the thermal instability of the lithium salt (LiPF$_6$ or LiBF$_4$) and the volatility of the solvents (DMC, EMC, etc) could possibly cause the resultant GPE to deviate from the desired composition or even to degrade. It is for this reason that in most of the literature on GPE the liquid electrolytes have to be based on LiIm, LiBeti as salts, and EC/PC as solvents. In Bellcore technology, on the contrary, the state-of-the-art electrolytes, the typical of which is LiPF$_6$/EC/DMC, could be used, since gellification occurs only after the cells are assembled.[556]

According to Tarascon and co-workers, the swelling of PVdF−HFP by liquid electrolytes was never complete due to the semicrystalline nature of the copolymer, which tends to microphase-separate after the activation by electrolyte. On the other hand, it is those crystalline domains in the gelled PVdF−HFP that provide mechanical integrity for the resultant GPE.[556] Thus, a dual phase structure was proposed for the Bellcore GPE by some authors, wherein the amorphous domain swollen by a liquid electrolyte serves as the ion conduction phase, while tiny crystallites act as dimensional stabilizer.

Apparently, the formation of the microporous structure within the PVdF−HFP copolymer was of critical importance to the success of Bellcore technology, and the ion conductivity was proportional to the uptake of the liquid electrolyte. To achieve the desired porosity of PVdF film, Bellcore researchers prepared the initial polymer blend of PVdF with a plasticizer dibutylphthalate (DBP), which was then extracted by low boiling solvents after film formation. Thus, a pore-memory would be left by the voids that were previously occupied by DBP. However, due to the incomplete dissolution of such high-melting DBP during the extraction process, the pore-memory could never be restored at 100% efficiency.[556,559] Beside the total volume of pores thus created by the plasticizer,
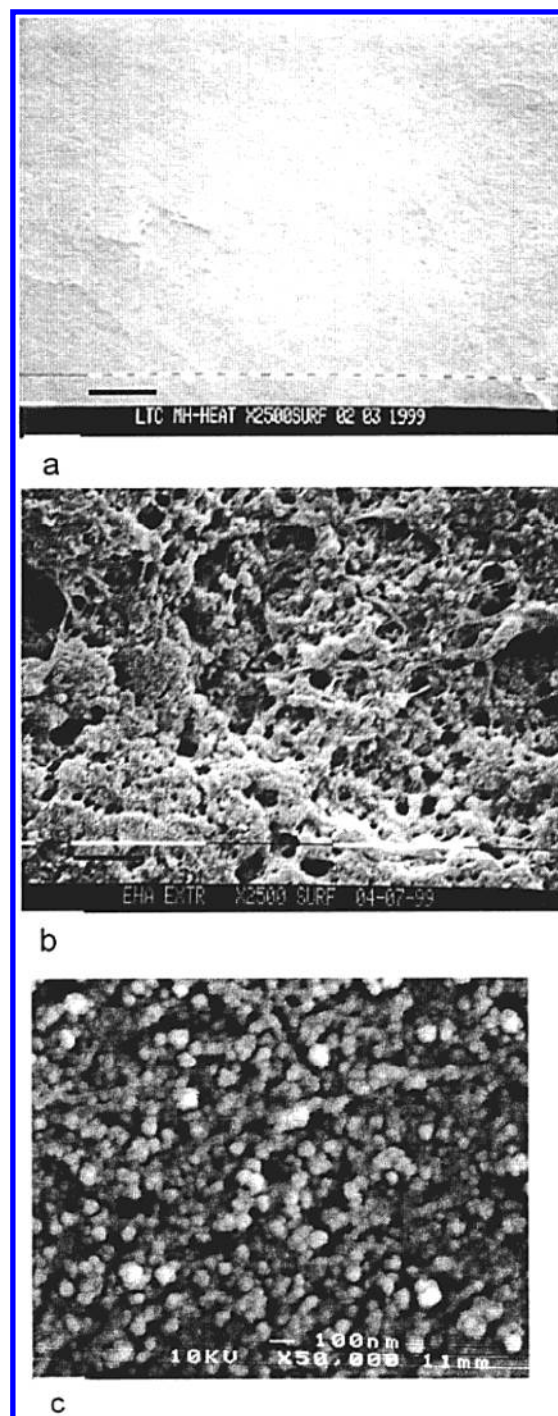


**Figure 79.** SEM of methanol-extracted separators prepared in the weight ratio of plasticizer/PVdF-HFP/SiO$_2$ of 5:3:2. The extracted plasticizer in parts a and c is DBP, and that in part b is an oligomer with molecular weight 450. Note that the scale in parts a and b is 5.0 $\mu$m and that in part c is 100 nm. (Reproduced with permission from ref 561 (Figure 2). Copyright 2000 The Electrochemical Society.)

the distribution of pore sizes, their interconnectivity, and the affinity of the inner wall of pores toward liquid electrolytes would all influence the final uptake of electrolytes.[560,561]

Improvements based on Bellcore technology were reported recently by Wunder and co-workers.[561,562] Using PEO oligomers instead of DBP, they obtained the PVdF−HFP microporous films with the pore size increased from nanoscale to microscale, as shown in

**Figure 80.** Cycle life of 2 A h cells (A and B) and a 25 A h cell (C) at 100% depth-of-charge at ambient temperature. (Reproduced with permission from ref 563 (Figure 7). Copyright 2001 Elsevier.)

Figure 79. As a result, the ion conductivity rose by ~70% from 0.2 mS cm$^{-1}$ of DBP-extracted GPE to 1.2 mS cm$^{-1}$ of the oligomer-extracted counterpart. The cycling tests in a lithium ion cell based on MCMB/LiCoO$_2$ showed an improvement in capacity b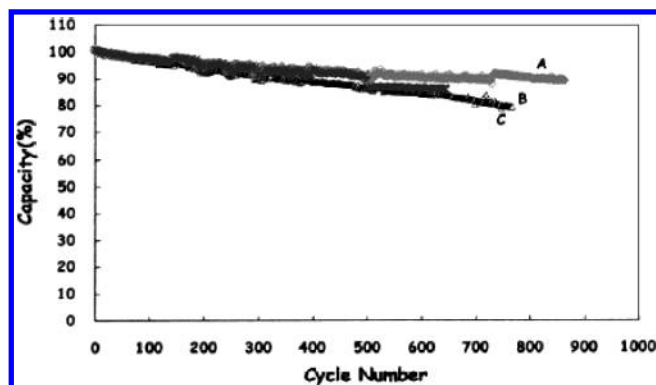y 40% and in rate capability by 70%. In their further work, Wunder and co-workers used polystyrene (PS) to form a blend with PVdF−HFP copolymer, which, via a "phase-inversion" technique, yielded a microporous film that could possess an ion conductivity as high as 4.0 mS cm$^{-1}$.[562] Characterization using various analytic means led the authors to conclude that the presence of PS increases pore volume, wherein the liquid electrolyte forms a highly conductive path, while the swollen PVdF−HFP region is relatively resistive, corresponding to the low ion conductivities found in the GPE based on homogeneous PVdF by previous investigators.[557−559] At this stage, the demarcation between GPE and the traditional microporous separators based on polyolefin materials becomes quite ambiguous.

The Bellcore GPE technology, bearing the brand name of "plastic lithium ion cells" or "PLion cells", has been licensed worldwide to various battery manufacturers, and a recent report by Han et al. described the adaptation of it to large lithium ion cells designed as traction power in electric vehicle applications.[563] Figure 80 shows the cycle life of such cells at room temperatures, while tests of an improved 28 A h cell carried out between 60 and −20 °C yielded 95% and 60% of the rated capacity, respectively. These cells also passed all the safety tests, including external short circuit, high current charge, impact, nail-penetration, and heating, with the exception of overcharge, where the cells became swollen and burst into flames between 105% and 150% of overcharged capacities. Since there is always a concern over the stability of the C−F bond in PVdF polymers with respect to the fully lithiated carbonaceous anode,[338] there is doubt once again about the appropriateness of fluorinated polymers as GPE hosts for lithium-based cell applications. However, it should be kept in mind that the lithium ion cells based on liquid electrolytes behave similarly under the same abusive conditions. A more likely situation is that the reaction of the fluorinated polymers with carbonaceous anodes occurs at much higher temper-

atures so that it is not responsible for the thermal runaway induced by overcharge. According to the investigations by Maleki et al.[360,361] and Dahn et al.,[369−371] cathode/electrolyte interaction, instead of anode/electrolyte interaction, should be the main source of the hazard to safe operation.

## 9. Concluding Remarks

The traditional role of electrolytes in batteries is of less consequence than the electrode materials. While the recent understandings about electrolytes in lithium-based rechargeable cells revealed that the chemical composition of electrolytes profoundly affects the cell performance in many aspects—from lithium cycling efficiency to rate capability, and from capacity retention at various temperatures to tolerance against abuses—the fact remains that the choice of electrolyte components is dictated by the electrode materials in use. Thus, the current state-of-the-art electrolyte systems in lithium ion cells are tailor-made for the specific cell chemistry in which the various electrolyte components yield ad hoc surface chemistries on metal oxide cathodes and especially on graphitic anodes. Radical change in electrolyte composition is not expected to be likely, as long as the cell chemistry remains the reversible shuttling of lithium ions between those metal oxides and graphitic carbons, but innovations will continue to be carried out concerning the rate performance, temperature range of service, safety of scaled-up cells, and "solidification" of the electrolyte.

On the other hand, the emergence of new cell chemistries would call for reformulation of the electrolytes, as has always been the case during the history of lithium battery development. There have been numerous such efforts in seeking more energetic or safer cathode materials, which include the novel 5.0 V class mixed metal oxides and the more recent olivine iron phosphate family, while metallic lithium remains a main attraction as a potential anode considering its tremendous energy density. In the latter case, electrolyte reformulation has been used as a main factor in controlling the undesired formation of dendritic lithium during the long-term cyclings, an example of which is the work of Aurbach et al., who found ad hoc surface chemistry on metallic lithium provided by an ether-based electrolyte similar to that of a carbonaceous anode.[14,18] Polymer-based electrolytes are also expected to be effective in regulating the surface morphology of metallic lithium. Upon the successful solution of the safety issue of the lithium electrode, the revival of the lithium cell is a possibility, along with new electrolyte formulations that cater to the new cell chemistries.

## 11. References

(1) For fundamentals of modern electrodics, see: Bockris, J. O'M.; Reddy, A. K. N. *Modern Electrochemistry*, 2nd ed.; Plenum Press: New York, 2000; Vol. 2.

(2) For elementary readings concerning battery technology and chemistry, see: Linden, D., Ed. *Handbook of Batteries*, 2nd ed.; McGraw-Hill: New York, 1995; 3rd ed.; McGraw-Hill: New York, 2001.

(3) The redox potentials against the standard hydrogen electrode (SHE) for various reactions, usually called "electrochemical series", are listed in the annually updated *CRC Handbook of Chemistry and Physics*; CRC Press: Boca Raton, FL. On the other hand, unless otherwise indicated, the potential values used in this review are all referred to the $Li^+/Li$ reference electrode.

(4) Jasinski, R. *High Energy Batteries*; Plenum Press: New York, 1967.

(5) Fraioly, A. V.; Barber, W. A.; Feldman, A. M. U.S. Patent 3,551,205, 1970.

(6) Schneider, A. A.; Moser, J. U.S. Patent 3,674,562, 1972.

(7) Moser, J. U.S. Patent 3,660,163, 1972.

(8) Fukuda, M.; Ijima, T. In *Power Sources*; Collins, D. H., Ed.; Academic Press: London, 1975; Vol. 5, p 713.

(9) Selim, R.; Bro, P. *J. Electrochem. Soc.* **1974**, *121*, 1457.

(10) Raul, R. D.; Brummer, S. B. *Electrochim. Acta* **1977**, *22*, 75.

(11) Koch, V. R.; Young, J. H. *J. Electrochem. Soc.* **1978**, *125*, 1371.

(12) Yoshimatsu, I.; Hirai, T.; Yamaki, J. *J. Electrochem. Soc.* **1988**, *135*, 2422.

(13) Broadhead, J.; Trumbore, F. A. In *Power Sources*; Collins, D. H., Ed.; Academic Press: London, 1975; Vol. 5, p 661.

(14) Dan, P.; Mengeritsky, E.; Geronov, Y.; Aurbach, D.; Weissman, I. *J. Power Sources* **1995**, *54*, 143.

(15) Aurbach, D.; Gofer, Y.; Ben-Zion, M. *J. Power Sources* **1992**, *39*, 163.

(16) Aurbach, D.; Weissman, I.; Zaban, A.; Ein-Eli, Y.; Mengeritsky, E.; Dan, P. *J. Electrochem. Soc.* **1996**, *143*, 2110.

(17) Aurbach, D.; Zaban, A.; Ein-Eli, Y.; Weissman, I.; Chusid, O.; Markovski, B.; Levi, M. D.; Levi, E.; Schechter, A.; Granot, E. *J. Power Sources* **1997**, *86*, 91.

(18) Aurbach, D.; Zinigrad, E.; Teller, H.; Dan, P. *J. Electrochem. Soc.* **2000**, *147*, 1274.

(19) Dominey, L. A. In *Nonaqueous Electrochemistry*; Aurbach, D., Ed.; Marcel-Dekker: New York, 1999; Chapter 8.

(20) Whittingham, M. S. *Science* **1976**, *192*, 1126.

(21) Whittingham, M. S. *Prog. Solid State Chem.* **1978**, *12*, 1.

(22) (a) Mizushima, K.; Jones, P. C.; Wiseman, P. J.; Goodenough, J. B. *Mater. Res. Bull.* **1980**, *15*, 783. (b) Mizushima, K.; Jones, P. C.; Wiseman, P. J.; Goodenough, J. B. *Solid State Ionics* **1981**, *3/4*, 171.

(23) Murphy, D. W.; Christian, P. *Science* **1979**, *205*, 651.

(24) Armand, M. In *Materials for Advanced Batteries*; Murphy, D. W., Broadhead, J., Steele, B. C. H., Eds.; Plenum Press: New York, 1980; p 145.

(25) Lazzari, M.; Scrosati, B. *J. Electrochem. Soc.* **1980**, *127*, 773.

(26) Auborn, J.; Barberio, Y. L. *J. Electrochem. Soc.* **1987**, *134*, 638.

(27) Semkov, K. W.; Sammels, A. F. *J. Electrochem. Soc.* **1987**, *134*, 766.

(28) Scrosati, B. *J. Electrochem. Soc.* **1992**, *139*, 2776.

(29) Nagaura, T.; Nagamine, M.; Tanabe, I.; Miyamoto, N. *Prog. Batteries Sol. Cells* **1989**, *8*, 84.

(30) Nagaura, T.; Ozawa, K. *Prog. Batteries Sol. Cells* **1990**, *9*, 209.

(31) Nishi, Y.; Azuma, H.; Omaru, A. U.S. Patent 4,959,281, 1990.

(32) Ohzhku, T.; Ueda, A.; Nagayama, M. *J. Electrochem. Soc.* **1993**, *140*, 1862.

(33) Bittihn, R.; Herr, R.; Hoge, D. *J. Power Sources* **1993**, *43/44*, 223.

(34) Nagaura, T. *Proceedings of the 5th International Seminar on Lithium Battery Technology and Applications*, Deerfield Beach, FL, March 5−7, 1990; Florida Educational Seminars, Inc.: Boca Raton, FL.

(35) Dahn, J. R.; von Sacken, U.; Fong, R. *Extended Abstracts of the 178th Electrochemical Society Meeting*, Seattle, WA, Oct. 14−19, 1990; Abstract No. 42; Electrochemical Society: Pennington, NJ.

(36) Fong, R.; von Sacken, U.; Dahn, J. R. *J. Electrochem. Soc.* **1990**, *137*, 2009.

(37) Peled, E. *J. Electrochem. Soc.* **1979**, *126*, 2047.

(38) Brodd, J. *Extended Abstracts of the 201st Electrochemical Society Meeting*, Philadelphia, PA, May 12−17, 2002; Abstract No. 259; Electrochemical Society: Pennington, NJ.

(39) Hannon, D. *Purchasing Magazine* **2002**, Feb. 21.

(40) Broussely, M. *11th International Meeting on Lithium Batteries*, Monterey, CA, June 23−28, 2002; Abstract No. 415; Electrochemical Society: Pennington, NJ.

(41) Megahed, S.; Scrosati, B. *J. Power Sources* **1994**, *51*, 79.

(42) Brandt, K. *Solid State Ionics* **1994**, *69*, 173.

(43) Sawai, K.; Iwakoshi, Y.; Ohzuhu, T. *Solid State Ionics* **1994**, *69*, 273.

(44) Guyomard, D.; Tarascon, J. M. *Solid State Ionics* **1994**, *69*, 222.

(45) Ebner, W.; Fouchard, D.; Xie, L. *Solid State Ionics* **1994**, *69*, 238.

(46) Arora, P.; White, R. E.; Doyle, M. *J. Electrochem. Soc.* **1998**, *145*, 3647.

(47) Tarascon, J. M.; Armand, M. *Nature* **2001**, *414*, 359.

(48) (a) Blomgren, G. E. *J. Power Sources* **1999**, *81/82*, 112. (b) Blomgren, G. E. *J. Power Sources* **2003**, *119/121*, 326.

(49) Fry, A. J. *Synthetic Organic Electrochemistry*, 2nd ed.; John Wiley: London, 1989.

(50) The physical data were extracted and compiled from the following literature sources: (a) Jang, G. J.; Tomkins, R. P. T. *Nonaqueous Electrolytes Handbook*; Academic Press: New York, 1972; Vol. 1. (b) Dudley, J. T.; Wilkinson, D. P.; Thomas, G.; LeVae, R.; Woo, S.; Blom, H.; Horvath, C.; Juzkow, M. W.; Denis, B.; Juric, P.; Aghakian, P.; Dahn, J. R. *J. Power Sources* **1991**, *35*, 59. (c) *Aldrich Handbook of Fine Chemicals and Laboratory Equipment*; Aldrich Chemical Co.: 2003−2004. (d) Ue, M.; Ida, K.; Mori, S. *J. Electrochem. Soc.* **1994**, *141*, 2989. (e) Ding, M. S.; Xu, K.; Zhang, S.; Jow, T. R. *J. Electrochem. Soc.* **2001**, *148*, A299.

(51) Harris, W. S. Electrochemical Studies in Cyclic Esters. Ph.D. Thesis, University of California, Berkeley, CA, 1958.

(52) Jasinski, R.; Kirkland, S. *Anal. Chem.* **1967**, *39*, 1663.

(53) Jasinski, R.; Carroll, S. *Anal. Chem.* **1968**, *40*, 1908.

(54) Rauh, R. D.; Reise, T. F.; Brummer, S. B. *J. Electrochem. Soc.* **1978**, *125*, 186.

(55) Aurbach, D.; Daroux, M. L.; Faguy, P. W.; Yeager, E. *J. Electrochem. Soc.* **1987**, *134*, 1611.

(56) Dey, A. N. *Thin Solid Films* **1977**, *43*, 131.

(57) Aurbach, D.; Gofer, Y.; Langsam, J. *J. Electrochem. Soc.* **1989**, *136*, 3198.

(58) Newman, G. H.; Francis, R. W.; Gaines, L. H.; Rao, B. M. *J. Electrochem. Soc.* **1980**, *127*, 2025.

(59) Rauh, R. D.; Brummer, S. B. *Electrochim. Acta* **1977**, *22*, 85.

(60) Koch, V. R.; Young, J. H. *J. Electrochem. Soc.* **1978**, *125*, 1371.

(61) Koch, V. R. *J. Electrochem. Soc.* **1979**, *126*, 181

(62) Koch, V. R.; Goldman, J. L.; Mattos, C. J.; Mulvaney, M. *J. Electrochem. Soc.* **1982**, *129*, 1.

(63) Koch, V. R.; Young, J. H. *Science* **1979**, *204*, 499.

(64) Goldman, J. L.; Mank, R. M.; Young, J. H.; Koch, V. R.; Young, J. H. *J. Electrochem. Soc.* **1980**, *127*, 1461.

(65) Desjardins, C. D.; Cadger, T. G.; Salter, R. S.; Donaldson, G.; Casey, E. J. *J. Electrochem. Soc.* **1985**, *132*, 529.

(66) Foos, J. S.; McVeigh, J. *J. Electrochem. Soc.* **1983**, *130*, 628.

(67) Foos, J. S.; Stolki, T. J. *J. Electrochem. Soc.* **1988**, *135*, 2769.

(68) Abraham, K. M.; Goldman, J. L.; Natwig, D. L. *J. Electrochem. Soc.* **1982**, *129*, 2404.

(69) Dampier, F. W. *J. Electrochem. Soc.* **1981**, *128*, 2501.

(70) Abraham, K. M.; Pasquariello, D. M.; Martin, F. J. *J. Electrochem. Soc.* **1986**, *133*, 661.

(71) Yoshimatsu, I.; Hirai, T.; Yamaki, J. *J. Electrochem. Soc.* **1988**, *135*, 2422.

(72) Abraham, K. M.; Foos, J. S.; Goldman, J. L. *J. Electrochem. Soc.* **1984**, *131*, 2197.

(73) Geronov, Y.; Puresheva, B.; Moshtev, R. V.; Zlatilova, P.; Kosev, T.; Staynov, Z.; Pistoia, G.; Pasquali, M. *J. Electrochem. Soc.* **1990**, *137*, 3338.

(74) Campbell, S. A.; Bowes, C.; McMillan, R. S. *J. Electroanal. Chem.* **1990**, *284*, 195.

(75) Xu, K.; Angell, C. A. *J. Electrochem. Soc.* **1998**, *145*, L70.

(76) Xu, K.; Ding, S.; Jow, T. R. *J. Electrochem. Soc.* **1999**, *146*, 4172.

(77) Simon, B.; Boeuve, J. P.; Broussely, M. *J. Power Sources* **1993**, *43/44*, 65.

(78) Plichta, E.; Slane, S.; Uchiyama, M.; Salomon, M.; Chua, D.; Ebner, W. B.; Lin, H. W. *J. Electrochem. Soc.* **1989**, *136*, 1865.

(79) Uchida, I.; Sato, H. *J. Electrochem. Soc.* **1995**, *142*, L139.

(80) Angell, C. A.; Choi, Y. *J. Microsc.* **1986**, *141*, 251.

(81) Xu, K.; Ding, S.; Jow, T. R. *J. Electrochem. Soc.* **2001**, *148*, A267.

(82) Elliott, W. Report No. 1, Contract NAS 3-6015 (N 65-11518), Sept 1964.

(83) Pistoia, G.; De Rossi, M.; Scrosati, B. *J. Electrochem. Soc.* **1970**, *117*, 500.

(84) Pistoia, G. *J. Electrochem. Soc.* **1971**, *118*, 153.

(85) Subbarao, S.; Shen, D. H.; Deligiannis, F.; Huang, C. K.; Halpert, G. *J. Power Sources* **1990**, *29*, 579.

(86) Takami, N.; Ohsaki, T.; Inada, K. *J. Electrochem. Soc.* **1992**, *139*, 1849.

(87) Arakawa, M.; Tobishima, S.; Hirai, T.; Yamaki, J. *J. Electrochem. Soc.* **1986**, *133*, 1527.

(88) Surampudi, S.; Shen, D. H.; Huang, C. K.; Narayanan, S. R.; Attia, A.; Halpert, G.; Peled, E. *J. Power Sources* **1993**, *43/44*, 21.

(89) Tobishima, S.; Arakawa, M.; Hirai, T.; Yamaki, J. *J. Power Sources* **1989**, *26*, 449.

(90) McMillan, R. S.; Juskow, M. W. *J. Electrochem. Soc.* **1991**, *138*, 1556.

(91) Yamaura, J.; Ozaki, Y.; Morita, A.; Ohta, A. *J. Power Sources* **1993**, *43/44*, 233.

(92) Zhang, S. S.; Liu, Q. G.; Yang, L. L. *J. Electrochem. Soc.* **1993**, *140*, L107.

(93) Guyomard, D.; Tarascon, J. M. *J. Electrochem. Soc.* **1992**, *139*, 937.

(94) Tarascon, J. M.; Guyomard, D.; Baker, G. L. *J. Power Sources* **1993**, *43/44*, 689.

(95) Dahn, J.; von Sacken, U.; Juzkow, M. W.; al-Janaby, H. *J. Electrochem. Soc.* **1991**, *138*, 2207.

(96) Ohzuku, T.; Iwakoshi, Y.; Sawai, K. *J. Electrochem. Soc.* **1993**, *140*, 2490.

(97) Huang, S. Y.; Kavan, L.; Exnar, I.; Grätzel, M. *J. Electrochem. Soc.* **1995**, *142*, L142.

(98) Guyomard, D.; Tarascon, J. M. *J. Electrochem. Soc.* **1993**, *140*, 3071.

(99) Tarascon, J. M.; Guyomard, D. *Solid State Ionics* **1994**, *69*, 293.

(100) Zheng, T.; Liu, Y.; Fuller, E. W.; Tseng, S.; von Sacken, U.; Dahn, J. *J. Electrochem. Soc.* **1995**, *142*, 2581.

(101) Morita, M.; Ichimura, T.; Ishikawa, M.; Matsuda, Y. *J. Electrochem. Soc.* **1996**, *143*, L26.

(102) Ein-Eli, Y.; Thomas, S. R.; Chadha, R.; Blakley, T. J.; Koch, V. R. *J. Electrochem. Soc.* **1997**, *144*, 823.

(103) Chu, A. C.; Josefowicz, J. Y.; Farrington, G. C. *J. Electrochem. Soc.* **1997**, *144*, 4161.

(104) Aurbach, D.; Ein-Eli, Y.; Markovsky, B.; Zaban, A.; Luski, S.; Carmeli, Y.; Yamin, H. *J. Electrochem. Soc.* **1995**, *142*, 2882.

(105) Koetschau, I.; Richard, M. N.; Dahn, J. R.; Soupart, J. B.; Rousche, J. C. *J. Electrochem. Soc.* **1995**, *142*, 2906.

(106) Peled, E.; Golodnitsky, D.; Menachem, C.; Bar-Tow, D. *J. Electrochem. Soc.* **1998**, *145*, 3482.

(107) Ein-Eli, Y.; Thomas, S. R.; Koch, V. R.; Aurbach, D.; Schechter, A.; Markovsky, B. *J. Electrochem. Soc.* **1996**, *143*, L273.

(108) Ein-Eli, Y.; McDevitt, S. F.; Aurbach, D.; Markovsky, B.; Schecheter, A. *J. Electrochem. Soc.* **1997**, *144*, L180.

(109) Sekai, K.; Azuma, H.; Omaru, A.; Fujita, S.; Imoto, H.; Endo, T.; Yamaura, K.; Nishi, Y. *J. Power Sources* **1993**, *43/44*, 241.

(110) Linden, D. In *Handbook of Batteries*, 2nd ed.; Linden, D., Ed.; McGraw-Hill: New York, 1995; Chapters 14 and 36.

(111) Ue, M. *J. Electrochem. Soc.* **1995**, *142*, 2577.

(112) Ravdel, B.; Abraham, K. M.; Gitzendanner, R.; Marsh, C. *Extended Abstracts of the 200th Electrochemical Society Meeting*, San Francisco, CA, Sept 2−7, 2001; Abstract No. 97; Electrochemical Society: Pennington, NJ.

(113) Xu, W.; Angell, C. A. *Electrochem. Solid State Lett.* **2001**, *4*, E1.

(114) Hossain, S. *Handbook of Batteries*, 2nd ed.; Linden, D., Ed.; McGraw-Hill: New York, 1995; Chapter 36.

(115) Schmidt, M.; Heider, U.; Kuehner, A.; Oesten, R.; Jungnitz, M.; Ignat'ev, N.; Sartori, P. *J. Power Sources* **2001**, *97/98*, 557.

(116) Walker, C. W.; Cox, J. D.; Salomon, M. *J. Electrochem. Soc.* **1996**, *143*, L80.

(117) Aurbach, D.; Zaban, A.; Schecheter, A.; Ein-Eli, Y.; Zinigrad, E.; Markovsky, B. *J. Electrochem. Soc.* **1995**, *142*, 2873.

(118) Aurbach, D.; Ein-Ely, Y.; Zaban, A. *J. Electrochem. Soc.* **1994**, *141*, L1.

(119) Jasinski, R.; Carroll, S. *J. Electrochem. Soc.* **1970**, *117*, 218.

(120) Nanjundiah, C.; Goldman, J. L.; Dominey, L. A.; Koch, V. R. *J. Electrochem. Soc.* **1988**, *135*, 2914.

(121) Koch, V. R. *J. Electrochem. Soc.* **1979**, *126*, 181.

(122) Webber, A. *J. Electrochem. Soc.* **1991**, *138*, 2586.

(123) Ein-Eli, Y.; Markovsky, B.; Aurbach, D.; Carmeli, Y.; Yamin, H.; Luski, S. *Electrochim. Acta* **1994**, *39*, 2559.

(124) Aurbach, D.; Ein-Eli, Y. *J. Electrochem. Soc.* **1995**, *142*, 1746.

(125) Gnanaraj, J. S.; Levi, M. D.; Levi, E.; Salitra, G.; Aurbach, D.; Fischer, J. E.; Claye, A. *J. Electrochem. Soc.* **2001**, *148*, A525.

(126) Matsuda, Y.; Morita, M.; Takada, K. *J. Electrochem. Soc.* **1984**, *131*, 1991.

(127) Matsuda, Y.; Morita, M.; Yamashita, T. *J. Electrochem. Soc.* **1984**, *131*, 2821.

(128) Takata, K.; Morita, M.; Matsuda, Y. *J. Electrochem. Soc.* **1985**, *132*, 126.

(129) Ue, M. *J. Electrochem. Soc.* **1994**, *141*, 3336.

(130) Ue, M.; Takeda, M.; Takehara, M.; Mori, S. *J. Electrochem. Soc.* **1997**, *144*, 2684.

(131) Ue, M.; Murakami, A.; Nakamura, S. *J. Electrochem. Soc.* **2002**, *149*, A1572.

(132) Zhang, S. S.; Xu, K.; Jow, T. R. *J. Electrochem. Soc.* **2002**, *149*, A586.

(133) Takami, N.; Ohsaki, T.; Hasebe, H.; Yamamoto, M. *J. Electrochem. Soc.* **2002**, *149*, A9.

(134) Zhang, S. S.; Xu, K.; Jow, T. R. *Electrochem. Commun.* **2002**, *4*, 928.

(135) Zhang, S. S.; Xu, K.; Jow, T. R. *J. Solid State Electrochem.* **2003**, *7*, 147.

(136) Xu, K.; Angell, C. A. *Electrochim. Acta* **1995**, *40*, 2401.

(137) Ito, K.; Ohno, H. *Electrochim. Acta* **1998**, *43*, 1247.

(138) Croce, F.; D'Aprano, A.; Nanjundiah, C.; Koch, V. R.; Walker, C.; Salomon, M. *J. Electrochem. Soc.* **1996**, *143*, 154.

(139) Naoi, K.; Mori, M.; Naruoka, Y.; Lamanna, W. M.; Atanasoski, R. *J. Electrochem. Soc.* **1999**, *146*, 462.

(140) Ishikawa, M.; Morita, M.; Asao, M.; Matsuda, Y. *J. Electrochem. Soc.* **1994**, *141*, 1105.

(141) Krause, L. J.; Lamanna, W.; Summerfield, J.; Engle, M.; Korba, G.; Loch, R.; Atanasoski, R. *J. Power Sources* **1997**, *68*, 320.

(142) Foropoulos, J.; DesMarteau, D. D. *Inorg. Chem.* **1984**, *23*, 3720.

(143) Armand, M.; Gorecki, W.; Andreani, R. *Proceedings of the 2nd International Meeting on Polymer Electrolytes*; Scrosati, B., Ed.; Elsevier: London, 1989; p 91.

(144) Xu, K.; Day, N. D.; Angell, C. A. *J. Electrochem. Soc.* **1996**, *143*, L209.

(145) Wang, X.; Yasukawa, E.; Kasuya, S. *J. Electrochem. Soc.* **2000**, *147*, 2421.

(146) Dominey, L. A.; Koch, V. R.; Blakley, T. *Electrochim. Acta* **1992**, *37*, 1551.

(147) Yang, H.; Kwon, K.; Devine, T. M.; Evans, J. W. *J. Electrochem. Soc.* **2000**, *147*, 4399.

(148) Kanamura, K.; Umegaki, T.; Shiraishi, S.; Ohashi, M.; Takehara, Z. *J. Electrochem. Soc.* **2002**, *149*, A185.

(149) Methlie, G. J. U.S. Patent 3,415,687, 1968.

(150) Wiesboeck, R. A. U.S. Patent 3,654,330, 1972.

(151) Kawamura, T.; Kimura, A.; Egashira, M.; Okada, S.; Yamaki, J. *J. Power Sources* **2001**, *104*, 260.

(152) Sloop, S. E.; Pugh, J. K.; Wang, S.; Kerr, J. B.; Kinoshita, K. *Electrochem. Solid-State Lett.* **2001**, *4*, A42.

(153) Behl, W. K.; Plichta, E. J. *J. Power Sources* **1998**, *72*, 132.

(154) Behl, W. K.; Plichta, E. J. *J. Power Sources* **2000**, *88*, 192.

(155) Xu, K.; Zhang, S.; Jow, T. R.; Xu, W.; Angell, C. A. *Electrochem. Solid-State Lett.* **2002**, *4*, A26.

(156) Zhang, S.; Jow, T. R. *J. Power Sources* **2002**, *109*, 458.

(157) Ozawa, K. *Solid State Ionics* **1994**, *69*, 212.

(158) Ding, M. S. *J. Electrochem. Soc.* **2003**, *150*, A455.

(159) Ding, M. S.; Xu, K.; Jow, T. R. *J. Electrochem. Soc.* **2000**, *147*, 1688.

(160) Ding, M. S.; Xu, K.; Jow, T. R. *J. Therm. Anal. Calorim.* **2000**, *62*, 177.

(161) Ding, M. S. *J. Electrochem. Soc.* **2002**, *149*, A1063.

(162) Angell, C. A. *Science* **1995**, *267*, 1924.

(163) Angell, C. A. *Chem. Rev.* **2002**, *102*, 2627.

(164) Plichta, E. J.; Behl, W. K. *Proceedings of the 38th Power Sources Conference*, Cherry Hill, NJ, 1998; p 444.

(165) Lin, H. P.; Chua, D.; Salomon, M.; Shiao, H. C.; Hendrickson, M.; Plichta, E.; Slane, S. *Electrochem. Solid-State Lett.* **2001**, *4*, A71.

(166) Ding, S. P.; Xu, K.; Zhang, S. S.; Jow, T. R.; Amine, K.; Henriksen, G. L. *J. Electrochem. Soc.* **1999**, *146*, 3974.

(167) Liu, Z. K. *J. Electrochem. Soc.* **2003**, *150*, A359.

(168) Zhang, S. S.; Xu, K.; Allen, J. L.; Jow, T. R. *J. Power Sources* **2002**, *110*, 217.

(169) Blint, J. R. *J. Electrochem. Soc.* **1995**, *142*, 696.

(170) Wang, Y.; Nakamura, S.; Ue, M.; Balbuena, P. B. *J. Am. Chem. Soc.* **2001**, *123*, 11708.

(171) Yanase, S.; Oi, T. *J. Nucl. Sci. Technol.* **2002**, *39*, 1060.

(172) Fukushima, T.; Matsuda, Y.; Hashimoto, H.; Arakawa, R. *Electrochem. Solid-State Lett.* **2001**, *4*, A127.

(173) Matsuda, Y.; Fukushima, T.; Hashimoto, H.; Arakawa, R. *J. Electrochem. Soc.* **2002**, *149*, A1045.

(174) It should be pointed out that the simple summation of the contribution from each individual ionic species comes from the assumption that the Kohlrausch independent ion rule, established for infinitely diluted solutions, still applies in the electrolytes of practical salt concentrations (~1.0 M), which is incorrect due to the intensive interionic couplings in the latter. However, eq 1 remains qualitatively useful (see ref 1).

(175) For an excellent introductory reading on ac impedance techniques for the purpose of ion conductivity measurement or study of interfacial properties, please see: Linford, R. G. In *Electrochemical Science and Technology of Polymers*, 2nd ed.; Linford, R. G., Ed.; Elsevier Applied Science: London, 1990; p 281.

(176) Blomgren, G. E. In *Lithium Batteries*; Gabano, J. P., Ed.; Academic Press: London, 1983.

(177) Tobishima, S.; Okada, T. *Electrochim. Acta* **1985**, *30*, 1715.

(178) Endo, E.; Ata, M.; Tanaka, K.; Sekai, K. *J. Electrochem. Soc.* **1998**, *145*, 3757.
(179) Tsuchida, E.; Kobayashi, N.; Ohno, H. *Macromolecules* **1988**, *21*, 96.
(180) Zhou, G.; Khan, I. M.; Smid, J. *Polym. Commun.* **1989**, *30*, 52.
(181) Zhang, S. S.; Wan, G. X. *J. Appl. Polym. Sci.* **1993**, *48*, 405.
(182) Tada, Y.; Sato, M.; Takeno, N.; Nakacho, Y.; Shigehara, K. *Chem. Mater.* **1994**, *6*, 27.
(183) Robinson, R. A.; Stokes, R. H. *Electrolyte Solutions*; Butterworths: London, 1959; p 392.
(184) Some organic nitrogen-containing compounds (nitriles, nitroalkyls, amides, etc.) are the rare exceptions to this rule. For example, for acetonitrile, $\epsilon = 36$ and $\eta = 0.3$ cP at room temperature. However, the poor electrochemical stability of these compounds prevented them from being used in batteries.
(185) Jasinski, R. *Electrochem. Technol.* **1968**, *6*, 28.
(186) Saito, T.; Ikeda, H.; Matsuda, Y.; Tamura, H. *J. Appl. Electrochem.* **1976**, *6*, 85.
(187) Matsuda, Y.; Satake, H. *J. Electrochem. Soc.* **1980**, *127*, 877.
(188) Tobishima, S.; Yamaji, A. *Electrochim. Acta* **1984**, *29*, 267.
(189) Tobishima, S.; Yamaji, A.; Okada, T. *Electrochim. Acta* **1984**, *29*, 1471.
(190) Arakawa, M.; Tobishima, S.; Hirai, T.; Yamaki, J. *J. Electrochem. Soc.* **1986**, *133*, 1527.
(191) Tobishima, S.; Arakawa, M.; Hirai, T.; Yamaki, J. *J. Power Sources* **1987**, *20*, 293.
(192) Tobishima, S.; Arakawa, M.; Yamaki, J. *Electrochim. Acta* **1990**, *35*, 383.
(193) Matsuda, Y.; Nakashima, H.; Morita, M.; Takasu, Y. *J. Electrochem. Soc.* **1981**, *128*, 2552.
(194) Matsuda, Y.; Morita, M.; Kosaka, K. *J. Electrochem. Soc.* **1983**, *130*, 101.
(195) Ding, M. S.; Xu, K.; Zhang, S. S.; Amine, K.; Henriksen, G. L.; Jow, T. R. *J. Electrochem. Soc.* **2001**, *148*, A1196.
(196) Ding, M. S.; Jow, T. R. *J. Electrochem. Soc.* **2003**, *150*, A620.
(197) Blint, R. *J. Electrochem. Soc.* **1997**, *144*, 787.
(198) Choquette, Y.; Brisard, G.; Parent, M.; Brouillette, D.; Perron, G.; Desnoyers, J. E.; Armand, M.; Gravel, D.; Lougui, N. *J. Electrochem. Soc.* **1998**, *145*, 3500.
(199) Chen, H. P.; Fergus, J. W.; Jang, B. Z. *J. Electrochem. Soc.* **2000**, *147*, 399.
(200) Smedley, S. I. *The Interpretation of Ionic Conductivity in Liquids*; Plenum Press: New York, 1980; Chapter 3.
(201) Evans, D. H.; O'Connell, K. M.; Petersen, R. A.; Kelly, M. J. *J. Chem. Educ.* **1983**, *60*, 290.
(202) Bard, A. J.; Faulkner, L. R. *Electrochemical Methods—Fundamentals and Applications*, 2nd ed.; John Wiley & Sons: New York, 2000.
(203) Ue, M.; Murakami, A.; Nakamura, S. *J. Electrochem. Soc.* **2002**, *149*, A1572.
(204) Eggert, G.; Heitbaum, J. *Electrochim. Acta* **1986**, *31*, 1443.
(205) Guyomard, D.; Tarascon, J. M. *J. Power Sources* **1995**, *54*, 92.
(206) Koch, V. R.; Dominey, L. A.; Nanjundiah, C.; Ondrechen, M. J. *J. Electrochem. Soc.* **1996**, *143*, 798.
(207) Kita, F.; Kawakami, A.; Sonoda, T.; Kobayashi, H. In *New Sealed Rechargeable Batteries and Supercapacitors*; Barnett, B. M., Dowgiallo, E., Halpert, G., Matsuda, Y., Takehara, Z., Eds.; The Electrochemical Society Proceedings Series; Pennington, NJ, 1993; PV 93-23, p 321.
(208) Aurbach, D.; Gottlieb, H. *Electrochim. Acta* **1989**, *34*, 141.
(209) Aurbach, D. *J. Electrochem. Soc.* **1989**, *136*, 906.
(210) Aurbach, D.; Gofer, Y. *J. Electrochem. Soc.* **1991**, *138*, 3529.
(211) Goren, E.; Chusid, O.; Aurbach, D. *J. Electrochem. Soc.* **1991**, *138*, L6.
(212) Aurbach, D.; Gofer, Y.; Ben-Zion, M.; Aped, P. *J. Electroanal. Chem.* **1992**, *339*, 451.
(213) Aurbach, D.; Chusid, O. *J. Electrochem. Soc.* **1993**, *140*, L155.
(214) Zhang, X.; Kostecki, R.; Richardson, T. J.; Pugh, J. K.; Ross, P. N. *J. Electrochem. Soc.* **2001**, *148*, A1341.
(215) Tiedemann, W. H.; Bennion, D. N. *J. Electrochem. Soc.* **1973**, *120*, 1624.
(216) Jorne, J.; Tobias, C. W. *J. Electrochem. Soc.* **1974**, *121*, 994.
(217) Jorne, J.; Tobias, C. W. *J. Appl. Electrochem.* **1975**, *5*, 279.
(218) Peled, E. In *Lithium Batteries*; Gabano, J. P., Eds.; Academic Press: London, 1983; p 43.
(219) Peled, E.; Straze, H. *J. Electrochem. Soc.* **1977**, *124*, 1030.
(220) Dousek, F. P.; Jansta, J.; Rihaz, J. *J. Electroanal. Chem.* **1973**, *46*, 281.
(221) Nazri, G.; Muller, R. H. *J. Electrochem. Soc.* **1985**, *132*, 1385.
(222) Kanamura, K.; Tamura, H.; Shiraishi, S.; Takehara, Z. *J. Electrochem. Soc.* **1995**, *142*, 340.
(223) Kanamura, K.; Shiraishi, S.; Takehara, Z. *J. Electrochem. Soc.* **1996**, *143*, 2187.
(224) Epelboin, I.; Froment, M.; Garreau, M.; Thevenin, J.; Warin, D. *J. Electrochem. Soc.* **1980**, *127*, 2100.
(225) Thevenin, J. G.; Muller, R. H. *J. Electrochem. Soc.* **1987**, *134*, 273.
(226) Gaberšček, M.; Jamnik, J.; Pejovnik, S. *J. Electrochem. Soc.* **1993**, *140*, 308.
(227) Gaberšček, M.; Pejovnik, S. *J. Electrochem. Soc.* **1999**, *146*, 933.
(228) Naoi, K.; Mori, M.; Shinagawa, Y. *J. Electrochem. Soc.* **1996**, *143*, 2517.
(229) Geronov, Y.; Schwager, F.; Muller, R. H. *J. Electrochem. Soc.* **1982**, *129*, 1422.
(230) Hérold, A. *Bull. Soc. Chim. Fr.* **1955**, *187*, 999.
(231) Guérard, A.; Hérold, A. *Carbon* **1975**, *13*, 337.
(232) Billaud, D.; Hérold, A. *Carbon* **1979**, *17*, 183.
(233) *Graphite Intercalation Compounds*, Vol. I and II; Zabel, H., Solin, S. A., Eds.; Springer-Verlag: New York, 1990 and 1992.
(234) Bagouin, M.; Guérard, D.; Hérold, A. *C. R. Acad. Sci., Ser. C* **1966**, *262*, 557.
(235) Guérard, D.; Hérold, A. *C. R. Acad. Sci., Ser. C* **1972**, *275*, 571.
(236) Avdeev, V. V.; Nalimova, V. A.; Semenenko, K. N. *High-Pressure Res.* **1990**, *6*, 11.
(237) Dey, A. N.; Sullivan, B. P. *J. Electrochem. Soc.* **1970**, *117*, 222.
(238) Eichinger, G. *J. Electroanal. Chem.* **1976**, *74*, 183.
(239) Besenhard, J. O. *Carbon* **1976**, *14*, 111.
(240) Besenhard, J. O.; Möhwald, H.; Nickl, J. J. *Carbon* **1980**, *18*, 399.
(241) Besenhard, J. O.; Fritz, H. P *Angew. Chem., Int. Ed. Engl.* **1983**, *22*, 950.
(242) Besenhard, J. O.; Fritz, H. P. *J. Electroanal. Chem.* **1974**, *53*, 329.
(243) Arakawa, M.; Yamaki, J. *J. Electroanal. Chem.* **1987**, *219*, 273.
(244) Yazami, R.; Touzain, P. *J. Power Sources* **1983**, *9*, 365.
(245) Yazami, R.; Guérard, D. *Power Sources* **1993**, *43/44*, 39.
(246) Kanno, R.; Takeda, Y.; Ichikawa, T.; Nakanishi, K.; Yamamoto, O. *J. Power Sources* **1989**, *26*, 535.
(247) Mohri, M.; Yanagisawa, N.; Tajima, Y.; Tanaka, H.; Mitate, T.; Nakajima, S.; Yoshida, M.; Yoshimoto, Y.; Suzuki, T.; Wada, H. *J. Power Sources* **1989**, *26*, 545.
(248) The configuration of the "half anode cell" enables the separate evaluation of the anode material alone; thus, it is widely used as a convenient tool. However, it should be kept in mind that the "anode materials" under study are actually "cathode materials" in this half-cell: Li|electrolyte|carbonaceous "anode". To make things more confusing, different researchers use both "charge" (referring to this carbonaceous material in an imaginary full lithium ion cell, therefore, conceptually correct) and "discharge" (referring to this half-cell, therefore, operationally correct) to describe the same process of lithiating the carbon electrode in this half-cell. Since there is no standard convention, caution must be taken when electrochemical literature concerning this topic is being studied. This review will use less ambiguous terms such as "lithiation" or "delithiation" for the cycling of anode half-cells.
(249) Chusid, O.; Ein Ely, Y.; Aurbach, D.; Babai, M.; Carmeli, Y. *J. Power Sources* **1993**, *43/44*, 47.
(250) Aurbach, D.; Ein-Eli, Y.; Chusid, O.; Carmeli, Y.; Babai, M.; Yamin, H. *J. Electrochem. Soc.* **1994**, *141*, 603.
(251) Besenhard, J. O.; Winter, M.; Yang, J.; Biberacher, W. *J. Power Sources* **1993**, *54*, 228.
(252) Dahn, J. R. *Phys. Rev. B* **1991**, *44*, 9170.
(253) Jiang, Z.; Alamgier, M.; Abraham, K. M. *J. Electrochem. Soc.* **1995**, *142*, 333.
(254) Aurbach, D.; Levi, M. D.; Levi, E.; Schechter, A. *J. Phys. Chem. B* **1997**, *101*, 2195.
(255) Chung, G.; Kim, H.; Yu, S.; Jun, S.; Choi, J.; Kim, M. *J. Electrochem. Soc.* **2000**, *147*, 4391.
(256) Although by the solution method the ternary GICs composed of [Li$^+$(solv)]−graphite] were indeed synthesized and identified by XRD, the solvents used were mostly ether compounds that have high donicity toward lithium ion. Similar Li GICs with carbonate molecules were never obtained. On the contrary, even via the solution method, binary GICs (i.e., bare lithium ion intercalation without solvent) instead of ternary ones were often preferentially formed in these ether solvents, casting more doubt about the possibility of their formation via lithium ion cells. The large *c*-axis distance measured by XRD for these ternary GICs ranged between 7 and 11 Å and confirmed from another angle that in situ XRD carried out on a graphite anode during its cycling never detected such GICs. See refs 257−260 for the preparation and characterization of various ternary GICs based on ether compounds and lithium ion.
(257) Mizutani, Y.; Abe, T.; Ikeda, K.; Ihara, E.; Asano, M.; Harada, T.; Inaba, M.; Ogumi, Z. *Carbon* **1997**, *35*, 61.
(258) Abe, T.; Mizutani, Y.; Tabuchi, T.; Ikeda, K.; Asano, M.; Harada, T.; Inaba, M.; Ogumi, Z. *J. Power Sources* **1997**, *68*, 216.
(259) Mizutani, Y.; Abe, T.; Inaba, M.; Ogumi, Z. *Synth. Met.* **2002**, *125*, 153.
(260) Abe, T.; Kawabata, N.; Mizutani, Y.; Inaba, M.; Ogumi, Z. *J. Electrochem. Soc.* **2003**, *150*, A257.
(261) Shu, Z. X.; McMillan, R. S.; Murray, J. J. *J. Electrochem. Soc.* **1993**, *140*, 922.
(262) Matsumura, Y.; Wang, S.; Mondori, J. *J. Electrochem. Soc.* **1995**, *142*, 2914.
(263) Kim, Y.; Park, S. *J. Electrochem. Soc.* **2001**, *148*, A194.
(264) Huang, W.; Frech, R. *J. Electrochem. Soc.* **1998**, *145*, 765.

(265) Inaba, M.; Siroma, Z.; Funabiki, A.; Ogumi, Z.; Abe, T.; Mizutani, Y.; Asano, M. *Langmuir* **1996**, *12*, 1535.
(266) Chu, A. C.; Josefowicz, J. Y.; Farrington, G. C. *J. Electrochem. Soc.* **1997**, *144*, 4161.
(267) Hirasawa, K. A.; Sato, T.; Asahina, H.; Yamaguchi, S.; Mori, S. *J. Electrochem. Soc.* **1997**, *144*, L81.
(268) Alliata, D.; Kötz, R.; Novák, P.; Siegenthaler, H. *Electrochem. Commun.* **2000**, *2*, 436.
(269) Inaba, M.; Siroma, Z.; Kawatate, Y.; Funabiki, A.; Ogumi, Z. *J. Power Sources* **1997**, *68*, 221.
(270) Peled, E.; Golodnitsky, D.; Ardel, G. *J. Electrochem. Soc.* **1997**, *144*, L208.
(271) Ein-Eli, Y.; McDevitt, S. F.; Laura, R. *J. Electrochem. Soc.* **1998**, *145*, L1.
(272) Ein-Eli, Y. *Electrochem. Solid-State Lett.* **1999**, *2*, 212.
(273) Aurbach, D.; Markovsky, B.; Gamolsky, K.; Levi, E.; Ein-Eli, Y. *Electrochim. Acta* **1999**, *45*, 67.
(274) Aurbach, D.; Levi, M. D.; Levi, E.; Schechter, A. *J. Phys. Chem. B* **1997**, *101*, 2195.
(275) Aurbach, D.; Teller, H.; Levi, E. *J. Electrochem. Soc.* **2002**, *149*, A1255.
(276) Chung, G.; Kim, H.; Jun, S.; Kim, M. *Electrochem. Commun.* **1999**, *1*, 493.
(277) Andersson, A. M.; Edström, K. *J. Electrochem. Soc.* **2001**, *148*, A1100.
(278) Zhuang, G.; Ross, P. *Electrochem. Solid-State Lett.* **2003**, *6*, A136.
(279) Aurbach, D.; Markovsky, B.; Schechter, A.; Ein Eli, Y. *J. Electrochem. Soc.* **1996**, *143*, 3809.
(280) Naji, A.; Ghanbaja, J.; Humbert, B.; Willmann, P.; Billaud, D. *J. Power Sources* **1996**, *63*, 33.
(281) Bar-Tow, D.; Peled, E.; Burstein, L. *J. Electrochem. Soc.* **1999**, *146*, 824.
(282) Kanamura, K.; Tamura, H.; Takehara, Z. *J. Electroanal. Chem.* **1992**, *333*, 127.
(283) Kanamura, K.; Tamura, H.; Shiraishi, S.; Takehara, Z. *J. Electroanal. Chem.* **1995**, *394*, 49.
(284) Lee, C.; Mun, B.; Ross, P. N. *J. Electrochem. Soc.* **2002**, *149*, A1286.
(285) Zhang, X.; Pugh, J. K.; Ross, P. N. *Electrochem. Solid-State Lett.* **2001**, *4*, A82.
(286) Imhof, R.; Novák, P. *J. Electrochem. Soc.* **1998**, *145*, 1081.
(287) Zhang, S.; Ding, M. S.; Xu, K.; Allen, J.; Jow, T. R. *Electrochem. Solid-State Lett.* **2001**, *4*, A206.
(288) Some metal oxide structures are unstable when over-delithiated, and as a consequence, the crystal lattice collapses to form a new phase that is electrochemically inactive. Examples are the so-called "Jahn−Teller effect" for spinel cathodes and similar behavior for $LiNiO_2$ and $LiCoO_2$ materials as well. These irreversible processes are considered to be caused by the intrinsic properties of the crystalline materials instead of electrolytes and are, therefore, beyond the scope of the current review. See ref 46 for a detailed review.
(289) Mansour, A. *Surf. Sci. Spectrosc.* **1996**, *3*, 279.
(290) Aurbach, D.; Levi, M. D.; Levi, E.; Teller, H.; Markovsky, B.; Salitra, G.; Heider, U.; Heider, L. *J. Electrochem. Soc.* **1998**, *145*, 3024.
(291) Aurbach, D. *J. Power Sources* **2000**, *89*, 206.
(292) Aurbach, D.; Gamolsky, K.; Markovsky, B.; Salitra, G.; Gofer, Y.; Heider, U.; Oesten, R.; Schmidt, M. *J. Electrochem. Soc.* **2000**, *147*, 1322.
(293) Eriksson, T.; Andersson, A. M.; Bishop, A. G.; Gejke, C.; Gustafsson, T.; Thomas, J. O. *J. Electrochem. Soc.* **2002**, *149*, A69.
(294) Andersson, A. M.; Abraham, D. P.; Haasch, R.; MacLaren, S.; Liu, J.; Amine, K. *J. Electrochem. Soc.* **2002**, *149*, A1358.
(295) Thomas, M. G. S. R.; Bruce, P. G.; Goodenough, J. B. *J. Electrochem. Soc.* **1985**, *132*, 1521.
(296) Jang, D. H.; Shin, Y. J.; Oh, S. M. *J. Electrochem. Soc.* **1996**, *143*, 2204.
(297) Xia, Y.; Zhou, Y.; Yoshio, M. *J. Electrochem. Soc.* **1997**, *144*, 2593.
(298) Zhang, X.; Ross, P. N.; Kostecki, R.; Kong, F.; Sloop, S.; Kerr, J. B.; Striebel, K.; Cairns, E. J.; McLarnon, F. *J. Electrochem. Soc.* **2001**, *148*, A463.
(299) Wang, Y.; Guo, X.; Greenbaum, S.; Liu, J.; Amine, K. *Electrochem. Solid-State Lett.* **2001**, *4*, A68.
(300) Matsuo, Y.; Kostecki, R.; McLarnon, F. *J. Electrochem. Soc.* **2001**, *148*, A687.
(301) Du Pasquier, A.; Blyr, A.; Courjal, P.; Larcher, D.; Amatucci, G.; Gérand, B.; Tarascon, J. M. *J. Electrochem. Soc.* **1999**, *146*, 428.
(302) Balasubramanian, M.; Lee, H. S.; Sun, X.; Yang, X. Q.; Moodenbaugh, A. R.; McBreen, J.; Fischer, D. A.; Fu, Z. *Electrochem. Solid-State Lett.* **2002**, *5*, A22.
(303) Zhang, S. S.; Xu, K.; Jow, T. R. *Electrochem. Solid-State Lett.* **2002**, *5*, A92.
(304) Zhang, S. S.; Xu, K.; Jow, T. R. *J. Electrochem. Soc.* **2002**, *149*, A1521.
(305) Croce, F.; Nobili, F.; Deptula, A.; Lada, W.; Tossici, R.; D'Epifanio, A.; Scrosati, B.; Marassi. *Electrochem. Commun.* **1999**, *1*, 605.

(306) Rasch, B.; Cattaneo, E.; Novak, P.; Vielstich, W. *Electrochim. Acta* **1991**, *36*, 1397.
(307) Kanamura, K.; Toriyama, S.; Shiraishi, S.; Takehara, Z. *J. Electrochem. Soc.* **1995**, *142*, 1383.
(308) Ossola, F.; Pistoia, G.; Seeber, R.; Ugo, P. *Electrochim. Acta* **1988**, *33*, 47.
(309) Matsuta, S.; Kato, Y.; Ota, T.; Kurokawa, H.; Yoshimura, S.; Fujitani, S. *J. Electrochem. Soc.* **2001**, *148*, A7.
(310) Blyr, A.; Sigala, C.; Amatucci, G.; Guyomard, D.; Chabre, Y.; Tarascon, T. M. *J. Electrochem. Soc.* **1998**, *145*, 194.
(311) Cattaneo, E.; Ruch, J. *J. Power Sources* **1993**, *43/44*, 341.
(312) Imhof, R.; Novák, P. *J. Electrochem. Soc.* **1999**, *146*, 1702.
(313) Sun, X.; Lee, H. S.; Lee, S.; Yang, X. Q.; McBreen, J. *Electrochem. Solid-State Lett.* **1998**, *1*, 239.
(314) Xu, K.; Angell, C. A. *J. Electrochem. Soc.* **2002**, *149*, A920.
(315) Fey, G. T.; Li, W.; Dahn, J. R. *J. Electrochem. Soc.* **1994**, *141*, 2279.
(316) Seel, J. A.; Dahn, J. R. *J. Electrochem. Soc.* **2000**, *147*, 892.
(317) Lu, Z. H.; Dahn, J. R. *J. Electrochem. Soc.* **2001**, *148*, A710.
(318) Shembel, E. M.; Apostolova, R. D.; Strizhko, A. S.; Belosokhov, A. I.; Naumenko, A. F.; Rozhkov, V. V. *J. Power Sources* **1995**, *54*, 421.
(319) Zhang, S. S.; Ding, M. S.; Jow, T. R. *J. Power Sources* **2001**, *102*, 16.
(320) Lopez, S.; Petit, J. P.; Dunlop, H. M.; Butruille, J. R.; Tourillon, G. *J. Electrochem. Soc.* **1998**, *145*, 823.
(321) Braithwaite, J. W.; Gonzales, A.; Nagasubramanian, G.; Lucero, S. J.; Peebles, D. E.; Ohlhausen, J. A.; Cieslak, W. R. *J. Electrochem. Soc.* **1999**, *146*, 448.
(322) Chen, Y.; Devine, T. M.; Evans, J. W.; Monteiro, O. R.; Brown, I. G. *J. Electrochem. Soc.* **1999**, *146*, 1310.
(323) Munshi, M. Z. A.; Gopalienger, R.; Owens, B. B. *Solid State Ionics* **1988**, *27*, 259.
(324) Xu, K.; Zhang, S.; Poese, B. A.; Jow, T. R. *Electrochem. Solid-State Lett.* **2002**, *5*, A259.
(325) Diard, J. P.; LeCanut, J. M.; LeGorrec, B.; Montella, C. *Electrochim. Acta* **1998**, *43*, 2469.
(326) Casparac, R.; Martin, C. R.; Lisac, E. S.; Mandic, Z. *J. Electrochem. Soc.* **2000**, *147*, 991.
(327) Kanamura, K.; Okagawa, T.; Takehara, Z. *J. Power Sources* **1995**, *57*, 119.
(328) Atanasoski, R. T.; Law, H. H.; Tobias, C. W. *Electrochim. Acta* **1987**, *32*, 877.
(329) Atanasoski, R. T.; Serb, J. *J. Chem. Soc.* **1992**, *57*, 935.
(330) Christe, K. O.; Dixon, D. A.; McLemore, D.; Wilson, W. W.; Sheehy, J. A.; Boatz, J. *J. Fluorine Chem.* **2000**, *101*, 151.
(331) Polypropylene or stainless steel containers are normally used, but glass containers can be severely corroded by $LiPF_6$-containing electrolytes, because the formation of gaseous $SiF_4$ serves as the driving force for the reaction between the fluorinated Lewis acids $PF_5$ or HF and the main composition of glass $Na_2SiO_3$.
(332) Vogdanis, L.; Heitz, W. *Macromol. Rapid Commun.* **1986**, *7*, 543.
(333) Vogdanis, L.; Martens, B.; Uchtmann, H.; Hensel, F.; Heitz, W. *Macromol. Chem.* **1990**, *191*, 465.
(334) Terasaki, M.; Yosjida, H.; Tukamoto, H.; Mizutani, M.; Yamachi, M. *Denki Kagaku* **1993**, *61*, 1417.
(335) Ohta, A.; Koshina, H.; Okuno, H.; Murai, H. *J. Power Sources* **1995**, *54*, 6.
(336) Takeuchi, E. S.; Gan, H.; Palazzo, M.; Leising, R. A.; Davis, S. M. *J. Electrochem. Soc.* **1997**, *144*, 1944.
(337) Endo, E.; Ata, M.; Sekai, K.; Tanaka, K. *J. Electrochem. Soc.* **1999**, *146*, 49.
(338) Du Pasquier, A.; Disma, F.; Bowmer, T.; Gozdz, A. S.; Amatucci, G.; Tarascon, J. M. *J. Electrochem. Soc.* **1998**, *145*, 472.
(339) Zheng, T.; Gozdz, A. S.; Amatucci, G. G. *J. Electrochem. Soc.* **1999**, *146*, 4014.
(340) Richard, M. N.; Dahn, J. R. *J. Electrochem. Soc.* **1999**, *146*, 2068.
(341) Richard, M. N.; Dahn, J. R. *J. Electrochem. Soc.* **1999**, *146*, 2078.
(342) MacNeil, D. D.; Larcher, D.; Dahn, J. R. *J. Electrochem. Soc.* **1999**, *146*, 3596.
(343) Pistoia, G.; Antonini, A.; Rosati, R.; Zane, D. *Electrochim. Acta* **1996**, *41*, 2683.
(344) Amatucci, G. G.; Schmutz, C. N.; Blyr, A.; Sigala, C.; Gozdz, A. S.; Larcher, D.; Tarascon, J. M. *J. Power Sources* **1997**, *69*, 11.
(345) Antonini, A.; Bellito, C.; Pasquali, M.; Pistoia, G. *J. Electrochem. Soc.* **1998**, *145*, 2726.
(346) Tsunekawa, H.; Tanimoto, S.; Marubayashi, R.; Fujita, M.; Kifune, K.; Sano, M. *J. Electrochem. Soc.* **2002**, *149*, A1326.
(347) Levy, S. C.; Bro, P. *Battery Hazards and Accident Prevention*; Plenum Press: New York, 1994; p 115.
(348) von Sacken, U.; Nodwell, E.; Sundher, A.; Dahn, J. *Solid State Ionics* **1994**, *69*, 284.
(349) Chen, Y.; Evans, J. W. *J. Electrochem. Soc.* **1996**, *143*, 2708.
(350) Song, L.; Evans, J. W. *J. Electrochem. Soc.* **1998**, *145*, 2327.
(351) Tobishima, S.; Yamaki, J. *J. Power Sources* **1999**, *81/82*, 882.
(352) Leising, R. A.; Palazzo, M.; Takeuchi, E. S.; Takeuchi, K. J. *J. Electrochem. Soc.* **2001**, *148*, A838.
(353) Hasegawa, K.; Arakawa, Y. *J. Power Sources* **1993**, *43/44*, 523.

(354) Gee, M. A.; Laman, F. C. *J. Electrochem. Soc.* **1993**, *140*, L53.
(355) Chen, Y.; Evans, J. W. *J. Electrochem. Soc.* **1994**, *141*, 2947.
(356) Newman, J.; Tiedemann, W. *J. Electrochem. Soc.* **1995**, *142*, 1054.
(357) Pals, C. R.; Newman, J. *J. Electrochem. Soc.* **1995**, *142*, 3274.
(358) Pals, C. R.; Newman, J. *J. Electrochem. Soc.* **1995**, *142*, 3282.
(359) Joho, F.; Novák, P.; Spahr, M. E. *J. Electrochem. Soc.* **2002**, *149*, A1020.
(360) Maleki, H.; Al Hallaj, S.; Selman, J. R.; Dinwiddie, R. B.; Wang, H. *J. Electrochem. Soc.* **1999**, *146*, 947.
(361) Maleki, H.; Deng, G.; Anani, A.; Howard, J. *J. Electrochem. Soc.* **1999**, *146*, 3224.
(362) Zhang, Z.; Fouchard, D.; Rea, J. R. *J. Power Sources* **1998**, *70*, 16.
(363) Biensan, P.; Simon, B.; Pérès, J. P.; de Guibert, A.; Brousely, M.; Bodet, J. M.; Perton, F. *J. Power Sources* **1999**, *81/82*, 906.
(364) Dahn, J. R.; Fuller, E. W.; Obrovac, M.; von Sacken, U. *Solid State Ionics* **1994**, *69*, 265.
(365) Arai, H.; Okada, S.; Sakurai, Y.; Yamaki, J. *J. Electrochem. Soc.* **1997**, *144*, 3117.
(366) Schilling, O.; Dahn, J. R. *J. Electrochem. Soc.* **1998**, *145*, 569.
(367) MacNeil, D. D.; Christensen, L.; Landucci, J.; Paulsen, J. M.; Dahn, J. R. *J. Electrochem. Soc.* **2000**, *147*, 970.
(368) MacNeil, D. D.; Hatchard, T. D.; Dahn, J. R. *J. Electrochem. Soc.* **2001**, *148*, A663.
(369) MacNeil, D. D.; Dahn, J. R. *J. Electrochem. Soc.* **2001**, *148*, A1205.
(370) MacNeil, D. D.; Dahn, J. R. *J. Electrochem. Soc.* **2001**, *148*, A1211.
(371) MacNeil, D. D.; Dahn, J. R. *J. Electrochem. Soc.* **2003**, *150*, A21.
(372) Matsuda, Y. *J. Power Sources* **1993**, *43*, 1.
(373) Hirai, T.; Yoshimatsu, I.; Yamaki, J. *J. Electrochem. Soc.* **1994**, *141*, 2300.
(374) Kovač, M.; Milićev, S.; Kovač, A.; Pejovnik, S. *J. Electrochem. Soc.* **1995**, *142*, 1390.
(375) Mogi, R.; Inaba, M.; Jeong, S.; Iriyama, Y.; Abe, T.; Ogumi, Z. *J. Electrochem. Soc.* **2002**, *149*, 2002.
(376) Besenhard, J. O.; Wagner, M. W.; Winter, M.; Jannakoudakis, A. D.; Jannakoudakis, P. D.; Theodoridou, E. *J. Power Sources* **1993**, *43/44*, 413.
(377) Gong, J. B.; Tsumura, T.; Nakamura, H.; Yoshio, M.; Yoshitake, H.; Abe, T. *202nd Meeting of the Electrochemical Society,* Salt Lake City, UT, Oct 20−24, 2002; Abstract No. 200; Electrochemical Society: Pennington, NJ.
(378) Izatt, R. M.; Bradshaw, J. S.; Nielsen, S. A.; Lamb, J. D.; Christensen, J. J. *Chem. Rev.* **1985**, *85*, 271.
(379) Morita, M.; Hayashida, H.; Matsuda, Y. *J. Electrochem. Soc.* **1987**, *134*, 2107.
(380) Nagasubramanian, G.; Di Stefano, S. *J. Electrochem. Soc.* **1990**, *137*, 3830.
(381) Salomom, M. *J. Solution Chem.* **1990**, *19*, 1225.
(382) Nagasubramanian, G.; Attia, A. I.; Halpert, G. *J. Electrochem. Soc.* **1992**, *139*, 3043.
(383) Lonergan, M. C.; Ratner, M. A.; Shriver, D. *J. Am. Chem. Soc.* **1995**, *117*, 2344.
(384) Lee, H. S.; Yang, X. Q.; McBreen, J.; Choi, L. S.; Okamoto, Y. *J. Electrochem. Soc.* **1996**, *143*, 3825.
(385) Lee, H. S.; Sun, X.; Yang, X. Q.; McBreen, J.; Callahan, J. H.; Choi, L. S. *J. Electrochem. Soc.* **2000**, *146*, 9.
(386) Lee, H. S.; Yang, X. Q.; Xiang, C. L.; McBreen, J.; Choi, L. S. *J. Electrochem. Soc.* **1998**, *145*, 2813.
(387) Sun, X.; Lee, H. S.; Yang, X. Q.; McBreen, J. *J. Electrochem. Soc.* **1999**, *146*, 3655.
(388) Sun, X.; Lee, H. S.; Yang, X. Q.; McBreen, J. *J. Electrochem. Soc.* **2002**, *149*, A355.
(389) Sun, X.; Lee, H. S.; Yang, X. Q.; McBreen, J. *Electrochem. Solid-State Lett.* **2001**, *4*, A184.
(390) Sun, X.; Lee, H. S.; Yang, X. Q.; McBreen, J. *Electrochem. Solid-State Lett.* **2002**, *5*, A248.
(391) Sun, X.; Lee, H. S.; Yang, X. Q.; McBreen, J. *Electrochem. Solid-State Lett.* **2003**, *6*, A43.
(392) Lee, H. S.; Sun, X.; Yang, X. Q.; McBreen, J. *J. Electrochem. Soc.* **2002**, *149*, A1460.
(393) Tasaki, K.; Nakamura, S. *J. Electrochem. Soc.* **2001**, *148*, A984.
(394) Morita, M.; Ishikawa, M.; Matsuda, Y. In *Lithium Ion Batteries: Fundamentals and Performance*; Wakihara, M., Yamamoto, O., Eds.; Wiley-VCH: New York, 1999; p 156.
(395) Ein-Eli, Y.; Thomas, S. R.; Koch, V. R. *J. Electrochem. Soc.* **1996**, *143*, L195.
(396) Ein-Eli, Y.; Thomas, S. R.; Koch, V. R. *J. Electrochem. Soc.* **1997**, *144*, 1159.
(397) Wilkinson, D.; Dahn, J. R. U.S. Patent 5,130,211, 1992.
(398) Shu, Z. X.; McMillan, R. S.; Murray, J. J. *J. Electrochem. Soc.* **1993**, *140*, L101.
(399) Wrodnigg, G. H.; Besenhard, J. O.; Winter, M. *J. Electrochem. Soc.* **1999**, *146*, 470.
(400) Simon, B.; Boeuve, J.-P. U.S. Patent 5,626,981, 1997.
(401) Barker, J.; Gao, F. U.S. Patent 5,712,059, 1998.
(402) Naruse, Y.; Fujita, S.; Omaru, A. U.S. Patent 5,714,281, 1998.

(403) Jehoulet, C.; Biensan, P.; Bodet, J. M.; Broussely, M.; Moteau, C.; Tessier-Lescourret, C. In *Batteries for Portable Applications and Electric Vehicles*; Holmes, C. F., Landgrebe, A. R., Eds.; The Electrochemical Society Proceeding Series; Pennington, NJ, 1997; P. V. 97-18, P974.
(404) Aurbach, D.; Gamolsky, K.; Markovsky, B.; Gofer, Y.; Schmidt, M.; Heider, U. *Electrochim. Acta* **2002**, *47*, 1423.
(405) Contestabile, M.; Morselli, M.; Paraventi, R.; Neat, R. J. *J. Power Sources* **2003**, *119/121*, 943.
(406) Herreyre, S.; Huchet, O.; Barusseau, S.; Perton, F.; Bodet, J. M.; Biensan, Ph. *J. Power Sources* **2001**, *97/98*, 576.
(407) Broussely, M.; Blanchard, P.; Biensan, Ph.; Planchat, J. P.; Nechev, K.; Staniewicz, R. J. *J. Power Sources* **2003**, *119/121*, 859.
(408) Oesten, R.; Heider, U.; Schmid, M. *Solid State Ionics* **2002**, *148*, 391.
(409) Wang, C.; Nakamura, H.; Komatsu, H.; Yoshio, M.; Yoshitake, H. *J. Power Sources* **1998**, *74*, 142.
(410) Naji, A.; Ghanbaja, J.; Willmann, P.; Billaud, D. *Electrochim. Acta* **2000**, *45*, 1893.
(411) Matsuo, Y.; Fumita, K.; Fukutsuka, T.; Sugie, Y.; Koyama, H.; Inoue, K. *J. Power Sources* **2003**, *119/121*, 373.
(412) Santer, H. J.; Möller, K.-C.; Ivanco, J.; Ramsey, M. G.; Netzer, F. P.; Yamaguchi, S.; Besenhard, J. O.; Winter, M. *J. Power Sources* **2003**, *119/121*, 368.
(413) Möller, K.-C.; Santer, H. J.; Kern, W.; Yamaguchi, S.; Besenhard, J. O.; Winter, M. *J. Power Sources* **2003**, *119/121*, 561.
(414) Holleck, G. L.; Harris, P. B.; Abraham, K. M.; Buzby, J.; Brummer, S. B. Technical Report No. 6, Contract N00014-77-0155; EIC Laboratories: Newton, MA, 1982.
(415) Abraham, K. M.; Brummer, S. B. In *Lithium Batteries*; Gabano, J., Ed.; Academic Press: New York, 1983.
(416) Narayanan, S. R.; Surampudi, S.; Attia, A. I.; Bankston, C. P. *J. Electrochem. Soc.* **1991**, *138*, 2224.
(417) Abraham, K. M.; Pasquariello, D. M.; Willstädt, E. B. *Proceedings of the 33rd International Power Sources Symposium*, Cherry Hill, NJ, June 13−16, 1988; The Electrochemical Society, Inc.: 1988; p 38.
(418) Behl, W. K.; Chin, D. T. *J. Electrochem. Soc.* **1988**, *135*, 16.
(419) Behl, W. K.; Chin, D. T. *J. Electrochem. Soc.* **1988**, *135*, 21.
(420) Behl, W. K. *J. Electrochem. Soc.* **1989**, *136*, 2305.
(421) Abraham, K. M.; Pasquariello, D. M. U.S. Patent, 4,857,423, 1989.
(422) Abraham, K. M.; Pasquariello, D. M.; Willstaedt, E. B. *J. Electrochem. Soc.* **1990**, *137*, 1856.
(423) Abraham, K. M. *Electrochim. Acta* **1993**, *38*, 1233.
(424) Mason, J. G.; Rosenblum, M. *J. Am. Chem. Soc.* **1960**, *82*, 4206.
(425) Wilkinson, D. P.; Dudley, J.; Golovin, N. In *Rechargeable Lithium Batteries*; Subbarao, S., Koch, V. R., Owens, B. B., Smyrl, W. H., Eds.; The Electrochemical Society: Pennington, NJ, 1990; PV 90-5, p 77.
(426) Abraham, K. M. In *Rechargeable Lithium Batteries*; Subbarao, S., Koch, V. R., Owens, B. B., Smyrl, W. H., Eds.; The Electrochemical Society: Pennington, NJ, 1990; PV 90-5, p 1.
(427) Cabrera, C. R.; Bard, A. J. *J. Electroanal. Chem.* **1989**, *273*, 147.
(428) Cha, C. S.; Ai, X. P.; Yang, H. X. *J. Power Sources* **1995**, *54*, 255.
(429) Golovin, M. N.; Wilkinson, D. P.; Dudley, J. T.; Holonko, D.; Woo, S. *J. Electrochem. Soc.* **1992**, *139*, 5.
(430) Halpert, G.; Surampudi, S.; Shen, D.; Huang, C. K.; Narayanan, S.; Vamos, E.; Perrone, D. *J. Power Sources* **1994**, *47*, 287.
(431) Richardson, T. J.; Ross, P. N. *J. Electrochem. Soc.* **1996**, *143*, 3992.
(432) Adachi, M.; Tanaka, K.; Sekai, K. *J. Electrochem. Soc.* **1999**, *146*, 1256.
(433) Hammerich, O.; Parker, V. D. *Electrochim. Acta* **1973**, *18*, 537.
(434) Kerr, J. B.; Tian, M. U.S. Patent 6,045,952, 2000.
(435) Mao, H.; Wainwright, D. S. Canadian Patent 2,205,683, 1997.
(436) Yoshio, M.; Yoshitake, H.; Abe, K. *204th Meeting of Electrochemical Society*, Orlando, FL, Oct 12−16, 2003; Abstract No. 280.
(437) Kuboki, T.; Ohsaki, T. U. S. Patent 6,413,679, 2002.
(438) Reimers, J. N.; Way, B. M. U.S. Patent 6,074,777, 2000.
(439) Mao, H. Canadian Patent 2,163,187, 1995.
(440) Yoshino, A. In *Proceedings of the 4th Hawaii Battery Conference*, ARAD Enterprises, Hilo, HI, Jan 8, 2002; ARAD Enterprises: Hilo, HI; p 102.
(441) Besenhard, J. O.; von Werner, K.; Winter, M. US. Patent 5,-916,708, 1999.
(442) McMillan, R.; Slegr, H.; Shu, Z. X.; Wang, W. *J. Power Sources* **1999**, *81/82*, 20.
(443) Inaba, M.; Kawatate, Y.; Funabiki, A.; Jeong, S. K.; Abe, T.; Ogumi, Z. *Electrochim. Acta* **1999**, *45*, 99.
(444) Petrella, R. V. In *Flame Retardant Polymeric Materials*; Lewin, M., Atlas, S. M., Pearce, E. M., Eds.; Plenum Publishing: New York, 1978; Vol. 2, p 159.
(445) Cullis, C. F.; Hirshler, M. M. *The Combustion of Organic Polymers*; Clarendon Press: Oxford, 1981.
(446) Shu, Z. X.; McMillan, R. S.; Murray, J. J.; Davidson, I. J. *J. Electrochem. Soc.* **1995**, *142*, L161.

(447) Shu, Z. X.; McMillan, R. S.; Murray, J. J.; Davidson, I. J. *J. Electrochem. Soc.* **1996**, *143*, 2230.

(448) For this reason ClEC and FEC were treated as cosolvents in this review, instead of as additives as they were in most literature sources.

(449) Winter, M.; Novák, P. *J. Electrochem. Soc.* **1998**, *145*, L27.

(450) Naji, A.; Ghanbaja, J.; Willmann, P.; Billaud, D. *J. Power Sources* **1999**, *81/82*, 207.

(451) Winter, M.; Imhof, R.; Joho, F.; Noák, P. *J. Power Sources* **1999**, *81/82*, 818.

(452) Nagasubramanian, G. The 1999 Joint International Meeting of the Electrochemical Society, Honolulu, HI, Oct 17−22, 1999; Abstract 334; Electrochemical Society: Pennington, NJ.

(453) Arai, J.; Katayama, H.; Akahoshi, H. *J. Electrochem. Soc.* **2002**, *149*, A217.

(454) Salomon, M.; Plichta, E. J. *Electrochim. Acta* **1985**, *30*, 113.

(455) Chagnes, A.; Carré, B.; Willmann, P.; Lemordant, D. *J. Power Sources* **2002**, *109*, 203.

(456) Fukushima, T.; Matsuda, Y.; Hashimoto, H.; Arakawa, R. *J. Power Sources* **2002**, *110*, 34.

(457) Rendek, L. J.; Chottiner, G. S.; Scherson, D. A. *J. Electrochem. Soc.* **2003**, *150*, A326.

(458) Takami, N.; Sekino, M.; Ohsaki, T.; Kanda, M.; Yamamoto, M. *J. Power Sources* **2001**, *97/98*, 677.

(459) Lanz, M.; Novák, P. *J. Power Sources* **2001**, *102*, 277.

(460) Chagnes, A.; Carré, B.; Willmann, P.; Dedryvére, R.; Gonbeau, D.; Lemordant, D. *J. Electrochem. Soc.* **2003**, *150*, A1255.

(461) Smart, M. C.; Ratnakumar, B. V.; Surampudi, S.; Wang, Y.; Zhang, X.; Greenbaum, S. G.; Hightower, A.; Ahn, C. C.; Fultz, B. *J. Electrochem. Soc.* **1999**, *146*, 3963.

(462) Smart, M. C.; Ratnakumar, B. V.; Surampudi, S. *J. Electrochem. Soc.* **2002**, *149*, A361.

(463) Vetter, J.; Novák, P. *J. Power Sources* **2003**, *119/121*, 338.

(464) Nakajima, T.; Dan, K.; Koh, M. *J. Fluorine Chem.* **1998**, *87*, 221.

(465) Yamaki, J.-I.; Yamazaki, I.; Egashira, M.; Okada, S. *J. Power Sources* **2001**, *102*, 288.

(466) Smart, M. C.; Ratnakumar, B. V.; Ryan-Mowrey, V. S.; Surampudi, S.; Prakash, G. K. S.; Hu, J.; Cheung, I. *J. Power Sources* **2003**, *119/121*, 359.

(467) Zhang, S. S.; Angell, C. A. *J. Electrochem. Soc.* **1996**, *143*, 4047.

(468) Choquette, Y.; Brisard, G.; Parent, M.; Brouillette, D.; Perron, G.; Desnoyers, J. E.; Armand, M.; Gravel, D.; Slougui, N. *J. Electrochem. Soc.* **1998**, *145*, 3500.

(469) Matsuda, Y.; Morita, M.; Yamada, K.; Hirai, K. *J. Electrochem. Soc.* **1985**, *132*, 2538.

(470) Morita, M.; Okada, Y.; Matsuda, Y. *J. Electrochem. Soc.* **1987**, *134*, 2665.

(471) Bach, S.; Baffier, N.; Pereira-Ramos, J. P.; Messina, R. *J. Power Sources* **1993**, *43/44*, 569.

(472) Yan, W.; Lerner, M. M. *J. Electrochem. Soc.* **2001**, *148*, D83.

(473) Park, S. H.; Winnick, J.; Kohl, P. A. *J. Electrochem. Soc.* **2002**, *149*, A1196.

(474) Dominey, L. A. U.S. Patent, 5,273,840, 1993.

(475) Barthel, J.; Wühr, M.; Buestrich, R.; Gores, H. J. *J. Electrochem. Soc.* **1995**, *142*, 2527.

(476) Barthel, J.; Buestrich, R.; Carl, E.; Gores, H. J. *J. Electrochem. Soc.* **1996**, *143*, 3565.

(477) Barthel, J.; Buestrich, R.; Carl, E.; Gores, H. J. *J. Electrochem. Soc.* **1996**, *143*, 3572.

(478) Barthel, J.; Buestrich, R.; Gores, H. J.; Schmidt, M.; Wühr, M. *J. Electrochem. Soc.* **1997**, *144*, 3866.

(479) Barthel, J.; Schmidt, M.; Gores, H. J. *J. Electrochem. Soc.* **1998**, *145*, L17.

(480) Barthel, J.; Schmidt, M.; Gores, H. J. *J. Electrochem. Soc.* **2000**, *147*, 21.

(481) Sasaki, Y.; Handa, M.; Kurashima, K.; Tonuma, T.; Usami, K. *J. Electrochem. Soc.* **2001**, *148*, A999.

(482) Handa, M.; Fukuda, S.; Sasaki, Y.; Usami, K. *J. Electrochem. Soc.* **1997**, *144*, L235.

(483) Xu, W.; Angell, C. A. *Electrochem. Solid-State Lett.* **2000**, *3*, 366.

(484) Xu, W.; Angell, C. A. *Solid State Ionics* **2002**, *147*, 295.

(485) Videa, M.; Xu, W.; Geil, B.; Marzke, R.; Angell, C. A. *J. Electrochem. Soc.* **2001**, *148*, A1352.

(486) Xu, W.; Shusterman, A.; Videa, M.; Velikov, V.; Marzke, R. L.; Angell, C. A. *J. Electrochem. Soc.* **2003**, *150*, E74.

(487) Lischka, U.; Wietelmann, U.; Wegner, M. DE 19829030 C1, 1999.

(488) Xu, K.; Zhang, S.; Jow, T. R. *Electrochem. Solid-State Lett.* **2003**, *6*, A117.

(489) Xu, K.; Lee, U.; Zhang, S.; Wood, M.; Jow, T. R. *Electrochem. Solid-State Lett.* **2003**, *6*, A144.

(490) Amine, K.; Liu, J.; Kang, S.; Belharouak, I.; Hyung, Y.; Vissers, D.; Henriksen, G. *J. Power Sources* **2004**, *129*, 14.

(491) Jiang, J.; Dahn, J. R. *Electrochem. Solid-State Lett.* **2003**, *6*, A180.

(492) Jow, T. R.; Ding, M. S.; Xu, K.; Zhang, S. S.; Allen, J. L.; Amine, K.; Henriksen, G. L. *J. Power Sources* **2003**, *119/121*, 343.

(493) Yamaguchi, H.; Takahashi, H.; Kato, M.; Arai, J. *J. Electrochem. Soc.* **2003**, *150*, A312.

(494) Handa, M.; Suzuki, M.; Suzuki, J.; Kanematsu, H.; Sasaki, Y. *Electrochem. Solid-State Lett.* **1999**, *2*, 60.

(495) Eberwein, M.; Schmidt, A.; Schmidt, M.; Zabel, M.; Burgemeister, T.; Barthel, J.; Kunz, W.; Gores, H. J. *J. Electrochem. Soc.* **2003**, *150*, A994.

(496) Sartori, P.; Ignatyev, N. The 194th Meeting of the Electrochemical Society, Boston, MA, Nov 1−6, 1998; Abstract 160.

(497) Sartori, P.; Ignatyev, N. U.S. Patent 6,210,830, 2001.

(498) Schmidt, M.; Heider, U.; Kuehner, A.; Oesten, R.; Jungnitz, M.; Ignat'ev, N.; Sartori, P. *J. Power Sources* **2001**, *97/98*, 557.

(499) (a) Gnanaraj, J. S.; Levi, M. D.; Gofer, Y.; Aurbach, D.; Schmidt, M. *J. Electrochem. Soc.* **2003**, *150*, A445. (b) Gnanaraj, J. S.; Zinigrad, E.; Asraf, L.; Sprecher, M.; Gottlieb, H. E.; Geissler, W.; Schmidt, M.; Aurbach, D. *Electrochem. Commun.* **2003**, *5*, 946.

(500) Gnanaraj, J. S.; Zinigrad, E.; Levi, M. D.; Aurbach, D.; Schmidt, M. *J. Power Sources* **2003**, *119/121*, 799.

(501) Egashira, M.; Scrosati, B.; Armand, M.; Béranger, S.; Michot, C. *Electrochem. Solid-State Lett.* **2003**, *6*, A71.

(502) Barbarich, T. J.; Driscoll, P. F. *Electrochem. Solid-State Lett.* **2003**, *6*, A113.

(503) Plichta, E. J.; Behl, W. K. *Proceedings of the 38th Power Source Conference*, Cherry Hill, NJ, 1998; p 444.

(504) Plichta, E. J.; Hendrickson, M.; Thompson, R.; Au, G.; Behl, W. K.; Smart, M. C.; Ratnakumar, B. V.; Surampudi, S. *J. Power Sources* **2001**, *94*, 160.

(505) Hamlen, R.; Au, G.; Brundage, M.; Hendrickson, M.; Plichta, E.; Slane, S.; Barbarello, J. *J. Power Sources* **2001**, *97/98*, 22.

(506) Nagasubramanian, G. *J. Appl. Electrochem.* **2001**, *31*, 99.

(507) Fan, J. *J. Power Sources* **2003**, *117*, 170.

(508) Smart, M. C.; Ratnakumar, B. V.; Surampudi, S. *J. Electrochem. Soc.* **1999**, *146*, 486.

(509) Shiao, H. C.; Chua, D.; Lin, H.; Slane, S.; Salomon, M. *J. Power Sources* **2000**, *87*, 167.

(510) Sawai, K.; Ohzuku, T. *J. Electrochem. Soc.* **2003**, *150*, A674.

(511) Wang, C.; Appleby, A. J.; Little, F. E. *J. Electrochem. Soc.* **2002**, *149*, A754.

(512) Zhang, S. S.; Xu, K.; Jow, T. R. *J. Power Sources* **2003**, *115*, 137.

(513) Huang, C.-K.; Sakamoto, J. S.; Wolfenstine, J.; Surampudi, S. *J. Electrochem. Soc.* **2000**, *147*, 2893.

(514) Gitzendanner, R.; Ehrlich, G.; Marsh, C.; Marsh, R. The 194th Meeting of the Electrochemical Society, Boston, MA, Nov 1−6, 1998; Abstract 157; Electrochemical Society: Pennington, NJ.

(515) Smart, M. C.; Ratnakumar, B. V.; Whitcanack, L. D.; Chin, K. B.; Surampudi, S.; Croft, H.; Tice, D.; Staniewicz, R. *J. Power Sources* **2003**, *119/121*, 349.

(516) The physical significance of the impedance response corresponding to the semicircle at lower frequency has been ambiguous. Conventionally it was assigned to the "charge-transfer" for the electrochemical reactions; hence, conceptually, it should not be influenced by electrolytes due to the presence of the electronically insulating surface films. However, experiences show that it is in fact readily affected by the chemical composition of the electrolytes; therefore, it should involve an interfacial process that is sensitive to the surface film formation. There was a suggestion (see ref 518) that the SEI is a mixed conductor for both ions and electrons, so that the electrons can transport across it to reach the redox reaction sites. This hypothesis is well able to explain why $R_{ct}$ is affected by SEI chemical composition, however, at the risk of overturning the fundamentals of lithium ion chemistry.

(517) Mohamedi, M.; Takahashi, D.; Itoh, T.; Uchida, I. *Electrochim. Acta* **2002**, *47*, 3483.

(518) Chen, C. H.; Liu, J.; Amine, K. *J. Power Sources* **2001**, *96*, 321.

(519) Roth, E. P.; Crafts, C. C.; Doughty, D. H. The 202nd Meeting of the Electrochemical Society, Salt Lake City, UT, Oct 20−24, 2002; Abstract 216.

(520) (a) Yokoyama, K.; Fujita, S.; Hiwara, A.; Naruse, Y.; Toriida, M.; Omaru, A. U.S. Patent 5,580,684, 1996. (b) Narang, S. C.; Ventura, S. C.; Dougherty, B. J.; Zhao, M.; Smedley, S.; Koolpe, G. U.S. Patent 5,830,600, 1998. (c) Narang, S. C.; Ventura, S. C.; Cox, P. U.S. Patent 6,168,885, 2001.

(521) Lyons, J. W. *The Chemistry and Uses of Flame Retardants*; John Wiley & Sons: New York, 1970.

(522) Cullis, C. F.; Hirshler, M. M. *The Combustion of Organic Polymers*; Clarendon Press: Oxford, 1981.

(523) Lee, C. W.; Venkatachalapathy, R.; Prakash, J. *Electrochem. Solid-State Lett.* **2000**, *3*, 63.

(524) Wang, X.; Yasukawa, E.; Kasuya, S. *J. Electrochem. Soc.* **2001**, *148*, A1058.

(525) Wang, X.; Yasukawa, E.; Kasuya, S. *J. Electrochem. Soc.* **2001**, *148*, A1066.

(526) Xu, K.; Ding, M. S.; Zhang, S.; Allen, J. L.; Jow, T. R. *J. Electrochem. Soc.* **2002**, *149*, A622.

(527) Xu, K.; Zhang, S.; Allen, J. L.; Jow, T. R. *J. Electrochem. Soc.* **2002**, *149*, A1079.

(528) Ding, M. S.; Xu, K.; Jow, T. R. *J. Electrochem. Soc.* **2002**, *149*, A1489.

(529) Xu, K.; Ding, M. S.; Zhang, S.; Allen, J. L.; Jow, T. R. *J. Electrochem. Soc.* **2003**, *150*, A161.
(530) Xu, K.; Zhang, S.; Allen, J. L.; Jow, T. R. *J. Electrochem. Soc.* **2003**, *150*, A170.
(531) Hyung, Y. E.; Vissers, D. R.; Amine, K. *J. Power Sources* **2003**, *119/121*, 383.
(532) Ota, H.; Kominato, A.; Chun, W.-J.; Yasukawa, E.; Kasuya, S. *J. Power Sources* **2003**, *119/121*, 393.
(533) Granzow, A. *Acc. Chem. Res.* **1978**, *11*, 177.
(534) Arai, J. *J. Electrochem. Soc.* **2003**, *150*, A219.
(535) Arai, J. *J. Power Sources* **2003**, *119/121*, 388.
(536) Ratner, M. A.; Shriver, D. F. *Chem. Rev.* **1988**, *88*, 109.
(537) Watanabe, M. In *Solid State Ionics: Materials and Applications*; Chowdari, B. V. R., Ed.; World Scientific Publishing Co.: Singapore, 1992; p 149.
(538) Sanchez, J.-Y. In *Solid State Ionics: Materials and Applications*; Chowdari, B. V. R., Ed.; World Scientific Publishing Co.: 1992; p 159.
(539) Armand, M. *Solid State Ionics* **1994**, *69*, 309.
(540) Shriver, D. F.; Bruce, P. G. In *Solid State Electrochemistry*; Bruce, P. G., Ed.; Cambridge University Press: Cambridge, U.K., 1995; p 95.
(541) Song, J. Y.; Wang, Y. Y.; Wan, C. C. *J. Power Sources* **1999**, *77,* 183.
(542) Dias, F. B.; Plomp, L.; Veldhuis, J. B. J. *J. Power Sources* **2000**, *88*, 169.
(543) (a) Fenton, D. E.; Parker, J. M.; Wright, P. V. *Polymer* **1973**, *14*, 589. (b) Wright, P. V. *Br. Polym. J.* **1975**, *7*, 319. (c) Wright, P. V. *J. Polym. Sci., Polym. Phys. Ed.* **1976**, *14*, 955.
(544) (a) Armand, M. B.; Chabagno, J. M.; Duclot, M. *The 2nd International Conference on Solid Electrolytes*, St. Andrews, Scotland, 1978; Abstract No. 65. (b) Armand, M. B.; Chabagno, J. M.; Duclot, M. In *Fast Ion Transport in Solids*; Duclot, M. J., Vashishta, P., Mundy, J. N., Shenoy, G. K., Eds.; North-Holland, Amsterdam, 1979.
(545) Angell, C. A.; Liu, C.; Sanchez, E. *Nature* **1993**, *362*, 137.

(546) Angell, C. A.; Fan, J.; Liu, C.; Lu, Q.; Sanchez, E.; Xu, K. *Solid State Ionics* **1994**, *69*, 343.
(547) Angell, C. A.; Xu, K.; Zhang, S.-S.; Videa, M. *Solid State Ionics* **1996**, *86/88*, 17.
(548) Imrie, C. T.; Ingram, M. D.; McHattie, G. S. *J. Phys. Chem. B* **1999**, *103*, 4132.
(549) Zheng, Y.; Chia, F.; Ungar, G.; Wright, P. V. *Chem. Commun.* **2000**, *16*, 1459.
(550) Anderman, M. *Solid State Ionics* **1994**, *69*, 336.
(551) Scrosati, B.; Croce, F.; Persi, L. *J. Electrochem. Soc.* **2000**, *147,* 1718.
(552) Persi, L.; Croce, F.; Scrosati, B.; Plichta, E.; Hendrickson, M. A. *J. Electrochem. Soc.* **2002**, *149*, A212.
(553) Pamero, S.; Satolli, D.; D'Epifano, A.; Scrosati, B. *J. Electrochem. Soc.* **2002**, *149*, A414.
(554) Aihara, Y.; Appetecchi, G. B.; Scrosati, B. *J. Electrochem. Soc.* **2002**, *149*, A849.
(555) Appetecchi, G. B.; Aihara, Y.; Scrosati, B. *J. Electrochem. Soc.* **2003**, *150*, A301.
(556) Tarascon, J.-M.; Gozdz, A. S.; Schmutz, C.; Shokoohi, F.; Warren, P. C. *Solid State Ionics* **1996**, *86/88*, 49.
(557) Feuillade, G.; Perche, P. *J. Appl. Electrochem.* **1975**, *63*, 5.
(558) Tsuchida, E.; Ohno, H.; Tsunemi, K. *Electrochim. Acta* **1983**, *28*, 591.
(559) Tsunemi, K.; Ohno, H.; Tsuchida, E. *Electrochim. Acta* **1983**, *28*, 833.
(560) Du Pasquier, A.; Zheng, T.; Amatucci, G. G.; Gozdz, A. S. *J. Power Sources* **2001**, *97/98*, 758.
(561) Wang, H.; Huang, H.; Wunder, S. L. *J. Electrochem. Soc.* **2000**, *147*, 2853.
(562) Huang, H.; Wunder, S. L. *J. Electrochem. Soc.* **2001**, *148*, A279.
(563) Han, K. N.; Seo, H. M.; Kim, J. K.; Kim, Y. S.; Shin, D. Y.; Jung, B. H.; Lim, H. S.; Eom, S. W.; Moon, S. I. *J. Power Sources* **2001**, *101*, 196.